



**DEVELOPMENT OF USERS-GROUPING AND POWER-ALLOCATION
ALGORITHMS FOR FAIRNESS MAXIMIZATION OF NOMA-BASED MULTIBEAM
SATELLITE NETWORKS INTENDED FOR 5G IMPLEMENTATION**

by

Joel BIYOGHE

Thesis submitted in fulfilment of the requirements for the degree

Doctor of Engineering in Electrical Engineering

in the Faculty of Engineering and the Built Environment

at the Cape Peninsula University of Technology

Supervisor: Dr Vipin BALYAN

Bellville Campus

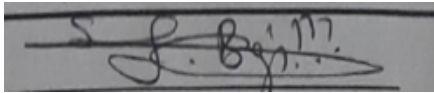
March 2023

CPUT Copyright Information

The thesis may not be published either in part (in scholarly, scientific or technical journals), or as a whole (as a monograph), unless permission has been obtained from the university.

DECLARATION

I, Joel S. BIYOGHE, declare that the contents of this thesis represent my own unaided work, and that the thesis has not previously been submitted for academic examination towards any qualification. Furthermore, it represents my own opinions and not necessarily those of the Cape Peninsula University of Technology.



14/03/2023

Signed

Date

ABSTRACT

Non-Orthogonal Multiple Access (NOMA), Multi-Input Multi-Output (MIMO) and Satellites technologies, are identified as key technology enablers for implementing 5G networks. Thus, the development of NOMA-based Multibeam Satellite Networks (MBSNs) for the realisation of 5G networks is a current research trend in the international telecommunication industry. 5G networks intend to provide extremely high speeds and reliability to all users; and, therefore, set a critical requirement for both high system capacity and high system fairness. However, most reported works on designed subsystems for NOMA-MBSNs focused on maximising the network's capacity alone, without much regard for the high fairness requirement. Therefore, this research suggests to address this need, by proposing a novel users-grouping algorithm (UGA) and two novel power-allocation algorithms (PAAs); which all seek to maximize the fairness of 2users-NOMA-MBSNs.

The proposed users-grouping algorithm was developed by combining the concept of bipartite-matching between the far-users set and the near-users set, the minimum channel-gains margin restriction, and the minimum channel-correlation coefficient restriction between paired users. The resulting restricted problem was formulated as a restricted Hungarian-matrix problem of channel-correlation coefficients between far and near users; which was then solved by the Restricted Hungarian method. The developed *UGA* was then implemented and tested on both Matlab and real-time processor (Arm Cortex-R5) platforms. The results showed that the algorithm ensures high channel-gain margin and channel-correlation between paired users and high fairness amongst resulting pairs. Results also demonstrated that the proposed *UGA* outperforms other existing user-grouping algorithms in terms of resulting pairing fairness.

The proposed power-allocation algorithms were designed based on the *OCTR*-ratios convergence concept (*PAA-1*) and the Max-Min Fairness Concept (*PAA-2*), respectively. In each design, since the original fairness maximization power-allocation problem for the *NOMA-MBSN* is non-convex and NP-hard, it was thus decomposed into two sub-problems, namely, intra-beam and inter-beams power allocations. Each of these sub-problems was then solved using the selected concept amongst the two above; and yielded in intra-beam and inter-beam power-allocation algorithms, respectively. The final algorithm (*PAA-1* or *PAA-2*) combined both sub-algorithms. The developed algorithm in each design (*PAA1* or *PAA-2*) was implemented and tested on both Matlab and the real-time processor (Cortex-R5). In each case, the results demonstrated that the proposed algorithm maximizes the network's fairness; and exhibits sound superiority to other existing power-allocation algorithms, in achieving network fairness.

In sum, to the author's best knowledge, all three algorithms proposed are novel contributions in the field of NOMA-MBSN's development for 5G implementation.

LIST OF PUBLICATIONS

Some of the work presented in this Thesis has been published in international journals and conferences proceedings. The published articles are listed below.

1. Biyoghe, J. & Balyan, V. 2020. A comprehensive survey of existing researches in NOMA Based Integrated Satellite-Terrestrial Networks for 5G. *5th International Conference on Information and Communication Technology for Competitive Strategies (ICTCS-2020)*, India, 11-12 December, 2020, pp 369-378.
2. Biyoghe, J. & Balyan, V. 2021a. A Survey of Existing Studies on NOMA Application to Multi-Beam Satellite Systems for 5G. *5th International Conference on Inventive Systems and Control (ICISC)*, Coimbatore, 7-8 January 2021, pp. 244-255.
3. Biyoghe, J. & Balyan, V. 2021b. NOMA Application to Satellite Communication Networks for 5G: A comprehensive Survey of Existing Studies. *Journal of Communications*, 16(6): 217-227, June.

ACKNOWLEDGEMENTS

I wish to thank all those who contributed in making this journey a success.

To God, the beginning of all things, thank you.

To all my parents, brothers and sisters, across the globe, thank you all for your support, motivations and prayers.

To all friends, appreciators, thank you all.

To the CPUT community at large, thank you very much.

Special thanks to the CPUT staff at the former International-Office: Ms Merle Hodges (Mama Merle – RIP), Mr Makoema Matome, Ms Tandi Jiba (Mama T), Ms Mbolekwa (Mama Portia); you made my stay at CPUT a life lasting enjoyable experience.

Special thanks to two beautiful people who showed me unconditional love during my stay at CPUT: Mr Mornay de Vos (AGC) (Mr de Vos), and Ms Taylia Green (PGO: FEBE) (Momy Taylia).

To the Staff in the Department of Electrical , Electronis, and Computer Engineering, Thank you.

To the Pan-Africanist Students Movement of Azania (PASMA), thank you for the opportunity you gave me to serve the poor students from all corners of Afrika and be an inspiration to many. This PhD is for us; and may this inspire many more PASMA cadres to succeed academically and professionally. iZwe lethu, iAfrika.

To the government of the Republic of South Africa for the support throughout this Doctoral research, thank you.

To the government of the Gabon Republic, for support throughout my academic journey up to Masters level, thank you.

To my supervisor, Dr Vipin, thank you.

To God, the end of all things, thank you.

DEDICATION

This PhD is the fruit of close to 30 years of hard work and dedication which started when I was a kid. Its completion is a combined effort between various part-players; including, God, myself, my parents, my various guides throughout my academic journey, as well as my brothers and sisters across the globe. I choose to celebrate this accomplishment with you all, who, from near or from far, have contributed in making this a reality. The list below is not exhaustive; but I choose to highlight these individuals, for the special role they played in my academic journey.

Name	Role
Meyo Me Ndong Joseph	The first person to identify my gift and help me develop it.
Edzome Ndong Victor (Dallys)	The very first person who accepted to be my teacher.
Effangone Ndje Raymond Bernard (Bner)	My initiator in Sciences; the one who help me develop my scientific mind-set.
Boucalt Desiré	Another one of my teachers who instigated my Scientific mind-set. He taught me that discipline is key in Sciences.
Fassinou Simon	Another one of my teachers who guided me in the Sciences field.
Gabriels (HoP Mech-Eng)	The one who opened the doors of University for me.
Raji Atanda & Adonis Marco	Two of my biggest motivators during my journey as a student at the Department of Electrical & Electronics Engineering (at CPUT).
Whaits Clive	My initiator and coach into the Telecommunications field. Enhanced my Scientific & Engineering mind-set.
Van Zyl Robert	My initiator to the field of Satellite Systems Engineering. Played a significant role in my Post-graduate studies.
Balyan Vipin	My PhD Research Supervisor
Nse Esseng Germaine	My library, my school, my university, in Life-Orientation. She always taught me life, high moral and high ethical values.
Obiang Meyo Michel (Grand OB)	My mind-opener, answers' machine, motivator.
Mme Kie & Mr Moyi (DGBS-2007)	People who valued Excellence. I can only say, thank you.
Memaghe Biteghe Hongrile	My guide, and advisor during my first steps away from home.
Obone Ndong Marie (Puri), Bella Ndong Pascaline (Chimene), Minkwe Alexia (Mémé), Nzoghe Mba Lazare, Obame Bekale Ronald, Obame Maingoua Axel, Ona Biyoghe Cirille, Nkoghe Esseng, Ndong Jean Michel (Papa Gentil), <i>Et al.</i>	All those who have left this world and wanted to witness this achievement, I dedicate this to you.
Parents and Supporters	To you all, my parents and supporters throughout this journey, your support, efforts, contribution, advices as well as patience toward me, have all produced this fruit. It is yours to reap. This PhD belongs to you all.
All my Brothers, Sisters around the world.	To you, who have been waiting for this achievement, from wherever you are reading this, I dedicate this to you all, collectively, and individually. We have made it!
Etsameyong - Medouneu	My Village, my Origines, This PhD is for you!

This PhD is for us all, and to God the Glory!

ABBREVIATIONS

4G	4 th Generation Mobile Networks
5G	5 th Generation Mobile Networks
AP	Access-Point
BPM	Bipartite-Matching
CSI	Channel-State Information
ICI	Inter-Channel Interference
IoT	Internet-of-Things
ITU	International Telecommunication Union
JI	Jain's Index
MA	Multiple-Access
MBSN	Multi-Beam Satellite Network
MIMO	Multiple-Input Multiple-Output
MISO	Multiple-Input Single-Output
MMF	Maximum-Minimum Fairness
NOMA	Non-Orthogonal Multiple-Access
OCTR	Offered-Capacity to Traffic-Request
OMA	Orthogonal Multiple-Access
PA	Power-Allocation
PAA	Power-Allocation Algorithm
PAS	Power-Allocation Subsystem
PC	Precoding
PCA	Precoding Algorithm
PCS	Precoding Subsystem
RAN	Radio-Access Network
UG	Users Grouping
UGA	Users Grouping Algorithm
UGS	Users Grouping Subsystem
USS	Users Scheduling Subsystem
ZF	Zero-Forcing

TABLE OF CONTENT

Declaration	i
Abstract	ii
List of Publications	iii
Acknowledgements.....	iv
Dedication.....	v
Abbreviations	vi
Table of Content	vii
List of Figures	xiii
List of Tables	xv
Chapter 1 : Introduction	1
1.1. Problem background.....	1
1.1.1. Mobile networks' evolution and 5G development requirements	1
1.1.2. Background on Users' Grouping Subsystem Design for NOMA-MBSNs	3
1.1.3. Background on Power-Allocation Subsystem Design for NOMA-MBSNs	4
1.2. Problem Statement	5
1.3. Research Objectives.....	5
1.4. Research Questions	6
1.5. Research Delineation.....	6
1.6. Research Relevance.....	6
1.7. Research Methodology	7
1.8. Thesis layout.....	8
1.9. Chapter summary	8
Chapter 2 : System Description and Modelling.....	9
2.1. Introduction	9
2.2. System description.....	9
2.3. Brief overview of PD-NOMA.....	10
2.4. User's channel-vector modelling	13
2.4.1. modelling of user's channel-coefficients	13
2.4.1.1. Channel's power-gain modelling.....	15
2.4.1.2. Channel-phase modelling.....	16
2.4.1.3. Summary on channel-coefficient modelling.....	17
2.4.2. Modelling of user's channel vector in a MBSN link	17
2.4.3. The Hermitian of a channel-vector.....	19
2.4.4. Summary on user's channel-vector estimation	19

2.5.	Users' scheduling	19
2.6.	Important terminology and notations	20
2.7.	Chapter summary	21
Chapter 3 : NOMA Users' Grouping System Design		22
3.1.	Introduction	22
3.2.	Modelling of Channel-Correlation and Channel gain-margin between users	23
3.3.	UGA's Design Concept	25
3.4.	UGA's Design discussion.....	26
3.4.1.	Step 1: splitting the $2M$ -users into 2 subsets of M -users:.....	26
3.4.2.	Step 2: formulate the user-pairing problem as a bipartite matching problem:....	26
3.4.3.	Step 3: Introduce the <i>fair-pairing</i> requirement into the BPMP in step2 and use the Hungarian Method to solve the problem.....	27
3.4.4.	Step 4: Introduce the <i>minimum channel-gain margin</i> requirement into the BPMB to yield a restricted BPMB and solve it using restricted-HM.....	28
3.4.5.	Step 5: Reduce C_{gr_min} and re-iterate the restricted HM process in step4.....	29
3.5.	Resulting UGA	31
3.6.	Precoding Weight-vectors calculation	32
3.6.1.	Background	32
3.6.1.1.	Role of pc section	32
3.6.1.2.	Classification of Precoding techniques	33
3.6.2.	Selection of the Zero-Forcing technique	34
3.6.3.	Calculation of the precoding weight-vector matrix (W) in a 2-users NOMA case	34
3.7.	Chapter summary	35
Chapter 4 : Modelling of the power-allocation Subsystem in a 2-users NOMA-MBSN.....		36
4.1.	Introduction	36
4.2.	Overview of the power-allocation subsystem in a mobile network	36
4.2.1.	Role of the power-allocation subsystem	36
4.2.2.	PA system's design goals and considerations	37
4.3.	The proposed power-allocation algorithms design work	38
4.4.	Design requirement and specifications for the proposed PA subsystem	38
4.5.	Link between System's fairness, users' OCTR-ratios and users' capacities	39
4.6.	Modelling of the network's users' capacities.....	41
4.6.1.	General model of the user's capacity in terms of user's SINR	41
4.6.2.	SINR of the near-user (n) in any beam (b).....	42
4.6.3.	SINR of the far-user (f) in beam (b)	43
4.6.4.	Effect of the Precoding on users' SINRs and capacities	44
4.6.5.	Link between beam's users' capacities and the P_b and α_b	45

4.7.	Formulation of the system's fairness maximization as an optimization problem ...	47
4.7.1.	The original optimization problem	47
4.7.2.	Decomposition of original problem into 2 sub-problems.....	48
4.7.3.	Variations of beam's users' capacities versus beam's power (P_b).....	49
4.7.4.	Variations of beam's users' capacities versus α_b	49
4.8.	Common power-allocation design concepts for system's fairness-maximization ..	51
4.9.	Chapter summary	52
Chapter 5 : Power-Allocation Algorithm Based on the OCTR-Ratios Convergence Concept		53
5.1.	Introduction	53
5.2.	Description of the OCTR-ratios Convergence concept.....	53
5.3.	Intra-beam power-allocation algorithm design.....	54
5.3.1.	Overview	54
5.3.2.	Step1: Process initialization.....	55
5.3.2.1.	Input parameters definition	55
5.3.2.2.	Notion of OCTR-ratios convergence within a beam	56
5.3.2.3.	Convergence error definition	57
5.3.2.4.	Increment and decrement step-sizes:.....	57
5.3.2.5.	Initial power-set definition for the intra-beam power-allocation.....	58
5.3.3.	Step2: Iterative Convergence Search	59
5.3.3.1.	Step2-a: Receive the new value of " α_b "	59
5.3.3.2.	Step2-b: Evaluate the OCTR-ratios R_{bn} and R_{bf} based on received " α_b "	60
5.3.3.3.	Step2-c: Check for OCTR-ratios convergence.....	60
5.3.3.4.	Step2-d: Check if power-share of minimum OCTR-ratio can still be increased.....	60
5.3.3.5.	Step2-e: Increment " α_b " if applicable:.....	60
5.3.3.6.	Step2-f: Decrement " α_b " if applicable:	61
5.3.4.	Step3: Terminate the search process and determine the beam's OCTR-ratio .	61
5.3.5.	Resulting intra-beam PA-algorithm based on the OCTR-ratios convergence concept	62
5.4.	Inter-beam power-allocation algorithm design.....	62
5.4.1.	Overview	62
5.4.2.	Step1: Process initialization.....	63
5.4.2.1.	System's power budget specification	63
5.4.2.2.	Notion of OCTR-ratios Convergence in the context of inter-beam	64
5.4.2.3.	Convergence-error definition	65
5.4.2.4.	Beam's power increment step-size definition	65
5.4.2.5.	Beam's power decrement step-size definition.....	69

5.4.3.	Step2: Iterative convergence search process	69
5.4.3.1.	Step2-a: Receive the new beam's powers set ($P_{b\text{-set-new}}$).....	70
5.4.3.2.	Step2-b: Evaluate OCTR-ratios of respective beams (R_b)	70
5.4.3.3.	Step2-c: Check for OCTR-ratios convergence.....	70
5.4.3.4.	Step2-d: Check whether the beam' power for $R_{b\text{-min}}$ can still be increased....	70
5.4.3.5.	Step2-e: Determine $P_{b\text{-inc-new}}$ and calculate new P_b for beam with $R_{b\text{-min}}$	71
5.4.3.6.	Step2-f: Determine $P_{b\text{-dec-new}}$ and calculate new P_b for beam with $R_{b\text{-max}}$	71
5.4.4.	Step3: Terminate the process and save the resulting $P_{b\text{-set}}$	72
5.4.5.	Resulting inter-beam PA-algorithm based on the OCTR-ratios convergence concept	72
5.5.	Global System's Power-Allocation Algorithm -1	73
5.6.	Novelty of the proposed PAA-1.....	74
5.7.	Chapter summary	74
Chapter 6 : Power-allocation Algorithm based on the Maximum-Minimum Fairness Concept.....		75
6.1.	Introduction.....	75
6.2.	Description of the max-min fair concept	75
6.2.1.	Merit of the Max-Min Fairness Concept.....	75
6.2.2.	Step-flow of the max-min fairness concept	77
6.3.	Intra-beam power-allocation algorithm design.....	78
6.3.1.	Overview	78
6.3.2.	Step1: Process Initialisation	79
6.3.2.1.	Input parameters definition	79
6.3.2.2.	Defining the user's right:.....	79
6.3.2.3.	Deserving shares of the beam's power for beam's near and far-users.....	79
6.3.2.4.	Generate initial power-set.....	80
6.3.3.	Step2: Iterative intra-beam power-sharing coefficient's adjustment	80
6.3.3.1.	Step2-a: Receive the new value of " α_b "	80
6.3.3.2.	Step2-b: Evaluate the OCTR-ratios R_{bn} and R_{bf} based on received " α_b "	80
6.3.3.3.	Step2-c: Check if both users satisfy $R \geq 1$	80
6.3.3.4.	Step2-d: Check if all users are unsatisfied ($R \leq 1$).....	81
6.3.3.5.	Step2-e: Adjustment of the intra-beam power-sharing coefficient (α_b).....	81
6.3.4.	Step3: Terminate the process and determine the beam's OCTR-ratio (R_b).....	83
6.3.5.	Resulting intra-beam PA-algorithm based on the max-min fair concept.....	84
6.4.	Inter-beam power-allocation algorithm design.....	84
6.4.1.	Overview	84
6.4.2.	Step 1: Process Initialization	85

6.4.2.1. System's power budget specification	85
6.4.2.2. Define the right of every user	86
6.4.2.3. Calculate the deserving share of power of every user from $P_{\text{tot-sat}}$:	86
6.4.2.4. Generate the initial power-set for all user	86
6.4.3. Step2: Iterative redistribution of the excess-power amongst unsatisfied beams	86
6.4.3.1. Step2-a: Receive the new beam's powers set ($P_{\text{b-set-new}}$)	86
6.4.3.2. Step2-b: Evaluate the <i>OCTR</i> -ratio of each respective beam (R_b)	87
6.4.3.3. Step2-c: Conditions-1: Check if all beams are satisfied (i.e. all $R_b \geq 1$)	87
6.4.3.4. Step2-d: Condition-2: Check if any beam is over-satisfied	87
6.4.3.5. Step2-e: Redistribution of excess power amongst unsatisfied users:	89
6.4.4. Stage3: Terminate the inter-beam power allocation process	94
6.4.5. Resulting inter-beam PA-algorithm based on Max-Min Fairness concept	95
6.5. Global System's power-allocation Algorithm -2	96
6.6. Novelty of the proposed <i>PAA-2</i>	97
6.7. Chapter summary	98
Chapter 7 : Implementation, Testing and Validation of all the developed Algorithms (<i>UGA</i> , <i>PAA-1</i> and <i>PAA-2</i>)	99
7.1. Introduction	99
7.2. Matlab Implementation, Testing and Validation	99
7.2.1. The implementation	99
7.2.2. The ATPs of the subsystems under test	99
7.2.3. Mobile network's Parameters specification:	101
7.2.4. Generation of network's input-data sets:	102
7.2.4.1. Users' traffic-requests generation	103
7.2.4.2. Users channel-vectors generation	103
7.2.5. <i>UGA</i> 's Code running and results discussion	105
7.2.5.1. Test results	105
7.2.5.2. Performance validation	107
7.2.5.3. Superiority of the proposed <i>UGA</i>	112
7.2.6. Precoding weight-vector Code results	113
7.2.7. <i>PAA-1</i> 's Code running and results discussion	114
7.2.7.1. Test results	114
7.2.7.2. Performance validation	116
7.2.7.3. Effect of different average-TRs on the system's <i>OCTR</i> -ratios convergence value	117
7.2.7.4. Superiority of the proposed algorithm <i>PAA-1</i> over existing <i>PAAs</i>	118
7.2.8. <i>PAA-2</i> 's Code running and results discussion	119

7.2.8.1. Test results.....	119
7.2.8.2. Performance validation.....	122
7.2.8.3. Effect of different average-TRs on the network’s Fairness-Metric.....	122
7.2.8.4. Superiority of the proposed algorithm PAA-2 over existing PAAs.....	123
7.3. On-Processor Implementation, Testing and Validation.....	124
7.3.1. Implementation.....	124
7.3.2. Tests process and input-data generation.....	125
7.3.3. Results and Validation of the UGA’s Code.....	127
7.3.4. Results and Validation of the Zero-forcing Precoding Code.....	128
7.3.5. Results and Validation of the PAA-1’s Code.....	129
7.3.6. Results and Validation of the PAA-2’s Code.....	130
7.4. Chapter summary.....	132
Chapter 8 : Conclusion and Recommendations.....	133
8.1. Conclusion.....	133
8.1.1. Summary.....	133
8.1.2. Responses to research questions.....	135
8.2. Recommendations.....	135
References.....	137
Appendices.....	145
Appendix-A: Matlab Codes for the “Matlab Implementation” of the Algorithms.....	145
Appendix-A1: The “Main Function” which calls the UGA, PCA, PAA-1 and PAA-2.....	145
Appendix-A2: The Top-Level-Function of the “proposed-UGA”.....	146
Appendix-A3: The Top-Level-Function of the “PCA”.....	147
Appendix-A4: The Top-Level-Function of the “PAA-1”.....	148
Appendix-A5: The Top-Level-Function of the “PAA-2”.....	149
Appendix-B: Vitis Codes for the “On-Processor Implementation” of the Algorithms.....	150
Appendix-B1: The “MA-Encoder Function” which calls the UGA, PCA, PAA-1 & PAA-2.....	150
Appendix-B2: The Top-Level-Function of the “proposed-UGA”.....	151
Appendix-B3: The Top-Level-Function of the “PCA”.....	153
Appendix-B4: The Top-Level-Function of the “PAA-1”.....	155
Appendix-B5: The Top-Level-Function of the “PAA-2”.....	157

LIST OF FIGURES

Figure 1.1: illustration of mobile networks: (a): the TMN and (b): the MBSN (adopted from Li et al., 2019:277 and Yin et al., 2019:11848, respectively).	1
Figure 1.2: Illustration of the MA-Encoder of a NOMA-MBSN (adapted from Wang et al., 2016:55).	3
Figure 2.1: Geo-spatial illustration of a 2-users NOMA MBSN (adapted from Biyoghe & Balyan, 2021:247).....	10
Figure 2.2: Illustration of PD-NOMA concept: OMA vs NOMA (adapted from Biyoghe & Balyan, 2020:370).....	11
Figure 2.3: Geo-spatial illustration of a 3users-NOMA beam.....	12
Figure 2.4: User’s channel-vector estimation block in the MA-encoder.	13
Figure 2.5: Illustration of the channel link between satellite and user in a MBSN.	18
Figure 2.6: User’s scheduling block in the MA-encoder.....	19
Figure 3.1: The NOMA Users’ Grouping System (UGS) in the MA-Encoder block.	22
Figure 3.2: Illustrations of outcomes to the BPMP: (a) maximum matching, (b) perfect matching.....	27
Figure 3.3: Illustration of the border region for far- and near- users’ channel-gains.....	29
Figure 3.4: The Precoding system in the MA-Encoder block.	32
Figure 4.1: The Power-Allocation Subsystem in the MA-Encoder block	36
Figure 4.2: Variations of C_{bn} , C_{bf} , R_{bn} and R_{bf} , with respect to “ α_b ”	50
Figure 5.1: The Power-Allocation System in the MA-Encoder block.....	53
Figure 5.2: Illustration of the intra-beam power-allocation stage in a multi-beams satellite system.	55
Figure 5.3: Illustration of inter-beam power-allocation stage	63
Figure 5.4: Illustration of: (a) the max possible beam’s power increment ($P_{b-inc-max}$); (b) the maximum possible OCTR-ratios gap (Gap_{max}).	67
Figure 6.1: Illustration of the intra-beam power-allocation stage in a multi-beams satellite system.....	78
Figure 6.2: illustration of the sliding process of “ α_b ” and its effect on of R_{bn} and R_{bf} : (a): case of $R_{bn} > 1$; (b): case of $R_{bf} > 1$	83
Figure 6.3: Illustration of inter-beam power-allocation stage	85
Figure 7.1: Geo-spatial illustration of 80-users’ distribution in the network (3D view).	104
Figure 7.2: Geo-spatial illustration of the 80-users’ distribution in the network (Top-view)..	105
Figure 7.3: Highlight of the generated pairs on the network’s spatial-distribution view.	106
Figure 7.4: Highlight of the generated pairs on the network’s spatial-distribution view.	109
Figure 7.5: Highlight of the generated pairs on the network’s spatial-distribution view.	111

Figure 7.6: Fairness-Metric the proposed <i>UGA</i> for case of 3, 4, 5, and 6 antennas on the satellite.	112
Figure 7.7: Fairness-metrics of various users-grouping algorithms for different number of antennas.....	112
Figure 7.9: Beams' powers per iteration and Total power used on Satellite.	115
Figure 7.10: Intra-beam power-sharing coefficient (α_b) of respective beams, per iteration..	115
Figure 7.11: Beams' capacities per iteration and total satellite's throughput.....	115
Figure 7.12: <i>OCTR</i> -ratio (R_b) of respective beams at each iteration.....	116
Figure 7.13: Fairness-Metric of the Multi-Beam Satellite's Network per iteration of the <i>PAA-1</i>	116
Figure 7.14: <i>OCTR</i> -ratios convergence value (a) and Network's Fairness Metric (b); of the proposed <i>PAA-1</i> , for different Average Users' Traffic-Requests.....	118
Figure 7.15: Fairness-Metric of various <i>PAAs</i>	119
Figure 7.16: Beams' powers per iteration and Total power used on Satellite.	120
Figure 7.17: Intra-beam power-sharing coefficient (α_b) of respective beams, per iteration..	120
Figure 7.18: Beams' capacities per iteration and total satellite's throughput.....	121
Figure 7.19: <i>OCTR</i> -ratio (R_b) of respective beams at each iteration.....	121
Figure 7.20: Fairness-Metric of the Multi-Beam Satellite's Network per iteration of the <i>PAA-2</i>	121
Figure 7.21: Achievable fairness-metric of the <i>PAA-2</i> for different average traffic-requests.....	123
Figure 7.22: Fairness-Metric of various <i>PAAs</i>	124
Figure 7.23: <i>Zynq UltraScale+ MPSoC</i> running applications/codes of our proposed algorithms.	125
Figure 7.24: Beam's powers and Total power used, per iteration of the <i>PAA-1</i>	129
Figure 7.25: Beam's Capacities and Total networks throughput, per iteration of the <i>PAA-1</i>	129
Figure 7.26: Beam's <i>OCTR</i> -ratios and resulting network's Fairness-metric, per iteration of the <i>PAA-1</i>	130
Figure 7.27: Beam's powers and Total power used, per iteration of the <i>PAA-2</i>	131
Figure 7.28: Beam's Capacities and Total networks throughput, per iteration of the <i>PAA-2</i>	131
Figure 7.29: Beam's <i>OCTR</i> -ratios and resulting network's Fairness-metric, per iteration of the <i>PAA-2</i>	131

LIST OF TABLES

Table 2.1: Basic Classification of the Tx-Rx propagation link in terms of signal paths.	14
Table 2.2: List of common notations in this document and their meaning.....	21
Table 3.1: Illustration of square matrix of near-far users channel-correlation coefficients.....	28
Table 3.2: Proposed Users' Grouping Algorithm for 2-users NOMA-based MBSNs	31
Table 5.1: General step-flow of the OCTR-ratios Convergence concept	54
Table 5.2: Proposed Intra-beam PA Algorithm for 2-users NOMA, based on the OCTR-ratios Convergence Concept	62
Table 5.3: Proposed Inter-beam PA Algorithm for M -beams, based on the OCTR-ratios Convergence Concept	72
Table 5.4: Proposed Global PA-Algorithm-1 for 2-users NOMA MBSN, based on the OCTR- ratios Convergence Concept.	74
Table 6.1: General step-flow of the Max-Min Fairness concept.....	77
Table 6.2: Proposed Intra-beam PA Algorithm for 2-users NOMA, based on the Max-Min Fairness Concept	84
Table 6.3: Proposed Inter-beam PA Algorithm for M -beams, based on the Max-Min Fairness Concept.....	95
Table 6.4: Proposed Global PA-Algorithm-2 for 2-users NOMA MBSN, based on the Max- Min Fairness Concept.....	97
Table 7.1: Acceptance Test Procedure (ATP) of the Users-Grouping Subsystem (UGS)...	100
Table 7.2: : Acceptance Test Procedure (ATP) of the Power-Allocation Subsystem (PAS)	100
Table 7.3: Mobile Network's Parameters Specification.....	101
Table 7.4: a set of traffic-requests for the 8-selected users, with an average value of 3bps/Hz.	103
Table 7.5: Ground distances and Angle-of-Arrival of selected 8-users	104
Table 7.6: Channel-vectors of the selected 8-users	104
Table 7.7: Near-users and far-users' sets as well as the resulting C_3 -matrix.	106
Table 7.8: Generated pairs of near-far users.	106
Table 7.9: channel-gain ratio of resulting pairs.....	107
Table 7.10: C_3 of the resulting pairs and algorithm's fairness-metric.	107
Table 7.11: Ground distances and Angle-of-Arrival of selected 10-users.	108
Table 7.12: Channel-vectors of the selected 10-users	108
Table 7.13: Near-users and far-users' sets as well as the resulting C_3 -matrix.	108
Table 7.14: Generated pairs of near-far users.....	109
Table 7.15: Channel-gain ratio (C_{gr}) of resulting pairs.	109
Table 7.16: C_3 of the resulting pairs and algorithm's fairness-metric.	109
Table 7.17: Ground distances and Angle-of-Arrival of selected 12-users.	110

Table 7.18: Channel-vectors of the respective 12-users.	110
Table 7.19: Near-users and far-users' sets as well as the resulting C_3 -matrix.	110
Table 7.20: Generated pairs of near-far users.....	110
Table 7.21: Channel-gain ratio (C_{gr}) of resulting pairs.	111
Table 7.22: C_3 of the resulting pairs and algorithm's fairness-metric.	111
Table 7.23: Channel matrix of near-users (H_{nu}).	113
Table 7.24: The generated Zero-forcing precoding matrix.....	113
Table 7.25: The Q-Matrix obtained.....	113
Table 7.26: Sets of users' traffic requests with different average values.	117
Table 7.27: Ground distances and Angle-of-Arrivals of selected 8-users.	127
Table 7.28: Channel-vectors of the respective 8-users	127
Table 7.29: Resulting pairs from the <i>UGA</i> -Code	128
Table 7.30: Channel-gain ratio of resulting pairs.	128
Table 7.31: C_3 of resulting pairs and the achieved grouping fairness-metric.	128
Table 7.32: precoding weight-vectors of the 4 respective antennas	128
Table 7.33: The Q-Matrix obtained.....	129

CHAPTER 1: INTRODUCTION

1.1. Problem background

1.1.1. Mobile networks' evolution and 5G development requirements

Wireless radio access networks, commonly referred to as mobile networks, allows mobile users to access the network's resources (frequency and power) in order to either transmit or receive information (Islam et al., 2017:721). Figure 1.1 below gives an illustration of common types of mobile networks, including the terrestrial base-station network (TBN) and the multi-beam satellite network (MBSN). They are generally evaluated in terms of their total capacity, reliability (quality of service (QoS), and user-fairness), latency as well as geographical coverage or span (Aldababsa et al., 2018:2; Bai et al., 2018:38). Based on their achievable performances, mobile networks have been classified from 1G to 4G over the past years; and current generation being proposed is classified as 5G.

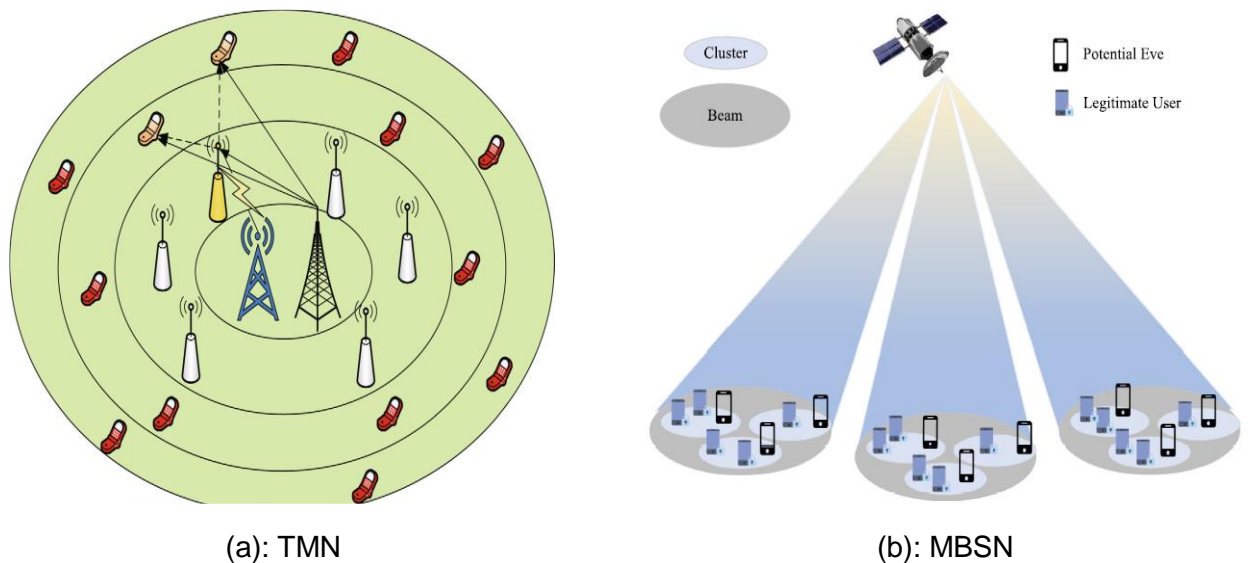


Figure 1.1: Illustration of mobile networks: (a): the TMN and (b): the MBSN (adopted from Li et al., 2019:277 and Yin et al., 2019:11848, respectively).

The last and most advanced generation of mobile networks is the 4G networks. These networks mainly employ OFDMA and their top achievable performances include, a connectivity density of up to 10^5 connections per Km^2 , an end-to-end latency of maximum 10ms, as well as minimum user-experienced data rate of 10Mbps and a peak user data rate 1Gbps (Liu & Jiang, 2016:7; Wang et al., 2016:53). With such performances, services offered by 4G in addition to those provided by 3G include HD video calling and live-streaming.

With the ongoing technology advancement, the telecommunication industry intends providing throughout the 2020 decade, services such as Smart grids, home automation, industrial internet, remote surgery, Intelligent Transportation System (ITS), and the whole-world connection ... etc. (Khan & Jayakody, 2020: 15758). All these services constitute elements of the bigger project of the international mobile telecommunication (IMT) called the *achievement of the internet of things (IoT)*; which consists of being able to interconnect millions of devices that can interchange data accurately, reliably and in near real-time (Aldababsa et al., 2018:2; An et al., 2019:63531). These services set the requirement for network performances such massive-connectivity (i.e. ultra-high density), ultra-reliable, ultra-low latency and ubiquity (i.e. seamless and large geographical coverage) (Islam et al., 2017:721; Anwar et al., 2019:2).

Visibly, the performances of 4G networks appear to be insufficient to support the new intended services (Zhu et al., 2019:204). For this reason, the international telecommunication union (ITU) has developed standards for the next generation of WRANs known as the 5G networks, which should be capable of supporting the new intended services. Some of the 5G performance standards include to achieve: a) a minimum connectivity density of 10^6 connections per Km^2 , b) an ultra-low end-to-end latency of maximum 1ms, c) a user-experienced data rate of 100Mbps and a peak user data rate of about 10Gbps (Liu & Jiang, 2016:7; Wang et al., 2016:53).

The development of networks that meet the 5G requirements constitutes the current challenge of the telecommunication industry. However, some possible technologies that are considered key enabler of 5G network's development have already been proposed; including the non-orthogonal multiple-access (NOMA) technology, Multi-users multiple-input multiple-output (MIMO) technology, as well as the satellite technology as the access-point component to allow a ubiquitous coverage (Bai et al., 2018:38; Ejaz et al., 2020:6-7; Balyan & Gupta, 2021:1). Thus, in the field of mobile networks development, researches are currently trending toward the development of mobile networks that employs NOMA, MIMO and the Satellite altogether, to achieve 5G networks. This research subscribes to this trend. These types of mobile networks are commonly called NOMA-based Multi-Beam Satellite Networks (NOMA-MBSNs).

Without loss of generality, the essential part of a mobile network's design implies designing the multiple-access (MA) encoder of the network. As illustrated in Figure 1.2 below, the MA-encoder of a NOMA-MIMO mobile network generally consists amongst others of the following fundamental subsystems: the users' channel-state information (CSI) acquisition subsystem, users scheduling subsystem (USS), NOMA-users grouping subsystem (UGS), Precoding subsystem (PCS) and the power-allocation subsystem (PAS). The users' CSI-acquisition subsystem estimates the channel-vector and traffic-request of all users, at a given time-slot.

The USS then decides which users amongst the all active network's users should be serve in this time-slot. Subsequently, the UGS decides the best combination of users to put in same group, to successfully perform NOMA technology. The PCS then, determines the precoding weight-vectors of respective antennas, necessary for successful mitigation of the excessive Inter-Channel Interferences (ICIs) caused by usage of MIMO technology. Finally, the PAS is in charge of determining the adequate amount of power to be allocated to each user, in order to achieve a desired network's service goal. Because of the level of complexity involved in the development of these subsystems, their designs constitute respectively subfields of research. Thus, in this research, we focus on the design of UGS and PAS, for NOMA-MBSNs.

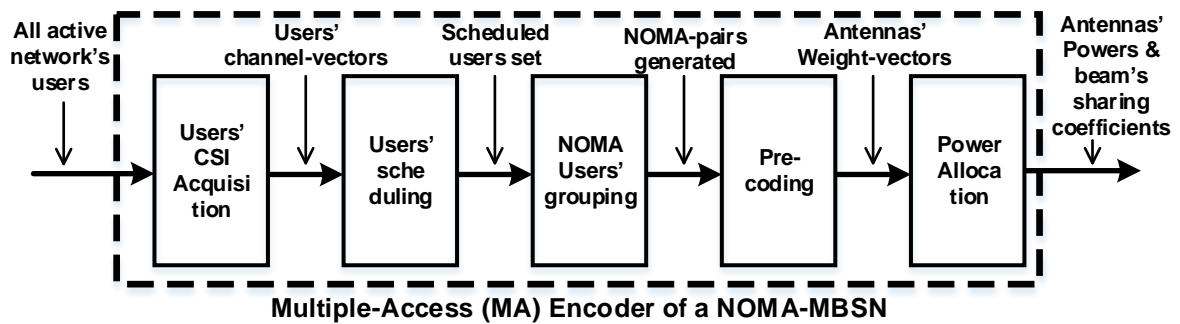


Figure 1.2: Illustration of the *MA*-Encoder of a NOMA-MBSN (adapted from Wang et al., 2016:55).

1.1.2. Background on Users' Grouping Subsystem Design for NOMA-MBSNs

In mobile networks that would employ NOMA technology coupled with MIMO technology, each antenna of the access-point will serve 2 or more users simultaneously by means of NOMA protocol. Thus, network users need to be put into subgroups called NOMA-groups, in order to be served simultaneously by the same antenna; that is known as NOMA users' grouping. In order to implement NOMA protocol at transmission and successfully decode respective user's information at reception, it is required that users grouped in the same NOMA group must have distinct channel gains (Ding et al., 2016:6011; Zhu et al., 2017:2257; Aldababsa et al., 2018:3). Also, due to excessive ICIs caused by employment of MIMO technology, users grouped together must have high channel-correlation; in order for all group's users to successfully mitigate the ICI from other groups by means of the unique group's precoding weight-vector (Caus et al., 2016:500; Neira et al., 2019:61). Subsequently, since poorly correlated users will achieve poor capacities, and given that providing good quality of service to all users (i.e. achieving high system's fairness) is a critical requirement of 5G networks, it is therefore necessary to avoid situation where some groups have extremely high correlations while others have extremely poor correlation. Thus, it is necessary to ensure fairness during grouping, in terms of channel-correlation of resulting groups. Consequently, it appears clearly that, for the

development of NOMA-MIMO networks for 5G implementation, the UGS of the network must ensure that the three following requirements are met:

- a) In all the pairs, a minimum channel gain margin between the group's users is satisfied;
- b) In all the pairs, a minimum channel-correlation between the group's users is satisfied;
- c) Fairness amongst the generated pairs is preserved with respect to channel-correlation of each group.

From the existing literature, very few studies have presented a users' grouping algorithm for their work on NOMA-based MIMO networks. To the author's best knowledge, only the following authors proposed an algorithm for their NOMA-MBSN (case of 2-users per NOMA-group):

- 1) Caus et al., (2016:500): proposed a UGA based on Minimum-Euclidian-Norm (*MEN*) technique. The proposed algorithm meets the requirement (b), but with not much considerations of requirements (a) and (c).
- 2) Vazquez et al., (2016:91): also proposed a UGA based on Geographical User's Clustering (*GUC*) technique. This algorithm meets the requirement (b), but with not much considerations of requirements (a) and (c).
- 3) Zhu et al., (2019:3): presented a UGA in which they consider both maximum channel-correlation and channel-gain margin. This algorithm ensures that requirements (a) and (b) are met; but without considering fairness during pairing, i.e. requirement (c).
- 4) Lin et al., (2019:661): Similar to Zhu et al., 2019:3, authors in this article also presented a *UGA* in which they consider both maximum channel-correlation and channel-gain margin between users. But yet again, there was no much consideration ensuring fairness between resulting pairs. Therefore, this algorithm also meets requirements (a) and (b); but without much consideration of requirement (c).
- 5) Zhu et al., (2017:2258): proposed a UGA that considers maximum channel-correlation as well as fair-grouping. But there was no specific attention in ensuring that all resulting pairs satisfy a minimum channel-gain margin. Therefore, this algorithm ensures that requirements (b) and (c) are met, but not much consideration of requirement (a).

Therefore, from the above survey, it appears that, no work has managed to address all three requirements simultaneously. As such, the need to have a UGS that ensures these three requirements are met, in order to improve the network's fairness, remains relevant and must be addressed.

1.1.3. Background on Power-Allocation Subsystem Design for NOMA-MBSNs

The role of the power-allocation subsystem is to determine the adequate amount of power to allocate to respective users, in order to achieve the defined network's goal. This would be

either to maximise the network's total capacity, or maximise network's fairness, or to achieve a trade-off of these two fundamental performance parameters of the network (Kumar et al., 2008:70-71; Shams et al., 2014:137). In terms of development, the field of 5G mobile networks development is still relatively new; and the amount of proposed design works therein is still fairly young. Subsequently, to the author's best knowledge, only a few authors have reported power-allocation algorithm's design for *NOMA-MBSNs*. In this regards, the authors (Biyoghe & Balyan, 2020:372-373; Biyoghe & Balyan, 2021a:220-222; Biyoghe & Balyan, 2021b:247-251) presented a detailed review of existing studies which, at the time of starting this research, had proposed *PA* algorithms for their *NOMA-MIMO* networks; including, satellite's, terrestrial's, as well as integrated satellite-terrestrial's networks.

From these surveys, it results that, most of the studies that proposed a *PAA* for 2-users *NOMA-MBSNs*, designed their *PAA* to maximise the system's capacity; without much attention given to system's fairness. And only one study attempted to design a *PAA* for system's fairness maximization (Biyoghe & Balyan, 2021a:223; Biyoghe & Balyan, 2021b:252). This indicates that, the design of *PA* algorithms for fairness maximization of *NOMA*-based satellite networks still remains an unattended field which requires rapid attention. Because, system's fairness is a critical performance requirement for 5G networks; and *NOMA*-based *MBSNs* are planned to be part of 5G mobile networks' implementation. Furthermore, the only identified work listed above developed their algorithm based on the *OCTR*-ratios convergence concept. *Thus, to the author's best knowledge, no reported work has proposed a fairness-maximization PA algorithm based on the maximum-minimum fairness concept, for NOMA-based networks in general, and NOMA-MBSNs in particular.*

1.2. Problem Statement

5G networks, which *NOMA-MBSNs* seeks to realise, set critical requirements for both high system's capacity and high system's fairness; because they aim to offer to every network's user a seamless connectivity, irrespective of user's channel conditions. However, existing works that thus far developed users' grouping and power-allocation subsystems for *NOMA-MBSNs*, designed their subsystems to maximize the network's capacity; without much consideration of the fairness aspect. Thus, the need to have network's subsystems (including *UGS* and *PAS*) which maximize the network's fairness, remains unattended and is a high priority concern in the field of *NOMA-MBSNs* development.

1.3. Research Objectives

This research seeks to address the above outlined need, by proposing to design a users' grouping algorithm (*UGA*) and power-allocation algorithms (*PAAs*) for *NOMA-MBSNs*, which maximise the network's fairness. Thus, the research objectives can be listed as follows:

- To propose a novel users-grouping algorithm (UGA) for 2-users-NOMA-MBSNs, which increases network's fairness.
- To propose a novel Power-Allocation Algorithms (PAA-1) based on the OCTR-ratios convergence concept, which maximises the fairness of a 2-users-NOMA-MBSNs.
- To propose a novel Power-Allocation Algorithms (PAA-2) based on the Maximum-Minimum Fairness concept, which maximises the fairness of a 2-users-NOMA-MBSNs.
- To Implement, Test and Validate each algorithm on *matlab* (emulation).
- To Implement, Test and Validate each algorithm on a *real-time processor* (on-chip).

1.4. Research Questions

The research addresses the following questions:

- 1) What approach would be adequate for the design of a *UGA* which satisfies the three pairing requirements of a 2-users-NOMA-MBSN?
- 2) Which concept would be adequate for the design of a *PAA* that maximizes fairness of a 2-users-NOMA-MBSN?
- 3) What approach would be suitable to solve the non-convex and *NP*-hard fairness maximization power-allocation problem, for 2-users-NOMA-MBSNs?

1.5. Research Delineation

- In this research, it will be assumed that, the channel-state information (CSI) of all users, are known to the network at the time of executing the proposed UGA and PAAs.
- Due to the complexity involved in integrating all the software of the satellite onto the satellite's On-Board Computer (OBC), the hardware testing and validation of the proposed algorithms will be done using a programmable hardware (Real-time processor) available, not the satellite's OBC.

1.6. Research Relevance

All the 3 algorithms proposed from this research are novel in the field of NOMA-MBSNs development for 5G. Thus, this research is relevant at multiple levels.

First, in the international telecommunication industry, the development of 5G mobile networks is the technology race of the 2020 decade. Thus, the knowledge proposed through this research will be relevant to 5G networks' developers across the globe.

Secondly, this project is part of the French South African Institute of Technology (F'SATI)'s space program. F'SATI is part of the QB50 nanosatellite project, which is an international nanosatellites' mission in which 50CubeSats are deployed in a constellation, in Low-Earth Orbit; to study the layers of the Atmosphere and facilitate the exchange of data at very fast

links, to ground users deployed across the globe. This constellation is forming a satellite mobile network in which multiple users will require to access network information simultaneously, at a good quality-of-service. Also, F'SATI in collaboration with the South African National Space Agency (SANSA), intend having multiple launches of nanosatellite through the 2020 decade, to form a CubeSat constellation. This constellation will be used for real-time in-situ monitoring of South-African boarder and coastal lines; and will have to provide real time data to users on the ground at very high speed. It is also therefore, forming a satellite's mobile network, in which multiple users will require to access network information simultaneously, at a good quality-of-service. Consequently, the knowledge developed in this research is relevant for use in the various satellite networks development missions, in which F'SATI is involved; for better network's service delivery to the multiple mobile ground users.

Lastly, the knowledge developed in this research will be relevant to any ground, aerial and low altitude mobile communication networks in which multiple users need to be provided high-speed links simultaneously, by a single access point equipped with multiple antennas. This is particularly relevant to the Department of Defence & Military Veterans, which would make use of aerial vehicles (eg. drones) to transfer information to various ground points simultaneously, at very high speed; for the purpose of land and territorial guarding and monitoring.

1.7. Research Methodology

To achieve the objectives of this research, the following methodology is adopted:

1. Start by giving a clear description of the network under design;
2. Then, design the proposed UGA, following the stages below:
 - a) develop a model of the users-grouping subsystem that relates the output parameters of the UGS to its input parameters;
 - b) investigate by means of literature review, existing approaches based on which users' grouping algorithms are often designed.
 - c) Select the approach to be considered for the design of the proposed UGA.
 - d) Design the proposed UGA based on selected approach.
3. Then, design the proposed power-allocation algorithms, following the stages below:
 - a. develop a model of the users-grouping subsystem that relates the output parameters of the PAS to its input parameters;
 - b. investigate by means of literature review, existing concepts commonly used for the design of PA algorithms to achieve network's fairness maximization.
 - c. Design a PAA for the described network, based on the OCTR-ratios convergence concept, to obtain the first proposed power-allocation algorithm (PAA-1).

- d. Design a PAA for the described network, based on the Max-Min Fairness concept, to obtain the second proposed power-allocation algorithm (PAA-2).
4. Thereafter, implement, test and validate each of the proposed UGA, PAA-1 and PAA-2 on the *Matlab platform*, for first functional performance review.
5. Finally, implement, test and validate each of the proposed UGA, PAA-1 and PAA-2 on the *real-time processor platform*, for further functional performance review.

1.8. Thesis layout

This thesis comprises of 8 chapters. Chapter-1 introduces the research, by highlighting the research problem, objectives, questions, relevance as well as the adopted methodology. Chapter-2 describes the network under development; i.e. a 2-users NOMA-MBSN. It also gives a details discussion on user's channel-vector estimation in MIMO networks; as well as on precoding weight-vectors calculation for the respective antennas. Chapter 3: presents the design of the proposed users-grouping algorithm for the described network. Chapter-4: discusses the modelling of the power-allocation subsystem; as well as the identification of adequate concepts to be employed for the design of fairness-maximization power-allocation algorithms, including the OCTR-ratios convergence concept and the Maximum-Minimum Fairness concept. Chapter-5 presents the design of the power-allocation algorithm based on the OCTR-ratios convergence concept, and yields the first proposed power-allocation algorithms (PAA-1). Chapter-6 presents the design of the power-allocation algorithm based on the Max-Min Fairness concept, and yields the second proposed power-allocation algorithms (PAA-2). Chapter-7 discusses the implementation, testing and validation of the proposed algorithms on two platforms, namely, *matlab*, and *on-processor (real-time)*. For the implementation on each platform, the chapter presents for each algorithm, the codes wrote, the tests performed, as well as the results obtained. This presentation for each algorithm is then concluded by a discussion of the results obtained, to validate the proposed algorithm against the defined design requirements. Chapter-8 outlines the conclusions and recommendations for future work.

1.9. Chapter summary

This chapter gave an overview of the project covered in this research. It outlined the research objectives, the problem that the research seeks to address, the questions that the research seeks to answer; as well as the methodology adopted in this research to achieve the intended goals. It also presented some important delineations of the research, the relevance of the research; as well as the layout of the rest of this thesis.

CHAPTER 2: SYSTEM DESCRIPTION AND MODELLING

2.1. Introduction

In this research, we are proposing to design the user-grouping system (UGS) and the power-allocation system (PAS), for a NOMA-based MBSS network. The UGA is in charge of deciding which users should be served by the same antenna for using NOMA protocol; and the PAS decides of the amount of power that should be assigned to each antenna as well as to each user within the antenna beam. The design goal of the UGA in this work is to ensure that the following conditions are satisfied: (a) all users grouped in same NOMA beam satisfy a minimum channel-gain margin; (b) all users grouped in same NOMA beam have highly correlated channel-vectors; (c) fair grouping is obtained between the different groups, in terms of groups' correlation coefficients. The design goal for the PAS is to maximize the network's fairness in terms of resource allocation. The intended network can be described as presented below.

2.2. System description

The mobile network under development can be described as follows:

- *Architecture:*

An Earth orbiting satellite is used to provide network coverage to mobile users distributed on the ground. In this scenario, the satellite in space acts as the access-point (AP) and the mobile users on the ground acts as user terminal. For simplicity, in this study, the satellite is assumed to be a GEO satellite so that the beam coverage on the ground are assumed to be static.

- *Antenna topology:*

The satellite is equipped with M -antennas pointing to the ground and forming M distinct beams on the earth's surface, while each user-terminal is equipped with a single antenna. Each satellite's antenna serves a designated group of users on the ground, while reusing the entire spectrum available. As such, each user is exposed to all the M -satellite's antennas, thus resulting in a many-to-one downlink architecture between the satellite and the user terminal; also known as MISO system. Subsequently, since the satellite serves multiple users simultaneously, the resulting network's downlink architecture is a multiple-MISO, often referred to as multi-user MIMO system (Panah & Yogeewaran, 2016:19; Rahayu et al., 2019:469; Ejaz et al., 2020:1).

- *Multiple-access technology:*

Power-domain NOMA, commonly referred to simply as NOMA, will be employed in this study; as opposed to traditional OMA used in 4G networks. By means of NOMA, each satellite

antenna will be serving 2-users simultaneously in its beam; forming what is known as a NOMA-beam or NOMA-group. In this study, the number of users per antenna's beam is limited to 2; because the complexity involved in the decoding process of a NOMA signal increases exponentially as the number of users per NOMA beam gets bigger (Aldababsa et al., 2018:3; Anwar et al., 2019:35; Trivedi et al., 2019:10). The proposed system will therefore result in a total of M NOMA-groups being served by the satellite; which implies a total of $2M$ users being served simultaneously.

- *Propagation medium:*

The satellite-to-ground link is a free-space channel which is commonly described by the Rician fading Model over multiple ranges of frequencies (Beigi & Soleymani, 2018:2; An et al., 2019:1507; Yan et al., 2019:63533). In this study, it will be assumed that the channel-state-information (CSI) of all users are available to the satellite; that is, the satellite has perfect knowledge of the channel vectors of all users.

Figure 2.1 below gives a geo-spatial illustration of the resulting NOMA-based MBSN. This network is basically a MU-MIMO network with NOMA technology and satellite component; and is a practical example of futuristic 5G networks.

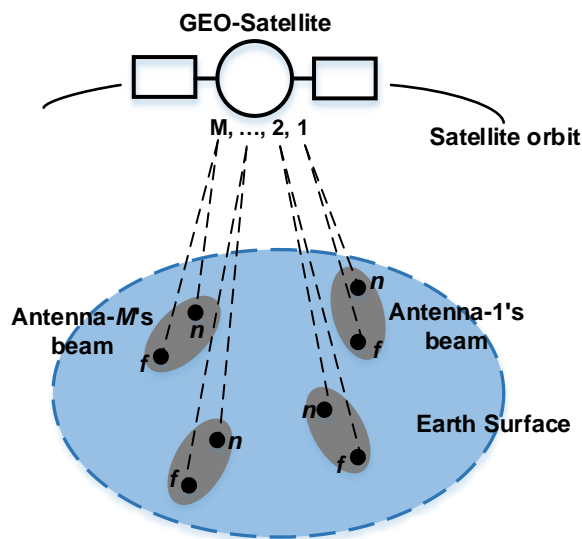


Figure 2.1: Geo-spatial illustration of a 2-users NOMA MBSN (adapted from Biyoghe & Balyan, 2021:247).

The network's design in this context implies the design of the multiple-access (MA) encoder of the network; which without loss of generality, comprises the fundamental blocks presented in Figure 1.2 above (Chistopoulos et al., 2015:4696; Wang et al., 2016:55).

2.3. Brief overview of PD-NOMA

In an orthogonal multiple access (OMA) technology of RANs, only one user is assigned a designated frequency band at a time. This is the case of the traditional multiple access (MA)

techniques such as time-division multiple access (TDMA) and frequency-division multiple access (FDMA) as well as the latest offset-FDMA (OFDMA) used in the 4G era (Botsinis et al., 2018: 47443; Wang et al., 2019:139173). The non-orthogonal multiple access (NOMA) is a new multiple-access technology of radio-access networks (RANs), in which more than 1 user are allowed to utilize the same frequency resources simultaneously (Wang et al., 2016:57; Ligwa & Balyan, 2022:621). In this format, the separation of information between the users sharing the same frequency resource is done either by assigning different power levels to users: power-domain NOMA (PD-NOMA); or by assigning different codes to users: code-domain NOMA (CD-NOMA) (Aldababsa et al., 2018:4; Balyan, 2021:273). Figure 2.2 below illustrates a comparison in power-domain between OMA and NOMA technologies.

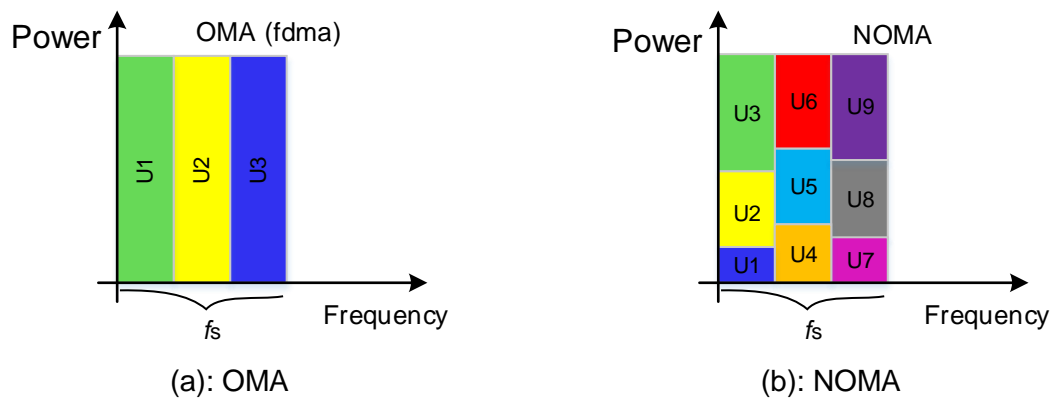


Figure 2.2: Illustration of PD-NOMA concept: OMA vs NOMA (adapted from Biyoghe & Balyan, 2020:370).

Figure 2.3 below gives a geo-spatial illustration a multi-users NOMA beam, with 3 users in the beam. During PD-NOMA implementation, all the beam's users must share the power allocated to the beam; thus, each user is assigned a portion of the beam's power. The portion of the beam's power allocated to each user is defined by the power-sharing coefficient (α) of that user. Beam's users with poorer channel conditions are given bigger shares of the beam's power; and users with better channel conditions are given smaller shares (Aldababsa et al., 2018:7; An et al., 2019:1106). Thus, the power-sharing coefficient of each user in the beam is inversely proportional to user's channel condition; and the sum of all power-sharing coefficients should be equal to 1 (Balyan, 2020:752; Ernest et al., 2020:18). The resulting transmitted signal is a superposition of multiple signals with same frequency; and thus the process is often known as superposition coding (Wang et al., 2016:57; Anwar et al., 2019:35). In the illustration below, it is assumed that $|h_3| < |h_2| < |h_1|$; which implies $\alpha_3 > \alpha_2 > \alpha_1$ and $\alpha_3 + \alpha_2 + \alpha_1 = 1$; where, $|h_3|$, $|h_2|$ and $|h_1|$ are the channel gains of user-3, user-2 and user-1 respectively, and α_3 , α_2 and α_1 their respective beam's power-sharing coefficient coefficients.

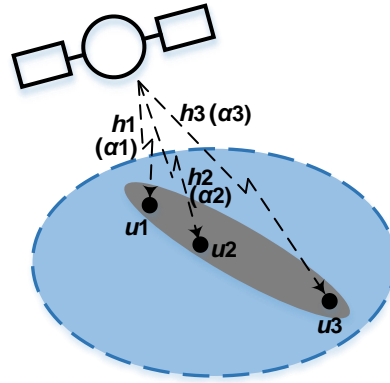


Figure 2.3: Geo-spatial illustration of a 3users-NOMA beam.

To decompose this signal at the receiver, the concept of successive interference cancellation (SIC) is employed (Wang et al., 2016:57; Anwar et al., 2019:35). In the SIC process, the user with highest power-sharing coefficient (i.e. worst channel condition) decomposes its signal directly because it sees others signals as noise; and the users with smaller power coefficients (i.e. better channel conditions) must first decompose stronger signals before decoding their own (Saito et al., 2013:612; Caus et al., 2016:512).

By virtue of serving two or more users simultaneously within the same frequency slot, NOMA provides the following advantages over OMA:

- It increases the spectral efficiency of the network, compared OMA, and thus resulting increased system's throughput (Yan et al., 2019:63532; Daniels & Balyan, 2022:15; Kumar & Kumar, 2020:11).
- It increases the system's fairness; as it continuously serves and guaranties minimum QoS to both users with poor and good channel (Islam et al., 2017:728; Yan et al., 2018:978).
- It increases the system's latency, as users are served more frequently, which implies shorted waiting time compared to OMA system (Dai et al., 2015:76; Dai et al., 2018:2298).

While it has not been employed for 4G networks up until now, NOMA technology is considered one of the pioneers' technologies of 5G networks development (Wan et al., 2018:109; Kumar & Kumar, 2020:12). However, it is to be noted that, while NOMA provides better system performances that OMA in most aspects, the complexity induced by the implementation of the SIC constitutes a considerable concern of the NOMA technology (Anwar et al., 2019:35; Trivedi et al., 2019:10).

It is to be noted that, in this work, we focus on the case of 2users per NOMA-group, as illustrated in Figure 2.1 above; and the illustration with 3users-per beam was just to give a better description of the NOMA protocol.

2.4. User's channel-vector modelling

The block diagram in above shows that, in order to implement other subsystems of the MA Encoder, including, the users-scheduling, users-grouping, precoding, and power-allocation subsystems, it is necessary to have knowledge of users' CSI (also known as users' channel vectors). Thus, the CSI-acquisition system is the first block in the chain. Note that, in this work as it is common practice in the field, we will assume that the acquisition of the CSI has been performed and all user's channel vectors are available to the satellite. Therefore, the design of the users' CSI-acquisition system is outside the scope of this work. However, for ease of reference, we opt to give an overview of how users' CSI are often estimated in mobile networks, by means of analytical methods known as user's channel-vector modelling. Figure 2.4 below outlines the block under discussion in this section.

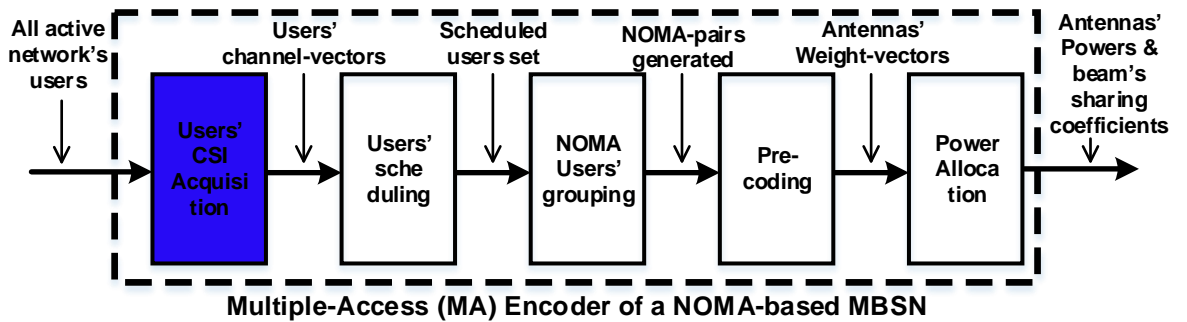


Figure 2.4: User's channel-vector estimation block in the MA-encoder.

The CSI of users in a mobile network are commonly estimated through pilot measurement (Yand & Choi, 2013:4; Panah & Yogeewaran, 2016:19; Ali et al., 2017:756). However, in some cases where the propagation environment is well characterised, and the setup does not lead to complex mathematical computations, users' channel vectors can also be estimated by means of analytical models. The modelling process of a user's channel vector in the mobile network can be presented as follows.

2.4.1. modelling of user's channel-coefficients

The propagation environment between a transmit-antenna and a receive-antenna is often characterised by a channel coefficient, commonly noted (h), which describes the channel condition of this link. Due to the complex-exponential nature of the signal propagating through the wireless channel between a transmit-antenna and a receive-antenna, the channel coefficient (h) is described as a complex-exponential coefficient:

$$h = |h|e^{j\theta} \quad (2-1)$$

where, " $|h|$ " is the channel-amplitude (or voltage-gain), and describes the voltage-drop of the transmitted signal throughout the propagation medium; while " θ " is the channel-phase, and

describes the phase-shift suffered by transmitted signal through the channel (Goldsmith, 2004:29).

The electromagnetic propagation environment can be seen as an electronic system where the transmit-antenna is the input port and the receive-antenna is the output port. The analysis of RF-signal transfer through electronic circuits is generally done in power-domain, and not in voltage-domain. Thus, the analysis of the channel being traversed by RF-signals is best done in power-domain. The power-gain of an electronic circuit is the square of the voltage-gain; which means that the channel's power-gain is the square of the channel's voltage gain. Therefore, with P_{rx} and P_{tx} referring to transmit and receive power respectively, it can be written that:

$$\frac{P_{rx}}{P_{tx}} = \left(\frac{V_{rx}}{V_{tx}} \right)^2 = |h|^2, \text{ and} \quad (2-2)$$

$$|h| = \sqrt{P_{rx}/P_{tx}} \quad (2-3)$$

Subsequently, the channel-coefficient can be expressed in terms of the power-gain as:

$$h = \sqrt{P_{rx}/P_{tx}} e^{j\theta} \quad (2-4)$$

Thus, the estimation of channel gain “|h|” is achieved by first estimating the channel-power gain (P_{rx}/P_{tx}) and then take the square-root of it.

Consequently, the modelling of the channel coefficient (h) between a transmit- and receive-antenna, simply implies modelling the channel's power-gain ($P_{rx}/P_{tx} = |h|^2$) and channel-phase (θ). Table 2.1 below summarises common configurations of the propagation channel between a transmit- and receive- antenna (Parsons, 2000:114; Patzold, 2002:4; Reddy & Chakravarthula, 2017:21).

Table 2.1: Basic Classification of the Tx-Rx propagation link in terms of signal paths.

Families	Description/ Configuration (LoS = Line-of-sight)	Common characterisation	Implication/ Meaning
Non-Multipath Fading	1. No LoS + No Multipath	Non-conductive channel	Signal totally blocked
	2. LoS + No Multipath	Free-space channel	Strong signal received
Multipath Fading	1. No LoS + Multipath	Rayleigh model channel	Weak signal received with possible fluctuations
	2. LoS + Multipath	Rician model channel	Strong signal received with possible fluctuations

The modelling of the channel power-gain and channel-phase are done using different procedures; but are both strongly dependent on the type propagation environment, as discussed in the following sections.

2.4.1.1. Channel's power-gain modelling

The power-gain of a wireless channel is commonly characterised by three independent components, namely, the path-loss (PL), the shadow (shad) or slow-fading (SF), and the multipath fading (MPF) or fast-fading (FF); and can be described as (Goldsmith, 2004:47; Neira et al., 2011:130; Yan et al., 2018:31328):

$$|h|^2 \text{ (dB)} = PL(\text{dB}) + Shad(\text{dB}) + MPF(\text{dB}) \quad (2-5)$$

Each of these three components can be described as follows.

A. *Path-loss:*

The path-loss describes the power loss in the transmitted signal due to distance travelled away from transmitter; and is often referred to as “distanced based power-loss”. It constitutes the main component of the channel's power-gain, and is commonly characterised using Friis-equation as (Fenech et al., 2012:993; Chistopoulos et al., 2015:4698; Habib & Moh, 2019:8):

$$PL(\text{dec}) = \frac{P_{rx}}{P_{tx}} = G_{tx} G_{rx} \left(\frac{\lambda_c}{4\pi D} \right)^2 \quad (2-6)$$

$$PL(\text{dB}) = 10\log(G_{tx}) + 10\log(G_{rx}) + 20\log(\lambda_c) - 20\log(D) - 20\log(4\pi) \quad (2-7)$$

Where, “dec” is short for “decimal scale”, G_{tx} is the transmit-antenna gain, G_{rx} the receive-antenna gain, λ_c is the signal's wavelength in free-space (in *meters*), and D is the line-of-sight distance between the two antennas (in *meters*).

B. *shadow (or SF):*

The shadow describes the power attenuation on the transmit signal caused by possible obstructing elements that the signal traverses during its propagation toward the receiver. This component causes the signal's power-loss (and subsequently the channel's power-gain) to fluctuate relatively slowly about its main component which is the path-loss (Comisso, 2008:27; Neira et al., 2011:130). The most common model for shadowing in wireless communication environment is the “*log-normal shadowing*”, in which the shadowing (or attenuation) follows a log-normal distribution expressed below (in dB), with mean (μ) and variance σ^2 ; where σ is the max deviation (Goldsmith, 2004:44).

$$p(x) = \frac{1}{\sqrt{2\pi}\sigma} \exp\left(-\frac{(x - \mu)^2}{2\sigma^2}\right) \quad (2-8)$$

C. *multipath fading (or FF):*

the multipath-fading describes the fluctuation on the received signal's power due to combination of various arriving components of the transmitted signal emanating from the

different reflected/ or refracted paths. This component causes a fast fluctuation of the channel's power-gain about the path-loss (Comisso, 2008:22; Neira et al., 2011:130). The modelling of MPF component is strongly dependent on the type of propagation environment at hand. Thus, in a propagation environment which is assumed to have multiple paths with no strong LoS path (case of terrestrial urban environment), the Rayleigh fading model is the most commonly used method for describing MPF of the environment (Zhu et al., 2018:983; Wang et al., 2019:139177; Ernest et al., 2020:5). And the pdf of the channel-gain $|h|$ is expressed as (Comisso, 2008:24; Mahmood et al., 2015:3):

$$\rho(x) = \frac{x}{\sigma^2} \exp\left(-\frac{x^2}{2\sigma^2}\right), x \geq 0 \quad (2-9)$$

Where, σ^2 is the variance of the Rayleigh channel. Similarly, in a propagation environment which is assumed to have multiple paths with a strong LoS path (case of satellite environment), the Rician fading model is the most commonly used method for describing MPF of the environment (An et al., 2019:1106; Yan et al., 2020:8818). And the pdf of the channel gain $|h|$ is expressed as: (An et al., 2019:1507; Zhang et al., 2019:172323):

$$\rho(x) = \frac{x}{\sigma^2} \exp\left(-\frac{x^2 + r^2}{2\sigma^2}\right) I_0\left(\frac{xr}{\sigma^2}\right), x \geq 0 \quad (2-10)$$

Where, “ r ” is the rice-factor, “ I_0 ” and is the modified Bessel function of the first kind and zero-order, and σ^2 is the variance of the Rician channel.

In sum, by means of the selected model for the *PL*, *Shad* and the MPF, the channel's power-gain $|h|^2$ between a transmit-antenna and a receive-antenna can be estimated as in equation (2-5) above; and the channel gain $|h|$ can then be derived. In this particular study where the environment is the satellite-to-ground link, the above outline models, including, the Friis equation, log-normal distribution and the Rician distribution, will be used to describe the *PL*, *Shad* and the MPF respectively.

2.4.1.2. Channel-phase modelling

The phase-offset of the propagation channel is critically dependent on the geometries of the communication link between the transmit and receive antennas. Thus, the modelling of the channel's phase-offset is really specific to a given antenna-to-antenna geometrical setup (Tse & Viswanath, 2005:297; Neira et al., 2011:1230; Chistopoulos et al., 2015:4698).

For example, when the environment is described using the Rayleigh fading model, it is assumed that there is no strong line-of-sight path between the transmit and receive antennas,

but only multipath components. In such a case, it will be a highly complex task to try to derive the model of the channel phase-offset, due to multiple components arriving at different phase offsets.

However, in a free-space environment, or a Rician modelled environment, it is assumed that there is a strong line-of-sight (LoS) path between the transmit and receive antennas, and weak multipath components. In such a case, the angle-of-arrival (AoA) of the strong LoS path together with the antennas geometrics, could be used to produce an estimate of the channel phase-offset, with reduced complexity (Tse & Viswanath, 2005:297; Neira et al., 2011:130; Chistopoulos et al., 2015:4698).

2.4.1.3. Summary on channel-coefficient modelling

In sum, an estimate of the channel-coefficient (h) for a propagation link between a transmit and receive antenna is generated as in Equation (2-1) above, after obtaining estimates of the channel's gain " $|h|$ " and phase-offset " θ ". Generally, the channel-gain " $|h|$ " is derived from the channel's power-gain " $|h|^2$ ", which can be estimated as in Equation (2-5), by using selected models for the *PL*, Shadow and MPF presented in Equations (2-6), (2-8), and (2-10) respectively. The channel phase-offset " θ " however, is geometric specific, and strongly depends on both the antenna setup as well as the link's geometrics. Thus, it is quite complex to characterise; and its modelling may require the designer to derive a quite detailed geometrical layout of the link.

2.4.2. Modelling of user's channel vector in a MBSN link

The MBSN is a MU-MIMO system in which the satellite is equipped with multiple antennas (i.e. M -antennas) and the user terminals are equipped with 1 antenna. Figure 2.5 below illustrates the link between a satellite with M -antennas and different user-terminals (u, v, \dots, z) with a single antenna each. As shown on the diagram, there exists a channel coefficient between the user's antenna and each of the respective satellite's antennas. Subsequently, the CSI between the user " u " and the satellite can be expressed as a vector, (commonly called user's channel-vector " h_u "); which consists of all the channel-coefficients between the user's antenna and the respective satellite's antennas:

$$h_u = \begin{bmatrix} h_{u1} \\ h_{u2} \\ \dots \\ h_{uM} \end{bmatrix} \quad (2-11)$$

Where, " h_{uM} " is the channel-coefficient between the user's antenna and the M^{th} satellite's antenna.

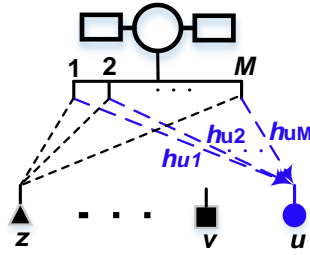


Figure 2.5: Illustration of the channel link between satellite and user in a MBSN.

In essence, each channel-coefficient (h_{uM}) in the channel vector (h_u) must be estimated as discussed in the section “*channel-coefficient modelling*” above. However, performing modelling of each coefficient independently can yield a tedious process. Therefore, to render the modelling process of the user’s channel-vector less hectic, some simplifications are often performed based on common assumptions, as follows.

- ***Assumption 1: the gains of all the channel-coefficients of a designated user (u) are relatively equal.***

Due to extremely high distance between satellite antennas and user terminal antenna, the distance between each satellite antenna and the user antenna is approximately the same. Consequently, it is common assumption that, the path-loss will be the same; and the channel gains of each coefficient will be approximately the same. However, there will be slight fluctuation between these channel gains of respective antenna’s coefficients due channel fading (Zhu et al., 2017:2261; Zhu et al., 2019:206).

- ***Assumption 2: the phase-angles of all the channel-coefficients of a designated user (u) will be relatively equal:***

Again, due to extremely high distance between satellite antennas and user’s antenna, the angle-of-arrival of the main line-of-sight signal path at respective satellite’s antennas, from a designated user, will be similar (Neira et al., 2011:130; Chistopoulos et al., 2015:4698).

Consequently, it results that, in the satellite-to-earth link, all the channel-coefficients forming the channel-vector of a given user (u) will be relatively equal; with possible small variations between them due to channel fading.

This means that, for each user terminal (u), an estimate of the user’s channel-vector will be derived as follows. In terms of phase-offset, the phase-offset of one channel-coefficient will first be estimated; that is, the phase-offset between the user’s antenna and one of the satellite’s antennas. Then, the same channel phase-offset will be used for all the other satellite’s antennas. In term of the channel-gain, the gain of one channel-coefficient will first be estimated according to the channel-gain modelling process outlined above. Then, this channel gain will be attributed to all the other coefficients; with possible small variation to mimic fluctuations on the channel due to MPF. Thereafter, from the channel-gain and phase-offset of each

coefficient, the channel-coefficient will be generated; and all the channel-coefficients will be listed together to form the user's channel-vector as in equation (2-11) above.

2.4.3. The Hermitian of a channel-vector

Denoted $[-]^H$, the Hermitian of a channel-vector is the transpose of a channel-vector when the vector consists of complex channel-coefficients. When the channel-coefficients are all real, then the Hermitian operation is simply a transpose, and the transposed of the channel-vector is denoted $[-]^T$.

2.4.4. Summary on user's channel-vector estimation

The estimation of users' CSI via analytical models is a quite complex exercise which often requires lots of environment's specifics assumptions, as well as lots of details on both antennas and links' geometries. For the purpose of conceptual design and quick proof-of-concept during mobile networks' designs, the models-based user's channel-vector estimation is often used. However, in practice, the acquisition of user's channel-vector is commonly achieved through pilot-measurement. In this work, similar to other popular studies on NOMA based MBSS design, it will be assumed that the CSI of all users are available at the satellite at the time of operation, for usage by other blocks of the MA encoder, such as USS, UGS, PCS and PAS.

2.5. Users' scheduling

The users' scheduling is another subsystem of the MA-encoder of mobile networks, as highlighted in Figure 2.6 below.

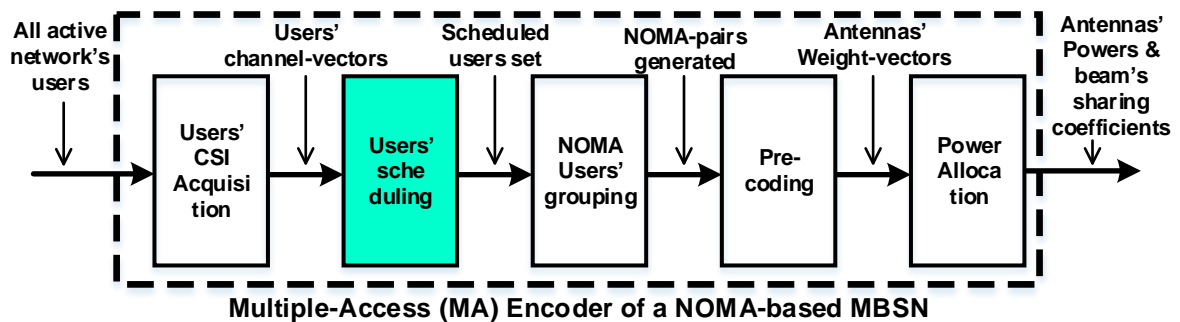


Figure 2.6: User's scheduling block in the MA-encoder.

Without loss of generality, in the MA encoder of a mobile network, the users' scheduling block is responsible amongst other things, for deciding which users should be given access to network resources at a given time of service. The user's scheduling is often designed to achieve the following goals:

- a. *Fair access for all users*: to ensure that some users are not ignored by network for too long;

- b. *System's Capacity maximization*: to ensure that, only users with good channel conditions are mostly considered by network;
- c. *Trade-off between the two above*: to ensure a middle-point between fair access to all users and system's capacity maximization.

Amongst other parameters, the users' channel-conditions and queuing-time are commonly considered parameters when performing users scheduling.

Various different concepts have been proposed to date for implementing users' scheduling in mobile networks. Random scheduling is the most concept for users' scheduling and is widely employed in mobile network's design (Shah & Shin, 2012:128; Jamali & Ghiasian, 2019:138). However, additional concepts are proposed from existing literature. For example, authors in (Saito et al., 2013:612) and (Ramirez & Mosquera, 2020:8813) proposed a proportional-fair scheduling (PFS) concept. Also, Guidotti & Coralli (2018:2) implemented a geographical-users scheduling (GUS) concept. Furthermore, Chistopoulos et al. (2015:4702) proposed a custom user scheduling technique.

The design of the users scheduling system is outside the scope of this research. Therefore, we assume in this work that, the user scheduling has been performed and that the $2M$ users to be served by the satellite, at a given time slot have been selected. As such, we will not discuss user scheduling in further details. However, for the sake of demonstration our work later, we consider in this study the random scheduling concept.

2.6. Important terminology and notations

The following terminology will be used extensively in this text:

Antenna group or beam: represents a group of users served by same antenna using NOMA technology. Each antenna will form a beam that covers its intended users.

Beam's notation: " b " will represent the antenna's number within the antenna set; or simply the beam's number. Since there are M -satellite antennas, therefore $b = 1, 2, \dots, M$.

NOMA group size: number of users served by same antenna (i.e. under same beam). In this application it has been specified to 2.

Near-field versus far-field beam's users: as indicated earlier, an effective implementation of PD-NOMA technology requires that users in same NOMA group shall have distinct channel conditions. Therefore, amongst the 2 users in each antenna group, the one with a better channel conditions will be noted as "*near-field user*" and the other one will be "*far-field user*".

User's Channel vector: refers to the channel conditions or CSI of each user in the network.

Beam's power: will refer to the transmit power allocated to the associated antenna for a particular beam.

Beam's weight vector: refers to the precoding-weight vector associated with each satellite's antenna, for ICI mitigation at transmission.

The following notations will be used extensively in the models presented in this document:

Table 2.2: List of common notations in this document and their meaning.

Notation	Description
b	Beam's number (Satellite antenna number), $1 \leq b \leq M$
P_b	Power allocated to beam "b" (i.e. to antenna "b")
W_b	Precoding weight-vector associated with beam "b" (i.e. antenna "b")
h_u	User's channel vector
h_u^H	Hermitian of the user's channel vector
$\ h_u\ , \Omega$	Respectively, the Norm and the phase of the channel-vector.
2	Number of users per antenna beam for NOMA.
h_{nb}	channel vector of the "near-user" in beam "b"
h_{fb}	channel vector of the "far-user" in beam "b"; $\ h_{nb}\ > \ h_{fb}\ $
α_b	Power-sharing coefficient in each beam "b" for NOMA implementation.

2.7. Chapter summary

This chapter provided a description of the system under design; in this case, a multi-beams satellite network which employs PD-NOMA and MIMO technologies. It also gave a brief overview of PD-NOMA and MIMO technologies, respectively. Furthermore, it gave an overview of the users' CSI (channel-vectors) acquisition process in a MIMO network; which is a very crucial stage, since the users' scheduling, grouping, precoding and power allocation processes, all depend on the user's channel-vectors.

CHAPTER 3: NOMA USERS' GROUPING SYSTEM DESIGN

3.1. Introduction

In this chapter, we propose a novel Users-Grouping Algorithm (UGA) for a 2-users NOMA based Multi-Beam Satellite Network. This work falls within the design of the Users' Grouping Subsystem (UGS) of the network's MA-Encoder, as illustrated in Figure 3.1 below.

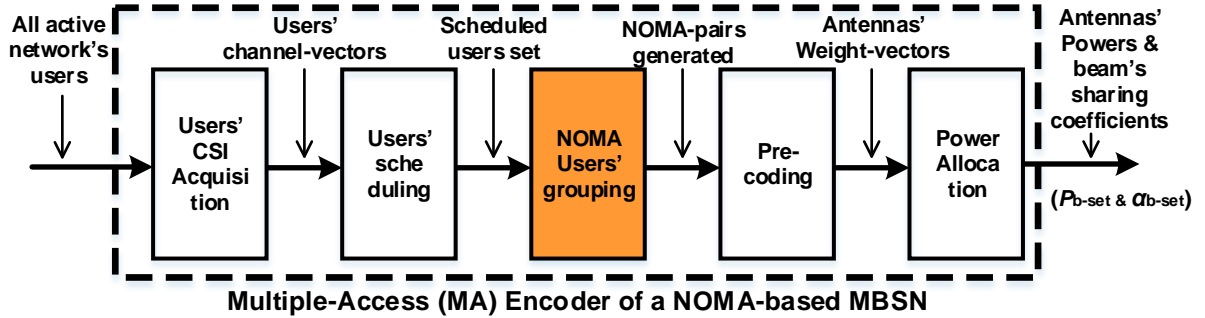


Figure 3.1: The NOMA Users' Grouping System (UGS) in the MA-Encoder block.

The role of the UGS can briefly be explained as follows. In the traditional Orthogonal Multiple-Access (OMA)-based networks used up to 4G, each antenna of the access-point only serves one user per designated sub-frequency band. Therefore, if the access point is equipped with M -antennas, M -users will be scheduled in a given time frame, and each antenna will serve one user alone. However, in a NOMA-based multicast mobile networks, each antenna of the access-point serves 2 or more users simultaneously per designated sub-frequency band, by means of NOMA protocol. When the number of users per antenna is 2, the system is called a 2-users NOMA. With M -antennas at the access-point, a total of $2M$ -users will be scheduled to be served in a particular time frame. Within this population of $2M$ -users that are to be served in a NOMA-based network, a decision of the users set that should be served by the same antenna must be made; that is known as users-grouping, and is achieved by the users grouping system. In the case of a 2-users-NOMA system, the grouping process is simply referred to as users-pairing, and the output of the UGS is a set of M -pairs of users that should be served together by means of NOMA.

As indicated earlier in section-1.1.2, when developing a users' pairing algorithm for a 5G mobile network, which employs NOMA and MIMO technologies simultaneously, there are three fundamental requirements that the algorithm must satisfy. These include, to ensure that:

- d) In all the pairs, a minimum channel gain margin between the group's users is satisfied;
- e) In all the pairs, a minimum channel-correlation between the group's users is satisfied;

- f) Fairness amongst the generated pairs is preserved with respect to channel-correlation of each group.

From the survey of existing *UGA* design works presented in section-1.1.2 above, it appears that, no work has managed to address all three requirements simultaneously. Therefore, this work proposes a user-grouping algorithm for 2users NOMA-based satellite network, which seeks to satisfy all 3 requirements above; and thus, improve the network's fairness.

The rest of this chapter presents the design process for the proposed *UGA*. In order to carry out the design of our proposed *UGA*, the system's description, assumptions and specifications to be considered were presented in Chapter-2.

3.2. Modelling of Channel-Correlation and Channel gain-margin between users

In this application, two users need to be paired for each antenna, based on the requirements (a), (b) and (c) outlined above. Therefore, the output parameters of the user-grouping system under design include the channel-correlations and channel gain-margin between users of each antenna group; and the input parameters include the number of antennas (i.e. number of pairs to generate) as well as the users' channel-vectors. A mathematical model which links these two sets of parameters can be derived as presented below. To develop these models, we consider the system's description and specifications made in section 2.2 which indicated that:

- the number of antennas on the satellite is M ;
- The number of users per antenna group (i.e. beam) is 2;
- The channel vector of all users are known.

The model of the channel correlation between the two users can be derived as follows. With h_1 and h_2 being the complex channel-vectors of user1 and user2 respectively, the channel-correlation (chx_corr) between the two users is the inner product of the two channel-vectors, and can be expressed as (Joyce, 2015:1):

$$chx_corr(u_1, u_2) = h_1 \circ h_2 = h_1^H \times h_2 = \|h_1\| \times \|h_2\| \times e^{j(\Omega_2 - \Omega_1)} \quad (3-1)$$

Where, $\|h_1\|$ and $\|h_2\|$ are the norms of user1 and user2's channel-vectors respectively; and Ω_1 and Ω_2 are their phase-offsets. The channel-correlation factor (chx_corr_fac) describes the angular difference the two vectors, is expressed as $e^{j(\Omega_2 - \Omega_1)}$; and can be derived from the channel-vectors' correlation as:

$$chx_corr_fac(u_1, u_2) = e^{j(\Omega_2 - \Omega_1)} = \frac{h_1^H \times h_2}{\|h_1\| \times \|h_2\|} \quad (3-2)$$

The correlation-factor is a complex number $e^{j(\Omega_2 - \Omega_1)} = \cos(\Omega_2 - \Omega_1) + j\sin(\Omega_2 - \Omega_1)$, when the channel vectors are complex. However, the meaningful information desired can be obtained

from its real-part alone. Therefore, the channel-correlation-coefficient (chx_corr_coef) is the real-part of the correlation-factor, and gives an accurate estimation of the angular difference between the two vectors. It is expressed as:

$$chx_corr_coef(u_1, u_2) = \cos(\Omega_2 - \Omega_1) = Real\left(\frac{h_1^H \times h_2}{\|h_1\| \times \|h_2\|}\right) \quad (3-3)$$

From this model, it can be seen that, when the angle between the two vectors is very small (i.e. tends to 0), the correlation-coefficient is maximum (i.e. tends to 1); and the two users are said to have highly correlated channels. Oppositely, when the angle between the two vectors is wide (i.e. tends to 90), the correlation-coefficient is minimum (i.e. tends to 0); and the two users are said to have uncorrelated or orthogonal channels.

The model of the channel-gain margin between the two users can be derived as follows. To compare the channel gains of user1 and user2, this is usually done by calculating the gain-margin between the two channel gains $|h_1|$ and $|h_2|$. The channel-gain margin is generally expressed as the difference between the two channel-gains; hence the term channel-gains margin (C_{gm}), as shown in equation-(3-4) below. Alternatively, it is also often expressed in form of a ratio between the two channel-gains; hence the term channel-gain ratio (C_{gr}), as shown in equation-(3-5) below.

$$C_{gm} = |h_1| - |h_2| \quad (3-4)$$

$$C_{gr} = \frac{|h_1|}{|h_2|} \quad (3-5)$$

If $|h_1| \geq |h_2|$, $C_{gm} \geq 0$ and $C_{gr} \geq 1$; and if $|h_1| \leq |h_2|$, $C_{gm} \leq 0$ and $C_{gr} \leq 1$. In this application, we prefer to work with a positive C_g ; thus, we will always consider the user with the bigger channel gain to be h_1 and the user with the smaller channel gain to be h_2 .

Considering that the satellite is equipped with M -antennas, and that each antenna is serving a pair of users, the user-grouping algorithm is supposed to results into M -pairs; with each pair consisting of a user with bigger channel gain (h_1) and a user with smaller channel gain (h_2). As it will be explained in the next section below, according to most UGAs for 2-users NOMA systems, in each beam (b), ($b \in M$), the user with the bigger channel gain is usually called *near-user* of the beam, and its channel-vector is noted (h_{bn}); and the one with smaller channel-gain is called *far-user* of the beam, and its channel-vector is noted (h_{bf}). Therefore, the channel-correlation coefficient and channel-gain margin in each beam (b), ($b \in M$), will be:

$$chx_corr_coef(b) = C_3(NU_b, FU_b) = Real \left(\frac{h_{bn}^H \times h_{bf}}{\|h_{bn}\| \times \|h_{bf}\|} \right) \quad (3-6)$$

$$C_{gm}(b) = C_{gm}(NU_b, FU_b) = |h_{bn}| - |h_{bf}| \quad (3-7)$$

$$C_{gr}(b) = C_{gr}(NU_b, FU_b) = \frac{|h_{bn}|}{|h_{bf}|} \quad (3-8)$$

Where, “ b ” represents the beam number in the set from 1 to M ; NU is the *near-user*, FU is the *far-users*, and C_3 stands for “ chx_corr_coef ”.

3.3. UGA’s Design Concept

To achieve a successful grouping of all users in a 2-users NOMA system, a widely used concept is a two-stage grouping process, which includes:

- Stage1: first split the $2M$ users into 2 sets of M -far-users and M -near-users, based on their channel-gains;
- Stage2: then, formulate pairs of far-near users, based on channel-correlation coefficients between far users and near users.

This concept has been employed by most studies that presented a UGA for 2-users NOMA system; including Caus et al., (2016:500); Vazquez et al., (2016:91); Zhu et al., (2017:2258); Lin et al., (2019:661); Zhu et al., (2019:1). Therefore, in this work, we opt to design our algorithm based on this concept. However, our implementation of this concept, which constitutes our proposed algorithm to achieve desired goal, will differ from others’ implementations.

To group $2M$ users into M -pairs, and obtain an outcome (set of pairs) which satisfies all three requirements (a), (b) and (c) outlined in section-3.2 above, can indeed be a highly complex grouping exercise to fulfil; as there is no direct mathematical link between the three parameters. Thus, to fulfil the task with reduced complexity, we propose to implement the concept enounced above in the following sequence of steps, which constitute the design steps for our proposed UGA:

- Step 1: *Split the $2M$ users set into a set of M -near and M -far users, based on the users’ channel gains.*
- Step 2: *Formulate the pairing problem as a channel-correlation maximization bipartite matching-problem (BPMP).*
- Step 3: *Introduce the “fair-pairing requirement” into step2 above; and address the resulting BPMP by means of the Hungarian-Method (HM), to meet both the “channel-correlation maximization” and “fair-pairing” requirements.*
- Step 4: *Introduce the “minimum gain-margin requirement” into the BPMP formulated in “step3”, to yield a “restricted BPMP”; and solve it by means of Restricted-HM.*

- Step 5: *Introduce “iteration” of step 4 above*; and adjust the “minimum gain-margin” initially defined, until perfect matching is obtained.

The “perfect-matching solution” resulting from the restricted Hungarian Method (step 4) ensures that, the obtained pairs satisfy the minimum channel-gain margin, the high channel-correlation, as well as fair-pairing with-respect-to pairs’ correlation coefficients. Each of the above outlined steps is discussed in the following section.

3.4. UGA’s Design discussion

The design steps outlined above our proposed UGA can be further discussed as follows.

3.4.1. Step 1: splitting the $2M$ -users into 2 subsets of M -users:

The channel state information acquisition block of the MA -Encoder ensures that the channel-vectors of all users in the network are known to the access-point (in this case the satellite) at all times. By means of the user-scheduling system, the $2M$ -users to be served by the satellite at a given time are selected. Therefore, the user-grouping system, receives the channel-vectors of the designated $2M$ -users. From the channel-vectors of the $2M$ -users, their respective channel-gains are calculated, by simply computing the norm the channel-vector. Thereafter, the resulting channel-gains of the $2M$ -users are ranked in an increasing order; and the M -users with the highest channel-gains are put together to form what is noted as the “*near-users set (NUs-set)*”. The remaining M -users with lower channel gains are also put together to form the “*far-users set (FUs-set)*”.

3.4.2. Step 2: formulate the user-pairing problem as a bipartite matching problem:

After obtaining the far-users and near-users sets, the aim is to formulate pairs consisting of a user from the FU -set and a user from the NU -set, with high channel-correlation. This becomes a pairing problem, which is a special case of matching problems. Since both sets consist of M -users, that is, they are of equal size; and a user from one set can only be matched to a unique user in the other set, this pairing problem becomes a bipartite matching problem (BPMP) or a bipartite graph (Han et al., 2017:11; Zhu et al., 2019:206).

A few different techniques can be used to solve BPMPs and yield a desired set of pairs, but the outcome is generally influenced by the conditions set. Ideally, if no conditions or restrictions is put between some users of NU -set and FU -set, the pairing process should yield a maximum matching of M -pairs. That is known as *perfect-matching* or *stable matching*, and indicates that the $BPMP$ has a solution (Chowdhury, 2019:13). Figure 3.2 (b) below illustrates this scenario with the case of four users per set; i.e. $M = 4$. However, if some restrictions are put between users, the pairing process could result in a certain number of maximum matching pairs which is less than M . This will mean that some users have not been matched. That is known as

incomplete or *imperfect matching*; and indicates that the *BPMP* has no solution (Salvatore, 2008:6). This scenario is illustrated in Figure 3.2 (a) below, again with the case of four users per set (i.e. $M = 4$).

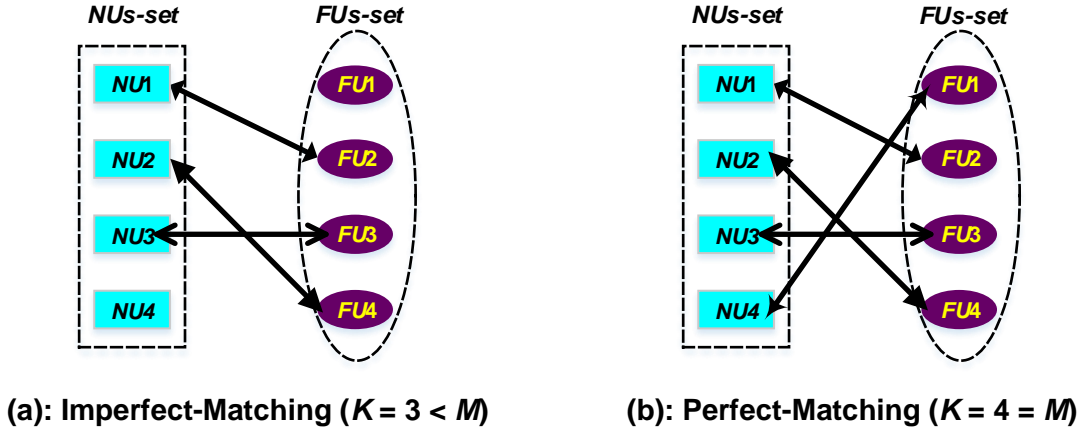


Figure 3.2: Illustrations of outcomes to the BPMP:
(a) maximum matching, (b) perfect matching

3.4.3. Step 3: Introduce the *fair-pairing* requirement into the BPMP in step2 and use the Hungarian Method to solve the problem.

If the formulated channel-correlation maximization's *BPMP* is solved using any arbitrary technique, we could result in a set of M -pairs in which some pairs have excellent channel correlation-coefficients, while others have extremely poor ones. But, such a situation is not acceptable in this application. Because, one of the design requirements for this algorithm is to ensure high fairness between the resulting pairs, in terms of their respective channel correlation-coefficients; that is, to avoid having some pairs with extremely high correlations, while others have extremely poor correlations (i.e. requirement "c"). For example, If the pairing process is performed as in Lin et al., (2019:661) and Zhu et al., 2019:3, where users with the highest channel correlation are grouped together first, remaining users with poorer correlation will have to be grouped together; resulting in an unfair pairing; which does not satisfy requirement (c). Therefore, we opt to employ the Hungarian-Method (*HM*) to solve the formulated *BPMB*, and so to to achieve this high fairness. The Hungarian-Method is a widely used technique for providing optimal solutions to "maximization-*BPMP*" (or bipartite graph), while simultaneously ensuring fairness amongst the resulting pairs (Zeng et al., 2013:221; Rusdiana et al., 2019:25). As such, employing the *HM* will minimize possibility of having cases where some pairs have extremely good channel-correlation while others are having extremely poor channel-correlations; which satisfies the fair-pairing requirement (c).

To solve our channel-correlation maximization's *BPMB* using the *HM*, we generate a Hungarian-matrix by calculating the channel-correlation coefficients (*chx_corr_coef* or C_3) between each near-user and each far-user, as illustrated in Table 3.1: Illustration of square

matrix of near-far users channel-correlation coefficients Table 3.1 below. These chx_corr_coefs (C_3) are calculated using equation-(3-6) above. Once the matrix is generated, the HM can then be executed. As indicated earlier, the correlation coefficient between two channel-vectors is basically a cosine function of the angular difference between the two vectors; which means that, it can go from -1 to +1. In this application, it is assumed that the satellite is employing pointing antennas to formulate beams on the ground. Therefore, only users whose channel vectors are in the same positive direction should be considered for grouping. This means that, all channel-correlation coefficients that are negative should be discarded automatically.

Table 3.1: Illustration of square matrix of near-far users channel-correlation coefficients

	NU_1	NU_2	...	NU_M
FU_1	$C_3(NU_1, FU_1)$	$C_3(NU_M, FU_1)$
FU_2		
...	
FU_M	$C_3(NU_1, FU_M)$...	$C_3(NU_M, FU_M)$

3.4.4. Step 4: Introduce the *minimum channel-gain margin* requirement into the BPMB to yield a restricted BPMB and solve it using restricted-HM

The employment of the *HM* in step3 above ensures that a pairing outcome which satisfies the requirement (a) and (c) is obtained. However, under the setup described in step1, there is a risk of having pairs from step3, in which users do not satisfy an acceptable channel-gain margin necessary for a successful implementation of NOMA protocol. Figure 3.3 below illustrates this possible scenario which can be explained as follows. By separating the $2M$ -users into a set of M -near and M -far users based on their respective channel-gains, we could possibly run into a scenario where the highest channel-gains in the *far-users set* and the lowest channel-gains in the *nears-user set* are very close. This is the case with *near-user-4* and *far-user1*, in the bubbled-illustration in Figure 3.3 below. In this scenario, if this *near-user4* and *far-user1* from this border-region have a relatively high channel-correlation, they could end-up being paired. Consequently, this resulting pair will not be able to successfully implement NOMA, because the two users do not have distinct channel-gains. This is the limitation identified in the users' grouping work proposed by Zhu et al., (2017:2258), which only satisfies requirement (a) & (c).

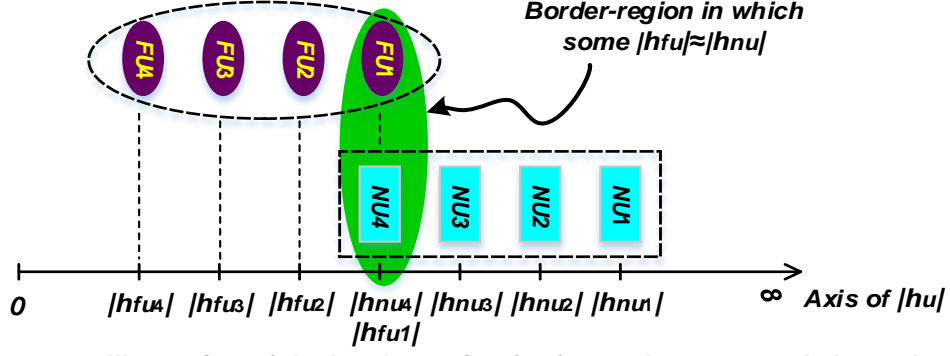


Figure 3.3: Illustration of the border region for far- and near- users' channel-gains.

Therefore, in order to avoid the above described situation, we introduce the need for a minimum channel-gain ratio C_{gr_min} that should be satisfied between far- and near-users, in order for them to be considered for pairing. This is the minimum channel-gain margin requirement (i.e. requirement-b); which can be described by the equation below:

$$C_{gr}(NU, FU) \geq C_{gr_min} \quad (3-9)$$

In essence, the (FU, NU) pair which does not satisfy that minimum channel-gain ratio will be restricted; that is, will not be allowed to be paired. The problem will become a “*restricted channel-correlation maximization bipartite matching problem*”. This restricted BPMB will be solved by means of the “*restricted Hungarian Method*”. If *perfect matching* is obtained from the restricted HM process at this stage, the resulting sets of M -pairs will satisfy all three requirements stipulated in section-3.2 above. However, due to possible restrictions introduced between some users of the FUs -set and NUs -set by the enforcement of the C_{gr_min} , the restricted-*HM* process could result in imperfect-matching; which is a problem, because all the M -pairs are expected from the *UGA*. The step6 below therefore discuss what should be done in such case.

3.4.5. Step 5: Reduce C_{gr_min} and re-iterate the restricted HM process in step4.

The step4 above should provide an optimal pairing outcome with M -pairs which satisfy all three design requirements outlined. However, often, when the minimum channel-gain margin defined is relatively high, this results in a lot of restricted (FU, NU) -pairs; and subsequently lead to a high probability of having imperfect-matching outcome from the restricted HM process.

As said above, having *imperfect-matching* outcome from the *UGA* would be a problem, because in this application, all users are expected to be paired; so that *NOMA* can be implemented in all M -antennas. Since there are M -antennas on the satellite, M -pairs are therefore expected from the users-grouping algorithm. Let's consider K , the number of pairs obtained from the restricted-*HM* process in step5. Having perfect matching would mean that,

K is equal to M . However, having imperfect-matching would mean that $K < M$; would be a problem and thus will not be acceptable.

To alleviate the problem in case of an *imperfect-matching* outcome, we opt to iteratively reduce the value of C_{gr_min} after each restricted-*HM* process, from the initial value defined “ $C_{gr_min}(init)$ ”, until a *perfect-matching* outcome is eventually obtained.

To define “ $C_{gr_min}(init)$ ”, the following discussion is considered. In this application, we adopt to work with the channel-gain margin in the form of channel-gain ratio (C_{gr}) as presented in equation (3-5) above. From this equation, it appears that, the minimum possible channel gain ratio is 1; this is when the far-user and the near-user have relatively same channel-gain. If the minimum channel-gain ratio “ C_{gr_min} ” is set to 2 for the purpose of grouping far-users and near-users, this means that, the gain of the near-user will need to be at least twice that of the associated far-user. While this could be possible for few users, we consider this to be realistically unlikely. We thus, select to set C_{gr_min} to an initial value less than 2; where, 1.5 is therefore, naturally selected since being middle range between 1 and 2. This means that we set: $C_{gr_min}(init) = 1.5$.

Since the case of imperfect-matching outcome will require a decrease of C_{gr_min} from the $C_{gr_min}(init)$ after each iteration, a decrement-step for C_{gr_min} needs to be defined. To define this decrement-step the following is considered. In the worst case scenario, the perfect matching result may only be obtained when C_{gr_min} reaches 1. This would mean that the C_{gr_min} went from the initial value defined “ $C_{gr_min}(init)$ ” down-to 1. The number of iterations necessary to go from $C_{gr_min}(init)$ down-to 1 will depend on the *decrement-step* defined. To avoid having an everlasting iterative process, we choose the set the *decrement-step* as a percentage of the range to cover. We arbitrary select that, in the worst case scenario, it should take not more than five-iterations for the pairing process to obtain perfect-matching. This therefore, means that, five iterations correspond to 100% of the range to cover, and 1 iteration will therefore correspond to 20% of the range. Subsequently, the *decrement-step* (*dec-step*) of the C_{gr_min} for the case of maximum five iterations will be:

$$dec_step = 20\% \{C_{gr_min}(init) - 1\} \quad (3-10)$$

Consequently, a more general expression is derived as:

$$dec_step = \frac{C_{gr_min}(init) - 1}{I_{max}} \quad (3-11)$$

Where I_{max} is the maximum number of iterations defined. After each execution of the restricted-*MH* process, if *imperfect-matching* is obtained, the new value of $C_{gr}(min)$ to be used for next iteration will be calculated as:

$$C_{gr_min} = C_{gr_min}(cur) - dec_step \quad (3-12)$$

Where, " $C_{gr_min}(cur)$ " is the current value of C_{gr_min} used in the just completed iteration. Note that, at the beginning of the *UGA*, C_{gr_min} will take the initial value $C_{gr_min}(init)$ defined, in order to execute the first iteration of the restricted-*HM* process. Then, after each iteration, if perfect-matching is not obtained, the value of C_{gr_min} will be reduced as in equation-(3-12) above and a new iteration of the restricted-*HM* process will be executed, until a *perfect-matching* is obtained from the restricted-*HM* process.

3.5. Resulting UGA

Table 3.2 below outlines the proposed UGA resulting from the above discussed steps (1 to 6)

Table 3.2: Proposed Users' Grouping Algorithm for 2-users NOMA-based MBSNs

Proposed NOMA Users' Grouping Algorithm (UGA) for 2-users NOMA-based MBSNs		
steps	lines	actions
Step0:		initial parameters specification:
(a)	1:	define $M, C_{gr_min}(init), l_{max}$,
(b)	2:	calculate $ h_u $ of each user by evaluating the norm of its channel-vector,
Step1:		split the $2M$-users into 2-subsets of M-users based on their channel-gains:
(a)	3:	Classify the users' channel-gains from step1-b, in ascending order;
(b)	4:	Make highest M -channel-gains = (NU s-set); and lowest M -channel-gains = (FU s-set).
Step2&3:		generate the Hungarian-Matrix of $C_3(NU, FU)$:
(a)	5:	Calculate $C_3(NU, FU)$ between every FU and NU , as in equation-(3-6);
(b)	6:	Then fill the Hungarian-Matrix of $C_3(NU, FU)$, as illustrated in Table 3.1;
(c)	7:	Then discard pairs that have negative channel-correlation coefficients.
repeat		repeat:
Step4:		execute the Restricted-Hungarian-Matrix Processing
A		generate the Restricted-Hungarian-Matrix based on the C_{gr_min} specified:
(a)	8:	Calculate the $C_{gr}(NU, FU)$ between each NU and FU as in equation-(3-8); then
(b)	9:	Compare each $C_{gr}(NU, FU)$ calculated, to C_{gr_min} , as in equation (3-9); then
(b)	10:	Discard pairs in the Hungarian-Matrix from "stage3" for which $C_{gr}(NU, FU) < C_{gr_min}$.
B		execute the restricted-<i>HM</i> on the Hungarian matrix from "step4-A".
(a)	11:	Call the restricted Hungarian-Method Function;
(b)	12:	Obtain the resulting K -pairs
Step5:		terminate user-grouping process or reiterate stage4:
(a)	13:	check for perfect-matching by comparing K and M ;
(b)	14:	if $K=M$: exit "repeat" => perfect-matching obtained ;
(c)	15:	else if $K < M$:
	16:	Calculate "dec-step" as in equation-(3-11); then,
	17:	Calculate new $C_{gr}(min)$ as in equation-(3-12); then
	18:	Return to step4.
Until		Until: perfect-matching is obtained
Step6:		Store final outcome (i.e. resulting M-pairs).

3.6. Precoding Weight-vectors calculation

This sections gives a brief description of the precoding system in the MA-Encoder block of the a MU-MIMO system, as highlighted in Figure 3.4 below. This discussion includes listing of common existing techniques as well as selection of an appropriate technique for our implementation.

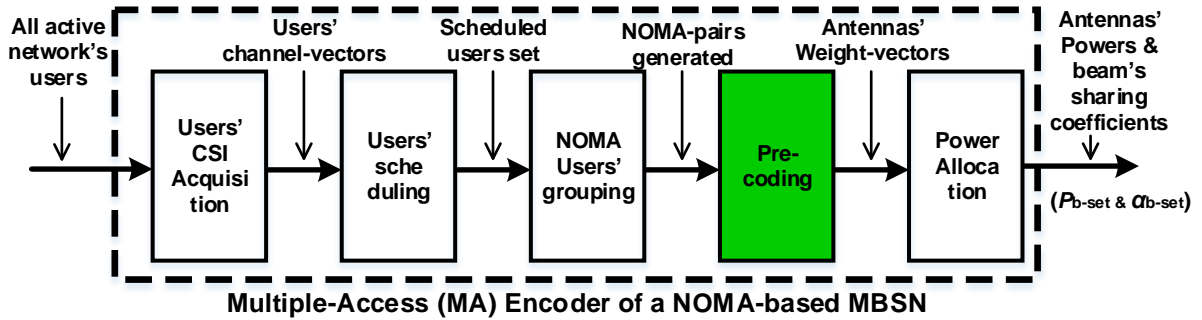


Figure 3.4: The Precoding system in the MA-Encoder block.

3.6.1. Background

3.6.1.1. Role of pc section

In the downlink scenario of the Multi-Users Multiple-Input Multiple-Output (MU-MIMO) system, the access-point transmits to multiple users simultaneously via multiple antennas; while reusing same frequency. This results in excessive Inter-Channel-Interference (*ICI*) on user-terminals (*UTs*) being served; and if not addressed, will subsequently lead to serious degradation of users' achievable capacities. The *ICI* suffered by the *UT* can be mitigated either at the receiver side (i.e. *UT*) by means the Multiple-Users-Detection (*MUD*) techniques. However, this may require a lot of resources from the receiver (*UT*) and will increment the receiver's complexity (Beigi & Soleymani, 2018:1; Neira et al., 2019:58; Yan et al., 2019:63532).

In the context of mobile communications, *UTs* are generally small handsets with limited resources; while the access-point (in this case the satellite) has a far larger resource capability. From this observation, the idea of addressing the *ICIs* at the access-point, instead of at the *UT* (i.e. handset) emerged. This idea is known as precoding technology and has gained more attention over recent years, with the emerging of MU-MIMO systems (Zhang et al., 2016:241; Trivedi et al., 2019:10; Zhang et al., 2020:8).

Precoding is the process of mitigating at the transmitter side (i.e. access-point), the *ICIs* that the receiver side (*UTs*) may be exposed to, in a "MU-MIMO system" (Caus et al., 2016:497; Vazquez et al., 2016:89; Neira et al., 2019:58). Through mitigation of the *ICIs*, the PC technology helps the system to achieve increased throughput; including increased spectral-

efficiency & power-efficiency (Islam et al., 2017:728; Aldababsa et al., 2018:7; Zhang et al., 2020:8).

3.6.1.2. Classification of Precoding techniques

Precoding techniques are commonly classified into two major families, namely, the non-linear and the linear techniques. Non-linear techniques include techniques such as the dirty-papers; are known to be very complex to implement (Zhang et al., 2016:241; Guidotti & Coralli, 2019:7-9). On the other side, linear techniques include techniques such maximum-ratio transmission (*MRT*), zero-forcing (*ZF*) and Minimum mean-square error (*MMSE*); and are known to be simpler to compute (Bharathi et al., 2017:1880; Guidotti & Coralli, 2018:1-3). For this reason, in this work, only linear precoding techniques will be considered.

Linear precoding techniques calculate the weight-vector matrix (W) for the multicast system by making use of the channel-matrix (H) consisting of the channel-vectors of the users being served by the respective antennas; that is:

$$W = [w_1 \ w_2 \ \dots \ w_M] \quad (3-13)$$

$$H = [h_1 \ h_2 \ \dots \ h_M] \quad (3-14)$$

where $1, 2, \dots, M$, are the antenna's number for the access-point, in this case the satellite.

The maximum ratio transmission (*MRT*) or Maximum ratio combining (*MRC*) is a precoding weight-vector calculation technique which implies allocating weight-vectors such as to maximise the *SNR* of each user. It is the most basic way of calculating weight-vector in the linear-precoding family, and the weight-vector matrix (W) is derived from the channel-matrix (H) as (Reddy & Chakravarthula, 2017:12; Wang et al., 2021:11102):

$$W_{MRT} = H^H \quad (3-15)$$

Where, $(*)^H$ is the *Hermitian* operator. One of the advantages of the *MRT* techniques is that it is simplest in terms of implementation computation; as it just implies calculating the Hermitian of the channel matrix. However, its drawback is that it is very sensitive to inter-channel-interference (*ICI*) and therefore, has very poor performance interference limited scenarios (Ali et al., 2017:757-758).

The zero-forcing is another linear precoding technique which implies calculating the weight-vectors such as to completely nullify the interference from other antennas (Vouyioukas, 2013:4; Hu & Rusek, 2017:3634). Importantly, this technique requires that the number of antennas at the access-point must be greater or equal to the number of users to be served (Yand & Choi, 2013:4; Panah & Yogeewaran, 2016:19). The weight-vector matrix (W) is

expressed in terms of system's channel matrix (H) as (Vazquez et al., 2016:2; Ali et al., 2017:757):

$$W_{ZF} = H^H(HH^H)^{-1} \quad (3-16)$$

The advantage of this technique is that, it cancels ICI completely, which makes it better than the MRT . Also, it is simpler to implement compared to the $MMSE$ technique, as the weight-vectors matrix is pseudo inverse of the channel matrix (Panah & Yogeewaran, 2016:19). However, its main drawback is that it involves channel matrix inversion. In fact, on one side, channel-matrix inversion often gets highly computational complex as the numb of antennas increases; and on other side, the channel-matrix can sometimes be non-invertible, making it impossible to implement the zero-forcing technique (Wagner et al., 2010:3; Hu & Rusek, 2017:3634). The minimum mean square error ($MMSE$) is also a linear precoding technique in which the precoding weight vector are calculated in such a way to minimise the mean square error between the transmitted and received signals of each user. The weight vectors matrix is a function of the channel matrix and the SINR of respective users; and can be expressed as (Bharathi et al., 2017:1880; Reddy & Chakravarthula, 2017:24; Guidotti & Coralli, 2018:3):

$$W_{MMSE} = H^H(HH^H + (1/SINR) \times I)^{-1} \quad (3-17)$$

Where, I is the identity matrix.

The $MMSE$ has increased computational complexity compare to other linear precoding techniques listed above; and thus is often strictly considered when others cannot be employed.

3.6.2. Selection of the Zero-Forcing technique

In this work, the zero-forcing technique will be the primary choice, due to its ability to completely mitigate ICI with reduced computational complexity. This assumes that, the channel matrix is invertible. However, in some cases, the channel matrix of satellite networks may be non-invertible due to very little variations in the coefficients that form users' channel vectors (Zhu et al., 2017:2261; Zhu et al., 2019:206). In this, case, inspired by the later cited works, we propose to combine the ZF and the MRT techniques; such that, when the channel is invertible, the ZF is used, but when the channel matrix may not be invertible, the MRT technique will then be employed.

3.6.3. Calculation of the precoding weight-vector matrix (W) in a 2-users $NOMA$ case

In traditional multi-beam networks that employed OMA technology, each antenna was serving a single user. As such, to calculate the weight-vector matrix, the channel matrix was formulated by considering channel vector of each user being by respective antennas. However, in $NOMA$

technology, each antenna is serving more than one user simultaneously (in this case 2 users). Therefore, since the channel matrix should be formulated by using only one user-per antenna, there has to be a selection of the user in antenna beam that will be used for the channel matrix formulation. This is mainly the reason why in the user-grouping, there was a requirement to group together, users with highly correlative channel vectors. Because, in this case, whichever user from the group may be chosen to formulate the channel matrix, the resulting antenna's weight vector will be able to cancel *ICI* for other users in the beam.

In this work, we are dealing with 2-users per antenna beam, namely, a far-user and a near-user. *We therefore, choose to use the channel-vector of near-user in each group, to formulate the channel-matrix (H) that will be used to derive the weight-vector matrix (W) by means of the ZF or MRT techniques.*

3.7. Chapter summary

This chapter principally presented the design of the proposed users' grouping algorithm. It started by presenting the models of the channel-gain margin and channel-correlation coefficient between two users; since these two parameters are important design parameters for the UGA. Then, it outlined the concept upon which the proposed UGA is designed; which is essentially, a two-stages approach involving: (a) the separation of users into a far and near users based on their respective channel-gains; and (b) the formulation of pairs of far-near users based on channel-correlation coefficients between respective users from these two groups. Thereafter it discussed the detailed design of the proposed UGA until final algorithm is obtained. In essence, the pairing problem is formulated into a restricted Hungarian matrix, which seeks to avoid users with low channel-gain margin from being paired; while at same time ensuring that users with channel-correlation are paired. Then, the problem is solve by means of Hungarian method, to ensure fairness amongst resulting pairs in terms of their respective channel-correlations coefficients. The outcome of Hungarian method ensure that the algorithm satisfies all there requirements, including high channel-gain margin and high channel-correlation coefficients between paired users; as well as high pairing fairness amongst resulting pairs. The chapter also gives a brief description of precoding weight vector calculation; and supports the choice of the zero-forcing technique for this application.

CHAPTER 4: MODELLING OF THE POWER-ALLOCATION SUBSYSTEM IN A 2-USERS NOMA-MBSN

4.1. Introduction

In this chapter, we present the necessary models that will be considered for designs of fairness-maximization power-allocation algorithms proposed by this research. The discussion in this chapter lays the fundamentals for designing the power-allocation system of the MA-Encoder block, as highlighted in Figure 4.1 below. However, the designs of our proposed power-allocation algorithms are covered in Chapter-5 and 6.

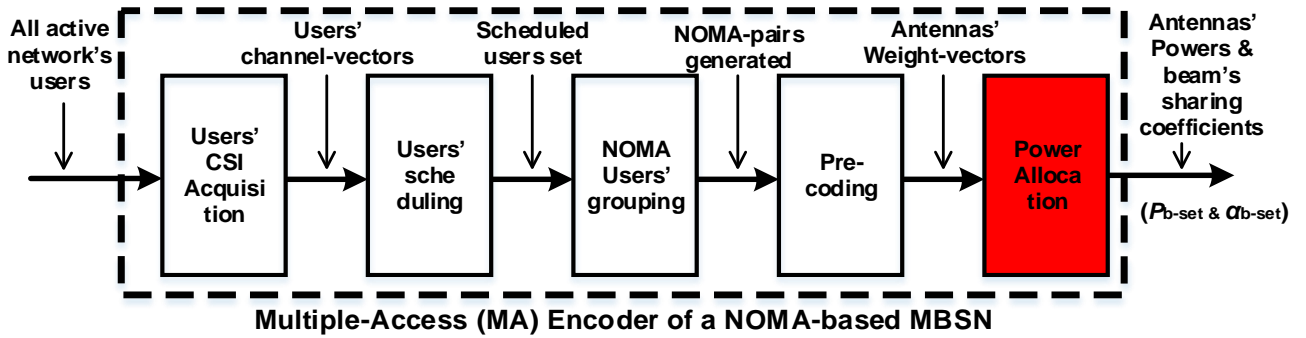


Figure 4.1: The Power-Allocation Subsystem in the MA-Encoder block

4.2. Overview of the power-allocation subsystem in a mobile network

4.2.1. Role of the power-allocation subsystem

The role of the power-allocation (*PA*) system in a mobile network can be explained as follows. Earlier generations of mobile networks usually assigned a fixed transmit power to all users serviced at a given time, regardless of their respective channel conditions. This usually led to two scenarios considered limitations for the network's global performance. One was the limited total capacity of the network due to the fact that a lot of power was given to users with poor channel conditions; while the achievable capacity of users with good channel conditions was limited by the standard power allocated to all users. The other limitation was the poor system's fairness, due to the fact that, with a fixed power assigned to users, some users could not satisfy their traffic requests, while other users were exceeding their traffic-requests. Therefore, in order to attempt addressing the outlined limitations, the idea of user's powers adjustment was introduced. The idea implies adjusting the power allocated to respective users being served at a given time, in order to achieve a defined network's global goal. Thus, the *PA* subsystem is in charge of determining the suitable power level that should be assigned to respective network's users being served at a given time, in order to achieve the desired network's goal (Kumar et al., 2008:70-71).

4.2.2. PA system's design goals and considerations

As indicated earlier, when serving users in a mobile network, the global goal of the operator is often either to maximise the network's total capacity, or maximise network's fairness, or to achieve a trade-off of these two fundamental performance parameters of the network (Kumar et al., 2008:70-71; Shams et al., 2014:137). Subsequently, the power allocation system is designed to achieve the defined network's goal (Saito et al., 2013:612; Islam et al., 2017:725). When the global network's goal is to maximize the system's total capacity (or network's total throughput), the *PA* system seeks to ensure that just enough power is given to users with poor channel conditions, for them to meet the minimum system's Quality-of-Service requirement. Then, the powers allocated to respective users with good channel conditions are maximised; so to easily maximize the total system capacity (Jiao et al., 2019:2; Sun et al., 2019:2; Wang et al., 2020:33634). When the global network's goal is to maximize system fairness, the *PA* system seeks to ensure that, powers allocated to respective users whose offered capacity by network exceeds their traffic-request; so that more power is given to respective users whose offered capacity by network is well below their traffic-request. In power allocation systems that seeks to maximize system's fairness, the parameter known as user's *OCTR*-ratio, is commonly considered; and is fundamental in maximizing system's users' fairness. The *OCTR*-ratio is basically, the ratio between the Capacity Offered to the user by the network, and the Traffic-Request of the user. In other words, this ratio is a numerical measure of the level of satisfaction of a user in the network. When a user is offered more capacity than its actual traffic-request, its *OCTR*-ratio will be greater than 1; and the user is said to be over-satisfied. Alternatively, when a user is offered less capacity than its actual traffic-request, its *OCTR*-ratio will be less than 1; and the user is said to be unsatisfied. Equally, when a user is offered a capacity equal to its actual traffic-request, its *OCTR*-ratio will be equal to 1; and the user is said to be satisfied. Thus, in fairness maximization applications, the power-allocation system usually seeks to improve the capacity of users with poor *OCTR*-ratios in order to improve these *OCTR*-ratios and thus achieve a better system's user' fairness (Pioro & Medhi, 2004:62; Le-Boudec, 2021:9).

It is critical to note that, in the context of 5G networks, which is what NOMA-based MBSNs seeks to implement, the needs to achieve high system capacity as well as high system fairness both constitute critical system requirements (Liu & Jiang, 2016:4; Aldababsa et al., 2018:2; Anwar et al., 2019:2).

In order to executes its expected function in a MU-MIMO system, the *PA* system needs to take in consideration parameters such as the number of antennas at the access-point, the

number of users to be served by each antenna, the precoding weight-vectors of respective antennas, as well as the channel-vectors for respective users to be served.

4.3. The proposed power-allocation algorithms design work

The surveys of existing power-allocation algorithms design works were outlined, earlier in section-1.1.3. From these surveys, it resulted that, most studies that proposed a *PAA* for 2-users *NOMA-MBSNs*, designed their *PAA* to maximise the system's capacity; without much attention given to system's fairness. This leaves the problem of high fairness requirement for 5G networks unattended.

Therefore, this work seeks to make a contribution in addressing this outlined gap, by proposing to design novel power-allocation algorithms that maximize the fairness of *NOMA-MBSNs*. Subsequently, two novel *PA* algorithms for 2-users *NOMA-MBSNs* are proposed by this research:

- First, a *PA* algorithm for fairness maximization of 2-users *NOMA-MBSNs*, based on the *OCTR-ratios convergence* concept;
- Second, a *PA* algorithm for fairness-maximization of 2-users *NOMA-MBSNs*, based on the *maximum-minimum fairness* concept; which in general, is an improvement of the *PA*-algorithm based on *OCTR-ratios convergence* concept.

4.4. Design requirement and specifications for the proposed *PA* subsystem

The fundamental design requirement for the proposed power-allocation subsystem is to maximise network's fairness. In order to design the *PA* subsystem, the network for which the *PA* subsystem is developed needs to be well described and the design parameters well defined. In this work, we consider the network's description given in "**section-2.2**"; which, for the purpose of *PAA*'s design can be re-clarified as follows:

- a) The number of antennas on the satellite is M ;
- b) Each satellite's antenna serves 2-users on the ground by means of *NOMA*-protocol; thus, each antenna's beam (b) consists of a near-user (n) and a far-user (f).
- c) The precoding weight-vector (w_b) of each satellite's antenna are available and were calculated based on the *ZF*-(or *MRT*) precoding techniques; where $b = 1, 2, \dots, M$.
- d) The channel-vectors of all users are known; thus, in each antenna's beam (b), the channel-vector (h_{bn}) of the near-user and (h_{bf}) of the far-user are assumed known.

The output parameter of interest for the *PA* system under design is the total system's users-fairness; and the input parameters include the number of antennas (M), number of users per *NOMA* group of each antenna (2), the precoding weight-vector of each respective antenna

(w_b), and the channel-vectors of respective users in all the beams (h_{bn} and h_{bf}). A mathematical model which links these two sets of parameters can be derived as presented in the following sections below.

4.5. Link between System's fairness, users' OCTR-ratios and users' capacities

In order to derive a description of system's fairness, the following cases should be considered. Firstly, when fixed power level is allocated to all users, as in traditional networks, some users may receive more power than they actually need to achieve their current traffic request; they are said to be overly satisfied. In contrast, others may receive far less power than they need to achieve their traffic requests; they are said to be unsatisfied. As results, the excess power received by the over-satisfied users, which could have been used to supplement unsatisfied users and improve their achievable traffic capacities, is wasted. This obviously leads to wastage of available resources. Secondly, when adjustable power is allocated to users with the aim of maximizing the network's throughput (total capacity), irrespective of their traffic requests, users with poor channel conditions are often intentionally given the minimum power possible, sufficient just for them to achieve the minimum QoS. And the rest of abundant power is given to users with good channel conditions; for them to maximize their achievable capacity, thus, maximizing the network's total capacity. This eventually leads to a serious imbalance in the network in terms of the achievable capacities of the different users; as users with poor channel conditions will most generally be unsatisfied, while those with good channel condition will be over-satisfied. In both of these highlighted cases, the power-allocation system is generally said to result in *poor system's fairness* due to existence of high gap between the level of satisfaction of respective users in the network.

Subsequently, the fairness of a mobile network with respect to resource allocation, is often described to be a metric that gives an indication of how well the systems tries to satisfy the capacity need (traffic request) of every user being served at a given time (Marinescu, 2018:185; Le-Boudec, 2021:10). It can be estimated by means of various metrics including the QoE's, Jain's, Gini's, Bossaer's etc... (Pinto-Roa et al., 2015:5; Roy et al., 2018:129). However, the Jain's and Gini's metrics are the most widely used for determining the system's fairness in terms of resources allocation (Obaidat et al., 2015:711; Pachon et al., 2015:256; Khan et al., 2016:18; Attiah et al., 2018:38). Jain's " $J(.,)$ " and Gini's " $G_i(.,)$ " fairness metrics can be expressed as follows:

$$\mathbf{J}(R_1, \dots, R_K) = \frac{\left(\sum_{u=1}^K R_u \right)^2}{K \times \sum_{u=1}^K (R_u)^2} \quad (4-1)$$

$$\mathbf{G}_i(R_1, \dots, R_K) = \prod_{u=1}^K \sin\left(\frac{\pi R_u}{2 \max(R_1, \dots, R_K)} \right)^{1/i} \quad (4-2)$$

Where, K is the total number of users being served, R_u is the *OCTR*-ratio of the u^{th} user in the set, $u = 1, 2, \dots, K$; and i is the order of the fairness-index and is a positive real.

There are two critical observations to make from these fairness metrics. The first one is that the estimation of the system's fairness is widely based on the evaluation of the level of satisfaction of all users being served at a given time. The level of satisfaction of a user is expressed by its *OCTR*-ratio, denoted as " R_u " in above metrics. This is the ratio between the capacity offered to the user by the network (*OC*, or simply C_u) and the traffic-request of the user (*TR*, or simply D_u); and can be written as:

$$\text{OCTR_ratio}(u^{\text{th}} \text{ user}) = R_u = \frac{C_u}{D_u} \quad (4-3)$$

The second observation is that the system's fairness is maximised when the gap between the different *OCTR-ratios* is minimised. Subsequently, from these observations, it appears clearly that, maximization of system's fairness implies minimization of gap between *OCTR-ratios* of respective users (R_u) being served.

There exists two fundamental ways to minimize the gap between the different *OCTR-ratios*; either by maximizing the minimum *OCTR*-ratio across all users, or by minimizing the maximum *OCTR*-ratio across all users. When no boundary is set for reducing the *OCTR*-ratio of some users, the later may often result in excessive loss of system's capacity, due to convergence toward the poorest *OCTR*-ratio in the system. Thus, it is not commonly considered. The former therefore, remains the most widely considered way of minimising the gap between the different *OCTR-ratios* in a users' set; and thus maximizing the system's fairness. Stated differently, a maximisation of the system's fairness is mostly achieved by maximizing the minimum *OCTR*-ratio across all users being served. In such cases, adjustable power is allocated to respective users in the network such as to maximize the minimum *OCTR*-ratio across all users, and thus, maximise the system's fairness.

Noting that at a given time frame of service, users' traffic requests (D_u) are generally assumed constants, the *OCTR*-ratio of each user (R_u) therefore, becomes a function solely of the offered-capacity (C_u) to the user. As such, the capacity offered to each user in the network, through power allocation, becomes the only adjustable variable, in order to adjust the user's *OCTR*-ratio. As explained earlier, when the user's *OCTR*-ratio is greater than 1, the user is said to be over-satisfied, which means that, the power allocated to the user is allowing it to achieve a capacity bigger than what it needs. Similarly, when the user's *OCTR*-ratio is less than 1, the user is said to be unsatisfied; which means that, the power allocated to the user is allowing it to achieve a capacity less than what it needs. Equally, when the user's *OCTR*-ratio is equal to 1, the user is said to be satisfied; which means that, the power allocated to the user is allowing it to achieve a capacity equal to what it needs. Consequently, in order to derive an explicit model of the user's *OCTR*-ratio with-respect-to its allocated power, it is necessary to derive a model of the capacity offered to each user (i.e. C_u) with-respect-to the power allocated the user.

4.6. Modelling of the network's users' capacities

4.6.1. General model of the user's capacity in terms of user's *SINR*

The general expression of the capacity (C) achievable by user in a free-space link, can be described as (Parker, 2017:174 and Willner, 2020:347):

$$C = B \times \log_2(\text{SINR} + 1) \quad [\text{bps}] \quad (4-4)$$

From this equation, the capacity can be normalised to the link's bandwidth, and user's capacity assuming a 1Hz bandwidth will be expressed as:

$$C = \log_2(\text{SINR} + 1) \quad [\text{bps/Hz}] \quad (4-5)$$

In this equation, the only independent variable is the user's *SINR*. Since the logarithmic function is monotonous and increasing in the positive real number set, i.e., $[0, +\infty]$, and the user's *SINR* is always a positive number, the following can be written:

$$\lim_{\text{SINR} \rightarrow +\infty} \{C\} = \lim_{\text{SINR} \rightarrow +\infty} \{\text{SINR} + 1\} = \lim_{\text{SINR} \rightarrow +\infty} \{\text{SINR}\} \Rightarrow +\infty \quad (4-6)$$

Subsequently, the affirmations below can be made:

- the normalised user's capacity (C) is a function of the user's *SINR* solely;
- the normalised user's capacity (C) is directly proportional to the user's *SINR*;
- A variation in the user's *SINR* leads to a like variation in the user's capacity (C).

Consequently, from these affirmations, it follows that, to derive the user's capacity model (C_u), it is necessary to derive the user's $SINR_u$. Thus, in the following section, we model the $SINR$ of any user in the system. This means, the $SINR$ of the near-user and far-user in beam (b), noted $SINR_{bn}$ and $SINR_{bf}$, respectively.

4.6.2. $SINR$ of the near-user (n) in any beam (b)

Considering the system's description given in section-2.2 and illustrated in Figure 2.1 above, and referring to Daniels & Balyan (2020:673), the total signal transmitted by the satellite through all its M -antennas can be expressed as:

$$S_{tx} = \sum_{b=1}^M w_b \sqrt{P_b} (\sqrt{\alpha_b} s_{bn} + \sqrt{1-\alpha_b} s_{bf}) \quad (4-7)$$

Where, " b " is the antenna's number, " w_b " is the antenna's precoding weight-vector, " P_b " is the power assigned to antenna " b ", " α_b " is the intra-beam $NOMA$ -power-sharing coefficient in beam " b "; and " s_{bn} " and " s_{bf} " are respectively the information signal of the near- and far-users in beam " b ".

This transmitted signal reaches all the users present in the system, via their respective channels. Thus, " h_{bn} " being the channel-vector of near-user (n) in any beam " b " of the network, the signal received by this user will be:

$$\begin{aligned} S_{rx-bn} &= h_{bn}^H \times S_{tx} \\ S_{rx-bn} &= h_{bn}^H \times \sum_{b=1}^M w_b \sqrt{P_b} (\sqrt{\alpha_b} s_{bn} + \sqrt{1-\alpha_b} s_{bf}) \end{aligned} \quad (4-8)$$

Where, $(*)^H$ is the Hermitian operator of the complex channel-vector. The above equation can further be expanded as follows:

$$S_{rx-bn} = \underbrace{h_{bn}^H w_b \sqrt{P_b} \sqrt{\alpha_b} s_{bn}}_{\text{Intended signal to the beam's near-user (bn)}} + \underbrace{h_{bn}^H w_b \sqrt{P_b} \sqrt{1-\alpha_b} s_{bf}}_{\text{Intra-beam interference (IBI) from the beam's far-user (bf) due to NOMA}} + \underbrace{\sum_{b^*=1; b^* \neq b}^M h_{bn}^H w_{b^*} \sqrt{P_{b^*}} (\sqrt{\alpha_{b^*}} s_{b^*n} + \sqrt{1-\alpha_{b^*}} s_{b^*f})}_{\text{Inter-beam interference (ICI) from other antennas}} \quad (4-9)$$

The normalised power of the received signal is the square of the signal's amplitude expressed above. Thus, from above equation, the signal power received by the near-user in any beam (b) would be:

$$P_{rx-bn} = (h_{bn}^H w_b \sqrt{P_b} \sqrt{\alpha_b})^2 + (h_{bn}^H w_b \sqrt{P_b} \sqrt{1-\alpha_b})^2 + \sum_{b^*=1; b^* \neq b}^M (h_{bn}^H w_{b^*} \sqrt{P_{b^*}})^2 + n \quad (4-10)$$

Where, “ n ” is the additive white Gaussian noise (AWGN). This equation can be rewritten as:

$$P_{rx-bn} = \underbrace{\left| h_{bn}^H w_b \right|^2 P_b \alpha_b}_{\text{Intended Power to (bn)}} + \underbrace{\left| h_{bn}^H w_b \right|^2 P_b (1 - \alpha_b)}_{\text{IBI Power from (bf)}} + \underbrace{\sum_{b^*=1; b^* \neq b}^M \left| h_{bn}^H w_{b^*} \right|^2 P_{b^*}}_{\text{ICI Power from other antennas}} + \underbrace{n}_{\text{AWGN}} \quad (4-11)$$

From this expression of the signal power received by the near-user of any beam (b) in the network, the actual power intended to the near-users as well as all other interfering powers are clearly expressed. Therefore, the signal-to-interference and noise ratio ($SINR$) of the near-user in beam (b) can easily be expressed as:

$$SINR_{bn} = \frac{\text{Intended Power}}{\text{IBI power} + \text{ICI power} + \text{AWGN}} \quad (4-12)$$

$$SINR_{bn} = \frac{\left| h_{bn}^H w_b \right|^2 P_b \alpha_b}{\left| h_{bn}^H w_b \right|^2 P_b (1 - \alpha_b) + \sum_{b^*=1; b^* \neq b}^M \left| h_{bn}^H w_{b^*} \right|^2 P_{b^*} + n} \quad (4-13)$$

Consequently, having the $SINR_{bn}$ of the near-user in any beam (b) of the network, its offered-capacity (C_{bn}) will be determined as described in equation- (4-5) above.

4.6.3. $SINR$ of the far-user (f) in beam (b)

Similar to the analysis completed above for the near-user in beam (b) of the network, the $SINR$ of the far-user in any beam (b) of the network, can be modelled in the following manner. As indicated earlier, it is known that the total transmitted signal by the satellite (S_{tx}), expressed in equation-(4-7) above, reaches all the users present in the system, via their respective channels. Thus, “ h_{bf} ” being the channel-vector of far-user (f) in any beam “ b ” of the network, the signal received by this user will be:

$$\begin{aligned} S_{rx-bf} &= h_{bf}^H \times S_{tx} \\ S_{rx-bf} &= h_{bf}^H \times \sum_{b=1}^M w_b \sqrt{P_b} \left(\sqrt{\alpha_b} s_{bn} + \sqrt{1 - \alpha_b} s_{bf} \right) \end{aligned} \quad (4-14)$$

The above equation can further be expanded as follows:

$$S_{rx-bf} = \underbrace{h_{bf}^H w_b \sqrt{P_b} \sqrt{\alpha_b} s_{bn}}_{\text{Intra-beam interference (IBI) from the beam's near-user (bn) due to NOMA}} + \underbrace{h_{bf}^H w_b \sqrt{P_b} \sqrt{1 - \alpha_b} s_{bf}}_{\text{Intended signal to the beam's far-user (bf)}} + \underbrace{\sum_{b^*=1; b^* \neq b}^M h_{bf}^H w_{b^*} \sqrt{P_{b^*}} \left(\sqrt{\alpha_{b^*}} s_{b^*n} + \sqrt{1 - \alpha_{b^*}} s_{b^*f} \right)}_{\text{Inter-beam interference (ICI) from other antennas}} \quad (4-15)$$

Again, the normalised power of the received signal is the square of the signal's amplitude expressed above. Thus, from above equation, the signal power received by the far-user in any beam (b) would be:

$$P_{rx-bf} = \left(h_{bf}^H w_b \sqrt{P_b} \sqrt{\alpha_b} \right)^2 + \left(h_{bf}^H w_b \sqrt{P_b} \sqrt{1-\alpha_b} \right)^2 + \sum_{b^*=1; b^* \neq b}^M \left(h_{bf}^H w_{b^*} \sqrt{P_{b^*}} \right)^2 + n \quad (4-16)$$

Where, n is the additive white Gaussian noise (AWGN). This equation can be rewritten as:

$$P_{rx-bf} = \underbrace{\left| h_{bf}^H w_b \right|^2 P_b \alpha_b}_{\text{IBI Power from (bn)}} + \underbrace{\left| h_{bf}^H w_b \right|^2 P_b (1-\alpha_b)}_{\text{Intended Power to (bf)}} + \underbrace{\sum_{b^*=1; b^* \neq b}^M \left| h_{bf}^H w_{b^*} \right|^2 P_{b^*}}_{\text{ICI Power from other antennas}} + \underbrace{n}_{\text{AWGN}} \quad (4-17)$$

From this expression of the signal power received by the far-user of any beam (b) in the network, the actual power intended to the far-users as well as all other interfering powers are clearly expressed. Therefore, the signal-to-interference and noise ratio ($SINR$) of the far-user in any beam (b) can easily be expressed as:

$$SINR_{bf} = \frac{\text{Intended Power}}{\text{IBI power} + \text{ICI power} + \text{AWGN}} \quad (4-18)$$

$$SINR_{bf} = \frac{\left| h_{bf}^H w_b \right|^2 P_b (1-\alpha_b)}{\left| h_{bf}^H w_b \right|^2 P_b \alpha_b + \sum_{b^*=1; b^* \neq b}^M \left| h_{bf}^H w_{b^*} \right|^2 P_{b^*} + n} \quad (4-19)$$

Consequently, having the $SINR_{bf}$ of the far-user in any beam (b) of the network, its offered-capacity (C_{bf}) will be determined as described in equation-(4-5) above.

4.6.4. Effect of the Precoding on users' $SINRs$ and capacities

The above derived equations (4-13) and (4-19), respectively, describe the $SINR$ of any near- and far-users in the network. The determination of the precoding weight-vectors for all the satellite's antennas, was discussed in "section 3.6". Subsequently, it was indicated in "section 3.6.2" that for this work, the zero-forcing technique for calculating precoding weight-vectors will be employed. It was also indicated in "section 3.6.3" that in this application, the channel-vector of the near-user in each beam will be selected for the calculation of the corresponding antenna's precoding weight vector.

From all this indications, it follows that, the purpose of the zero-forcing (ZF) precoding technique is to force inter-beam interference (ICI) to zero. Thus, if the ZF technique is well

implemented, the users whose channel-vectors were used to calculate the antennas' weight vectors will not suffer any *ICI*; as this will be completely cancelled on them. This implies that, in this application where channel-vectors of near-users have been selected for the calculation of antenna's weight-vectors, near users will not suffer any *ICI*.

Furthermore, it was indicated earlier that, in the decoding of NOMA protocol, the beam's user with better channel condition will first decode the signal of the user with poorer channel condition, before decoding its own signal. Thus, this user will not suffer intra-beam interference from the other beam's user with poorer channel condition. This implies that, in this application, the near-user, whose channel condition is better than that of the far-user, will not suffer any intra-beam interference from the far-user; since it will first decode the signal of the far-user before decoding its own.

Consequently, based on the two implications outlined supra, it results that in this application, the near-users in each beam (b) will not suffer any intra-beam interference, nor any inter-beam interference. Only the far-users in each beam will suffer both type of interferences. As such, a simplified expression of the *SINR* of the near-user ($SINR_{bn}$) in any beam (b) of the network, could be given as:

$$SINR_{bn} = \frac{|h_{bn}^H w_b|^2 P_b \alpha_b}{n} \quad (4-20)$$

However, the *SINR* of the far-user ($SINR_{bf}$) in any beam (b) of the network will still be as expressed in equation-(4-19) above.

Looking at the simplified expression of the near-user's *SINR* above, it can be seen that, the simplified *SINR* is bigger than the *SINR* when the precoding has not yet taken effect. Thus, increased *SINR* induces increased user's capacity. This in essence, is the purpose of employing the precoding; that is, to improve the capacities of respective users despite the presence of *ICIs*.

4.6.5. Link between beam's users' capacities and the P_b and α_b

From section-4.5 to section-4.6.3 above, the following has been shown:

- **Point1:** Considering that users' demands are constant over a given time of service, the *OCTR*-ratio (R_u) of any user (u) described by equation-(4-3) above, is purely a monotonous function of the user's offered-capacity (C_u). Thus, adjusting the user's offered capacity automatically results in adjusting its *OCTR*-ratio.

- **Point2:** The user's offered-capacity in the network is, without loss of generality, a monotonous function of the user's *SINR*, as described by equation-(4-5) above. Thus, adjusting the user's offered-capacity implies, adjusting its *SINR*.
- **Point3:** The *SINR* of any near-user or far-user in a 2-users *NOMA MBSN* have been derived in equations-(4-13) and (4-19) above respectively. It appears that, the *SINR* of the near-user in any beam (b) of the network, is a function of the user's channel-vector (h_{bn}), the weight-vectors (w_b) of the respective satellite's antennas ($b = 1, 2, \dots, M$), the power assigned to respective antennas (P_b); as well as the intra-beam power-sharing coefficient (α_b) in the designated beam (b) of the concerned user. It is common consideration that at a given time of service, the channel-vectors of all users are constant. Subsequently, since the both *ZF*- and *MRT*-precoding techniques only consider the users' channel-vectors in order to generate the antenna's weight-vectors, the weight-vectors of respective antennas are also considered constant at a given time of service. Consequently, the remaining adjustable parameters in the formula of the user's *SINR* are the powers allocated to respective antennas ($P_b, b = 1, 2, \dots, M$); and the intra-beam power-sharing coefficient (α_b) in the designated beam (b) of the concerned user. This analysis is also valid for the far-user (f) in any beam (b) of the network.

Thus, from these three observations, it can be seen that, by adjusting the power allocated to respective antennas, and by adjusting the intra-beam power-sharing coefficient (α_b) in the designated beam (b) of the concerned user, the *SINR* of the any near-user or far-user in the network can be adjusted accordingly; in yield in adjustment of the user's offered-capacity, and subsequently in the adjustment of the user's *OCTR*-ratio.

Therefore, the role of the power-allocation algorithm, in a system's fairness maximization scenario, is often to adjust the powers allocated to respective antennas (P_b), as well as the intra-beam power-sharing coefficient (α_b) in each respective beam; in order to improve the poorest *OCTR*-ratios in the network, and thus, maximise the network's fairness. The process of adjusting the powers allocated to respective antennas is commonly referred to as "*inter-beam power-allocation*"; and is performed by an *inter-beam power-allocation algorithm*. Equally, the process of adjusting the intra-beam power-sharing coefficient (α_b) in each beam, is generally known as *intra-beam power-allocation*; and is performed by an *intra-beam power-allocation algorithm*. The design concepts commonly used to develop power-allocation algorithms for system's fairness-maximization are presented in the following section.

4.7. Formulation of the system's fairness maximization as an optimization problem

4.7.1. The original optimization problem

The expression of the user's *OCTR*-ratio was given in equation-(4-3) above. As indicated above, the maximization of the system's fairness implies maximizing the minimum *OCTR*-ratio across the system. Therefore, considering that every user being served is annotated in terms of its beam's number ($b \in M$) and its rank within the beam ($r = n$ or f), the *OCTR*-ratio of any user being served in the network can be expressed as:

$$OCTR_ratio_{b,r} = R_{b,r} = \frac{C_{b,r}}{D_{b,r}} \quad (4-21)$$

Where $C_{b,r}$ is the capacity offered to the “ n ” or “ f ” user in beam “ b ”, and $D_{b,r}$ is the user's traffic request. As such, the system's fairness maximization request can be formulated as an optimization problem as follows:

$$\begin{array}{l} \text{Original System's} \\ \text{Fairness Maximization} \\ \text{Problem} \end{array} \left\{ \begin{array}{l} F: \max_{b \in M; r = n, f} \min (R_{b,r}) \quad (4-22a) \\ \text{s.t. } \sum_{b=1}^M P_b \leq P_{\text{tot}} \quad (4-22b) \\ P_b \leq P_{b\text{-max}} \quad (b \in M) \quad (4-22c) \\ 0 \leq \alpha_b \leq 1 \quad (b \in M) \quad (4-22d) \end{array} \right.$$

The constraint ((4-22d) emphasizes that, the intra-beam power-sharing coefficient in each beam (α_b) must be confined between 0 and 1. The constraint (4-22c) indicates that, the power allocated to each antenna (P_b) must not exceeds the defined maximum antenna acceptable power ($P_{b\text{-max}}$). The constraint ((4-22b) indicates that, the sum of the power allocated to respective antennas must not exceed the total power available on the satellite (P_{tot}).

Since the traffic request of each user ($D_{b,r}$) is constant at the time of service, the only adjustable variable is the user's capacity ($C_{b,r}$); which itself is a function of the user's *SINR*. But, equations-(4-13) and (4-19) of the near-user and far-user's *SINR* respectively, indicate that for a given beam power (P_b), the capacities of the beam's near-user and far-users are function of the NOMA intra-beam power-sharing coefficient (α_b). It is also known that, for a given beam power (P_b), “ α_b ” can take any value between [0,1], to adjust the near- and far-users' capacities toward some desired levels. As such, there is no linear relationship between the “amount of variation” in P_b and the resulting amount of variation in “ α_b ”. Subsequently,

there is no linear relationship between the “amount of variation” in the beam’s power (P_b) and the resulting amount of variation in the capacities of the respective beam’s users ($C_{b,r}$). Consequently, the functions “ $C_{b,r}$ ”, and subsequently “ $R_{b,r}$ ” are non-linear in terms of the amount of variation in the beam’s power. Therefore, the original problem is non-convex and *NP* hard; that is, it is very hard to solve by means of numerical computing methods (Wegener, 2003:67; Rao, 2009:248; Ramirez & Mosquera, 2020:8812).

4.7.2. Decomposition of original problem into 2 sub-problems

In order to reduce the complexity of the original problem above, we propose to decompose it into two sub-problems; namely, intra-beam fairness maximization problem and inter-beam fairness maximization problem; which can be formulated as follows:

$$\begin{array}{l} \text{Intra-beam's Fairness} \\ \text{Maximization Problem} \end{array} \left\{ \begin{array}{l} F_1 : \max \min (R_{bn}, R_{bf}) \quad (4-23a) \\ \text{s.t. } 0 \leq \alpha_b \leq 1 \quad (4-23b) \end{array} \right.$$

$$\begin{array}{l} \text{Inter-beam's Fairness} \\ \text{Maximization Problem} \end{array} \left\{ \begin{array}{l} F_2 : \max_{b \in M} \min (R_b) \quad (4-24a) \\ \text{s.t. } \sum_{b=1}^M P_b \leq P_{\text{tot}} \quad (4-24b) \\ P_b \leq P_{b\text{-max}} \quad (b \in M) \quad (4-24c) \end{array} \right.$$

In the intra-beam problem, the idea is to max the beam’s fairness, by maximizing the minimum *OCTR*-ratio within each beam; through careful adjustment of shares of the beam’s power given to respective users in the beam. Similarly, in the inter-beam problem, the idea is to adjust the powers allocated to respective beams, such as to maximise the inter-beam’s fairness; through improvement of the minimum *OCTR*-ratio across all beams. The solution to each of these sub-problems will come in a form of an algorithm; namely, an intra-beam and an inter-beam power allocation algorithm. Then, a global power-allocation algorithm for the system will combine these two algorithms, and run them iteratively, until an optimal solution for the original problem is obtained.

By decomposing the original problem into two sub-problems which we treat successively in iteration, we are reducing the complexity of the user’s *OCTR*-ratio adjustment process, from a non-linear two parameters dependency (P_b and α_b), to a single parameters dependency at the time (P_b or α_b). In essence, when addressing the intra-beam power-allocation problem through adjustment of the intra-beam power-sharing coefficients in each beam, the powers allocated to respective antennas are kept constant. Thus, in each beam (b), the beam’s power

(P_b) is assumed constant during intra-beam power-adjustment, and the only adjustable variable for the *SINR*, capacity and *OCTR*-ratio of a given user, is the intra-beam power-sharing coefficient (α_b). In the same manner, when addressing the inter-beam power-allocation problem through adjustment of the powers (P_b -s) to respective antennas, the intra-beam power-sharing coefficient (α_b) in each respective beam is assumed constant; and the beam is seen as a single user entity. Thus, the powers (P_b -s) allocated to respective antennas become the only adjustable variables for the *SINR* (and subsequently, of the capacity and the *OCTR*-ratio) of each beam.

4.7.3. Variations of beam's users' capacities versus beam's power (P_b)

Recall that, equations- (4-13) and (4-19), expressed respectively, the *SINR* of the near-user and far-user in any beam (b) of the network, respectively. From these two equations, it can be seen that, assuming a constant beam's power-sharing coefficient (α_b), the *SINRs* of the beam's users can be increased in two ways:

- a) Either by increasing their intended signal's power; that is, increasing the power (P_b) of the beam,
- b) Or by decreasing the interference from other antennas; that is, decreasing powers of other beams.

Similarly, the *SINRs* of the beam's users can be decreased in two ways:

- (i) Either by decreasing their intended signal's power; that is, decreasing the power (P_b) of the beam,
- (ii) Or by increasing the interference from other antennas; that is, increasing powers of other beams.

In this regards, authors Wang et al., 2019:(4-5), demonstrated that, the *SINRs* of the beam's users, and thus their capacities, increase much faster by increasing the beam's power; rather than by decreasing the powers of other beams. Similarly, the *SINRs* of the beam's users, and thus their capacities, decrease much faster by decreasing the beam's power; rather than by increasing the powers of other beams. These observations are critical for the design of the inter-beam power-allocation algorithm, and will be highly considered during the algorithms design discussion in the next chapters.

4.7.4. Variations of beam's users' capacities versus α_b

Similar to the above analysis, we look at the expressions of the *SINR* of the near-user and far-user in any beam (b) of the network, given in equations (4-13) and (4-19) above. Looking into

these equations, and considering that during the intra-beam power-sharing adjustment, the powers to respective beams are assumed constant; “ α_b ” therefore, becomes the only adjustable variable for the *SINRs*, capacities and *OCTR*-ratios, of the beam’s near- and far-users. Building from this outcome, and considering the models of the far- and near-user’s capacities resulting from equations (4-13), (4-19) and (4-5), the following observations shall be noted at this point:

- 1) “ α_b ” can take any value between [0,1], and thus is continuous in this interval;
- 2) “ C_{bn} ” is continuous and increasing when “ α_b ” increases in the interval [0,1]:
 - (i) When “ α_b ” is 0, “ C_{bn} ” is maximum; and
 - (ii) When “ α_b ” is 1, “ C_{bn} ” is minimum (theoretically, $C_{bn} = 0$).
- 3) “ C_{bf} ” is continuous and decreasing when “ α_b ” increases in the interval [0,1]:
 - (i) When “ α_b ” is 0, “ C_{bf} ” is minimum (theoretically, $C_{bf} = 0$); and
 - (ii) When “ α_b ” is 1, “ C_{bf} ” is maximum;
- 4) “ C_{bn} ” and “ C_{bf} ” have opposite variations as “ α_b ” varies in interval [0,1]:
 - (i) An increase in “ α_b ” leads to increase in “ C_{bn} ”, but a decrease in “ C_{bf} ”; and
 - (ii) A decrease in “ α_b ” leads to decrease in “ C_{bn} ”, but an increase in “ C_{bf} ”;
- 5) Consequently, “ R_{bn} ” and “ R_{bf} ” have opposite variations as “ α_b ” varies in interval [0,1]:
 - (i) An increase in “ α_b ” leads to increase in “ R_{bn} ”, but a decrease in “ R_{bf} ”; and
 - (ii) A decrease in “ α_b ” leads to decrease in “ R_{bn} ”, but an increase in “ R_{bf} ”;

The graphs in Figure 4.2 below illustrates the variations of C_{bn} , C_{bf} , R_{bn} and R_{bf} , as “ α_b ” varies from 0 to 1.

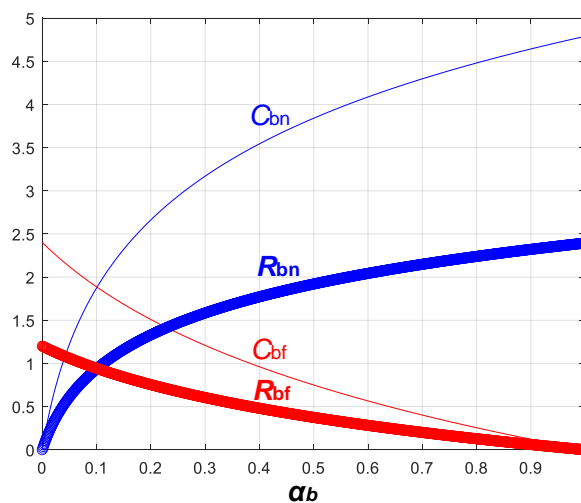


Figure 4.2: Variations of C_{bn} , C_{bf} , R_{bn} and R_{bf} , with respect to “ α_b ”

Again, the above listed observations are critical for the design of the intra-beam power allocation algorithm, and will be highly considered during the algorithms design discussion in the next chapters.

4.8. Common power-allocation design concepts for system's fairness-maximization

To solve each sub-problem individually and generate the resulting intra-beam and inter-beam power allocation algorithms, we opt to employ some commonly used concepts for addressing fairness maximization power-allocation problems in communications networks. These include the maximum-minimum fairness concept and the *OCTR-ratios* convergence concept (Piro & Medhi, 2004:63; Khan et al., 2016:16-17). The *OCTR-ratios* convergence concept implies that the available resources must be distributed to respective users in such a way that the *OCTR-ratios* of all users converge. In other words, the resources assigned to users with higher *OCTR-ratios* must be reduced “progressively”; and the resources assigned to users with smaller *OCTR-ratios* must be augmented, until all the *OCTR-ratios* are virtually equal (Kumar et al., 2008:71; Wang et al., 2019:5). The maximum-minimum fairness concept, usually simplified as “*max-min fairness*” implies that initial power must be distributed to respective users according to their deserving share of available power. Thereafter, if some users are over-satisfied (i.e. $R_u > 1$), then their excess powers must be redistributed to unsatisfied users ($R_u < 1$), in order to improve their achievable *OCTR-ratios* (Keshav, 1997:215-217; Marsic, 2013:313-316; Le-Boudec, 2021:10).

Instead of selecting one concept to address the formulated intra-beam and inter-beam power-allocation problems, and thereafter, produce one global power-allocation algorithm for the described system; in this research, we propose to use each of the two concepts separately, to solve the formulated power-allocation problems and yield two global *PA* algorithms that each solves the original problem (F). This means that, we propose two distinct works in this research with respect to power-allocation design as follows:

- Work 1: We first use the *OCTR-ratios convergence* concept to solve both the intra-beam and inter-beam *PA* problems, and generate intra-beam and inter-beam *PA* algorithms. These two sub-algorithms are thereafter combined, to produce a global power-allocation algorithm which is a solution to original problem. The produced algorithm (*Global-Algorithm-1*) will be noted “system's *PA algorithm based on OCTR-ratios convergence*”
- Work 2: We then repeat the same exercise with the *maximum-minimum fairness concept*. The produced algorithm (*Global-Algorithm-2*) will be noted “system's *PA algorithm based on Max-Min fairness*”

Therefore, the output of this work with respect to power-allocation, will be two novel power-allocation algorithms to maximize the fairness of the described 2-users NOMA MBSNs. One algorithm based on the *OCTR-ratios convergence* concept and the other based on the *maximum-minimum fairness* concept.

The designs of two proposed PA algorithms are presented in Chapter-5 and Chapter-6 as follows. In Chapter-5, we discuss the design of the system's *PA algorithm based on OCTR-ratios convergence*; and present the resulting Algorithm. In Chapter-6, we discuss the design of the system's *PA algorithm based on Max-Min fairness*; and present the resulting Algorithm.

4.9. Chapter summary

This chapter provided the foundation for the design of the power-allocation subsystem (*PAS*) of the mobile network's MA encoder. It started by giving an overview of the *PAS*; including, its role, design goals and considerations, as well as its design requirements in this application. Since in this application, the design requirement of the *PAS* is to maximize the network's fairness, a link between the network's fairness, and users' *OCTR-ratios* and capacities, was established. Then, a model of the capacities of beam's users (C_{bn} and C_{bf}), in a 2-Users NOMA-MBSN, in term of both, the allocated beams' powers (P_b) and the intra-beam NOMA power-coefficient (α_b), was derived. Furthermore, considering the derived models, the requirement for a power-allocation process that maximizes the system's fairness, was formulated as an optimization problem. The original optimization problem is NP-hard; and was then decomposed into two sub-optimal problems; namely, the intra-beam and inter-beam fairness-maximization power-allocation problems. Finally, the chapter presented the two commonly used concepts for solving sub-optimal fairness-maximization power-allocation problems; namely, the *OCTR-ratios convergence* and the *Max-min Fairness* concepts. Each one of these concepts will be employed independently, to solve the two sub-optimal problems obtained, and yield two suboptimal power-allocation algorithms. These two algorithms will thereafter be combined to yield a global power-allocation algorithm, which solves the original problem. Chapter 5 and 6, respectively, present the generation of fairness maximization power-allocation algorithms, based on the *OCTR-ratios convergence* concept and the *Max-Min fairness* concept.

CHAPTER 5: POWER-ALLOCATION ALGORITHM BASED ON THE OCTR-RATIOS CONVERGENCE CONCEPT

5.1. Introduction

This chapter presents the design of our proposed power-allocation algorithm for system's fairness-maximization, based on the OCTR-ratios convergence concept. This is the first approach employed to design the power-allocation subsystem for the MA-Encoder block of the described network, which is highlighted in the block-diagram in Figure 5.1 below.

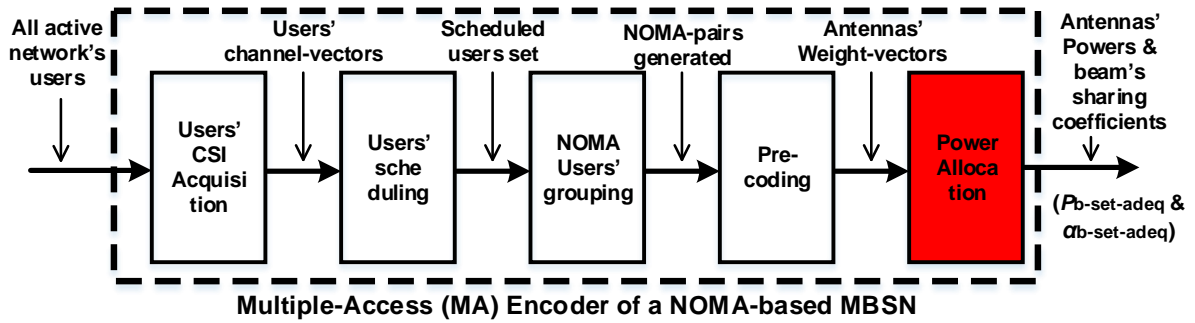


Figure 5.1: The Power-Allocation System in the MA-Encoder block

The rest of the chapter is outlined as follows. First, a description of the COTR-ratios convergence is given. This will be followed by detailed design discussion for the intra-beam power-allocation algorithm based on the OCTR-ratio convergence concept. Then, a detailed design discussion for the inter-beam power-allocation algorithm based on the OCTR-ratio convergence concept will also be given. Thereafter, the global power-allocation algorithm which combines the two sub-algorithms will be presented.

5.2. Description of the OCTR-ratios Convergence concept

The OCTR-ratio convergence concept is the most basic power-allocation approach for maximizing the system's fairness. It is an iterative search process which implies adjusting the power allocated to all users iteratively, until the gap between the OCTR-ratios of respective users becomes virtually 0; thus offering the most optimal system's fairness metric (Kumar et al., 2008:71; Wang et al., 2019:4). In other words, the power allocated to respective users is adjusted progressively, until all the OCTR-ratios converge towards the same value. The solution to this search process is the resulting powers-set that satisfies the OCTR-ratios convergence condition. This concept employs both the maximization of minimum OCTR-ratio and the minimization of maximum OCTR-ratio, in order to achieve a convergence of all OCTR-ratios. Generally, the minimum OCTR-ratio is first maximised, through increase of the user's allocated power; until either the convergence is achieved, or the user's power reaches its maximum. If the power reaches its maximum, which means the minimum OCTR-ratio cannot

be increased further; then the maximum *OCTR*-ratio starts to be minimised; through progressive decrease of its power; until the *OCTR*-ratios convergence is achieved. Therefore, based on the general computer programming logic, the execution of the *OCTR*-ratios convergence concept follows the step-flow outlined in Table 5.1 below.

Table 5.1: General step-flow of the *OCTR*-ratios Convergence concept

steps	actions
Step1:	Process initialization:
(a)	Receive: users' channel-vectors, users' demands, antennas' weight-vectors
(b)	Specify: initial users' powers, convergence-error, increment/decrement steps.
Step2:	Do iterative convergence search: increment or decrement of relevant user's power:
(i)	Receive the new power-set: from step1 (if first iteration), else from previous iteration;
(ii)	Evaluate the new <i>OCTR</i> -ratio of respective users based the new power-set received;
(iii)	Check for convergence of all <i>OCTR</i> -ratios; and if so, go to step3;
(iv)	If converge not achieved, check if the power of the user with minimum <i>OCTR</i> -ratio can still be incremented (i.e.: $P_u < P_{u-max}$ & $P_{tot-used} < P_{tot-sat}$):
	a) If YES: go to (v) below for user's power-increment;
	b) If NO: go to (vi) below for user's power decrement;
(v)	find the new-increment step-size and increase the power of user with minimum <i>OCTR</i> -ratio, to obtain a new power-set; then re-start step-2.
(vi)	find the new-decrement step-size and decrease the power of user with maximum <i>OCTR</i> -ratio, to obtain a new power-set; then re-start step-2.
Step3:	Terminate the process and Store the final power-set (i.e. relevant power to each user).

The techniques used to execute each of the above steps, can differ based on the designers' choices; or based on case-specific in which the concept is being used.

In this work, the *OCTR*-ratios convergence concept will be used in two cases as follows:

- i. for the design of the intra-beam *PA*-algorithm, so to maximize the beam's fairness; hence addressing the intra-beam fairness maximization problem (F_1).
- ii. for the design of the inter-beam *PA*-algorithm, so to maximize the inter-beam's fairness, hence addressing the inter-beam fairness maximization problem (F_2);

The designs these two power-allocation algorithms based on the *OCTR*-ratios convergence concept outlined above, are presented in the following section.

5.3. Intra-beam power-allocation algorithm design

5.3.1. Overview

The intra-beam power allocation process is particular to NOMA implementation. It is the process of determining how much share of the beam's power (P_b) should be given to each of the users sharing the same NOMA beam. As explained earlier, each user's share of the beam's power is determined by its coefficient (α); and the sum of all coefficients should be equal to 1. In the case of 2-users NOMA, where there are only two users per beam, namely, a near-user

and a far-user; there is only one coefficient per beam, called the intra-beam's power-sharing coefficient (α_b). This coefficient defines the near-user's share of beam's power, and the subtraction ($1-\alpha_b$) defines the far-user's share of beam's power. Subsequently, by assigning a value to the coefficient ($\alpha_b \in [0,1]$), one automatically defines the near-user's share (α_b) and far-user's share ($1-\alpha_b$) of the beam's power P_b . When the goal of the designed *PA*-algorithm is to maximize the beam's fairness as in this case, the allocation process consists of searching for the beam's power-sharing coefficient (α_{b-opt}) which maximizes the beam's fairness. When the algorithm design is based on the *OCTR*-ratios convergence concept, the intra-beam power allocation process implies, searching for the adequate shares of beam's power to respective users, which satisfies the *OCTR*-ratios convergence condition. In other words, searching the adequate value of the beam's power-sharing coefficient (α_{b-adeq}) which ensures that the *OCTR*-ratios of far- and near-users in the beam converge. Figure 5.2 below illustrates the focus of the intra-beam process, in the bigger picture of the network. In the figure below, only one arbitrary beam (b) is zoomed out (i.e. in red) for the purpose of illustration; but the same process occurs simultaneously in all the other beams.

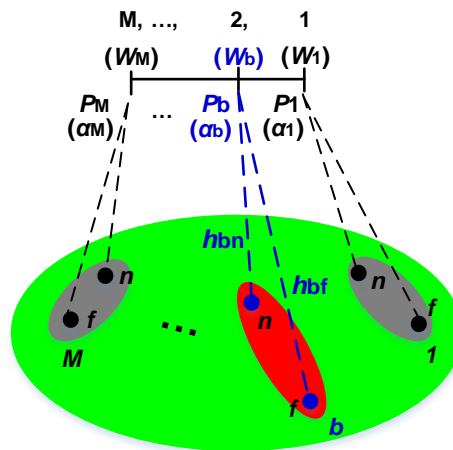


Figure 5.2: Illustration of the intra-beam power-allocation stage in a multi-beams satellite system.

Considering the design steps involved in the *OCTR*-ratios convergence concept as listed in Table 5.1 above, the design of the intra-beam power allocation algorithm based on *OCTR*-ratios convergence concept is presented in the following steps.

5.3.2. Step1: Process initialization

5.3.2.1. Input parameters definition

At this stage, all the input parameters necessary to perform the intra-beam power-allocation shall be known and well defined. It was indicated earlier that, fairness maximization implies adjusting the *OCTR*-ratio of each user in the beam. This in turn implies adjusting the offered

capacity of each user in the beam, through adjustment of their respective shares of the beam's power. Equations (4-13) and (4-19) provided models of the capacity of both the near- and far-users in each beam "b". These two models show that, in order to successfully perform intra-beam power adjustment through adjustment of the beam's power-sharing coefficient (α_b), it is necessary to know the following parameters:

- D_{bn} , D_{bf} , h_{bn} , h_{bf} , w_b , P_b and respective P_{b^*} of all other beams ($b^* \neq b$).

With all these parameters defined at the beginning of the intra-beam power adjustment process, the only adjustable variable in the presented capacity models of near- and far-users, will be the NOMA coefficient " α_b ". Thus, as said earlier, the adjustment of C_{bn} and C_{bf} ; and subsequently of R_{bn} and R_{bf} , becomes a single variable problem of " α_b ".

5.3.2.2. Notion of OCTR-ratios convergence within a beam

When using the OCTR-ratio convergence concept, the ultimate goal of the intra-beam power-shares determination is to ensure that the OCTR-ratios of both users are equal; that is, to obtain the condition $R_{bn} = R_{bf}$. This implies to obtain the condition:

$$R_{bn} - R_{bf} = 0; \quad (5-1)$$

or otherwise,

$$D_{bf} \times C_{bn} - D_{bn} \times C_{bf} = 0 \quad (5-2)$$

From the observations outlined earlier in 4.7.4, which are supported by the graph in Figure 4.2 above, it can be seen that, as " α_b " varies between 0 and 1, the capacities of near- and far-users are varying inversely to each other between 0 and their respective maximums. This implies that, there will always be an " α_b " for which the two capacities are equal; that is, $C_{bn} - C_{bf} = 0$. Subsequently, since D_{bn} and D_{bf} are positive constants, there will always be a " α_b " for which $D_{bf} \times C_{bn} - D_{bn} \times C_{bf} = 0$. This is supported by the Figure 4.2. Therefore, there will always be a " α_b " that satisfies the condition $R_{bn} - R_{bf} = 0$; or stated otherwise, $R_{bn} = R_{bf}$. However, because the users' capacities are logarithmic functions of " α_b ", it is hard to solve equation (5-2) by means of analytical calculations. Consequently, the determination of the value of " α_b " which is a solution to the equation is often done by means of numerical search-methods.

In numerical search-methods, the idea is generally to step " α_b " through a range of values, and verify in each step whether the condition in equation (5-1) is satisfied. However, in computer implementation, due to data resolution and step-size issues, it is extremely hard to always

achieve the exact equality condition $R_{bn} - R_{bf} = 0$; as that may require an infinitely running process. Therefore, to alleviate this difficulty, the notion of convergence is generally employed. In essence, instead of checking the equality condition in equation (5-1) at each search-step, the idea is to check whether the two terms converge. That is, we check if the difference of the terms is less than some define error, often called convergence-error (ce):

$$|R_{bn} - R_{bf}| < ce \quad (5-3)$$

Thus, it is crucial to carefully decide the convergence-error, increment step-size as well as the decrement size; because these parameters critically influence the time performance of the resulting algorithm.

5.3.2.3. Convergence error definition

The definition of the convergence-error for power-allocation process is dependent on a number of system specifications. In this application, as it will be presented later in the simulation section, the users' traffic requests are assumed to be in the range of 0.1 to 10 bps/Hz; and the achievable capacities of users are in practice usually greater than 0.1 bps/Hz. Thus, from this observation, it is reasonable to estimate that, the minimum possible *OCTR*-ratio in the worst case scenario, would be of the order $(0.1/10) = 0.01$. On feasibility, there do not seem to be a possible practical case where the *OCTR*-ratio of a user would be less than 0.01. For this reason, we opt to use the value of 0.01 as the sensitivity of the *OCTR*-ratio; and we subsequently set the convergence-error to be $ce = 0.01$. This therefore means that, we will consider that the *OCTR*-ratios within the beam are converging when their difference is less than 0.01. Note however that, if the extreme conditions assumed for the maximum traffic request (10bps/Hz) and minimum offered capacity (0.1bps/Hz) are relaxed, the convergence-error (ce) could be increased; and that will improve the convergence time of the algorithm.

5.3.2.4. Increment and decrement step-sizes:

In this concept, the search for the optimal shares of the beam's power amongst beam's users to yield the desired convergence point (i.e. almost equal *OCTR*-ratios), involves both the maximization of minimum *OCTR*-ratio and the minimization of the maximum *OCTR*-ratio. This therefore, means that, it is a search process which will oscillate around the optimal point. This search process is equivalent to the numerical step-search methods such as "steepest ascent" and "steepest descent" often used for optimal point search. These numerical search methods, mostly use a variable step-size, which progressively decreases every time the search crosses the optimal point. We therefore, opt to employ a variable step-size. We propose the following regarding the specification of the increment and decrement step-sizes:

- a) to start with an arbitrary “initial step-size ($Step_{init}$)” towards the direction of the optimal point;
- b) then, divide the step-size by 2 at every cross-over of the optimal point;
- c) continue the process until the convergence-error is satisfied.

We have defined the initial step-size ($Step_{init}$) to be a function of both the “gap between the two OCTR-ratios” as well as the initial power share “ α_{b-init} ”, as follows:

$$Step_{init} = 0.3\alpha_{b-init}, \quad \text{if } diff(R_{bn}, R_{bf}) > 2 \quad (5-4a)$$

$$Step_{init} = 0.2\alpha_{b-init}, \quad \text{if } 1 < diff(R_{bn}, R_{bf}) < 2 \quad (5-4b)$$

$$Step_{init} = 0.1\alpha_{b-init}, \quad \text{if } diff(R_{bn}, R_{bf}) < 1 \quad (5-4c)$$

From this initial step-size, a new step size ($Step_{new}$) will be determined for every iteration as follows. If the search direction for next iteration remains same as that of previous iteration, then the step-size will remain the same. However, if the search direction will have to change from that of the current iteration, then the new step-size will be calculated as half of the previous step-size. Thus, the determination of the new step-size for the next search iteration is dependent on whether the search direction will have to change in the next iteration. A general expression of the increment or decrement step-size at any iteration during the search process can be derived as follows:

$$Step_{new} = Step_{prev}, \quad (\text{if search direction is same}) \quad (5-5a)$$

$$Step_{new} = Step_{prev} / 2 \quad (\text{if search direction changed}) \quad (5-5b)$$

Where, the “ $Step_{prev}$ ” is function of the initial-step-size and number of times “ k ” that the search has changed the direction, and can be expressed as:

$$Step_{prev} = Step_{init}, \quad \text{if } k = 0; \quad (5-6a)$$

$$Step_{prev} = \frac{Step_{init}}{2^{(k-1)}}, \quad \text{if } k > 0, k \text{ is an integer.} \quad (5-6b)$$

5.3.2.5. Initial power-set definition for the intra-beam power-allocation

At the start of the intra-beam power allocation process, the available beam’s power (P_b) must first be shared equally between the two users. This implies, to start by setting “ α_b ” to an initial value (α_{b-init}) that ensures both users receive the same share of the beam’s power. Our interpretation of this request is that, the two users should be able to “receive at their terminals”, the same amount of power, from the beams power (P_b). Thus, to determine the initial “ α_{b-init} ”

for which both users receive same share of power at their respective terminals, the following is done. Consulting equations (4-13) and (4-19), the numerators represent the intended power received by each terminal, while the denominators represent the interference powers and noise. Thus, it can be written that:

$$P_{\text{rx-bf-intended}} = |h_{\text{bf}}^H w_b|^2 P_b (1 - \alpha_b) \quad (5-7a)$$

$$P_{\text{rx-bn-intended}} = |h_{\text{bn}}^H w_b|^2 P_b \alpha_b \quad (5-7b)$$

If these two powers are the same; that is, $P_{\text{rx-bn-intended}} = P_{\text{rx-bf-intended}}$, it results:

$$|h_{\text{bf}}^H w_b|^2 P_b (1 - \alpha_b) = |h_{\text{bn}}^H w_b|^2 P_b \alpha_b \quad (5-8)$$

Which subsequently leads to:

$$\alpha_{\text{b-init}} = \frac{|h_{\text{bf}}^H w_b|^2}{|h_{\text{bn}}^H w_b|^2 + |h_{\text{bf}}^H w_b|^2} \quad (5-9)$$

With this value of “ α_b ”, i.e. $\alpha_b = \alpha_{\text{b-init}}$, both the near-user and far-user of the beam “ b ” will receive same share of their beam’s power “ P_b ” at their respective terminals. This value of “ α_b ” represents the initial shares of beam-power between the far- and near user; and it will be sent to “Step-2” to commence the iterative intra-beam power-share adjustment process.

5.3.3. Step2: Iterative Convergence Search

Based on the initial power-set defined in “Step-1”, this step initiates the search process and continues it iteratively, until the convergence of OCTR-ratios of the near- and far-user is achieved. Following the steps outlined in Table 5.1 above, the search process in this step (Step-2) will be as follows:

5.3.3.1. Step2-a: Receive the new value of “ α_b ”

At this point, the new value of “ α_b ” is received, for the execution of a new iteration search. If this process is in its first iteration, this value will be coming from the “process initialization” process, i.e. “Step-1”. Otherwise, this new value of “ α_b ” will be coming from the previous iteration of the search process, i.e. “Step-2 (v or vi)”.

5.3.3.2. Step2-b: Evaluate the *OCTR*-ratios R_{bn} and R_{bf} based on received “ α_b ”

Using the new “ α_b ” received, the values of *SINR* for the near- and far-user will be calculated as in equations (4-13) and (4-19) respectively. Then, their resulting capacities (C_{bn} and C_{bf}) will be calculated as in equation (4-5). Thereafter, their *OCTR*-ratios (R_{bn} and R_{bf}) will be calculated according to equation (4-3).

5.3.3.3. Step2-c: Check for *OCTR*-ratios convergence

Using the calculated *OCTR*-ratios (R_{bn} and R_{bf}), the gap between them will be calculated and it will be compared to the convergence-error (ce) defined, as in equation (5-3); in order to establish whether the convergence has been reached or not. If the convergence has been achieved, no need to do any further adjustment of the beam’s power-sharing coefficient (α_b). This search loop must then be exited and the algorithm should go to Step-3, to terminate the intra-beam power allocation process. However, if convergence is not met, the search must proceed in the next step (step2-d) below.

5.3.3.4. Step2-d: Check if power-share of minimum *OCTR*-ratio can still be increased

If the convergence is not achieved, the user that has the minimum *OCTR*-ratio between the near- and far-user should be identified; and it should be checked whether it is possible to increase its share of power. In the case of the intra-beam power sharing, the available beam’s power is shared entirely amongst the beam’ users in an exclusive manner. Consequently, as illustrated in Figure 4.2 above, a decrease in the share of one user automatically leads to an increase in the share of other users. Thus, here, the situation will always be the need to increase the power share of the user with minimum *OCTR*-ratio; which then also directly means, the decrease of the power share of user with better *OCTR*-ratio. Again, as illustrated by Figure 4.2, if the near user has the minimum *OCTR*-ratio, then the current power-share (α_b) should be incremented, in order to increase the near-user’s capacity. Alternatively, if the far user has the minimum *OCTR*-ratio, then the current power-share (α_b) should be decremented, in order to increase the far-user’s capacity. Therefore, here, the exercise is rather to check which of the near or far-user in the beam has the minimum *OCTR*-ratio.

5.3.3.5. Step2-e: Increment “ α_b ” if applicable:

If the near user has the minimum *OCTR*-ratio in the beam, then the current intra-beam beam-power share “ α_b ” should be incremented; and thus, a new step-size need to be evaluated to perform the required increment. To determine the new step-size, it is necessary to first determine the new search direction, whether it should be the same as last direction or it should change. To identify what the direction should be, we check whether the “optimal point” has

been crossed or not. This is done by comparing the user with the current minimum ratio and the user with the previous minimum ratio. If it is the same user, it means that the optimal point has not yet been crossed. Therefore, the search must continue in the same direction and the step-size remains the same. But, if the user with minimum ratio has changed, it means that, the optimal point has been crossed. Thus, the search direction must change and the new step-size must be determined, by dividing the previous step-size by 2. The general formula for determining the new step-size at every iteration was presented in equation (5-5) above, and will therefore, be used to find the new step-size. Once the new step-size is determined, the incrementing of the current value of " α_b " will be performed and its value " $\alpha_{b\text{-new}}$ " for next iteration will be calculated as:

$$\alpha_{b\text{-new}} = \alpha_b + Step_{\text{new}} \quad (5-10)$$

5.3.3.6. Step2-f: Decrement " α_b " if applicable:

If the far user has the minimum *OCTR*-ratio in the beam, then the current intra-beam beam-power share " α_b " should be decremented. Thus, a new step-size need to be evaluated to perform the required decrement. The determination of the new step-size is as discussed in "Step2-e" (i.e. 5.3.3.5). Once the new step-size is determined, the decrementing of the current value of " α_b " will be done and its value " $\alpha_{b\text{-new}}$ " for next iteration will be calculated as:

$$\alpha_{b\text{-new}} = \alpha_b - Step_{\text{new}} \quad (5-11)$$

5.3.4. Step3: Terminate the search process and determine the beam's *OCTR*-ratio

In this step, the intra-beam search process will basically be terminated, and the intra-beam power allocation results will be stored. These include, the optimal intra-beam power-sharing coefficient " $\alpha_{b\text{-opt}}$ " obtained, the resulting capacities for near- and far-users (C_{bn} and C_{bf}), as well as their *OCTR*-ratios (R_{bn} and R_{bf}).

Also, noting that each beam will be represented by a unique *OCTR*-ratio for the purpose of inter-beam power allocation, the beam's *OCTR*-ratio must be decided by considering the resulting *OCTR*-ratios of the respective beam's users. Since the power allocation concept used in this section was the *OCTR*-ratio convergence, at this point, all *OCTR*-ratios of beam's users should have converged; that is, they are all relatively equal. Thus, the exercise of deciding the beam's *OCTR*-ratio become fairly simple, as the converged value for the *OCTR*-ratios, obtained from the process, will simply represent the beam's *OCTR*-ratio.

5.3.5. Resulting intra-beam PA-algorithm based on OCTR-ratios convergence concept

Following all the steps from the above discussion, the resulting intra-beam power-allocation algorithm based on the OCTR-ratios convergence concept, for fairness maximization within a 2-users NOMA beam, is summarised in Table 5.2 below.

Table 5.2: Proposed Intra-beam PA Algorithm for 2-users NOMA, based on the OCTR-ratios Convergence Concept

Algorithm 5.1: Proposed Intra-beam PA Algorithm for 2-users NOMA, based on OCTR-ratios Convergence Concept		
steps	lines	actions
Step1:		Process initialisation:
(a)	1:	Receive: $H, D, W, P_b\text{-set}$,
(b)		Specify:
	2:	$\alpha_{b\text{-init}}$, as in equation (5-9)
	3:	$ce = 0.01$, as discussed in step1-c.
	4:	$Step_{init}$, as in equation (5-4)
Step2:		Iterative Convergence Search Process:
repeat		repeat:
(a)	5:	Receive the new value of " $\alpha_{b\text{-new}}$ ";
(b)	6:	Evaluate the R_{bn} & R_{bf} using " $\alpha_{b\text{-new}}$ " based on equations (4-13), (4-19), (4-5) & (4-3);
(c)	7:	Check for OCTR-ratios convergence as in equation (5-3); and if Yes, go to Step-3.
(d)	8:	If no convergence, identify $\min(R_{bn}, R_{bf})$;
(e)		If R_{bn} is min: => increase α_b
	9:	Calculate $Step_{new}$ according to equation (5-5),
	10:	Calculate $\alpha_{b\text{-new}}$ according to equation (5-10),
	11:	Return to start of Step-2.
(f)		If R_{bf} is min: => decrease α_b
	13:	Calculate $Step_{new}$ according to equation (5-5),
	14:	Calculate $\alpha_{b\text{-new}}$ according to equation (5-11)
	15:	Return to start of Step-2.
Until		Until: OCTR-ratios convergence is obtained
Step3:		terminate the search process and determine "R_b" and also store "$\alpha_{b\text{-adeq}}$".

5.4. Inter-beam power-allocation algorithm design

5.4.1. Overview

In a general sense, the inter-beam power allocation is the process of determining the amount of power to be given to respective antennas of the access-point, in order to maximise the desired utility of the network. When the goal of the power-allocation block is to maximise the system's fairness, the inter-beam power allocation then consists of finding the adequate powers to be allocated to respective antennas, such as to maximise the fairness between all the beams. Subsequently, when the design concept used for the power-allocation system is the OCTR-ratios convergence, the inter-beam power allocation process implies, searching for the adequate set of powers that should be assigned to respective antennas, so that the OCTR-

ratios of all the beams converge. Figure 5.3 below gives an illustration of the inter-beam power allocation process. In this process, the access-point (i.e. the satellite in this case) with M -antennas, sees each beam (b) as a homogenous end-user, to whom a certain beam's power (P_b) was given through its antenna; and which in return, exhibits a certain *OCTR*-ratio (R_b). Consequently, the inter-beam *PA* process does the adjustment of respective beam's powers, by conserving purely, the *OCTR*-ratios of respective beams. It is highly important to note that, during the power adjustment process, because of a high number of beams, it is very hard to adjust the powers to all the beams simultaneously and expect a deterministic outcome. Therefore, to avoid this complexity, we propose to adjust the power of only one beam at the time (i.e. per search iteration); and the powers to all the other beams are kept constant. In this case, as discussed in section 4.7.3, it will be much simpler to adjust the *OCTR*-ratio (R_b) in the designated beam (b), through adjustment of its beam's power (P_b).

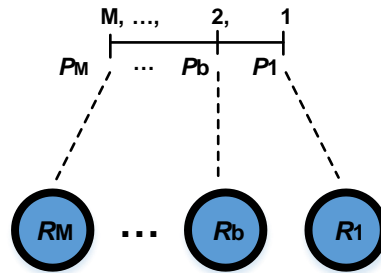


Figure 5.3: Illustration of inter-beam power-allocation stage

Considering the design steps involved in the *OCTR*-ratios convergence concept, as listed in Table 5.1 above, the design of the inter-beam power allocation algorithm based on the *OCTR*-ratios convergence concept is presented in the following steps.

5.4.2. Step1: Process initialization

5.4.2.1. System's power budget specification

Since the inter-beam power-allocation only considers the powers allocated to respective beams (P_b), as well as their resulting *OCTR*-ratios (R_b), to initiate the inter-beam *PA* process, it is necessary to specify power-related parameters such as, the total power available on the satellite ($P_{\text{tot-sat}}$), the maximum possible power beam's power ($P_{b\text{-max}}$) as well as the initial powers allocated to each beam ($P_{b\text{-init}}$).

Generally, the total power on the satellite and the maximum possible beam's power, must first be known and specified. Thereafter, based on the specified total satellite's powers, the maximum beam's power, and on the number of satellite's antennas, the initial power to assign

to each antennas ($P_{b\text{-init}}$) must be defined. The combination of all the " $P_{b\text{-init}}$ " into one power-vector gives the initial power-set described as:

$$P_{b\text{-set-init}} = [P_{1\text{-init}}, P_{2\text{-init}}, \dots, P_{M\text{-init}}] \quad (5-12)$$

In this work, we opt to start by assigning the same value of initial power ($P_{b\text{-init}}$) to all antennas; which is half of the maximum beam-power ($P_{b\text{-max}}$), that is, $P_{b\text{-init}} = \frac{1}{2}P_{b\text{-max}}$. Then, we generate the initial set of beams' power ($P_{b\text{-set-init}}$) as indicated in equation (5-12) here above. Thereafter, this initial " $P_{b\text{-set-init}}$ " is passed down to the "*iterative search-stage (step2)*" of the power-allocation process; to initiate and execute the inter-beam power-allocation search.

As outlined in the design steps-flow in Table 5.1 above, Step2, will start by determining the *OCTR*-ratio of each beam based on the beam's power-set provided. Then, the *OCTR*-ratios convergence will be checked; and thereafter, the decrement or increment of appropriate beam's power will be done. It is therefore, necessary to specify parameters such as the convergence-error (*ce*) against which the *OCTR*-ratios convergence will be checked; as well as the beam-power's increment or decrement step-size ($P_{b\text{-inc}}$, $P_{b\text{-dec}}$). These parameters are discussed in the following points.

5.4.2.2. Notion of *OCTR*-ratios Convergence in the context of inter-beam

When trying to solve the problem (F_2) by means of the *OCTR*-ratios convergence concept, the idea consists of adjusting the powers given to respective beams in order to increase the minimum *OCTR*-ratio amongst the beams, until the *OCTR*-ratios of all the beams converge. The *OCTR*-ratios convergence in this context of inter-beam system can be checked by successively checking the convergence between adjacent beams, as:

$$R_b - R_{b-1} = 0 ; \text{ for } b \geq 2 \text{ and } b \in M; \quad (5-13a)$$

$$R_b - R_{b-1} < ce ; \text{ for } b \geq 2 \text{ and } b \in M. \quad (5-13b)$$

Alternative, a more efficient way to check the convergence across all the beams, would be by checking the convergence between the maximum ($R_{b\text{-max}}$) and minimum ($R_{b\text{-min}}$) *OCTR*-ratios across all beams, as:

$$R_{b\text{-max}} - R_{b\text{-min}} = 0 \quad (5-14a)$$

$$R_{b\text{-max}} - R_{b\text{-min}} < ce \quad (5-14b)$$

Achieving the convergence would mean that the minimum *OCTR*-ratio amongst all beams has been maximized; and as such, the inter-beam fairness has been optimally maximized. As

discussed earlier in section 4.7.3, the capacity of each beam (b) and thus its *OCTR*-ratio (R_b), can be increased in two ways; either by increasing the beam's power (P_b), or by decreasing interference from other beams, through decrease of their powers. And Wang et al., (2019:4-5) further demonstrated that, it is easier to increase the beam's capacity by increasing its own power, rather than by decreasing other beams' powers. Therefore, based on these considerations, the inter-beam power-allocation process will consist of two major search phases in this work, in order to increase $R_{b-\min}$ amongst all beams until all *OCTR*-ratios converge. One phase will be to first increase the power of beam with $R_{b-\min}$ progressively, until either the convergence is achieved, or the constraints of problem (F_2) have been reached. In case the power of the beam with $R_{b-\min}$ can no longer be increased due to the constraints set, the other search phase will then be to progressively decrease the power of the beam with $R_{b-\max}$, until the convergence is achieved. Note that, since the ultimate goal in this concept is to achieve convergence no matter what, it does not put any limitation to how low the power of the beam with $R_{b-\max}$ can be reduced. These two phases, namely, the increasing of power of beam with $R_{b-\min}$, and the decreasing of power of the beam with $R_{b-\max}$, are performed iteratively, until the *OCTR*-ratios of all beams converge, and the resulting adequate set of antenna powers is stored.

Again, as stated before, because the above inter-beam power allocation process is a numerical step-search method which is looking for a convergence point, it is critically necessary to specify a convergence-error (ce) and a step-size ($P_{b-\text{inc}}$, $P_{b-\text{dec}}$), so that the search does not result in an infinite process.

5.4.2.3. Convergence-error definition

Similar to the discussion presented earlier in section 5.3.2.3 above, for the inter-beam power-allocation process, we maintain an *OCTR*-ratios convergence-error (ce) of 0.01, for the same reasons outlined earlier.

5.4.2.4. Beam's power increment step-size definition

In the inter-beam power allocation, the powers allocated to respective antennas are adjusted progressively. In this work, as explained above, we choose to adjust the power of only one beam at the time; that is, either the beam with minimum *OCTR*-ratio (i.e. increase the beam's power), or the beam with maximum *OCTR*-ratio (i.e. decrease the beam's power).

In numerical step-search methods, the step-size is usually dependent on both the search direction around the optimal point, as well as the estimated distance to the optimal point. In this case of the inter-beam power-allocation process based on the *OCTR*-ratio convergence,

the idea is to iteratively increase $R_{b-\min}$ across all beams or iteratively decrease $R_{b-\max}$ across all beams. Thus, we propose to define for both directions (increment and decrement), a step-size which is proportional to the gap between $R_{b-\max}$ and $R_{b-\min}$ in every iteration. At the end of each iteration, a new step-size for either the beam's power increment or the beam's power decrement, should be defined; in order to calculate the new beam's power and thus produce the new power-set for the next search iteration.

Therefore, to define the new beam's power increment-step-size at end of every iteration (when applicable), we consider the following points.

Point1: identify the maximum beam's power increment possible ($P_{b-inc-max}$):

we consider that at the start of the power-allocation process, all the beams are given the same power (P_{b-init}) which is half of the maximum beam power (P_{b-max}):

$$P_{b-init} = 1/2 P_{b-max} \quad (5-15)$$

Then, based on this, since the maximum possible beam power is P_{b-max} , it results that, the maximum possible power-increase for any beam is then the remaining half of P_{b-max} , as illustrated in Figure 5.4 (a) below.

$$P_{b-inc-max} = P_{b-max} - P_{b-init} = 1/2 P_{b-max} \quad (5-16)$$

Point2: identify the maximum gap possible between beam's OCTR-ratios (Gap_{max}):

After initially assigning all beams with same power ($P_{b-init} = 1/2 P_{b-max}$), we will obtain a set of OCTR-ratios from respective beams; and we will have an initial gap between $R_{b-\min}$ and R_{b-max} from the set. We then consider that, this initial gap (Gap_{init}) represents the maximum possible gap (Gap_{max}) that will exist between any $R_{b-\min}$ and R_{b-max} throughout the allocation process; since the purpose of the allocation process is to minimise this gap. This is illustrated in Figure 5.4 (b) below. Thus, we can write:

$$Gap_{max} \Rightarrow Gap_{init} \quad (5-17)$$

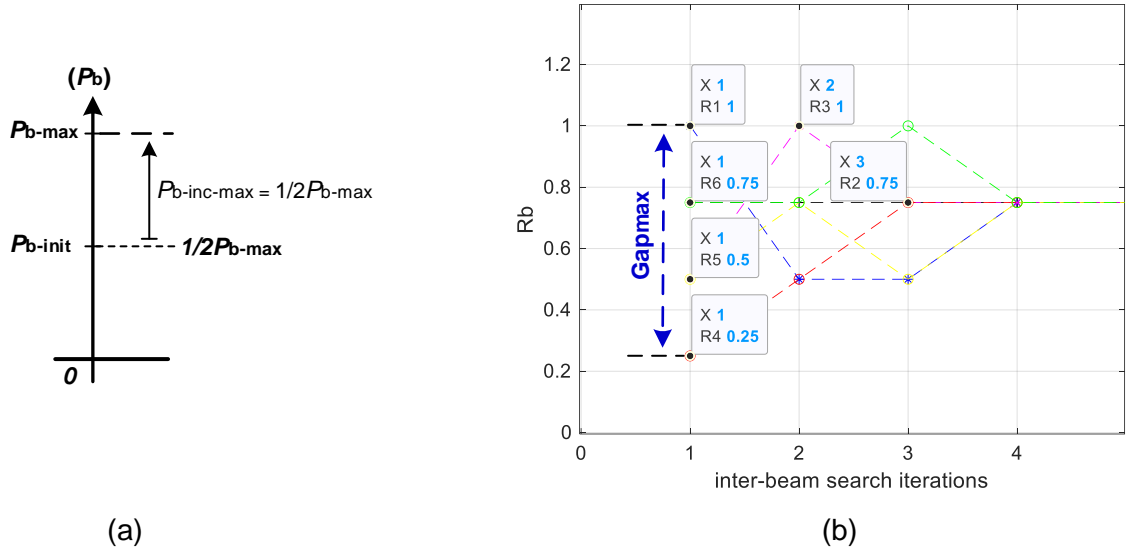


Figure 5.4: Illustration of: (a) the max possible beam's power increment ($P_{b-inc-max}$); (b) the maximum possible OCTR-ratios gap (Gap_{max}).

Point3: identify the needed beam's power increment ($P_{b-inc-nec}$):

From the above two points, we subsequently consider that, the maximum gap possible between beam's OCTR-ratios (i.e. Gap_{max}) induces a need for the maximum beam's power increment possible ($P_{b-inc-max}$) in order to improve R_{b-min} considerably. That is:

$$Gap_{max} \Rightarrow P_{b-inc-max} \quad (5-18)$$

Thus, from the three considerations above, we derive at every iteration, the current beam's power increment needed ($P_{b-inc-nec}$) for the next search, based on the current gap (Gap_{cur}) between R_{b-max} and R_{b-min} , as:

$$P_{b-inc-nec} = \left(\frac{Gap_{cur}}{Gap_{max}} \right) P_{b-inc-max} \quad (5-19)$$

Which, can be re-written based on equations (5-16) and (5-17) as:

$$P_{b-inc-nec} = \left(\frac{Gap_{cur}}{Gap_{init}} \right) \left(\frac{1}{2} \right) P_{b-max} \quad (5-20)$$

Point 4: identify the acceptable beam-power increment ($P_{b-inc-acc}$):

After determining the necessary increment for the beam's power (i.e. $P_{b-inc-nec}$) from above points, we then consider that, the beam's power increment in this power-allocation process is subject to the constraints of the inter-beam fairness maximization problem (F_2) as outlined in

equations (4-24b) and (4-24c). Therefore, in each iteration, before performing any possible increment of the beam's power for $R_{b-\min}$, we consider both, the remaining power-available for this beam ($P_{b-\text{avail}}$) as well as the remaining total power available on the satellite ($P_{\text{tot-avail}}$); which are both determined respectively as:

$$P_{b-\text{avail}} = P_{b-\text{max}} - P_{b-\text{cur}} \quad (5-21)$$

$$P_{\text{tot-avail}} = P_{\text{tot-sat}} - \sum_{b=1}^M P_{b-\text{cur}} \quad (5-22)$$

Since the power increment is subject to these two limitations, we determine the acceptable beam-power-increment ($P_{b-\text{inc-acc}}$) based on these two limitations. It follows that we could be confronted with the two following limiting scenarios.

- a) It could happen that, the beam can still accept a large power increase, but there is no more enough power on the satellite; meaning that $P_{\text{tot-avail}} < P_{b-\text{avail}}$. In this case, the acceptable beam's power increase ($P_{b-\text{inc-acc}}$) will only be up to remaining power available on the satellite (i.e. $P_{\text{tot-avail}}$).
- b) Alternatively, it could happen that, there is a large amount of power still available on the satellite, but the designated beam can now only accept a limited increase; meaning that $P_{b-\text{avail}} < P_{\text{tot-avail}}$. In this case, the acceptable beam's power increase ($P_{b-\text{inc-acc}}$) will only be up to the remaining power available in the beam (i.e. $P_{b-\text{avail}}$).

Thus, from these two scenarios, we derive the expression of the acceptable beam's power-increment ($P_{b-\text{inc-acc}}$) at every iteration, as:

$$P_{b-\text{inc-acc}} = \min\{P_{b-\text{avail}}, P_{\text{tot-avail}}\} \quad (5-23)$$

Point5: determine the new beam's power increment ($P_{b-\text{inc-new}}$) for the next iteration

In "point3" above, we have determined the currently needed beam's power increment ($P_{b-\text{inc-nec}}$) for $R_{b-\min}$, based on the current gap (Gap_{cur}) between $R_{b-\text{max}}$ and $R_{b-\min}$ across all beams. Furthermore, since in the optimization problem being solved by this algorithm, the power increase is subject to power constraints; in "point4" above, we determined the beam's power increment that can be accepted currently ($P_{b-\text{inc-acc}}$), given the power availability on both the beam with $R_{b-\min}$ and the satellite. Therefore, from these two parameters, we determine what should be the new beam's power-increment to be used for next search iteration, by comparing the two. If the needed beam's power increase is less than the

acceptable beam's power increase, then the new beam's power increment ($P_{b\text{-inc-new}}$) is the needed beam's power increase ($P_{b\text{-inc-nec}}$). Alternatively, if the acceptable beam's power increase is less than the needed beam's power increase, then $P_{b\text{-inc-new}}$ is the acceptable beam-power increase ($P_{b\text{-inc-acc}}$). Subsequently, we can write:

$$P_{b\text{-inc-new}} = \min\{P_{b\text{-inc-nec}}, P_{b\text{-inc-acc}}\} \quad (5-24)$$

5.4.2.5. Beam's power decrement step-size definition

Similar to previous discussion concerning the beam's power increment step-size calculation at every iteration; to determine the decrement step-size at the end of every iteration (where necessary), we still employ the considerations made in "point-1" and "point-2" of the section 5.4.2.4 above. Subsequently, based on these considerations, we formulate an expression of the necessary beam-power decrement ($P_{b\text{-dec-nec}}$) as a function of the current gap (Gap_{cur}) between $R_{b\text{-max}}$ and $R_{b\text{-min}}$ across all beams, the maximum possible gap (Gap_{max}) and the current power of the beam with $R_{b\text{-max}}$, which we denote $P_{b\text{-max-octr-ratio}}$:

$$P_{b\text{-dec-nec}} = \left(\frac{Gap_{cur}}{Gap_{max}}\right) \left(\frac{1}{2}\right) P_{b\text{-max-octr-ratio}} \quad (5-25)$$

Which can also be written in terms of the initial OCTR-ratios gap (Gap_{init}):

$$P_{b\text{-dec-nec}} = \left(\frac{Gap_{cur}}{Gap_{init}}\right) \left(\frac{1}{2}\right) P_{b\text{-max-octr-ratio}} \quad (5-26)$$

Then, since there are no constraints for power decrease in the OCTR-ratio convergence concept, there is no requirement to limit the decrease of power for the beam with $R_{b\text{-max}}$. Therefore, the only limit is 0. Consequently, the new beam's power decrement ($P_{b\text{-dec-new}}$) will simply take the calculated value of the necessary beam's power decrement ($P_{b\text{-dec-nec}}$), as:

$$P_{b\text{-dec-new}} = P_{b\text{-dec-nec}} \quad (5-27)$$

With all the above elements defined, the iterative inter-beam power-search for the convergence of OCTR-ratios, can then be executed adequately in step2.

5.4.3. Step2: Iterative convergence search process

After receiving all input parameters and setting up all necessary initial parameters in Step1, the inter-beam power-allocation search process will be executed iteratively as discussed in the steps below. As indicated in section 5.4.1 above, in this work, we propose to adjust the power

(P_b) of only one beam (b) at the time (i.e. in each search iteration) and keep the respective powers to other beams constant.

5.4.3.1. Step2-a: Receive the new beam's powers set ($P_{b\text{-set-new}}$)

At this point, the new beams' powers set ($P_{b\text{-set-new}}$) consisting of the new powers to respective beams (P_b) is received for the execution of a new iteration for *OCTR*-ratios convergence search. If this process is in its first iteration, this $P_{b\text{-set-new}}$ will be coming from the "process initialization" process, i.e. "Step-1". Otherwise, $P_{b\text{-set-new}}$ will be coming from the previous iteration of the search process, i.e. "Step-2 (e or f)".

5.4.3.2. Step2-b: Evaluate *OCTR*-ratios of respective beams (R_b)

From the new power-set, each beam ($b, b = 1, 2, \dots, M$) will receive its designated power (P_b); and from it, the new *OCTR*-ratio of the beam (R_b) will be evaluated. Then the set of new *OCTR*-ratios from the respective M -beams of the satellite will be obtained as:

$$R_{b\text{-set}} = [R_1, R_2, \dots, R_M] \quad (5-28)$$

5.4.3.3. Step2-c: Check for *OCTR*-ratios convergence

Using the new set of *OCTR*-ratios obtained from above step, $R_{b\text{-min}}$ and $R_{b\text{-max}}$ will be identified from the set. Then the gap between them will be calculated and it will be compared to the convergence-error (ce) defined, as in equation (5-14a); in order to establish whether the convergence has been reached or not. If the convergence has been achieved, it means that, the new received power-set is adequate for achieving optimal inter-beam's fairness. Therefore, no further power adjustment is necessary, and the algorithm must exist this search loop (i.e. "Step-2") and go to "Step-3" to terminate the inter-beam power-allocation process. However, if the convergence is not obtained, the search will proceed to point (d) below.

5.4.3.4. Step2-d: Check whether the beam' power for $R_{b\text{-min}}$ can still be increased

After determining that the convergence is not yet achieved, the current power ($P_{b\text{-cur}}$) of the beam with $R_{b\text{-min}}$ will be identified. Then it will be checked whether this beam-power can still be increased. To check this, we basically verify two power-availability conditions consecutively:

Verification-1: Has the current beam-power ($P_{b\text{-cur}}$) reached the maximum possible beam's power ($P_{b\text{-max}}$)?

This is verified by simply checking if current beam's power (P_{b-cur}) is less than P_{b-max} . If the answer to this verification is "YES", it means that, the power of this beam can no more be increased. In this case, the "Verification-2" will not be done; and the search will skip "Step2-e", and then go to "Step2-f" to decrease the power of beam with R_{b-max} . But, if the answer to this verification is "NO", it means that, the power of this beam can still be increased; and the "Verification-2" must then be done.

Verification 2: Is there still any power available on the satellite?

This is verified by simply checking if the total power currently used ($P_{tot-cur}$) is less than the total power on the satellite ($P_{tot-sat}$). If the answer to this verification2 is "YES", it means that there is still some power that can be given to the beam with R_{b-min} ; and as such, the search process will go to "Step2-e" below, to increase the power of R_{b-min} for the next iteration. However, if the answer is "NO", it will mean that, there is no more power that can be given to beam with R_{b-min} ; and as such, the power of the beam with R_{b-max} should be decreased. In this case, the search process will skip "Step2-e" (i.e. section 5.4.3.5 below) and go to "Step2-f" (i.e. section 5.4.3.6) to decrement the power of the beam with R_{b-max} , for the next iteration.

5.4.3.5. Step2-e: Determine $P_{b-inc-new}$ and calculate new P_b for beam with R_{b-min}

If from "Step2-d" above, it results that the power of the beam with R_{b-min} can still be increased, the current gap (Gap_{cur}) between R_{b-max} and R_{b-min} across all beams must be determined. Then, the new increment step-size ($P_{b-inc-new}$) will be calculated as in equation (5-24), following the discussion flow in section 5.4.2.4 above. Subsequently, the new incremented beam's power (P_{b-new}) for the concerned beam will be derived as:

$$P_{b-new} = P_{b-cur} + P_{b-inc-new} \tag{5-29}$$

Thereafter, the new beam-power for the beam with minimum OCTR-ratio will be updated in the power-set; and with the new power-set, the search process will return at the beginning of the iterative search loop (i.e. step2-a), for next search iteration.

5.4.3.6. Step2-f: Determine $P_{b-dec-new}$ and calculate new P_b for beam with R_{b-max}

Alternatively, if from "Step2-d" above, it results that the power of the beam with R_{b-min} can no more be increased, the current power ($P_{b-max-octr-ratio}$) of the beam with R_{b-max} must be identified; and the current gap (Gap_{cur}) between R_{b-max} and R_{b-min} across all beams must be determined. Then, the new decrement step-size ($P_{b-dec-new}$) will be calculated as in equation

(5-27), following the discussion flow in section 5.4.2.5 above. Subsequently, the new decremented beam's power ($P_{b\text{-new}}$) for the concerned beam will be derived as:

$$P_{b\text{-new}} = P_{b\text{-cur}} - P_{b\text{-dec-new}} \quad (5-30)$$

Thereafter, the new beam-power for the beam with minimum OCTR-ratio will be updated in the power-set; and with the new power-set, the search process will return at the beginning of the iterative search loop (i.e. step2-a), for next search iteration.

5.4.4. Step3: Terminate the process and save the resulting $P_{b\text{-set}}$

In this step, the inter-beam power-allocation search process will be terminated, and the last power-set obtained from the iterative search process (Step2) will be stored as the resulting adequate beams' powers-set ($P_{b\text{-set-adeq}}$). This power-set represents a set of the adequate powers that should be allocated to respective antennas ($P_{b\text{-adeq}}$), in order to achieve convergence of all OCTR-ratios from respective beams; and thus optimally maximize the inter-beam fairness.

5.4.5. Resulting inter-beam PA-algorithm based on OCTR-ratios convergence concept

Following all the steps from the above discussion, the resulting inter-beam power-allocation algorithm based on the OCTR-ratios convergence concept, for fairness maximization amongst M -beams, is summarised in Table 5.3 below.

Table 5.3: Proposed Inter-beam PA Algorithm for M -beams, based on the OCTR-ratios Convergence Concept

Algorithm 5.2: Proposed Inter-beam PA Algorithm for M-beams, based on the OCTR-ratios Convergence Concept		
steps	lines	actions
Step1:		Process initialisation:
(a)	1:	Receive: H, D, W
(b)	2:	Specify: $P_{\text{tot-sat}}, P_{b\text{-max}}, P_{b\text{-init}} = 1/2P_{b\text{-max}}, ce = 0.01$;
(c)	3:	Generate: $P_{b\text{-set-init}}$ as in equation (5-12);
Step2:		Iterative Convergence Search Process:
repeat		repeat:
(a)	5:	Receive the new beams powers set " $P_{b\text{-set-new}}$ ";
(b)	6:	Evaluate new R_b for each beam and generate new " $R_{b\text{-set}}$ " as in equation (5-28);
(c)	7:	Check for OCTR-ratios convergence as in equation (5-14a); if Yes, go to "Step-3".
(d)	8:	If no convergence, identify $R_{b\text{-min}}$, its " P_b "; and check if $P_b < P_{b\text{-max}}$ && $P_{\text{tot-cur}} < P_{\text{tot-sat}}$;
(e)		If condition in (d) is met: increase P_b as follows:
	9:	Calculate $P_{b\text{-inc-new}}$ as in equation (5-24);
	10:	Calculate $P_{b\text{-new}}$ according to equation (5-29)
	11:	Return to start of Step-2.
(f)		If condition in (d) is not met: decrease P_b as follows:
	13:	Calculate $P_{b\text{-dec-new}}$ as in equation (5-27)

	14:	Calculate $P_{b\text{-new}}$ according to equation (5-30)
	15:	Return to start of Step-2.
Until		Until: OCTR-ratios convergence is obtained
Step3:		terminate the search process store final beams powers set “ $P_{b\text{-set-adeq}}$ ”.

5.5. Global System’s Power-Allocation Algorithm -1

After obtaining the *intra-beam* (Algorithm 5.1) and the *inter-beam* (Algorithm 5.2) *power-allocation algorithms* based on the *OCTR-ratios convergence* concept, which respectively solve the intra-beam fairness-maximization problem (F_1) and inter-beam fairness-maximization problem (F_2); a global power-allocation algorithm that solves the original problem (F) is derived by combining the two sub-algorithms. In essence the combination of the two algorithms intervenes at “Step2-b” of the inter-beam algorithm. The “Step2-a” receives the new power-set; that is, the new beam-powers for all the respective antennas. Then, the “Step2-b” is supposed to calculate the new *OCTR-ratio* (R_b) of each beam (b), based on the powers allocated. If this application was *OMA* (i.e. 1 user per beam), all the allocated beam’s power would be used by the single beam’s user, and the calculation of the beam’s *OCTR-ratio* would be direct. However, in the case of *NOMA* applications (in this scenario 2-users per beam), the allocated beam’s power should be shared between the two beam’s users; and the determination of the resulting beam’s *OCTR-ratio* requires that an intra-beam power allocation first be performed. Thus, in the case of *NOMA*-based network, we introduce the intra-beam power allocation algorithm in the “Step2-b” of the inter-beam power allocation; so that the new *OCTR-ratio* of each beam can be determined. The combination of these two produces what we call the global power-allocation for the described “2-users *NOMA*-based *MBSN*”. Since the intra-beam power allocation maximizes the minimum *OCTR-ratio* within the beam, and the inter-beam power allocation maximizes the minimum *OCTR-ratio* across all beams, the combination of both therefore results in maximization of minimum *OCTR-ratio* in the entire system (network); which is the solution to the original system’s fairness maximization problem (F). The output parameters of the global power allocation algorithm generated are:

- *The inter-beam power share*: the set of adequate beams’ powers ($P_{b\text{-adeq}}$) to be allocated to respective antennas; $P_{b\text{-set-adeq}} = [P_{1\text{-adeq}}, P_{2\text{-adeq}}, \dots, P_{M\text{-adeq}}]$. This is the final set of beams’ powers received before terminating the search process.
- *The intra-beam power share in each beam*: the adequate beam’s power-sharing coefficient (α_b) obtained in each beam (b); $\alpha_{b\text{-set-adeq}} = [\alpha_{1\text{-adeq}}, \alpha_{2\text{-adeq}}, \dots, \alpha_{M\text{-adeq}}]$.

This is a set of the last power-sharing coefficient (α_b) received from each respective beam (b).

Where, “ M ” is the number of antennas on the satellite.

The proposed power-allocation algorithm based on *OCTR*-ratios convergence concept, to maximize fairness of 2users-NOMA MBSN, is summarised in Table 5.4 below.

Table 5.4: Proposed Global PA-Algorithm-1 for 2-users NOMA MBSN, based on the *OCTR*-ratios Convergence Concept.

Algorithm 5.3: Proposed Global PA Algorithm for 2-users NOMA MBSN, based on <i>OCTR</i>-ratios Convergence Concept (PAA-1)		
steps	lines	actions
Step1:		Process initialisation:
(a)	1:	Receive: $\mathbf{H}, \mathbf{D}, \mathbf{W}$;
(b)	2:	Specify: $P_{\text{tot-sat}}, P_{\text{b-max}}, P_{\text{b-init}} = 1/2P_{\text{b-max}}, ce = 0.01$;
(c)	3:	Generate: $\mathbf{P}_{\text{b-set-init}} = [P_{1\text{-init}}, P_{2\text{-init}}, \dots, P_{M\text{-init}}]$;
Step2:		Iterative Convergence Search Process:
repeat		repeat:
(i)	5:	Receive the new beams powers set " $\mathbf{P}_{\text{b-set-new}}$ ";
(ii)	6:	Do " <i>intra-beam power-allocation algorithm</i> " as in " Algorithm 5.1 " in Table 5.2;
		Receive the resulting new R_{b} and α_{b} for each respective beam;
		Generate new $\mathbf{R}_{\text{b-set}} = [R_1, R_2, \dots, R_M]$ and $\alpha_{\text{b-set}} = [\alpha_1, \alpha_2, \dots, \alpha_M]$;
(ii)	7:	Do " <i>inter-beam power-allocation algorithm</i> " as in "Algorithm 5.2" in Table 5.3;
		Execute "Step2-c" to "Step2-f" of "Algorithm 5.2" using $\mathbf{P}_{\text{b-set-new}}$ & $\mathbf{R}_{\text{b-set}}$.
		Receive, either $\mathbf{P}_{\text{b-set-new}}$ for next iteration, or an instruction to exit loop.
Until		Until: <i>OCTR</i>-ratios convergence is obtained
Step3:		terminate the search process store final powers set: "$\mathbf{P}_{\text{b-set-adeq}}$" & "$\alpha_{\text{b-set-adeq}}$".

5.6. Novelty of the proposed PAA-1

To the best of author's knowledge, the proposed algorithm (fairness-maximization power-allocation algorithm based on *OCTR*-ratio convergence concept) presents one principal novelty: it proposes a novel technique for determining the necessary increment or decrement step-size in each search iteration of the inter-beam PA process.

5.7. Chapter summary

In this chapter, the design of fairness maximization power-allocation algorithms for a 2-users NOMA-MBSN, based on the *OCTR*-ratios convergence concept, was presented. First, the general steps involved in the *OCTR*-ratios convergence concept were presented. Then based, on these steps, the intra-beam power-allocation algorithm was developed. To ensure that both users have same *OCTR*-ratio, the adequate value of α_{b} , noted $\alpha_{\text{b-a}}$, is determined analytically. Similarly, based on the above mentioned general steps, the inter-beam power-allocation algorithm was developed. A novel technique for determining the necessary increment or decrement step-size in each iteration of the inter-beam power-allocation process was proposed in this chapter. Finally, the global system's power-allocation algorithm (PAA-1) was generated by combining the intra-beam and inter-beam PA algorithms, in an iterative process.

CHAPTER 6: POWER-ALLOCATION ALGORITHM BASED ON THE MAXIMUM-MINIMUM FAIRNESS CONCEPT

6.1. Introduction

Similar to the work covered in the previous chapter, in this chapter, we present the design of our proposed power-allocation algorithm for system's fairness-maximization, based on the Maximum-Minimum Fairness concept. This is the second approach employed to design the power-allocation system for the *MA*-Encoder block of the described network, which was highlighted in the block-diagram in Figure 5.1 above.

The rest of the chapter is outlined as follows. First, a description of the *Max-Min Fair* concept is given. This will be followed by detailed design discussion for the intra-beam power-allocation algorithm based on the Max-Min Fair concept. Then, a detailed design discussion for the inter-beam power-allocation algorithm based on the Max-Min Fair concept will also be given. Thereafter, the global power-allocation algorithm which combines the two sub-algorithms will be presented.

6.2. Description of the max-min fair concept

6.2.1. Merit of the Max-Min Fairness Concept

Power-allocation processes that are intended to maximise the System's throughput eventually deliver the maximum possible system's throughput. However, they often deliberately neglect the needs of users with poor channel conditions, by serving them with the minimum power necessary just to achieve minimum Quality-of-Service (QoS). Subsequently, they create extremely high-gaps between the satisfaction-level (i.e. *OCTR*-ratios) of users with good channel conditions and those with poor channel conditions; which therefore, result in the worst system's fairness (extremely poor fairness).

Similarly, power-allocation processes that offer equal power to all users, results in mismanagement of available power-resource. Because, some over-satisfied users (*OCTR*-ratio > 1) waste their excess power, while it could have been used to increase the capacity of unsatisfied users (*OCTR*-ratio < 1) and thus improve their satisfaction-level. Therefore, due to relatively high gaps between the satisfaction-level (*OCTR*-ratio) of respective users, this types of power-allocation processes are not pareto-efficient; and thus, result in a system with relatively poor fairness (Le-Boudec, 2021:10).

Furthermore, power-allocation processes for system's fairness maximization, which are based on the *OCTR*-ratios convergence concept attempt to address the fairness problems observed in the two types of pa processes outlined above, by ensuring that all users are satisfied to the same level (*OCTR*-ratios converge). Thus, they deliver the most optimal (highest possible) system's fairness. However, they result in two critical resource allocation concerns: (1) when the user with worst *OCTR*-ratio has attained the maximum user's power, the allocation system forces all other users not to satisfy their respective traffic-needs, by reducing their respective powers unlimitedly, until they all match the worst *OCTR*-ratio in the system. (2) Subsequently, the allocation system leaves a lot of available access-point's power unused, while users are not satisfied. Consequently, in this approach, the amount of total power to be used by the access-point will be determined based on the user with the poorest *OCTR*-ratio. Thus, the approach results potentially in a degradation of global network's quality, due to under-usage of available resources. This is another case of mismanagement of available network resources, just like the constant power allocation process; and the approach is therefore, often considered inefficient (Kumar et al., 2008:71).

To address these above outlined limitations while ensuring that high system's fairness is still obtained, the *maximum-minimum fairness* concept, often simply termed *max-min fair* concept, is proposed. It introduces the notion of "*user's right to available power*" into the power allocation process; also known as "*user's deserving share of available power*". In essence, it stipulates that, every user has a deserving share (or rightful share of the available power); and thus at the beginning of the power allocation, every user must first be given its rightful share of the available power. Thereafter, if certain users are over-satisfied from their deserving share (i.e. their current traffic need is less than they rightful share), while others are unsatisfied (i.e. their current traffic need is more than they rightful share), only then should the excess power of the over-satisfied users be distributed to unsatisfied users to improve their capacities (Marsic, 2013:312-316; Le-Boudec, 2021:10).

Subsequently, through this principle, the max-min fairness addresses the concerns raised in above scenarios as follows:

- a) By giving to each user a rightful share of the available power, it addresses the problem of marginalization of users with poor channel conditions, encountered in capacity maximisation pa process.
- b) By redistributing the excess power from over-satisfied users amongst unsatisfied users, it addresses the problem of power wastage encountered in fix-pa processes.

- c) By limiting the extent to which the power of other users can be reduced (not below the minimum between their need and their rightful share), it addresses the problem encountered in the *OCTR*-ratio convergence concept.

Consequently, the max-min concept described above preserves equity amongst users while ensuring no wastage of network's power; and is thus, widely considered the most appropriate resource-allocation concept to achieve high system fairness (Keshav, 1997:215; Pioro & Medhi, 2004:63).

6.2.2. Step-flow of the max-min fairness concept

The max-min fairness concept can be outlined the sequence of steps listed in Table 6.1 below (Keshav, 1997:215-217; Kumar et al., 2008:276; Marsic, 2013:312; Le-Boudec, 2021:10-12).

Table 6.1: General step-flow of the Max-Min Fairness concept

steps	actions
Step1:	Process initialization:
(a)	Receive: users' channel-vectors, users' demands, antennas' weight-vectors, total power,
(b)	Define the right of every user,
(c)	Calculate the deserving power share of every user from total power available,
(d)	Generate the initial power-set for all users
Step2:	Do iterative redistribution of the excess-power amongst unsatisfied users:
(i)	Receive the new power-set: from step1 (if first iteration), else from previous iteration;
(ii)	Evaluate the new <i>OCTR</i> -ratio of respective users based the new power-set received;
(iii)	Check if all users are satisfied ($R \geq 1$); and if so, go to step3;
(iv)	Else, check if all users are unsatisfied ($R \leq 1$); and if so, go to step3;
(v)	Else (i.e. some users have $R \geq 1$ while others have $R \leq 1$), do power redistribution:
	1. Give to over-satisfied users ($R \geq 1$) the power necessary for their traffic-request;
	2. Gather the excess power from over-satisfied users;
	3. Redistribute the collected excess-power evenly among unsatisfied users ($R \leq 1$)
	4. Formulate the new "power-set" to respective users, for next check-iteration, and return at the start of "Step2";
Step3:	Terminate the process and Store the final power-set (i.e. relevant power to each user).

The techniques used to execute the different steps of the above outlined concept can differ based on the designers' choices; or based on case-specific in which the concept is being used. In this proposed work, the max-min fairness concept will be used in two cases:

- iii. To design the intra-beam *PA*-algorithm that maximizes the beam's fairness, and hence address the intra-beam fairness maximization problem (F_1); and
- iv. To design the inter-beam *PA*-algorithm that maximizes fairness between the beams, and hence address the inter-beam fairness maximization problem (F_2).

The designs these two power-allocation algorithms based on the max-min fair concept outlined above, are presented in the following section.

6.3. Intra-beam power-allocation algorithm design

6.3.1. Overview

As indicated earlier, the intra-beam power allocation is the process of determining how much share of the beam's power (P_b) should be given to each of the users sharing the same NOMA beam. In the case of 2-users NOMA, the share of the beam's power (P_b) for each user (near and far), is defined by a single intra-beam power-sharing coefficient " α_b ", which can take any value in the interval $[0,1]$. When the goal is to maximize the beam's fairness, the intra-beam power-allocation process implies finding the optimal value " α_{b-opt} " of the beam's power-sharing coefficient, which maximizes the minimum *OCTR*-ratio within the beam. This then results in maximizing the beam's fairness; and therefore, solves the optimization sub-problem (F_1). Subsequently, when the algorithm is based on the *max-min fair* concept, the exercise of the power-allocation process is to search for the adequate value " α_{b-adeq} " of the beam's power-sharing coefficient, which increases as much as possible the minimum *OCTR*-ratio within the beam; without impeding on the right of other users. By doing so, the beam's fairness is maximized. As shown before, Figure 6.1 below illustrates the focus of the intra-beam process, in the bigger picture of the network. In the figure below, only one arbitrary beam (b) is zoomed out (i.e. in red) for the purpose of illustration; but the same process occurs simultaneously in all the other beams.

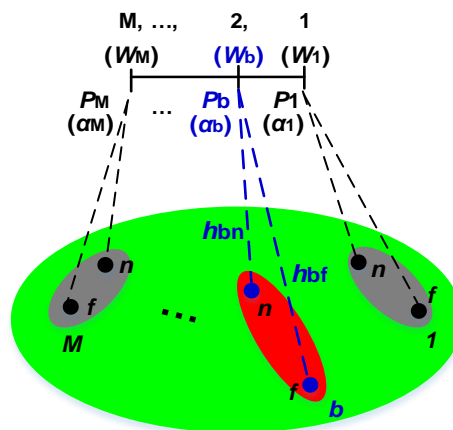


Figure 6.1: Illustration of the intra-beam power-allocation stage in a multi-beams satellite system

Following the design steps outlined above for the max-min fairness concept, the design of the proposed intra-beam power allocation algorithm based on max-min fairness concept is presented in the follows steps.

6.3.2. Step1: Process Initialisation

6.3.2.1. Input parameters definition

At this stage, all input parameters necessary to perform intra-beam power allocation shall be known and well defined; and according to equations (4-13) and (4-19), these fundamentally include:

- D_{bn} , D_{bf} , h_{bn} , h_{bf} , w_b , P_b and respective P_{b^*} of all other beams ($b^* \neq b$).

As indicated before, with all these parameters fixed, the adjustment of the beam's users capacities (C_{bn} and C_{bf}), becomes a single variable problem of " α_b ". Subsequently, given that users traffic requests (D_{bn} and D_{bf}) are constant over the service time, the adjustment of the *OCTR*-ratios of the beam's near-user (R_{bn}) and far-user (R_{bf}) users, is a single variable function of " α_b ".

The variation of R_{bn} , R_{bf} , C_{bn} and C_{bf} with-respect-to " α_b " were discussed in section 4.7.3 and illustrated in Figure 4.2 above. This figure showed that, an increase in " α_b " leads to the increase of R_{bn} but decrease of R_{bf} , and a decrease in " α_b " leads to the decrease of R_{bn} , but increase of R_{bf} .

6.3.2.2. Defining the user's right:

In system's throughput maximization, power-allocation process often deliberately prioritises users with good channel conditions and somehow neglects users with poorer channel conditions (Zhu et al., 2017:2259; Lin et al., 2019:661; Sun et al., 2019:86290). This situation is analogous to saying that, users with good channel conditions have more right to available powers than users with poor channel conditions; and generally results in system with extremely poor users' fairness. In 5G and beyond networks, in which *NOMA*-based MBSNs are expected to form a big component, all users are expected to receive a good quality of service, irrespective of their channel conditions. This set a critical requirement for high system's fairness; and this scenario is analogous to saying that, all users have the same right to the available power. Thus, in this intra-beam power-allocation design for beam's fairness maximization, we consider all beam's users to have the same right of access to available power.

6.3.2.3. Deserving shares of the beam's power for beam's near and far-users

For the intra-beam power allocation process, the power available for all users in the beam is the beam's power (P_b). Since the near- and far-users have the same right of access to the beam's power, we consider that they must receive at their respective terminals, the same share

of the beam's power. Thus, the unique intra-beam power sharing coefficient (α_{b-d}) which ensures that, both the near- and far-users receive the same deserving share of beam's power (P_b) is:

$$\alpha_{b-d} = \frac{|h_{bf}^H w_b|^2}{|h_{bn}^H w_b|^2 + |h_{bf}^H w_b|^2} \quad (6-1)$$

6.3.2.4. Generate initial power-set

By using the above calculated intra-beam power sharing coefficient " α_{b-d} ", both users will receive the same power " P_{rx-bu} " and " P_{rx-bf} " at their respective terminals. Therefore, " α_{b-d} " defines the initial power-set for the beam " b ", and will be sent to "Step2" for the execution of the iterative intra-beam power-share adjustment process, if applicable.

6.3.3. Step2: Iterative intra-beam power-sharing coefficient's adjustment

The "Step2" executes the search of the adequate intra-beam power-share " α_{b-d} ", in the sequence presented and discussed in the points below.

6.3.3.1. Step2-a: Receive the new value of " α_b "

At this point, the new value of " α_b " is received, for the execution of a new iteration search. If this process is in its first iteration, this value will be coming from the "process initialization" process, i.e. "Step-1". Otherwise, this new value of " α_b " will be coming from the previous iteration of the search process, i.e. "Step2-e".

6.3.3.2. Step2-b: Evaluate the *OCTR*-ratios R_{bn} and R_{bf} based on received " α_b "

Using the new " α_b " received, the values of *SINR* for the near- and far-user will be calculated as in equations (4-13) and (4-19) respectively. Then, their resulting capacities (C_{bn} and C_{bf}) will be calculated as in equation (4-5). Thereafter, their *OCTR*-ratios (R_{bn} and R_{bf}) will be calculated according to equation (4-3).

6.3.3.3. Step2-c: Check if both users satisfy $R \geq 1$

After calculating the *OCTR*-ratios of the far- and near-users (R_{bn} and R_{bf}), it should be checked whether they are both greater than 1. This check is basically executed by verifying if:

$$\min\{R_{bn}, R_{bf}\} \geq 1 \quad (6-2)$$

If so, this means that, no adjustment is needed, as the initial power-share “ α_{b-d} ” allows both users to satisfy their respective needs; meaning that $\alpha_{b-adeq} = \alpha_{b-d}$. Subsequently, the algorithm should go to “Step3” to terminate the process. However, if both *OCTR*-ratios are not greater than, the algorithm should continue to next step (Step2-d) below.

6.3.3.4. Step2-d: Check if all users are unsatisfied ($R \leq 1$)

If above step (Step2-c) is not satisfied, it should be checked whether both *OCTR*-ratios (R_{bn} and R_{bf}) are less than 1. This check is basically executed by verifying if:

$$\max\{R_{bn}, R_{bf}\} \leq 1 \quad (6-3)$$

If so, this means that, there is no excess power to do adjustment, as none of the user even satisfied their need from their deserving power share. In this case, the algorithm should go to “Step3” to terminate the process. However, if this condition is also not met, it would mean that, between the two beam’s users, one has a ratio greater than 1 and the other less than 1. This then implies that, the excess-power of the user with *OCTR*-ratio greater than 1 can be used to increase the current value of the *OCTR*-ratio which is less than 1; and thus maximize the beam’s fairness. Therefore, the algorithm should continue to next step (Step2-e) below to perform *adjustment of the intra-beam power-sharing coefficient*, and subsequently obtain the adequate coefficient “ α_{b-adeq} ” which maximizes the beam’s fairness.

6.3.3.5. Step2-e: Adjustment of the intra-beam power-sharing coefficient (α_b)

At this point, we should adjust the intra-beam power-sharing coefficient (α_b) in order to take the excess power of the user whose *OCTR*-ratio is greater than 1, and give it to the user whose *OCTR*-ratio is less than 1. In this regards, we indicated earlier that, by sliding “ α_b ” in the interval [0,1], the *OCTR*-ratio of the near- and far-users vary inversely; as illustrated in Figure 4.2 above. Thus, the exercise to perform is to slide “ α_b ” in the direction that decreases the *OCTR*-ratio greater than 1, until this *OCTR*-ratio is equal to 1. Subsequently, by doing so, we automatically increase the value of other *OCTR*-ratio. Figure 6.2 below illustrates this sliding process. So, if the near-user is the one whose *OCTR*-ratio is greater than 1 (i.e. $R_{bn} > 1$) based on the initial value of α_b (i.e. α_{b-d}), then we must decrease “ α_b ” from its current value “ α_{b-d} ” until it reaches the value “ α_{b-nd} ” for which $R_{bn} = 1$. Note that, α_{b-nd} is the value of “ α_b ” for which $C_{bn} = D_{bn}$, and can be calculated based on equation (4-13) and (4-5) as:

$$\alpha_{b-nd} = \frac{I_{bn}}{S_{bn}} (2^{C_{bn}} - 1) \quad (6-4a)$$

Where:

$$S_{bn} = |h_{bn}^H w_b|^2 P_b \quad (6-4b)$$

$$I_{bn} = \sum_{b^*=1; b^* \neq b}^M |h_{bn}^H w_{b^*}|^2 P_{b^*} + n \quad (6-4c)$$

As it can be observed in the Figure 6.2(a) below, since this new value “ α_{b-nd} ” is smaller than the initial value “ α_{b-d} ”, it produces an increased capacity for the far-user (C_{bf}) from the initial value; and consequently leads to an increased *OCTR*-ratio for the far-user (R_{bf}).

In a similar manner, if the far-user is the one whose *OCTR*-ratio is greater than 1 (i.e. $R_{bf} > 1$) based on the initial value of α_b (i.e. α_{b-d}), then we must increase “ α_b ” from its current value “ α_{b-d} ” until it reaches the value “ α_{b-fd} ” for which $R_{bf} = 1$. Note that, α_{b-fd} is the value of “ α_b ” for which $C_{bf} = D_{bf}$, and can be calculated based on equation (4-19) and (4-5) as:

$$\alpha_{b-fd} = \frac{S_{bf} + I_{bf} - (I_{bf} \times 2^{C_{bf}})}{S_{bf} \times 2^{C_{bf}}} \quad (6-5a)$$

Where:

$$S_{bf} = |h_{bf}^H w_b|^2 P_b \quad (6-5b)$$

$$I_{bf} = \sum_{b^*=1; b^* \neq b}^M |h_{bf}^H w_{b^*}|^2 P_{b^*} + n \quad (6-5c)$$

Again, as it can be observed in the Figure 6.2(b) below, since this new value “ α_{b-fd} ” is bigger than the initial value “ α_{b-d} ”, it produces an increased capacity for the near-user (C_{bn}) from the initial value; and consequently leads to an increased *OCTR*-ratio for the near-user (R_{bn}).

In either case, the resulting power-sharing coefficient “ $\alpha_b = \alpha_{b-nd}$ ” or “ $\alpha_b = \alpha_{b-fd}$ ”, is the new power-sharing coefficient for the next iteration, with which, the algorithm will go back to beginning of “Step2”. With this new power-sharing coefficient “ α_b ”, in the next iteration, at “step2-b”, the *OCTR*-ratio of one user will be equal to 1 and the other will be either less than 1, equal to 1 or greater than 1. This will subsequently result in meeting either the check in “Step2-c” or the check in “Step2-d”; which would also imply that, the received value of “ α_b ” in for this iteration, is the adequate value of “ α_b ” that maximizes the fairness in the beam, i.e.

“ $\alpha_{b\text{-adeq}} = \alpha_b$ ”. Consequently, the algorithm will jump to “Step3” to termination of the intra-beam power-allocation process.

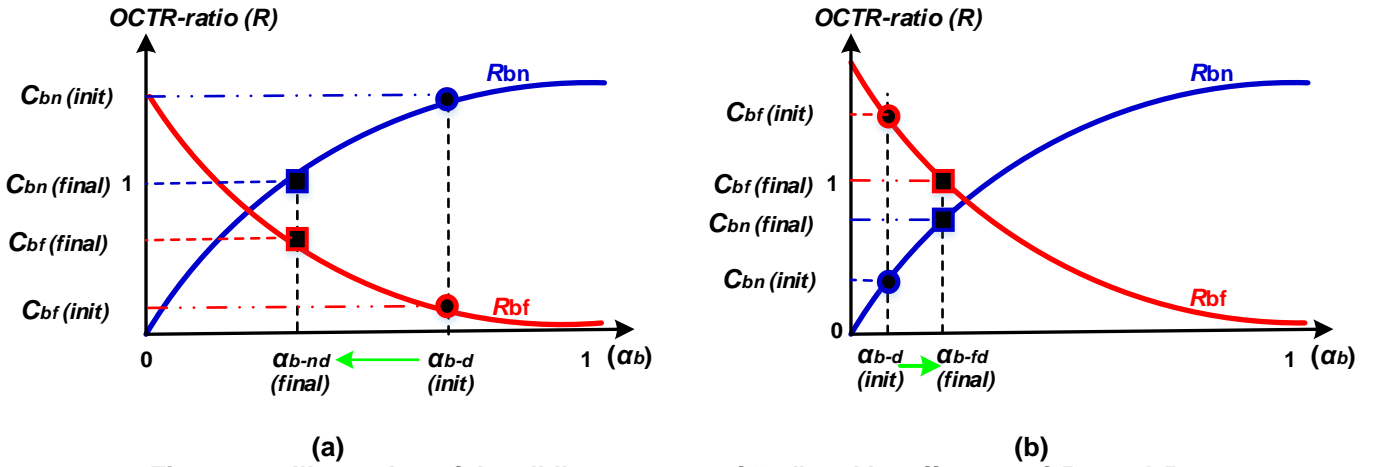


Figure 6.2: illustration of the sliding process of “ α_b ” and its effect on of R_{bn} and R_{bf} :
(a): case of $R_{bn} > 1$; (b): case of $R_{bf} > 1$.

6.3.4. Step3: Terminate the process and determine the beam’s $OCTR$ -ratio (R_b).

In this step, the intra-beam search process will be terminated, and the intra-beam power-allocation results will be stored. These include, the adequate intra-beam power-allocation coefficient “ $\alpha_{b\text{-adeq}}$ ” obtained, the resulting capacities for near- and far-users (C_{bn} , and C_{bf}), as well as their respective $OCTR$ -ratios (R_{bn} , and R_{bf}). Then, since each beam will be represented by a unique $OCTR$ -ratio for the purpose of inter-beam power-allocation, the beam’s $OCTR$ -ratio must be decided by considering the resulting $OCTR$ -ratios (R_{bn} , and R_{bf}) of the respective beam’s users. Given that the power-allocation concept used in this section was the *max-min fairness*, at this point, it may occur that beam’s users have different values of $OCTR$ -ratios; that is, $R_{bn} \neq R_{bf}$. Therefore, to determine the unique beam’s $OCTR$ -ratio (R_{bn}) that will be used for inter-beam power-allocation process, we consider the following:

Since the exercise of the power-allocation concept used here is to decrease the power of over-satisfied users, we propose that, in a beam where both users are over-satisfied, the beam’s $OCTR$ -ratio will be the maximum of the two $OCTR$ -ratios. That is,

$$R_b = \max\{R_{bn}, R_{bf}\}; \text{ if } R_{bn} \geq 1 \text{ and } R_{bf} \geq 1 \quad (6-6)$$

Similarly, since the goal of the power-allocation concept used here is to increase the minimum $OCTR$ -ratio across all beams, we propose that, in a beam where both users are unsatisfied, the beam’s $OCTR$ -ratio will be the minimum of the two $OCTR$ -ratios. That is,

$$R_b = \min\{R_{bn}, R_{bf}\}; \text{ if } R_{bn} \leq 1 \text{ and } R_{bf} \leq 1 \quad (6-7)$$

6.3.5. Resulting intra-beam PA-algorithm based on the max-min fair concept

Following all the steps from the above discussion, the resulting intra-beam power-allocation algorithm based on the max-min fair concept, for fairness maximization within a 2-users NOMA beam, is summarised in Table 6.2 below.

Table 6.2: Proposed Intra-beam PA Algorithm for 2-users NOMA, based on the Max-Min Fairness Concept

Algorithm 6.1: Proposed Intra-beam PA Algorithm for 2-users NOMA, based on the Max-Min Fairness concept		
steps	lines	actions
Step1:		Process initialisation:
(a)	1:	Receive: $H, D, W, P_{b\text{-set}}$,
(b)	2:	Define user's right => all users have same right;
(c)	3:	Extract the " P_b " from " $P_{b\text{-set}}$ " and calculate " $\alpha_{b\text{-d}}$ " as in equation (6-1);
(d)	4:	Use the calculated " $\alpha_{b\text{-d}}$ " to initiate "Step2";
Step2:		Iterative intra-beam power-sharing coefficient's adjustment:
repeat		repeat:
(a)	5:	Receive the new value of " $\alpha_{b\text{-new}}$ ";
(b)	6:	Evaluate the R_{bn} & R_{bf} using " $\alpha_{b\text{-new}}$ " based on equations (4-13), (4-19), (4-5) & (4-3);
(c)	7:	Check if both users are satisfied ($R \geq 1$) as in equation (6-2); and if so, go to "Step3";
(d)	8:	Else, Check if both users are satisfied ($R \leq 1$) as in equation (6-3); if so, go to "Step3";
(e)		Else: => Do adjustment of α_b as follows:
	9:	If $R_{bn} \geq 1$, => calculate " $\alpha_{b\text{-nd}}$ " as in equation (6-4a); assign $\alpha_b = \alpha_{b\text{-nd}}$; and go back to "Step2-a"
	10	If $R_{bf} \geq 1$, => calculate " $\alpha_{b\text{-fd}}$ " as in equation (6-5a); assign $\alpha_b = \alpha_{b\text{-fd}}$; and go back to "Step2-a"
Until		Until: Conditions 2c or 2d are met
Step3:		terminate the search process and determine the beam's OCTR-ratio for inter-beam.
	11	Store the resulting " $\alpha_{b\text{-adeq}}$ "
	12	Determine R_b as in equation (6-6) or (6-7).

6.4. Inter-beam power-allocation algorithm design

6.4.1. Overview

As indicated before, the inter-beam power allocation is the process of determining the amount of power to be given to respective antennas of the access-point, in order to maximise the desired utility of the network. When the goal is to maximize the system's fairness, inter-beam power-allocation process implies finding the adequate power-set to respective antennas, that maximizes the minimum OCTR-ratio across all beams. In so doing, it maximizes the inter-beam's fairness; therefore, solving the optimization sub-problem (F_2). Subsequently, when this power allocation process is executed based on the max-min fair concept, the exercise of the

inter-beam algorithm is to search for that adequate set of all the beams' powers ($P_{b\text{-set-adeq}}$) which increases as much as possible, the minimum *OCTR*-ratio across all beams, without impeding on the right of other beams. In so doing, the inter-beam's fairness is maximised. Figure 6.3 below provides an illustration of the inter-beam power-allocation process. As indicated before, in the inter-beam power-allocation process, the access-point (i.e. the satellite in this case) with M -antennas, sees each beam ($b, b \in M$) as a homogenous end-user, to whom a certain beam's power (P_b) was given through its antenna; and which in return, exhibits a certain *OCTR*-ratio (R_b). Therefore, the inter-beam *PA* process does the adjustment of respective beam's powers, by conserving purely, the *OCTR*-ratios of respective beams. Similar to the discussion presented in the previous Chapter (section 5.4.1), because it is very hard to adjust the powers of many beams simultaneously and expect a deterministic outcome; in this work also, we propose to adjust the power of only one beam at the time (i.e. per search iteration) while the powers to all the other beams are kept constant. In this case, as discussed in section 4.7.3, it will be much simpler to adjust the *OCTR*-ratio (R_b) in the designated beam (b), through adjustment of its beam's power (P_b).

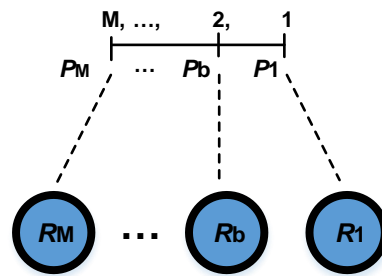


Figure 6.3: Illustration of inter-beam power-allocation stage

Considering the design steps involve in the max-min fairness concept, as listed in Table 6.1 above, the design of the proposed inter-beam power-allocation algorithm based on max-min fairness concept is presented the steps below.

6.4.2. Step 1: Process Initialization

6.4.2.1. System's power budget specification

At the start of the inter-beam power-allocation process, system's power related parameters must be specified. This include, the total power available on the satellite ($P_{\text{tot-sat}}$) and the maximum beam's antenna power $P_{b\text{-max}}$. Other input parameters such as such as the vector of all the users' traffic-demands (\mathbf{D}), channel-vectors of all the users (\mathbf{H}) and all the antennas' precoding weight vectors (\mathbf{W}), must be specified.

6.4.2.2. Define the right of every user

As discussed earlier, in the design of power-allocation algorithm for system's fairness maximization, we consider that all users have the same right of access to available power. Thus, since in the inter-beam power-allocation process, each beam is treated as a homogenous entity, we therefore, consider that all beams have the same right.

6.4.2.3. Calculate the deserving share of power of every user from $P_{\text{tot-sat}}$:

Given that all the beams have equal right of access to total system's power available, we start by dividing the total power equally amongst the beams, to get the deserving power-share of each beam. Thus, with " M " beams, the deserving power of each beam ($P_{\text{b-d}}$) will be:

$$P_{\text{b-d}} = \frac{P_{\text{tot-sat}}}{M} \quad (6-8)$$

6.4.2.4. Generate the initial power-set for all user

The initial power-set ($P_{\text{b-set-init}}$) consisting of deserving beam's power ($P_{\text{b-d}}$) from respective beams, is generated as in equation (6-9) below; and is then made available to "Step2" for inter-beam power-allocation search process to start.

$$P_{\text{b-set-init}} = [P_{1-d}, P_{2-d}, \dots, P_{M-d}] \quad (6-9)$$

6.4.3. Step2: Iterative redistribution of the excess-power amongst unsatisfied beams

After receiving all input parameters and setting up all necessary initial parameters in Step1, the inter-beam power allocation search process will be executed iteratively as discussed in the steps below. As indicated in 6.4.1 above, in this work, we propose to adjust the power (P_b) of only one beam (b) at the time (i.e. in each search iteration) and keep the respective powers to other beams constant.

6.4.3.1. Step2-a: Receive the new beam's powers set ($P_{\text{b-set-new}}$)

At this point, the new beams' powers set ($P_{\text{b-set-new}}$) consisting of the new powers to respective beams (P_b) is received for the execution of a new iteration of the inter-beam power redistribution process. If this process is in its first iteration, this $P_{\text{b-set-new}}$ will be coming from the "process initialization" stage, i.e. "Step-1". Otherwise, $P_{\text{b-set-new}}$ will be coming from the previous iteration of the search process, i.e. "Step2-e".

6.4.3.2. Step2-b: Evaluate the *OCTR*-ratio of each respective beam (R_b)

From the new power-set, each beam ($b, b = 1, 2, \dots, M$) will receive its designated power (P_b); and from it, the new *OCTR*-ratio of the beam (R_b) will be evaluated. Then the set of new *OCTR*-ratios from the respective M -beams of the satellite will be obtained as:

$$R_{b\text{-set}} = [R_1, R_2, \dots, R_M] \quad (6-10)$$

Using the input power-set received (i.e. $P_{b\text{-set-new}}$) and the beam's *OCTR*-ratios set generated ($R_{b\text{-set}}$), the inter-beam power-adjustment search process is divided into following the five (5) conditions below.

6.4.3.3. Step2-c: Conditions-1: Check if all beams are satisfied (i.e. all $R_b \geq 1$)

The first check is whether all beams are satisfied at this point; that is, if all *OCTR*-ratios are greater or equal to 1. This is verified by checking if:

$$\min\{R_{b\text{-set}}\} \geq 1 \quad (6-11)$$

If this condition is met, then, all other conditions below should be skipped, the search process should be exited and the algorithm terminated at "Step3". Because, this would mean that, all beams are satisfied and no need for further power adjustment.

6.4.3.4. Step2-d: Condition-2: Check if any beam is over-satisfied

After determining that not all beams are satisfied, the next check is whether there is any over-satisfied beam in the set. That is verified by checking if:

$$\max\{R_{b\text{-set}}\} > 1 \quad (6-12)$$

If it is found that there is an over-satisfied beam in the set, then the power (P_b) of that beam (b) should be reduced until its *OCTR*-ratio (R_b) is equal to 1. In a scenario where *NOMA* is not used, there is only one user in a beam. Subsequently, by fixing the powers of other beams, it would be less complex to directly evaluate the amount of beam's power (P_b) needed in a designated beam (b) to make $R_b=1$. However, in *NOMA*, such direct evaluation is difficult; and thus, the determination of such desired beam's power is done by means of step-search. In essence, by keeping the power to all other beams constant, we progressively reduce the power (P_b) of the over-satisfied beam (b) until $R_b=1$. At this point, it then becomes again critical to choose the decrement-step adequately. Therefore, to avoid unsettling or lengthy searches due

to arbitrary definition of the decrement-step, in this work, we proposed to use a decrement-step size for the beam-power, which is a function of both, the current beam's power (P_b) and the excess-margin of the *OCTR*-ratio above 1, which we denote $R_{b\text{-excess}}$. So we can write:

$$P_{b\text{-dec-step}} = R_{b\text{-excess}} \times \frac{1}{2} P_b \quad (6-13)$$

Where:

$$P_{b\text{-dec-step}} = \min\{1, (R_{b\text{-excess}} - 1)\} \quad (6-14)$$

From this decrement-step-size, the new beam power ($P_{b\text{-new}}$) will be derived as:

$$P_{b\text{-new}} = P_{b\text{-new}} - P_{b\text{-dec-step}} \quad (6-15)$$

Also, since it is extremely difficult to achieve perfect equality condition in numerical step-search methods when dealing with floating points numbers; it is therefore, critical to define an error against which the condition check can be done much more easily. In this regard, we propose again in this work, to use an *OCTR*-ratio convergence error $ce = 0.01$, as indicated in previous Chapter. Thus, because the perfect equality $R_b = 1$ is difficult to achieve, instead of checking this in order to detect settling of the beam's power decreasing's process; we would rather check the inequality below which is much easier to verify:

$$|R_b - 1| < ce \quad (6-16)$$

In sum, if there is an over-satisfied beam (b), the first thing to check is whether that R_b satisfies this equation (6-16). If so, it would mean that this *OCTR*-ratio should not be considered greater than; which implies that, that beam is not in fact over-satisfied. In such a case, the algorithm should proceed to "Step3". However, if not, then it would mean that, indeed the *OCTR*-ratio of the beam is greater than 1. In such as case, the power of that beam will be decreased iteratively until the beam's ratio is almost equal to 1. At each iteration, the beam-power decrement step-size ($P_{b\text{-dec-step}}$) will be determined as presented above and the new beam's power ($P_{b\text{-new}}$) will be derived. Thereafter, the new power-set will be updated for next iteration search.

When there is no more over-satisfied beam (i.e. beam that meets Condition-2), the inter-beam power allocation process should do redistribution of the excess-powers collected from over-satisfied beams in the manner presented below from "Condition-3 to 5".

6.4.3.5. Step2-e: Redistribution of excess power amongst unsatisfied users:

The redistribution of the excess-power collected from the over-satisfied users ($R_b > 1$), to the unsatisfied users ($R_b < 1$), is done by successively checking the following conditions:

Condition 3: Check if there is any beam (b) with $R_b < 1$ and $P_b < P_{b-d}$

The first thing is to check if amongst the unsatisfied beams (i.e. those with $R_b < 1$), there is any beam (b) whose power is less than the deserving beam power defined; i.e. $P_b < P_{b-d}$. If there is such a beam, its power must be increased until, either it becomes equal to P_{b-d} ; or its *OCTR*-ratio (R_b) becomes equal to 1. This is because, no beam should have a power less than the deserving beam's power defined, unless it is satisfied. The reason for having this case in the first place could be that, some iterations ago, the *OCTR*-ratio of this beam was 1 based on its beam's power at the time. But, after adjusting powers of others beams in more recent iterations, these adjusted powers from other beams have caused more interference to this beam, which resulted in reduction of its capacities and thus of its *OCTR*-ratio. To increase the power of this beam (b), we could simply take it from its current level (P_b) to the deserving level (P_{b-d}); which will mean, an increment in beam's power of an amount " P_{b-gap} ", where:

$$P_{b-gap} = P_{b-d} - P_b \quad (6-17)$$

However, in doing so, we could result in an over-satisfied situation again, and we will be forced to reduce the beam's power again; which will result in a lot more unnecessary search iterations. Therefore, to avoid this type of situations, we propose a beam's power increment step-size ($P_{b-inc-step}$) which takes in consideration the gap between the current beam's ratio (R_b) and the desired ratio (i.e. 1). That is:

$$R_{b-gap} = 1 - R_b \quad (6-18)$$

Then, we derive the needed increment step-size ($P_{b-inc-ned}$) proportional to both, the ratio gap (R_{b-gap}) to cover as well as the current beam power (P_b), as:

$$P_{b-inc-ned} = R_{b-gap} \times \frac{1}{2} P_b \quad (6-19)$$

Finally, we do not also want a situation where the needed increment is greater than the power-gap, because that would mean we will have to decrease power again to get down to P_{b-d} . Therefore, we propose a beam's power increment step-size which is the minimum of the two:

$$P_{b\text{-inc-step}} = \min\{P_{b\text{-inc-need}}, P_{b\text{-gap}}\} \quad (6-20)$$

The new beam's power ($P_{b\text{-new}}$) will be evaluated from the current beam's power (P_b) and the calculated increment step-size ($P_{b\text{-inc-step}}$) as:

$$P_{b\text{-new}} = P_b + P_{b\text{-inc-step}} \quad (6-21)$$

Again, as indicated before, to check the closeness of R_b to 1, we will employ a *OCTR*-ratio-error of $ce = 0.01$ and subsequently the inequality check presented in equation (6-16) above. Similarly, to check the closeness of the beam-power P_b to the deserving beam power ($P_{b\text{-d}}$), we propose an error which is a percentage of " $P_{b\text{-d}}$ "; since " $P_{b\text{-d}}$ " can be an arbitrary power-level depending on total system's power. To this effect, we propose:

$$P_{b\text{-error}} = 0.1\%(P_{b\text{-d}}) \quad (6-22)$$

Thus, instead of using the equality check $P_b = P_{b\text{-d}}$, we will utilise the inequality check:

$$|P_b - P_{b\text{-d}}| < P_{b\text{-error}} \quad (6-23)$$

In sum, if there is a beam (b) that satisfies "condition-3", the power of that beam will be increased iteratively until, either the beam's ratio (R_b) is almost equal to 1, or the beam's power (P_b) is almost equal to " $P_{b\text{-d}}$ ". At each iteration, the beam's power increment step-size ($P_{b\text{-inc-step}}$) will be determined as presented in equation (6-20) above; and the new beam's power ($P_{b\text{-new}}$) will be derived as in equation (6-21) above. Thereafter, the new beams' powers-set ($P_{b\text{-set-new}}$) will be updated for next iteration search and the algorithm will return to the start of "Step2".

When there is no more beam that meets "condition-3", the excess-power redistribution process will proceed to checking the next "condition4" below.

Condition 4: Check if there is a beam (b) with $P_{\text{tot-used}} < P_{\text{tot-sat}}$ and $P_b(R_{b\text{-min}}) < P_{b\text{-max}}$:

If "condition-3" is not met, the next condition to check during the excess-power redistribution process is whether there is still excess-power available that can be redistributed amongst the unsatisfied users. This basically implies to check if $P_{\text{tot-used}} < P_{\text{tot-sat}}$. If that is the case, it would mean that there is still available power that can be redistributed amongst unsatisfied users.

The conventional implementation of the max-min fairness concept proposes that this excess power should be redistributed equally amongst all unsatisfied users. However, in this work, we choose to bring a slight modification to this stage as follows. Since our aim is to maximise the minimum *OCTR*-ratio across all beams, we propose to focus initially on the beam with minimum *COTR*-ratio ($R_{b-\min}$) across all beams. In this regard, we suggest to progressively give the excess-power to that beam until either of the following events occur:

- a) There is no more excess-power ($P_{\text{tot-used}} = P_{\text{tot-sat}}$):
this is to adhere the constraint in equation (4-24b) of the sub-problem “ F_2 ”;
- b) This beam (b) has reached the maximum beam’s power ($P_b = P_{b-\max}$):
this is to adhere the constraint in equation (4-24c) of the sub-problem “ F_2 ”;

If the option (a) is not yet met but the option (b) is met, it would mean that the power of the current beam with “ $R_{b-\min}$ ” can no longer be increased despite availability of excess-power to redistribute. In this case, the redistribution process will consider the unsatisfied beam with the second minimum *OCTR*-ratio as the new minimum *OCTR*-ratio, and perform the same beam-power increment process as described in the following lines below.

To determine the beam’s power increment step-size ($P_{b-\text{inc-step}}$) at this stage, we consider the following. There two constraints that should be adhered to, namely, the maximum beam power ($P_{b-\max}$) and the total system’s power ($P_{\text{tot-sat}}$). Therefore, we propose an increment that is based on the available power from both constraints. The available beam’s power ($P_{b-\text{avail}}$) and the available total power ($P_{\text{tot-avail}}$) are obtained respective as:

$$P_{b-\text{avail}} = P_{b-\max} - P_b \quad (6-24)$$

$$P_{\text{tot-avail}} = P_{\text{tot-sat}} - P_{\text{tot-used}} \quad (6-25a)$$

$$P_{\text{tot-used}} = \sum_{b^*=1}^M P_{b^*} \quad (6-25b)$$

We first formulate the beam’s power increment needed when looking at “ $P_{b-\text{avail}}$ ”, as:

$$P_{b-\text{inc-ned1}} = \frac{1}{2} P_{b-\text{avail}} \quad (6-26)$$

We then formulate the beam’s power increment needed when looking at “ $P_{\text{tot-avail}}$ ”, as:

$$P_{b-\text{inc-ned2}} = \frac{1}{2} P_{\text{tot-avail}} \quad (6-27)$$

We consequently, derive the beam's power increment step-size to be used ($P_{b\text{-inc-now}}$) as the minimum of the two:

$$P_{b\text{-inc-now}} = \min\{P_{b\text{-inc-ned1}}, P_{b\text{-inc-ned2}}\} \quad (6-28)$$

Using the derived increment step-size ($P_{b\text{-inc-now}}$) and the current beam's power (P_b), the new beam's power ($P_{b\text{-new}}$) for this unsatisfied beam (b) will be obtained as:

$$P_{b\text{-new}} = P_b + P_{b\text{-inc-now}} \quad (6-29)$$

Again, as indicated above, to check the closeness of the beam's power (P_b) to the maximum beam power ($P_{b\text{-max}}$), we propose an error of:

$$P_{b\text{-max-error}} = 0.1\%(P_{b\text{-max}}) \quad (6-30)$$

Thus, instead of using the equality check $P_b = P_{b\text{-max}}$, we will utilise the inequality check:

$$|P_b - P_{b\text{-max}}| < P_{b\text{-max-error}} \quad (6-31)$$

Similarly, to check the closeness of the total power used ($P_{\text{tot-used}}$) to the total system's power ($P_{\text{tot-sat}}$), we propose an error of:

$$P_{\text{tot-error}} = 0.1\%(P_{\text{tot-sat}}) \quad (6-32)$$

Thus, instead of using the equality check $P_{\text{tot-used}} = P_{\text{tot-sat}}$, we will utilise the inequality check:

$$|P_{\text{tot-used}} - P_{\text{tot-sat}}| < P_{\text{tot-error}} \quad (6-33)$$

In sum, if there is a beam (b) that satisfies "condition-4", the power of that beam will be increased iteratively until, either the beam is no longer the minimum *OCTR*-ratio, or the beam's power (P_b) has reached maximum value ($P_{b\text{-max}}$), or the total power used ($P_{\text{tot-used}}$) has reached the total system's power ($P_{\text{tot-sat}}$). At each iteration, the beam's power increment step-size ($P_{b\text{-inc-now}}$) will be determined as presented in equation (6-28) above, and the new beam's power ($P_{b\text{-new}}$) will be derived as in equation (6-29) above. Thereafter, the new beams' powers-set ($P_{b\text{-set-new}}$) will be updated for next search iteration. Note that, if the unsatisfied beam with minimum R_b reaches the maximum beam's power while there is still excess power available for redistribution, the redistribution process will consider the unsatisfied beam with

the second minimum *OCTR*-ratio as the new minimum *OCTR*-ratio. Furthermore, if ever all the unsatisfied beams reach the maximum beam's power while there is still excess power available for redistribution (a very unfeasible case though), the redistribution process must be exited and the algorithm must go to "Step3" to terminate the inter-beam power-allocation process.

When there is no more excess-power to redistribute (i.e. condition 4 was not met) while all previous conditions (condition 1 to 3) have been met, the power redistribution process should proceed to checking if the total power used ($P_{\text{tot-used}}$) is greater than " $P_{\text{tot-sat}}$ "; that is "Condition 5".

Condition 5: Check if $P_{\text{tot-used}} > P_{\text{tot-sat}}$:

The purpose of this final check-condition is to avoid a situation where the total power used is greater than total power of the satellite; as that will violate the constraint in equation(4-24b) of the inter-beam power-allocation problem (F_2), which is being solve by this algorithm. Therefore, if this condition occurs, the total power used should be reduced gradually until it becomes equal to or less than " $P_{\text{tot-sat}}$ ". To execute this power reduction, we propose to start by decreasing progressively the biggest beam's power in the system ($P_{\text{b-biggest}}$). Note however that, this biggest beam-power should not be decreased below the deserving beam's power ($P_{\text{b-d}}$) defined. Also, the point of decreasing the beam's power is to achieve $P_{\text{tot-used}} = P_{\text{tot-sat}}$. Therefore, there is no need to excessively decrease the power such that " $P_{\text{tot-used}}$ " becomes far less than " $P_{\text{tot-sat}}$ ".

From these notes, we propose a decrement step-size ($P_{\text{b-dec-now}}$) for the beam's power (P_{b}) which takes in consideration these two outlined minimum limits. So, in order to calculate " $P_{\text{b-dec-now}}$ ", we start by extracting the beam's excess-power ($P_{\text{b-excess}}$) and the total excess-power ($P_{\text{tot-excess}}$) as:

$$P_{\text{b-excess}} = P_{\text{b}} - P_{\text{b-d}} \quad (6-34)$$

$$P_{\text{tot-excess}} = P_{\text{tot-used}} - P_{\text{tot-sat}} \quad (6-35a)$$

$$P_{\text{tot-used}} = \sum_{b^*=1}^M P_{b^*} \quad (6-35b)$$

Thereafter, we formulate two beam's power decrement needed. The first beam's power decrement needed when looking at the beam's excess power, is formulated as:

$$P_{\text{b-dec-ned1}} = \frac{1}{2} P_{\text{b-excess}} \quad (6-36)$$

The second beam's power decrement needed when looking at the total excess power is formulated as:

$$P_{b\text{-dec-ned2}} = \frac{1}{2} P_{\text{tot-excess}} \quad (6-37)$$

Consequently, we derive the beam's power decrement step-size to be used ($P_{b\text{-dec-now}}$) as the minimum of the two:

$$P_{b\text{-dec-now}} = \min\{P_{b\text{-dec-ned1}}, P_{b\text{-dec-ned2}}\} \quad (6-38)$$

Using the derived decrement step-size ($P_{b\text{-dec-now}}$) and the current beam's power (P_b), the new beam's power ($P_{b\text{-new}}$) for this beam (b) with the biggest power will be obtained as:

$$P_{b\text{-new}} = P_b - P_{b\text{-dec-now}} \quad (6-39)$$

Again, at this stage also, the closeness of the beam's power (P_b) to the deserving beam's power (P_{b-d}), is checked as described by equation (6-23) above; and the closeness of the total power used ($P_{\text{tot-used}}$) to the total system's power ($P_{\text{tot-sat}}$), is checked as described by equation (6-33) above.

In sum, if "condition-5" is met, the maximum beam's -power amongst all beams must be decreased iteratively until the total power used ($P_{\text{tot-used}}$) is equal to total system's power ($P_{\text{tot-sat}}$). At each iteration, the beam's power decrement step-size ($P_{b\text{-dec-now}}$) will be determined as presented in equation (6-38) above, and the new beam's power ($P_{b\text{-new}}$) will be derived as in equation (6-39) above. Thereafter, the new beams' powers-set ($P_{b\text{-set-new}}$) will be updated for next iteration search. However, with all previous conditions (condition 1 to 4) jumped, if this "condition 5" is also not met, the power redistribution process (i.e. Step2) should be exited and the algorithm should go to "Step3" to terminate the inter-beam power-allocation process.

6.4.4. Stage3: Terminate the inter-beam power allocation process

In this step, the inter-beam power-allocation search process will be terminated, and the last beams' powers-set obtained from the search process (Step2) will be stored as the resulting adequate beams' powers-set ($P_{b\text{-set-adeq}}$). This powers-set represents a set of the adequate powers that should be allocated to respective antennas ($P_{b\text{-adeq}}$) in order to produce the highest possible increase of the minimum *OCTR*-ratio amongst all beams, while preserving the rights of other beams; and thus maximize fairness between all beams.

6.4.5. Resulting inter-beam PA-algorithm based on Max-Min Fairness concept

Following all the steps from the above discussion, the resulting inter-beam power-allocation algorithm based on the Maximum-Minimum Fairness concept, for fairness maximization amongst M -beams, is summarised in Table 6.3 below.

Table 6.3: Proposed Inter-beam PA Algorithm for M -beams, based on the Max-Min Fairness Concept

Algorithm 6.2: Proposed Inter-beam PA-Algorithm for M-beams, based on the Max-Min Fairness concept		
steps	lines	actions
Step1:		Process initialisation:
(a)	1:	Receive: H, D, W ; and Define $P_{tot-sat}, P_{b-max}, ce=0.01$.
(b)	2:	Define beam's right => all beams have same right;
(c)	3:	Calculate P_{b-d} for all M -beams using equation (6-8);
(d)	4:	Generate: $P_{b-set-init}$ as in equation (6-9).
Step2:		Iterative excess-power redistribution to unsatisfied beams:
repeat		repeat:
(a)	5:	Receive the new beams powers set " $P_{b-set-new}$ ";
(b)	6:	Evaluate new R_b for each beam and generate new " R_{b-set} " as in equation(6-10);
(c)	7:	Check for condition-1 using equation (6-11); and if so, go to "Step3";
(d)	8:	Else, Check for condition-2 using equation (6-12):
	9	If "condition-2 = True" => using $ce=0.01$, verify if $R_b \approx 1$ using equation (6-16):
	10	If True: proceed to "condition-3"
	11	else: decrease P_b as in eqt (6-15), update P_{b-set} , and return to "Step2a".
(e)		Else: Check "Condition-3":
	13	If "Condition-3 = True" => using $ce=0.01$, verify if $R_b \approx 1$ using equation (6-16)
	14	If Eqt (6-16) not satisfied => Calculate $P_{b-error}$ as in equation (6-22);
	15	Then check if $P_b \approx P_{b-d}$ using equation (6-23):
	16	If equation (6-23) = True: => proceed to "Condition-4"
	17	else: calculate $P_{b-inc-new}$ and P_{b-new} as in equations (6-20) & (6-21), and update P_{b-set} then return to "Step2a"
		Else: Check "Condition-4":
	19	If "Condition-4 = True":
	20	Calculate $P_{b-max-error}$ and $P_{tot-error}$ as in equations (6-30) & (6-32);
	21	Check if $P_b \approx P_{b-max}$ (Eqt (6-31)) and $P_{tot-used} \approx P_{tot-sat}$ (Eqt (6-33));
	22	If True: proceed to "Condition-5"
	23	else: calculate $P_{b-inc-now}$ and P_{b-new} as in equations (6-28) & (6-29), and update P_{b-set} then return to "Step2a"
		Else: Check "Condition-5":
	25	If "Condition-5 = True":
	26	Calculate $P_{b-error}$ (Eqt (6-22)) and $P_{tot-error}$ Eqt (6-32);
	27	Check if $P_b \approx P_{b-d}$ (Eqt (6-23)) and $P_{tot-used} \approx P_{tot-sat}$ (Eqt (6-33));
	28	If True: Go to "Step3"
	29	else: calculate $P_{b-dec-now}$ and P_{b-new} as in equations (6-38) & (6-39). and update P_{b-set} then return to "Step2a"
	30	Else: Go to "Step3" (i.e. if none of above condition is met).
Until		Until: Either Condition 1 or 2 is met; or none of 5 conditions are met
Step3:		terminate the search process store final beams powers set "$P_{b-set-adeq}$".

6.5. Global System's power-allocation Algorithm -2

After obtaining the *intra-beam* (Algorithm 6.1) and the *inter-beam* (Algorithm 6.2) *power-allocation algorithms* based on the *maximum-minimum fairness* concept, which respectively solve the intra-beam fairness-maximization problem (F_1) and inter-beam fairness-maximization problem (F_2); a global power-allocation algorithm that solves the original problem (F) is derived by combining the two sub-algorithms. Similar to the previous concept, here also, the combination of the two algorithms intervenes at "Step2-b" of the inter-beam algorithm. The "Step2-a" receives the new power-set ($P_{b\text{-set-new}}$); that is, the new beam-powers for all the respective antennas. Then, the "Step2-b" is supposed to calculate the new *OCTR-ratio* (R_b) of each beam (b), based on the powers allocated. If this application was *OMA* (i.e. 1 user per beam), all the allocated beam's power would be used by the single beam's user, and the calculation of the beam's *OCTR-ratio* would be direct. However, in the case of *NOMA* applications (in this scenario 2-users per beam), the allocated beam's power should be shared between the two beam's users; and the determination of the resulting beam's *OCTR-ratio* requires that an intra-beam power allocation first be performed. Thus, in the case of *NOMA*-based network, we introduce the intra-beam power allocation algorithm in the "Step2-b" of the inter-beam power allocation; so that the new *OCTR-ratio* of each beam can be determined. The combination of these two produces what we call the global power-allocation for the described "2-users *NOMA*-based *MBSN*". Since the intra-beam power allocation maximizes the minimum *OCTR-ratio* within the beam, and the inter-beam power allocation maximizes the minimum *OCTR-ratio* across all beams, the combination of both therefore results in maximization of minimum *OCTR-ratio* in the entire system (network); which is the solution to the original system's fairness maximization problem (F). The output parameters of the global power allocation algorithm generated are:

- *The inter-beam power share*: the set of adequate beams' powers ($P_{b\text{-adeq}}$) to be allocated to respective antennas; $P_{b\text{-set-adeq}} = [P_{1\text{-adeq}}, P_{2\text{-adeq}}, \dots, P_{M\text{-adeq}}]$. This is the final set of beams' powers received before terminating the search process.
- *The intra-beam power share in each beam*: the adequate beam's power-sharing coefficient (α_b) obtained in each beam (b); $\alpha_{b\text{-set-adeq}} = [\alpha_{1\text{-adeq}}, \alpha_{2\text{-adeq}}, \dots, \alpha_{M\text{-adeq}}]$. This is a set of the last power-sharing coefficient (α_b) received from each respective beam (b).

Where, " M " is the number of antennas on the satellite.

The proposed power-allocation algorithm based on *Maximum-Minimum Fairness* concept, to maximize fairness of 2users-NOMA MBSN, is summarised in Table 6.4 below.

Table 6.4: Proposed Global PA-Algorithm-2 for 2-users NOMA MBSN, based on the Max-Min Fairness Concept

Algorithm 6.3: Proposed Global PA Algorithm for 2-users NOMA MBSN, based on Max-Min Fairness Concept (PAA-2)		
steps	lines	actions
Step1:		Process initialisation:
(a)	1:	Receive: $\mathbf{H}, \mathbf{D}, \mathbf{W}$; and Define $P_{\text{tot-sat}}, P_{\text{b-max}}$,
(b)	2:	Define beam's right => all beams have same right;
(c)	3:	Calculate $P_{\text{b-d}} = P_{\text{tot-sat}} / M$, for all M -beams;
(c)	3:	Generate: $\mathbf{P}_{\text{b-set-init}} = [P_{1-d}, P_{2-d}, \dots, P_{M-d}]$;
Step2:		Iterative Convergence Search Process:
repeat		repeat:
(i)	5:	Receive the new beams powers set " $\mathbf{P}_{\text{b-set-new}}$ ";
(ii)	6:	Do " <i>intra-beam power-allocation algorithm</i> " as in " <i>Algorithm 6.1</i> " in Table 6.2
		Receive the resulting new R_{b} and α_{b} for each respective beam;
		Generate new $\mathbf{R}_{\text{b-set}} = [R_1, R_2, \dots, R_M]$ and $\alpha_{\text{b-set}} = [\alpha_1, \alpha_2, \dots, \alpha_M]$;
(ii)	7:	Do " <i>inter-beam power-allocation algorithm</i> " as in " <i>Algorithm 6.2</i> " in Table 6.3
		Execute "Step2-c" to "Step2-e" of " <i>Algorithm 6.2</i> " using " $\mathbf{P}_{\text{b-set-new}}$ " & " $\mathbf{R}_{\text{b-set}}$ ".
		Receive, either $\mathbf{P}_{\text{b-set-new}}$ for next iteration, or an instruction to exit loop.
Until		Until: instruction to exit the loop is received from the <i>inter-beam PA-process</i>
Step3:		End the search process & store final powers set: "$\mathbf{P}_{\text{b-set-adeq}}$" & "$\alpha_{\text{b-set-adeq}}$".

6.6. Novelty of the proposed PAA-2

The work presented in the proposed algorithm 6.3 presents some novelty at various levels:

1. Firstly, to the best of author's knowledge, there is no other reported work that proposed a PA-algorithm based on max-min fairness concept, for 2Users NOMA MBSN. Thus, the *intra-beam*, *inter-beam* as well as the *global algorithms* proposed are individually and collectively, distinct novelties in this field of research.
2. Secondly, in the intra-beam power allocation algorithm, the techniques proposed for the adjustment of the beam's power-sharing coefficient (α_{b}) are author's original ideas and have not been reported before, to the best of author's knowledge.
3. Thirdly, In the inter-beam power allocation algorithm, we proposed a novel approach for redistributing the excess power amongst unsatisfied beams, which is orientated towards improving the minimum *OCTR-ratio* subject to beam's power constraints; rather than the liberal redistribution approach proposed in the conventional max-min concept.
4. Also, in the inter-beam power allocation algorithm, the methods used to determine the increment step-size necessary for the incrementing of the relevant beam's power in

each iteration (case of marginalised user (condition-3) or unsatisfied user(condition-4)) are author's own ideas. Similarly, the methods used to determine the decrement step-size necessary for the decrementing of the relevant beam's power in each iteration (case of marginalised user (condition-2) or unsatisfied user(condition-5)) are author's own ideas. To the best of the best of author's knowledge these proposed methods have not been reported before.

6.7. Chapter summary

This chapter presented the design of fairness maximization power-allocation algorithms for a 2-users *NOMA-MBSN*, based on the Max-Min fairness concept. First, the general steps involved in the max-min fairness concept were presented. Then based, on these steps, the intra-beam power-allocation algorithm was developed. In the case of max-min fairness concept, the desired value of α_b (noted, α_{b-d}) cannot be found analytically. Thus, the numerical search process was found to be one of the most reasonable approach to do so. Therefore, in this chapter, the author proposed a novel technique for adjusting α_b during iterations of the intra-beam power-allocation process. Similarly, based on the above mentioned general steps, the inter-beam power-allocation algorithm was developed. A novel approach for redistributing the excess power amongst desiring beams was proposed in this chapter. Furthermore, a novel method for determining the necessary increment or decrement step-size in each iteration of the inter-beam power-allocation process was proposed in this chapter. Finally, the global system's power-allocation algorithm (*PAA-2*) was generated by combining the intra-beam and inter-beam *PA* algorithms, in an iterative process.

CHAPTER 7: IMPLEMENTATION, TESTING AND VALIDATION OF ALL THE DEVELOPPED ALGORITHMS (UGA, PAA-1 AND PAA-2)

7.1. Introduction

This chapter discusses the implementation, testing and validation of our proposed algorithms for subsystems of the multiple-access encoder of a 2-Users *NOMA*-based *MBSN*; including the users-grouping algorithm, power-allocation algorithm based on the *OCTR*-ratio convergence concept as well as the power-allocation algorithm based on the maximum-minimum fairness concept.

After generating the algorithms, they need to be implemented into codes which will be executed on a programmable platform. In this research, we opted to implement our proposed algorithms on two platforms. First, we implemented them on the “*matlab platform*” (*emulation*) for initial check of their functional performances. Then, after satisfaction with initial performance achieved on matlab, we implemented the algorithms on a *real-time processor (on-chip implementation)* to further verify their performance on a real-hardware. Each of these two implementations as well as their respective tests and results are presented in details in the following sections.

7.2. Matlab Implementation, Testing and Validation

7.2.1. The implementation

Matlab is a user-friendly codes-development environment, which allows developers (software and firmware) to write codes for their algorithms and be able to easily test their functionalities. Matlab provides a C-like syntax format to write codes for algorithms; which can thereafter, be turned into the desired language of the targeted programmable devices (*C, C++, HDL, ... etc.*), by means of high-level synthesis (*HLS*). In this implementation, the “editor window” of Matlab was used to write codes that execute each of the proposed algorithms. An extract of the top-file code for each algorithm is presented in Appendix-A2, -A4 and -A5, respectively. After writing all the necessary codes for each algorithm, these codes were run in order to test the functional performance of the concerned algorithm. The test process for each algorithm is discussed in details in the next section below.

7.2.2. The ATPs of the subsystems under test

In Engineering systems’ design and development, in order to test functionalities of any proposed system, the acceptance test procedure (*ATP*) must first be defined for that system. This implies, clearly defining the following elements:

- The functions of the system which are to be tested,

- The requirements to be tested,
- The input parameters (data set) expected by the system in order to execute desired function: i.e. what will be needed to test each requirement?
- The output parameters (data set) measured in order to test each requirement: i.e. how will each requirement be tested?

Thereafter, the necessary input data set needs to be generated and supplied to the system in order for it to execute its functions.

Therefore, following the engineering system’s design and development approach, in order to test our proposed algorithms for the users-grouping subsystem (*UGS*) as well as the power-allocation subsystem (*PAS*), the *ATP* for each subsystem must first be defined. Thus, Table 7.1 and Table 7.2 below, respectively give a summary of the *ATP* for the *UGS* and *PAS* under test.

Table 7.1: Acceptance Test Procedure (ATP) of the Users-Grouping Subsystem (UGS)

Input parameters	Function to be tested	Requirements		Tests	Results display
<ul style="list-style-type: none"> ➤ Number of users per beam: $r = 2$; ➤ Number of antennas on the Satellite: $M = 4$; ➤ Channel vector (h_u) of all the $2M$-users in form of System’s channel-matrix (H). ➤ Initial minimum Channel-gain ratio ($C_{gr-init}$) 	The ability to generate M -pairs from the $2M$ -users according to the requirements set.	(a)	The algorithm shall generate M -pairs;	<ul style="list-style-type: none"> • Count the number of pairs K generated; and • Verify if it is less or equal to M. 	1) A table listing the generated pairs; 2) A plot of the top-level view of users spread in the network with highlight of the paired users;
		(b)	All pairs shall satisfy the minimum channel-gain margin defined;	<ul style="list-style-type: none"> • Measure the channel-gains ratios (C_{gr}) of all pairs, and • Verify that for all pairs, $C_{gr} \geq C_{gr-min}$ 	A table listing each pair and its C_{gr} , then the C_{gr-min} .
		(c)	All pairs should satisfy the high channel-correlation coefficient defined;	<ul style="list-style-type: none"> • Measure the channel-correlation coefficient (C_3) of all pairs, and • Verify that for all pairs, $C_3 \geq C_{3-min}$ 	1) A table of the C_3 -matrix with highlight of the paired users. 2) A table listing each pair and its C_3 , then the C_{3-min} .
		(d)	There must be high fairness amongst generated pairs with regards to their channel correlation;	<ul style="list-style-type: none"> • Calculate fairness metric of the algorithm by means of Jain’s Index, using the C_3 of all pairs. 	Write the numerical result.

Table 7.2: : Acceptance Test Procedure (ATP) of the Power-Allocation Subsystem (PAS)

Input parameters	Function to be tested	requirements		Tests	Results display
<ul style="list-style-type: none"> ➤ Number of antennas on the Satellite: M; ➤ $P_{tot-sat}$ and P_{b-max}; ➤ Operating frequency (F_c) and channel bandwidth (BW) 	The ability to allocate power to respective M antennas (i.e. P_b) and to respective beam’s users (i.e. α_b)	(a)	The algorithm shall generate: P_{b-set} : a set powers (P_b) to respective antennas, from the total available power (P_{tot}); α_{b-set} : and a set of “ α_b ” for each respective beam (b);	<ul style="list-style-type: none"> • Measure that algorithm generates a (i.e. P_{b-set} and α_{b-set}) at each iteration until it concludes the PA process. 	1) A Plot of P_b -set generated at each iteration; as well as P_{tot} used. 2) A Plot of α_b -set generated at each iteration.

<ul style="list-style-type: none"> ➤ Traffic demand (D_u) of each of the $2M$ users. ➤ Channel vector (h_u) of all the $2M$-users in form of System's channel-matrix (H). ➤ All M-pairs generated; ➤ Weight-vectors (w_b) of respective M-antennas in form of Weight-matrix (W). 	according to the requirements set.	(b)	The generated power sets (i.e. $P_{b\text{-set}}$ and $\alpha_{b\text{-set}}$) shall provide maximum system's fairness in terms of QoS.	<ul style="list-style-type: none"> • Measure the system's fairness metric at each iteration of the PAA, to observe whether it is being maximised or not through the process: this implies: <ul style="list-style-type: none"> ▪ Measure the C_{bn} & C_{bf} in each beam (b), based on the $P_{b\text{-set}}$ and $\alpha_{b\text{-set}}$ generated at each iteration; ▪ Then calculate the R_{bn} & R_{bf} in each beam. ▪ Thereafter, calculate the system's fairness metric by means of Jain's index, using the R_u of all the $2M$-users. 	<ul style="list-style-type: none"> 3) A Plot of C_{bn} & C_{bf} in each beam at each iteration; 4) A Plot of R_{bn} & R_{bf} as well as R_b, in each beams at each iteration; 5) A Plot of the system's FM measured at each iteration.
---	------------------------------------	-----	--	---	---

7.2.3. Mobile network's Parameters specification:

While the above *ATP* specifically indicate the necessary input-parameters for testing of the user-grouping and the power-allocation subsystems respectively, it should be noted that, in order to test any subsystem of the mobile-network's *MA*-encoder block, it is highly necessary to clearly describe the intended mobile network. As discussed in Section 2.2 , this implies specifying all the important factors and parameters of the mobile network which will influence the different subsystems; including the geo-spatial architecture, the casting and antennas technologies, the multiple-access technology, ...etc. Therefore, in this application, we consider implementing a 2-users *NOMA*-based multi-beams satellite network, with the network's parameters specification listed in Table 7.3 below.

Table 7.3: Mobile Network's Parameters Specification

Parameter	Specification
Access-point	LEO Satellite,
Satellite's altitude	Height = 1000km
Maximum network ground-coverage	$d_{\max} = 1000\text{km}$ from centre-beam
Angle-of-Arrival Span	$-\pi, +\pi$, with respect to centre-beam's axis
Number of Satellite's Antennas (M)	$M = 4$ (Multi-Cast),
Satellite's antennas casting technology	Full-frequency-reuse (<i>FFR</i>),
Frequency of operation for each antenna	$F_c = 20\text{GHz}$ (Ka Band)
Channel bandwidth	$BW = 500\text{MHz}$,
Gain of the satellite's antennas	$G_{\text{tx}} = 50\text{dBi}$,
Number of antenna at user-terminal	1
Gain of user-terminal's antenna	$G_{\text{rx}} = 0\text{dBi}$,
Multiple-access technology	<i>NOMA</i> (PD)
Number of <i>NOMA</i> users per antenna beam	$r = 2$,
Total satellite power available ($P_{\text{tot-sat}}$)	60W (48dBm),
Maximal antenna power ($P_{b\text{-max}}$)	20W (43dBm)
Noise Temperature & Spectral density	290Kelvin, -174dBm/Hz

Having specified all these input parameters of the mobile network, the *ATP* of each subsystem of the *MA*-encoder can then take effect, in order to run tests of each subsystem. Looking at the block-diagram in Figure 6.1 above for the *MA*-encoder block of the *NOMA*-based *MBSN*, it appears that, the user-grouping subsystem must execute before the power-allocation subsystem; because it must generate set of pairs which will be used by the *PAS*. Therefore, we test the proposed user-grouping algorithm for the *UGS* first. In this regard, looking at the *ATP* in Table 7.1 above for *UGS*, the remaining input-data set that still need to be defined for testing of the *UGA* is the set of channel vectors of the $2M$ -users to be grouped. The estimation of channel-vectors as well as traffic-requests of all users in a mobile network is commonly done by the *CSI-acquisition* subsystem of the *MA*-encoder block; which at every network service's time slot, provide a set of users' channel vectors and traffic requests. As such, for the purpose of testing our proposed algorithms, the generation of a set of users' traffic-requests and channel-vectors at a given network's service time-slot, is done as discussed below.

7.2.4. Generation of network's input-data sets:

In practice, the number of users that a mobile network can serve simultaneously (in this case $2M$) is generally far smaller than the number of active users in the network's coverage, requiring to be served. Therefore, mobile networks generally operate on a "service time-slot" basis. This means that, at every service time-slot, the "users' *CSI-acquisition subsystem*" of the network's *MA*-Encoder re-evaluates the statuses (i.e. traffic-request and channel-vector) of all the active network's users; and feeds them to the users-scheduling subsystem (*USS*) of the *MA*-Encoder. Then, from this population of active-users, the *USS* selects the $2M$ -users that will be served in the current time-slot; and only transfers their traffic-requests and channel-vectors as input-data sets to the other subsystems of the *MA*-encoder blocks, such as the *UGS* and *PAS*.

Thus, in our implementation, to mimic the operation of the real network, after specifying the network's static parameters as outlined in Table 7.3 above, we start by assuming a population of active-users of $10 \times 2M$ -users; and a network's service time-slot of T_{NS} . Then, at each network's service time (T_{NS}), we generate a new set users' traffic-requests and a new set of users' channel-vectors, for the $20M$ -users. Thereafter, we randomly select the $2M$ -users to be served, and we formulate their respective traffic-requests and channel-vectors into two input-data sets; which are then fed to the *UGS* and *PAS* for the execution of the proposed *UGA* and *PAA* respectively. The generation of the traffic-request and channel-vector for each of the respective $20M$ -users was done as discussed below.

7.2.4.1. Users' traffic-requests generation

To generate the traffic requests (TR) of all the $20M$ active-users, we randomly select the traffic request of each user between 0.5bps/Hz and 5.5bps/Hz . Due to the high number of users, it would be cumbersome to display the traffic-requests of all the $20M$ -users at each service time-slot. As such, in this document, we opt to only show, where applicable, the traffic-requests of the selected $2M$ -users in each network service time-slot. Thus, considering the case of 4-satellite's antennas, which means 8-users to be served and an active-users' population of 80-users; we generated the traffic-request for each of the 80-users as indicated above, and we only listed the TR of the 8-users selected. Table 7.4 below lists the set of traffic-requests for the selected 8-users; at a given network's service time-slot. Note that, the average- TR for the set listed below is 3bps/Hz . The average-demands of the generated TR -sets are made to range between 1bps/Hz and 5bps/Hz .

Table 7.4: a set of traffic-requests for the 8-selected users, with an average value of 3bps/Hz .

Average [bps/Hz]	D_{u1} [bps/Hz]	D_{u2} [bps/Hz]	D_{u3} [bps/Hz]	D_{u4} [bps/Hz]	D_{u5} [bps/Hz]	D_{u6} [bps/Hz]	D_{u7} [bps/Hz]	D_{u8} [bps/Hz]
3	2.6082	1.9074	3.1393	5.095	2.3788	4.8208	1.4845	0.7055

7.2.4.2. Users channel-vectors generation

To generate the channel-vectors of all active network's users, for the purpose of testing the functionality of the proposed algorithms, we considered the models described in Sections 2.4.1.3 and 2.4.2, for the estimation of user's channel-vector. These include, the path-loss model, the log-normal shadow distribution model as well as the *Rician* fading model; since the propagation medium is a satellite-to-ground link. The AWGN was generated by using a function provided on the *Matlab* environment.

Looking into these afore mentioned channel models, it can be seen that, without loss of generality, after specifying all the static network's parameters as listed in Table 7.3 above, the only parameters needed in order to estimate the channel-vector of a given user are its ground distance (d) to the satellite's centre-beam and angle-of-arrival (AoA). Therefore, to generate the channel vectors of all active network's users ($20M$), we randomly distributed users within the network's coverage, by randomly defining the ground distance of the user in the interval $0-1000\text{km}$; as well as its AoA in the interval $-\pi$ to $+\pi$.

As such, considering the case of 4-satellite's antennas, which means 8-users to be served and an active-users' population of 80-users; we generated the channel-vector for each of the 80-users as indicated above. Then, only the channel-vectors of the selected 8-users, are fed to the *UGS* and *PAS*. Again, for ease of presentation, since it would be cumbersome to tabulate the distances, $AoAs$, as well as resulting channel-vectors for all the 80-users, we opted to only

display the information of the selected 8-users. Subsequently, Table 7.5 below only lists the generated ground distance and AoA for each of the selected 8-users; and Table 7.6 below lists the resulting channel-vectors of respective 8-users. Figure 7.1 below gives a geo-spatial illustration (in 3D) of users' distribution across the network's coverage; for all the 80-users; while Figure 7.2 below gives the top-view (i.e. 2D) illustration of this users' distribution. On the plot, the 8-users randomly selected for service, which are tabulated in Table 7.5 and Table 7.6 below, are plotted in "red"; while the remain population of users are plotted in "black". Also, the blue dot in the centre of the plot represent the satellite's centre beam, which is the reference point of the satellite for all distances and AoAs of ground users.

Table 7.5: Ground distances and Angle-of-Arrival of selected 8-users

User No	1	2	3	4	5	6	7	8
Distance [km]	515	782	65	108	543	127	99	312
AoA [rad]	0.64π	0.05π	-0.41π	0.34π	0.42π	0.57π	0.21π	-0.32π

Table 7.6: Channel-vectors of the selected 8-users

h_1	h_2	h_3	h_4
$+0.0061 + 0.0411i$	$+0.0141 - 0.0148i$	$-0.0004 + 0.0128i$	$+0.0288 - 0.0483i$
$-0.0086 + 0.0406i$	$+0.0109 - 0.0174i$	$-0.0054 + 0.0116i$	$+0.0155 - 0.0541i$
$-0.0379 - 0.0169i$	$-0.0090 - 0.0184i$	$-0.0082 - 0.0098i$	$-0.0477 - 0.0298i$
$+0.0244 - 0.0336i$	$-0.0204 - 0.0021i$	$+0.0124 - 0.0033i$	$-0.0418 + 0.0377i$
h_5	h_6	h_7	h_8
$+0.0415 + 0.0236i$	$+0.0300 + 0.0343i$	$+0.0084 + 0.0011i$	$+0.0061 + 0.0105i$
$+0.0381 + 0.0287i$	$+0.0221 + 0.0399i$	$+0.0084 + 0.0013i$	$+0.0031 + 0.0117i$
$+0.0131 + 0.0459i$	$-0.0242 + 0.0387i$	$+0.0081 + 0.0026i$	$-0.0105 + 0.0061i$
$-0.0171 + 0.0445i$	$-0.0455 - 0.0024i$	$+0.0076 + 0.0039i$	$-0.0086 - 0.0086i$

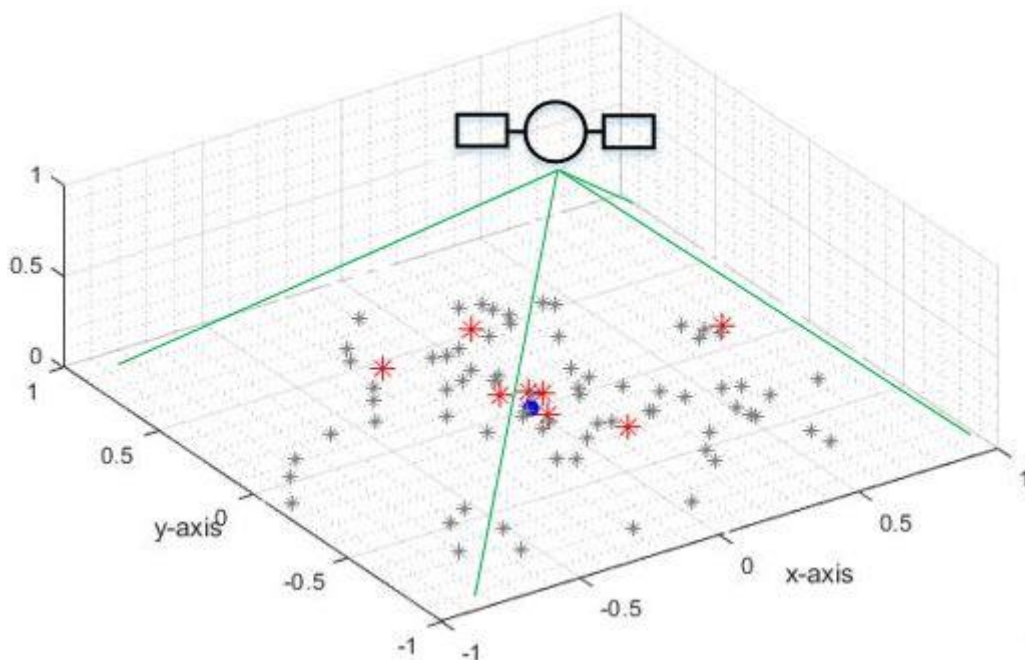


Figure 7.1: Geo-spatial illustration of 80-users' distribution in the network (3D view).

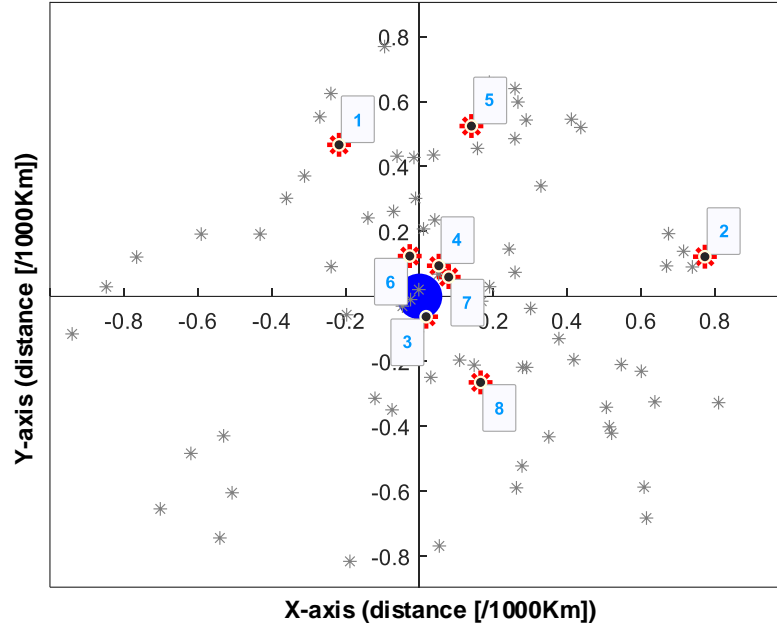


Figure 7.2: Geo-spatial illustration of the 80-users' distribution in the network (Top-view).

After producing all the necessary input-data sets as discussed above, the code generated for the proposed *users' grouping algorithm (UGA)* was then run and tested first; and thereafter those generated for each of the two power allocation algorithms (*PAA-1* and *PAA-2* respectively). Thus, the codes generated for all proposed algorithms were run in the following sequence:

- 1: First, the code for the *UGA*, in order to generate pairs;
- 2: Then, the code for precoding weight-vectors calculation based on Zero-Forcing;
- 3: Thereafter, the code for the *PAA* based on the *OCTR*-ratios convergence concept (i.e. *PAA-1*), to generate the power sets to respective antennas and beam's users;
- 4: Finally, the code for the *PAA* based on the Max-Min Fairness concept (i.e. *PAA-2*), to generate the power sets to respective antennas and beam's users;

7.2.5. *UGA's* Code running and results discussion

7.2.5.1. Test results

After defining all the input parameters required by the user-grouping system (UGS), they were provided to the code executing the users-grouping algorithm. This code was then run and provided expected output parameters. According to the *ATP* of the *UGS* in Table 7.1 above, the only expected data out of the *UGA* is the set of pairs generated. Thus, we provide here below, the generated pairs from the *UGA* process. In this regard, Table 7.7 (a) below lists the channel-gains of all the $2M$ -users in increasing order, for the above outlined input data-set (i.e. case of 4 satellite's antennas, 8-users). It also shows the M near-users (i.e. the 4 near-users) and M far-users (i.e. the 4 far-users). Then, Table 7.7 (b) below displays the channel-

correlation coefficients (C_3) between all near-users and far-users. Finally, Table 7.8 (a) below displays the resulting pairs of near-far users, obtained from running the code of the proposed UGA; and Table 7.8 (b) highlights them on the C_3 -matrix. Also, Figure 7.3 below highlights every pair (beams) generated from the $2M$ -users to be served, in the network's geo-spatial distribution presented earlier. Note that, for a given input data-set, the code was run over 100 times to investigate its reliability; and the generated pairs in each run were all the same.

Table 7.7: Near-users and far-users' sets as well as the resulting C_3 -matrix.

(a): channel gains of the 8-users

user	Channel Gains	Users-set
3	0.1126	} Near-users
7	0.0954	
4	0.0912	
6	0.0831	
8	0.0410	} Far-users
1	0.0256	
5	0.0243	
2	0.0170	

(b): far_users - near_users channel-correlation coefficients (C_3 -Matrix)

fu\neu	3	7	4	6
8	0.8631	0.1428	0	0.3223
1	0.4510	0.2075	0	0.9085
5	0.2058	0.3714	0.8943	0.6413
2	0.2016	0.6178	0	0.1554

Table 7.8: Generated pairs of near-far users.

(a): Resulting set of pairs

Near-user	Far-user
3	8
6	1
7	2
4	5

(b): The 4-pairs highlighted on the C_3 -matrix

fu\neu	3	7	4	6
8	0.8631	0.1428	0	0.3223
1	0.4510	0.2075	0	0.9085
5	0.2058	0.3714	0.8943	0.6413
2	0.2016	0.6178	0	0.1554

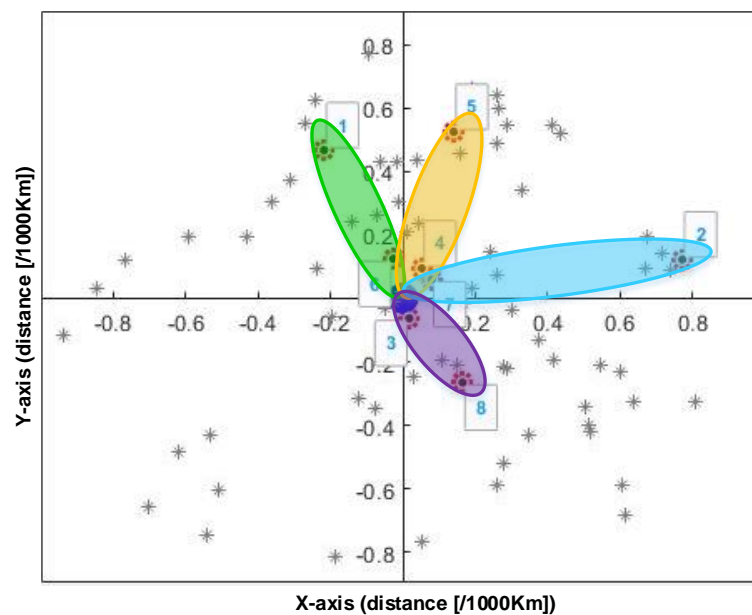


Figure 7.3: Highlight of the generated pairs on the network's spatial-distribution view.

7.2.5.2. Performance validation

The resulting pairs indicate that the code generates all expected M-pairs; *which shows that it satisfies the first requirement in the ATP of the UGS in Table 7.1 above.* Subsequently, in order to verify the performance of the algorithm with respect the other requirements listed in Table xxx, the generated pairs were used as follows. Firstly, to verify whether all pairs satisfy the minimum channel-gain margin (C_{gr-min}) defined, the channel-gain margin between the two users in each pair was calculated and tabulated in Table 7.9 below. The results captured in the table indicate that, for all users, the channel-gain ratio is greater than the defined minimum channel-gain ratio; *which shows that the algorithm also satisfies the second requirement in the ATP table.* Then, to verify whether all pairs satisfy the requirement of high channel-correlation coefficient, the channel-correlation coefficient between the two users in each pair was calculated and tabulated in Table 7.10 below. The results captured in the table indicate that, for all users, the channel-correlation coefficient obtained are relatively high; *which furthermore shows that the algorithm satisfies the third requirement in the ATP table.* Finally, to verify that the algorithm guaranties high fairness amongst pairs in terms of channel-correlation coefficients, the fairness-metric of the set of pairs generated was calculated by means of Jain's Index, using the channel-correlation coefficients of the respective pairs. Note that, according to the Jain's Index, the fairness metric range between 0 and 1, with 0 being worst and 1 being best system's fairness. The results from the grouping as displayed in Table 7.10below showed a very high fairness metric (in this case, greater than 0.9). *This also indicates that the algorithm satisfies the requirement (d) in the UGS's ATP table (Table 7.1 above).*

Table 7.9: channel-gain ratio of resulting pairs

Pair No	[nu-fu]	$ h_{nu} $	$ h_{fu} $	$Cgr = h_{nu} / h_{fu} $	Cgr-min
1	[3-8]	0.1126	0.0410	2.7470	1.5
2	[6-1]	0.0831	0.0256	3.2455	
3	[7-2]	0.0954	0.0170	5.6025	
4	[4-5]	0.0912	0.0243	3.7512	

Table 7.10: C_3 of the resulting pairs and algorithm's fairness-metric.

Pair No	[nu-fu]	Channel-correlation coefficient (C_3)	UGA's C3 fairness_metric
1	[3-8]	0.8634	0.9796
2	[6-1]	0.9085	
3	[7-2]	0.6178	
4	[4-5]	0.8943	

To further investigate the reliability of the performances of the proposed users-grouping algorithm with respect to all four requirements listed in the ATP table, the code was run multiple times with different sets of input-data. Also, different set of input-data were generated for the

cases of 5 and 6 antennas on the satellite; and in each case, the code of the *UGA* was run over 100 times. To test the *UGA* for the case of 5-antennas (i.e. 10-users to group in pairs), set of users' channel-vectors used are listed in Table 7.11 and Table 7.12 below. The near-users and far-users sets produced are given in Table 7.13 below. Finally, the generated 5-pairs obtained from running the algorithm, as well as their respective channel-gain ratios and respective channel-correlation coefficients, are displayed in Table 7.14, Table 7.15 and Table 7.16 below, respectively. These pairs are also highlighted on the geo-spatial distribution plot in Figure 7.4 below. The achieved fairness-metric of the *UGA* for this case of 5-antennas (i.e. 5-pairs) is about 0.957 as shown in Table 7.16 below.

Table 7.11: Ground distances and Angle-of-Arrival of selected 10-users.

User No	1	2	3	4	5	6	7	8	9	10
Distance [km]	450	560	80	131	509	600	639	200	122	150
AoA [rad]	-0.21π	0.42π	-0.3π	0.9π	0.94π	0.11	-0.91	-0.8π	0.37π	0.25π

Table 7.12: Channel-vectors of the selected 10-users

h_1	h_2	h_3	h_4	h_5
0.0106+0.0030i	-0.0124 - 0.0273i	0.0126 - 0.0074i	+0.0410 - 0.0385i	-0.0067 - 0.0079i
0.0104+0.0038i	-0.0240 - 0.0181i	0.0115 - 0.0090i	+ 0.0331 - 0.0455i	-0.0099 - 0.0030i
0.0085+0.0071i	0.0083 + 0.0289i	0.0035 - 0.0141i	-0.0174 - 0.0535i	0.0086 + 0.0058i
0.0055+0.0096i	0.0108 - 0.0280i	-0.0059 - 0.0133i	-0.0535 - 0.0174i	-0.0065 - 0.0081i
0.0019+0.0109i	-0.0255 + 0.0159i	-0.0129 - 0.0068i	-0.0455 + 0.0331i	0.0039 + 0.0096i
h_6	h_7	h_8	h_9	h_{10}
+0.0300+0.0343i	0.0324 + 0.0184i	-0.0124-0.0273i	0.0061 + 0.0105i	-0.0265 + 0.0320i
+0.0221+0.0399i	0.0297 + 0.0224i	-0.0240-0.0181i	0.0031 + 0.0117i	-0.0395 + 0.0128i
-0.0242+0.0387i	0.0103 + 0.0358i	0.0083+0.0289i	-0.0105 + 0.0061i	0.0336 - 0.0244i
-0.0455-0.0024i	-0.0133 + 0.0348i	0.0108-0.0280i	-0.0086 - 0.0086i	-0.0244 + 0.0336i
-0.0200-0.0410i	-0.0316 + 0.0197i	-0.0255+0.0159i	0.0061 - 0.0105i	0.0128 - 0.0395i

Table 7.13: Near-users and far-users' sets as well as the resulting C_3 -matrix.

(a): channel gains of the 10-users

user	Channel Gains	Users-set
3	0.1258	} Near-users
9	0.1020	
4	0.0929	
10	0.0833	
8	0.0671	} Far-users
1	0.0326	
5	0.0286	
2	0.0272	
6	0.0247	
7	0.0232	

(b): far_users - near_users channel-correlation coefficients (C_3 -matrix)

fu\nu	3	9	4	10	8
1	0.7784	0	0.2879	0	0
5	0.4026	0	0.9424	0.2494	0.2981
2	0.2176	0.8273	0	0.1206	0.4035
6	0	0	0.0621	0.7522	0.2060
7	0	0.4026	0	0.2879	0.6681

Table 7.14: Generated pairs of near-far users.

(a): Resulting set of pairs

Near-user	Far-user
3	1
10	6
8	7
4	5
9	2

(b): The 5-pairs highlighted on the C_3 -matrix

fu\ntu	3	9	4	10	8
1	0.7784	0	0.2879	0	0
5	0.4026	0	0.9424	0.2494	0.2981
2	0.2176	0.8273	0	0.1206	0.4035
6	0	0	0.0621	0.7522	0.2060
7	0	0.4026	0	0.2879	0.6681

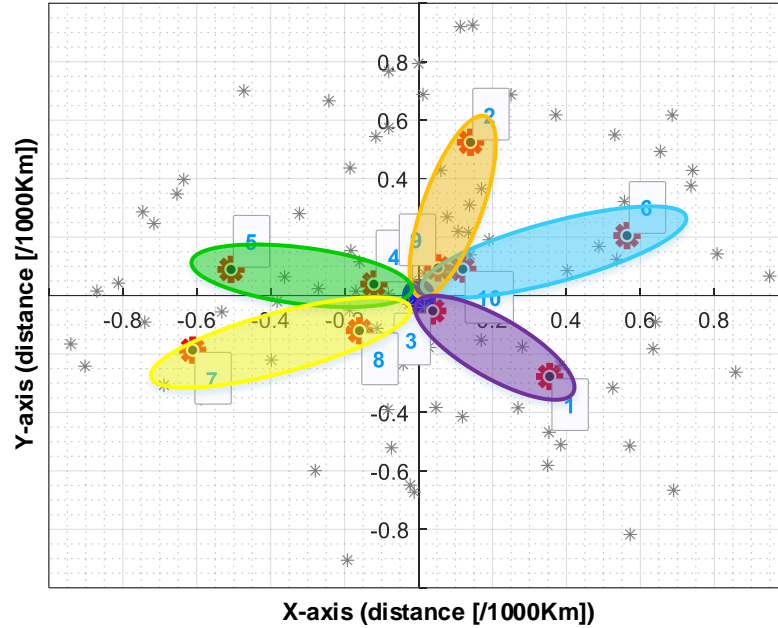


Figure 7.4: Highlight of the generated pairs on the network's spatial-distribution view.

Table 7.15: Channel-gain ratio (C_{gr}) of resulting pairs.

Pair No	[nu-fu]	$ h_{nu} $	$ h_{fu} $	$C_{gr} = h_{nu} / h_{fu} $	C_{gr-min}
1	[3-1]	0.1258	0.0326	3.8650	1.5
2	[10-6]	0.0833	0.0247	3.3741	
3	[8-7]	0.0671	0.0232	2.8925	
4	[4-5]	0.0929	0.0286	3.2455	
5	[9-2]	0.1020	0.0272	3.7512	

Table 7.16: C_3 of the resulting pairs and algorithm's fairness-metric.

Pair No	[nu-fu]	Channel-correlation coefficient (C_3)	UGA's $C_3_fairness_metric$
1	[3-1]	0.7784	0.9572
2	[10-6]	0.7522	
3	[8-7]	0.6681	
4	[4-5]	0.9414	
5	[9-2]	0.8273	

Similarly, to test the *UGA* for the case of 6-antennas (i.e. 12-users to group in pairs), set of users' channel-vectors used are listed in Table 7.17 and Table 7.18 below. The near-users and far-users sets produced are given in Table 7.19 below. Finally, the generated 6-pairs obtained from running the algorithm, as well as their respective channel-gain ratios and respective channel-correlation coefficients, are displayed in Table 7.20, Table 7.21 and Table

7.22 below, respectively. These pairs are also highlighted on the 2D geo-spatial distribution plot in Figure 7.5 below. The achieved fairness-metric of the UGA for this case of 6-antennas (i.e. 6-pairs) is about 0.9 as shown in Table 7.22 below.

Table 7.17: Ground distances and Angle-of-Arrival of selected 12-users.

User No	11	9	4	10	3	1	5	12	6	8	2	7
Dist [km]	99	127	170	175	200	312	500	515	543	648	782	907
AoA [rad]	0.26π	0.57π	-0.5π	0.34π	0.84π	-0.82π	0.06π	0.5π	0.4π	-0.87π	0.9π	0.46π

Table 7.18: Channel-vectors of the respective 12-users.

h_1	h_2	h_3	h_4	h_5	h_6
0.0061+0.0105i	0.0415+0.0236i	0.0130+0.0018i	-0.0150+0.0260i	0.0029-0.0067i	0.0061 + 0.0411i
0.0031+0.0117i	0.0381+0.0287i	0.0130+0.0023i	-0.0260+0.0150i	0.0009-0.0073i	-0.0086 + 0.0406i
-0.0105+0.0061i	0.0131+0.0459i	0.0124+0.0045i	0.0150-0.0260i	-0.0071-0.0018i	-0.0379 - 0.0169i
-0.0086-0.0086i	-0.0171+0.0445i	0.0114+0.0066i	0.0000+0.0300i	-0.0026+0.0069i	0.0244 - 0.0336i
0.0061-0.0105i	-0.0405+0.0253i	0.0101+0.0085i	-0.0150-0.0260i	0.0065+0.0035i	0.0278 + 0.0309i
0.0117+0.0031i	-0.0475-0.0042i	0.0085+0.0101i	0.0260+0.0150i	0.0042-0.0060i	-0.0360 + 0.0208i
h_7	h_8	h_9	h_{10}	h_{11}	h_{12}
0.0041 + 0.0121i	0.0219+0.0251i	-0.0061+0.0059i	0.0174-0.0292i	-0.0102-0.0177i	-0.0067-0.0079i
0.0002 + 0.0128i	0.0161+0.0291i	-0.0084+0.0015i	0.0094-0.0327i	-0.0177-0.0102i	-0.0099-0.0030i
-0.0128 + 0.0004i	-0.0176+0.0282i	0.0080-0.0029i	-0.0289-0.0180i	0.0102+0.0177i	0.0086+0.0058i
-0.0007 - 0.0128i	-0.0333-0.0017i	-0.0074+0.0043i	-0.0253+0.0228i	0.0000-0.0205i	-0.0065-0.0081i
0.0128 - 0.0009i	-0.0146-0.0299i	0.0065-0.0055i	0.0149+0.0306i	-0.0102+0.0177i	0.0039+0.0096i
0.0011 + 0.0127i	0.0191-0.0273i	-0.0055+0.0065i	0.0335-0.0059i	0.0177-0.0102i	-0.0009-0.0103i

Table 7.19: Near-users and far-users' sets as well as the resulting C_3 -matrix.

(a): user's channel gains

user	Channel Gains	Users-set
11	0.1168	Near-users
9	0.1017	
4	0.0834	
10	0.0816	
3	0.0735	
1	0.502	Far-users
5	0.0322	
12	0.0313	
6	0.0298	
8	0.0254	
2	0.0209	
7	0.0180	

(b): far_users - near_users channel-correlation coefficients (C_3 -matrix)

fu\ngu	11	9	4	10	3	1
5	0.5581	0.0285	0.1031	0	0	0
12	0	0.7787	0	0.2218	0	0
6	0	0.2581	0	0.7464	0.1086	0
8	0	0	0.0621	0	0	0.7787
2	0	0.0497	0	0	0.5278	0
7	0	0	0.8897	0	0	0.0379

Table 7.20: Generated pairs of near-far users.

(a): resulting set of pairs

Near-user	Far-user
11	5
10	6
4	7
9	12
1	8
3	2

(b): The 5-pairs highlighted on the C_3 -matrix

fu\ngu	11	9	4	10	3	1
5	0.5581	0.0285	0.1031	0	0	0
12	0	0.7787	0	0.2218	0	0
6	0	0.2581	0	0.7464	0.1086	0
8	0	0	0.0621	0	0	0.7787
2	0	0.0497	0	0	0.5278	0
7	0	0	0.8897	0	0	0.0379

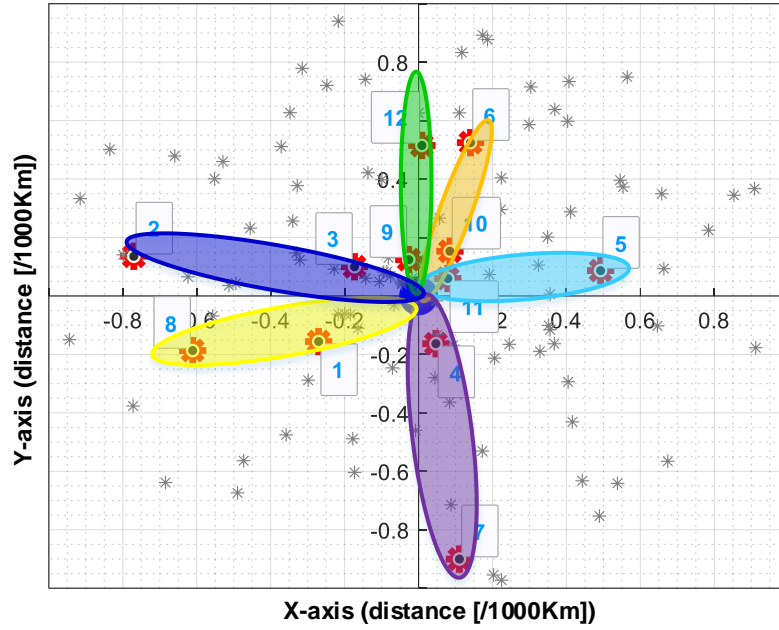


Figure 7.5: Highlight of the generated pairs on the network's spatial-distribution view.

Table 7.21: Channel-gain ratio (C_{gr}) of resulting pairs.

Pair No	[nu-fu]	$ h_{nu} $	$ h_{fu} $	$C_{gr} = h_{nu} / h_{fu} $	C_{gr-min}
1	[11-5]	0.1168	0.0322	3.6236	1.5
2	[10-6]	0.0816	0.0298	2.7393	
3	[4-7]	0.0834	0.0180	4.6265	
4	[9-12]	0.1017	0.0313	3.2455	
5	[1-8]	0.0502	0.0254	1.9741	
6	[3-2]	0.0735	0.0209	3.5257	

Table 7.22: C_3 of the resulting pairs and algorithm's fairness-metric.

Pair No	[nu-fu]	Channel-correlation coefficient (C_3)	UGA's $C_3_fairness_metric$
1	[11-5]	0.5581	0.9080
2	[10-6]	0.7464	
3	[4-7]	0.8897	
4	[9-12]	0.7787	
5	[1-8]	0.7585	
6	[3-2]	0.5278	

After running tests of the *UGA* for different number of antennas, we registered in each case, the achieved fairness-metric of the algorithm in terms of channel-correlation coefficients of respective pairs. Figure 7.6 below therefore, gives a plot of the resulting fairness-metric of the proposed *UGA*, for different number of satellite's antennas. The graph clearly indicates that, the resulting fairness metric remains relatively high, for different scenarios of satellite's antennas number.

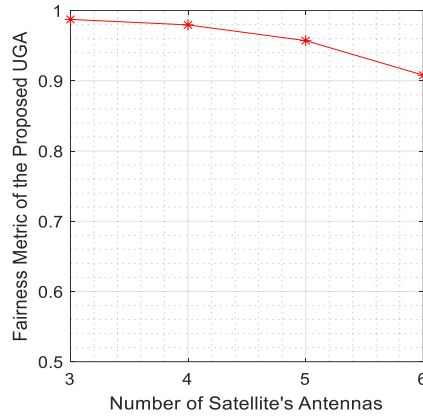


Figure 7.6: Fairness-Metric the proposed UGA for case of 3, 4, 5, and 6 antennas on the satellite.

7.2.5.3. Superiority of the proposed UGA

To demonstrate the superiority of our proposed algorithm over existing users-grouping algorithms listed earlier in section-1.1.2, we implemented: (A) the “Algorithm” in Lin et al., (2019:671), which we denoted here “UGA-in-source-1”; (B) the “Algorithm-1” in Zhu et al., (2019:4), which we denote here “UGA-in-source-2”; and (C) a UGA that automatically puts together far and near users with highest channel correlation coefficient, which we called here “HCP-UGA”. We then compared their fairness performances. Just like ours, these algorithms were individually run with test cases of 3, 4, 5 and 6 antennas on the satellite. In each of these cases, the resulting fairness-metric in terms of channel-correlation coefficients of respective pairs was calculated. below displays the fairness metric of our proposed UGA against “UGA-in-source-1”, “UGA-in-source-2”, as well as “HCP-UGA”; for different number of satellite’s antennas. We remember that, according to Jain’s Index, the fairness-metric is bounded in the interval 0 to 1, with 0 being the worst and 1 being the best system’s fairness. Therefore, *the graphs on Figure 7.7 below clearly demonstrate that our proposed UGA algorithm outperforms the cited algorithms in terms of fairness amongst generated pairs.*

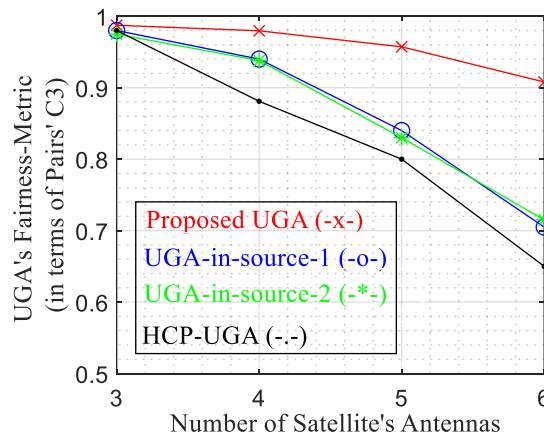


Figure 7.7: Fairness-metrics of various users-grouping algorithms for different number of antennas.

7.2.6. Precoding weight-vector Code results

After obtaining the M -pairs of users, both the set of pairs and the channel-vectors of all the $2M$ -users, were fed into the code which executes the precoding weight-vectors calculation. The code was run and produced the precoding matrix, which contains the expected M -precoding weight-vectors. During design of the precoding block (section 3.6.3 above), it was indicated that, in this design, only the channel vectors of the near-user in each pair will be used for the calculation of the precoding matrix. Thus, in the case of 4-satellite's antennas, considering the generated pairs listed in Table 7.8 above, as well as the respective channel-vectors of these 8-users, presented Table 7.6 above; the channel-matrix generated by the code, using the channel-vectors of near-users in each pair is displayed in Table 7.23 below.

Table 7.23: Channel matrix of near-users (H_{nu}).

h_3	h_7	h_4	h_6
-0.0004 + 0.0128i	+0.0084 + 0.0011i	+0.0288 - 0.0483i	+0.0300 + 0.0343i
-0.0054 + 0.0116i	+0.0084 + 0.0013i	+0.0155 - 0.0541i	+0.0221 + 0.0399i
-0.0082 - 0.0098i	+0.0081 + 0.0026i	-0.0477 - 0.0298i	-0.0242 + 0.0387i
+0.0124 - 0.0033i	+0.0076 + 0.0039i	-0.0418 + 0.0377i	-0.0455 - 0.0024i

Subsequently, Table 7.24 below gives the zero-forcing precoding matrix produced using the above generated channel-matrix of near-users (H_{nu}).

Table 7.24: The generated Zero-forcing precoding matrix.

w_1	w_2	w_3	w_4
1.3469 - 22.9739i	-140.14 - 175.28i	-24.85 + 123.74i	320.70 + 18.80i
5.1527+ 29.3910i	182.61 + 173.25i	23.45 - 150.02i	-364.45 + 12.20i
-9.4740-2.1989i	-58.78 - 38.60i	-7.41 + 44.63i	97.99 - 24.55i
1.7310 - 2.3265i	40.05 - 8.70i	-1.82 - 19.28i	-41.30 + 39.17i

From this precoding matrix, the precoding weight-vector of each of the 4-antennas is extracted from each column of the matrix; where the rank of the column is also the rank of the pair. This means that, the weight-vector in column-2 is for pair number-2, and should therefore, be used by the antenna serving this pair; which is our case is simply antenna number-2. And the same applies to all the other 3 pairs; in this case of 4-pairs. To verify that the produced precoding matrix is indeed a zero-forcing type, the product $Q = H_{nu}^H W$ must give an identity matrix. In this regard, Table 7.25 below shows the Q -matrix obtained using the H_{nu} in Table 7.23 above and the produced W in Table 7.24 above. The Q -matrix obtained is indeed an identity matrix; which certifies that the produced precoding-matrix (W) is indeed a zero-forcing precoding matrix.

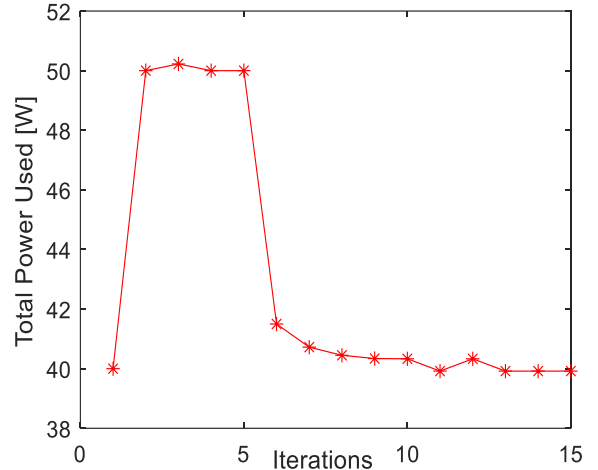
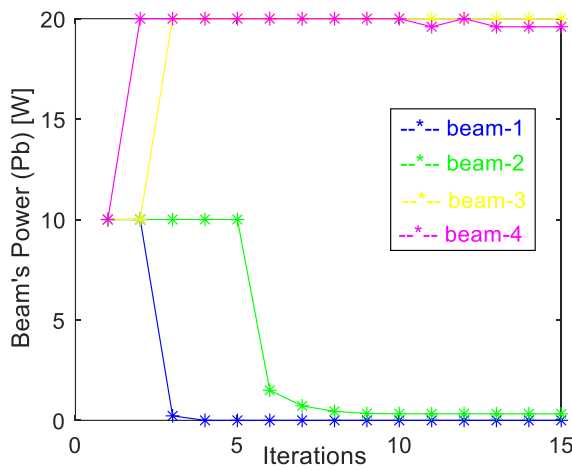
Table 7.25: The Q -Matrix obtained

Q_1	Q_2	Q_3	Q_4
1.0000 - 0.0000i	-0.0000 - 0.0000i	-0.0000 + 0.0000i	0.0000 + 0.0000i
0.0000 - 0.0000i	1.0000 - 0.0000i	-0.0000 - 0.0000i	-0.0000 + 0.0000i
-0.0000 + 0.0000i	-0.0000+0.0000i	1.0000 + 0.0000i	-0.0000 - 0.0000i
0.0000 + 0.0000i	0.0000 - 0.0000i	0.0000 - 0.0000i	1.0000 + 0.0000i

7.2.7. PAA-1's Code running and results discussion

7.2.7.1. Test results

After obtaining all the input-parameters required by the power-allocation subsystem as listed in the PAS's *ATP* (Table 7.2 above), they were fed to the code executing the power-allocation algorithm based on the *OCTR*-ratios convergence concept (*PAA-1*). The code was then run, to test its functional performance. In the case of the *OCTR*-ratios convergence concept, the code runs over a number of iterations, until all the *OCTR*-ratios converges; then it terminates. According to the these *PAS*'s *ATP*, the main output parameters of the power-allocation subsystem are the set of allocated beam's power ($P_{b\text{-set}}$), as well as the set of intra-beam power-sharing coefficient of respective beams ($\alpha_{b\text{-set}}$). From these two sets, other parameters are calculated, including the capacities of respective users, their resulting *OCTR*-ratios; and subsequently the system's fairness metric. Since the code is running over multiple iterations before it terminates, we have opted to output the " $P_{b\text{-set}}$ " and " $\alpha_{b\text{-set}}$ " at each iteration. Subsequently, we are able to calculate respective users' capacities, *OCTR*-ratios, as well as the system fairness metric, at each iteration. This also allows us to monitor the evolution of the system's fairness metric throughout the power-allocation process; in order to indeed verify that it is being maximised. Figure 7.8, to Figure 7.12 below display the results obtained from running the code of *PAA-1*, for the case of 4-satellite's antennas; using the relevant network's parameters defined in Table 7.3, the traffic-requests of the selected 8-users listed in Table 7.4, the 8 users' channel-vectors displayed in Table 7.6, the 4-user-pairs shown in Table 7.8, as well as the 4-precoding weight-vectors displayed in Table 7.24 above. Figure 7.8 below displays the respective beam's power over the different run iterations (a); as well as the total power used at each iteration (b). Then, Figure 7.9 below displays the respective beam's power-sharing coefficient (α_b) over the different run iterations. Note that, the power-sharing coefficients of beam-2 and beam-3 do not appear clearly on the graph because their values are extremely small (in the order of 10^{-12}) compared to values of power-sharing coefficients in beam-1 and beam-4 (which are in the order of 10^{-2}). Also, Figure 7.10 below displays the respective beams' capacities over the different run iteration (a); as well as the total throughput achieved at each iteration (b). Furthermore, Figure 7.11 below displays the respective user's *OCTR*-ratios over the different run iterations. Finally, Figure 7.12 below displays the system's fairness metric over the different run iterations. To verify reliability of the proposed code, the code was executed over 100 times; to check that the results are still the same in each execution.



(a): Respective beam's powers (P_b)
 (b): Total power used
Figure 7.8: Beams' powers per iteration and Total power used on Satellite.

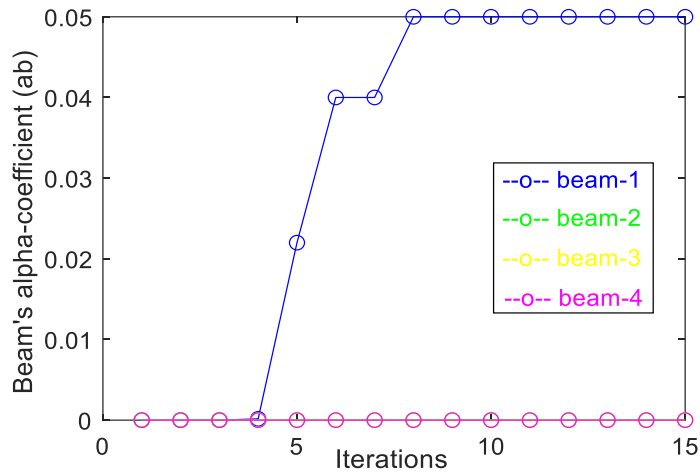
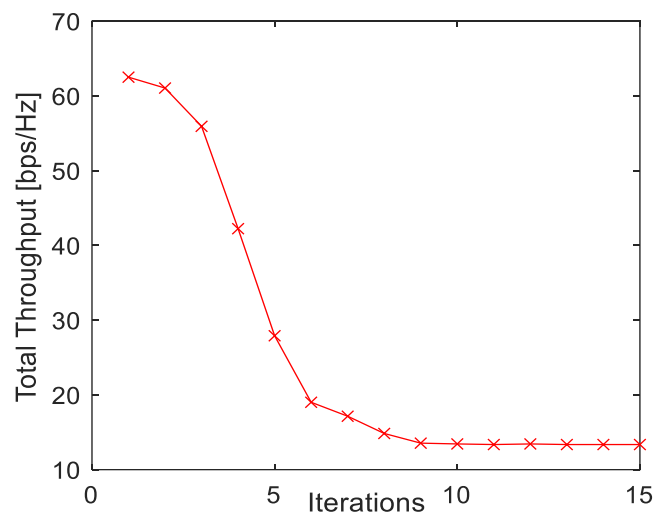
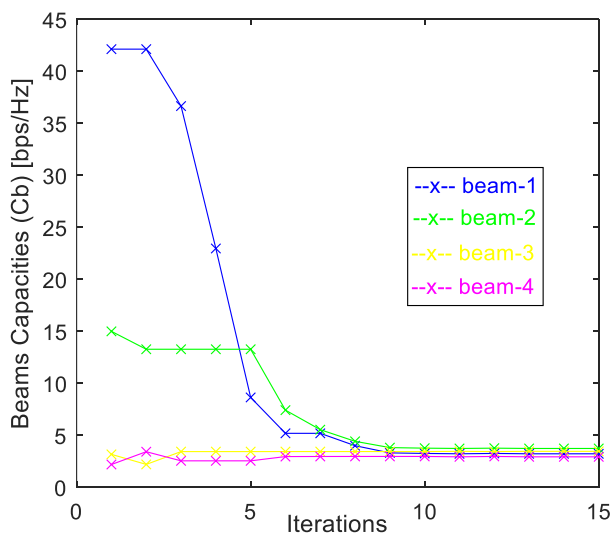


Figure 7.9: Intra-beam power-sharing coefficient (α_b) of respective beams, per iteration.



(a): Respective beam's Capacities
 (b): Total achievable Capacity
Figure 7.10: Beams' capacities per iteration and total satellite's throughput.

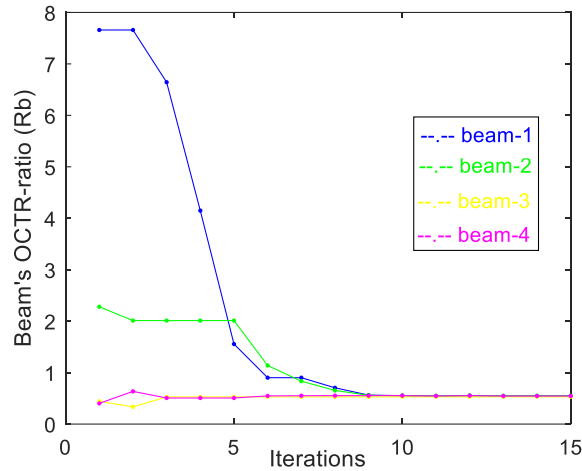


Figure 7.11: OCTR-ratio (R_b) of respective beams at each iteration.

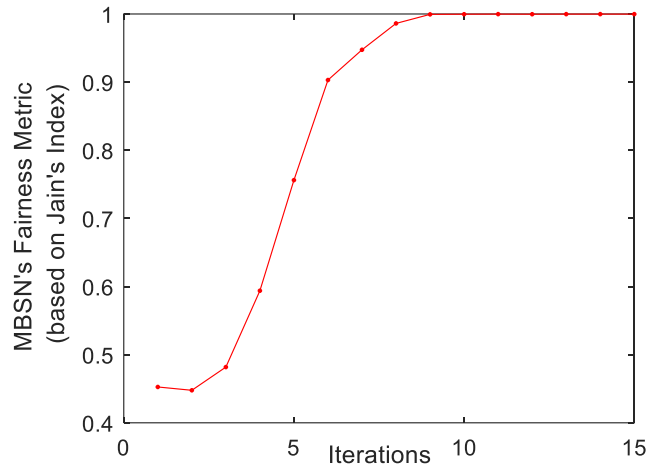


Figure 7.12: Fairness-Metric of the Multi-Beam Satellite's Network per iteration of the PAA-1.

7.2.7.2. Performance validation

Figure 7.11 above shows that, the OCTR-ratio of all beams indeed converge after a certain amount of iterations of the power-allocation algorithm. *This then confirms that the proposed algorithm indeed implements the OCTR-ratios convergence concept.* Furthermore, Figure 7.12 above shows the evolution of the network's fairness metric throughout the power-allocation process. It is worth reminding that, in this work, the network's fairness metric is calculated is based on Jain's Index. Jain's Index stipulates that, the fairness metric is bounded between 0 and 1; 0 being the worst and 1 being the best system's fairness metrics. Therefore, the graph in Figure 7.12 indicates that, the algorithm indeed maximises the network's fairness; from an initial minimum obtained with equal beam's power allocation, to a maximum of 1 obtained with the final beam's power allocation for which all OCTR-ratios converge. *This outcome therefore, satisfies the principal design requirement of the proposed power-allocation algorithm, as indicated in the ATP of the PAS (see Table 7.2 above). A fairness metric of 1 is the highest network's fairness value that can be obtained, and is in general only achieved by the OCTR-*

ratios convergence concept; which is its strongest positive characteristic. However, Figure 7.8 above shows that the total satellite's power used when the algorithm has executed is 40W, instead of the 60W available. This implies that, the algorithm forces the system to leave out a lot of its available power unused (in this case, 20W); which is a typical negative characteristic of power-allocation algorithm based on *OCTR*-ratio convergence concept. The consequence of leaving out a lot of available power unused is that the total achievable throughput of the system is ridiculously reduced while there is still power available; which is another negative characteristic of power-allocation algorithms based on the *OCTR*-ratios convergence concept. This characteristic is confirmed by Figure 7.10 (b) above which shows that, the total satellite's throughput achievable using *PAA-1* is significantly reduced.

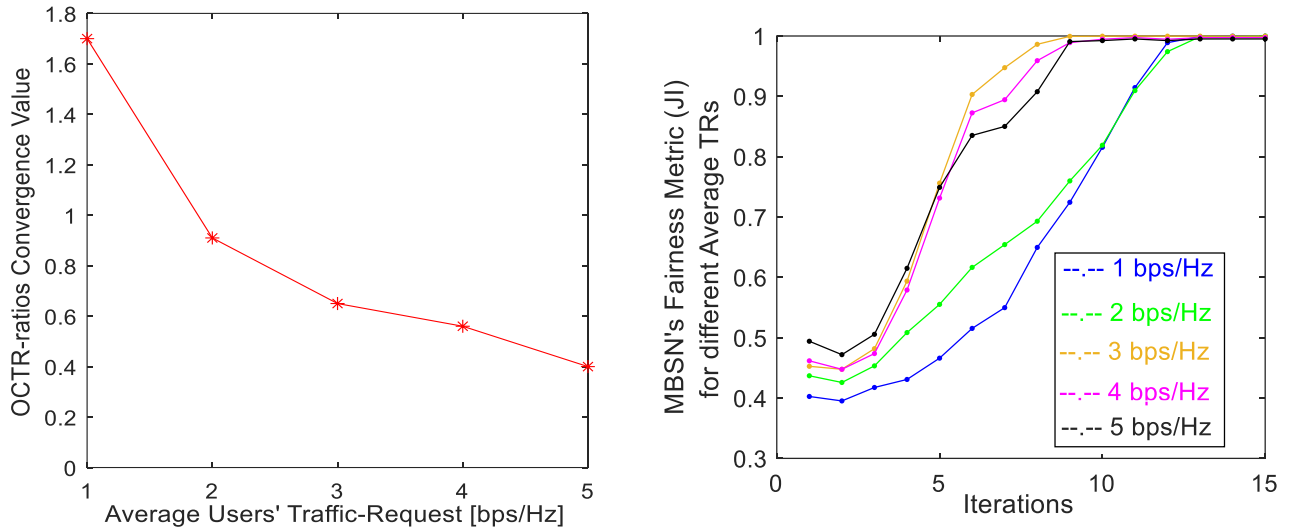
7.2.7.3. Effect of different average-TRs on the system's *OCTR*-ratios convergence value

The functional performance of the proposed Power-Allocation Algorithm-1 (*PAA-1*) were tested for different average values of the users' traffic-requests. To achieve these tests, in each test, we considered the same set of channel-vectors for the 8-users as listed in Table 7.6 above, and we generated a different set of traffic-requests (*TR*) for these 8-users, with a desired average-traffic-requests. Then, we fed the two input-data sets to the code executing the *PAA-1*. Table 7.26 below lists the different sets of generated traffic-requests for the 8-users, for different tests; with different average-*TR*.

Table 7.26: Sets of users' traffic requests with different average values.

Average [bps/Hz]	D _{u1} [bps/Hz]	D _{u2} [bps/Hz]	D _{u3} [bps/Hz]	D _{u4} [bps/Hz]	D _{u5} [bps/Hz]	D _{u6} [bps/Hz]	D _{u7} [bps/Hz]	D _{u8} [bps/Hz]
1	1.1248	0.5086	1.8063	0.6315	0.7319	0.8059	1.0984	1.2641
2	1.8850	1.6408	2.7081	1.9077	5.4081	1.135	2.063	0.5075
3	2.6082	1.9074	3.1393	5.095	2.3788	4.8208	1.4845	0.7055
4	5.265	3.4786	4.8037	2.9562	0.6840	3.7110	5.1083	4.0891
5	5.9253	4.8064	5.0878	5.2385	4.3857	5.1494	4.9002	4.7216

In each case, the code provided a final set of powers ($P_{b\text{-set}}$ and $\alpha_{b\text{-set}}$) which ensure that all user's *OCTR*-ratios converge, thus providing a system's fairness metric of 1. Figure 7.13 (a) below gives a plot of *OCTR*-ratios convergence value of the proposed *PAA-1*, for different average users' traffic-requests. The graph shows that, as the average traffic-requests increases, the *OCTR*-ratio convergence value decreases. This is a logical outcome, since, the higher the traffic-requests of respective users, the lower the users' *OCTR*-ratios. Figure 7.13 (b) below shows the network's fairness metric over run-iterations of the *PAA-1*, for different average traffic-requests ranging from 1 to 5 bps/Hz. The plots show that, for all the average traffic-requests, the algorithm always results in a system's fairness metric of 1; which again demonstrates that, the algorithm indeed implements the *OCTR*-ratios convergence concept, whatever the input data set.



(a): OCTR-ratios Convergence Values (b): Network's Fairness Metrics
Figure 7.13: OCTR-ratios convergence value (a) and Network's Fairness Metric (b); of the proposed PAA-1, for different Average Users' Traffic-Requests.

7.2.7.4. Superiority of the proposed algorithm PAA-1 over existing PAAs

To demonstrate the superiority of our proposed *PAA-1* over some existing power-allocation algorithms, in terms of system's fairness, we ran a few different power-allocation algorithms (*PAA*) with the same input set-up used to run our algorithm. And for each algorithm, we recorded the fairness-metric of the system throughout the power-allocation process. We ran the *PAA* ("Algorithm-3" in Zhu et al., (2017:2261)), which we call here "*PAA-in-source3*"; the *PAA* ("Figure-3" in Liu et al., (2015:4)), which we call here "*PAA-in-source4*"; as well as the *PAA* ("Algorithm-1" in Sun et al., (2019:5)), which we call here "*PAA-in-source5*". Taking in account all the network's parameters as listed in Table 7.3 above, we assumed the case of 4-satellite's antennas, and thus considered the users' channel-vectors given in Table 7.6 above, the generated *NOMA* pairs presented in Table 7.8 above, as well as the produced precoding weight-vectors presented in Table 7.24 above for the respective pairs. With all these input elements defined, we ran each *PAA*; and considering a generated set of user's traffic-requests, we calculated the fairness-metric of the system throughout the power-allocation process. Thus, Figure 7.14 (a) below displays the measured system's fairness-metric of each *PAA*, throughout the power-allocation process; for an average users' traffic-requests of 3bps/Hz. Then Figure 7.14 (b) displays the final system's fairness-metric obtained after executing each *PAA* completely; for different average traffic-requests. The graphs in Figure 7.14 (b) shows that, in terms of resulting system's fairness-fairness, over different average traffic-requests, our proposed *PAA-1* delivers a higher system's fairness metric (i.e. 1) than the other algorithms (i.e. 0.47, 0.56 and 0.53 for *PAAs* in source-3, -4 and -5 respectively). Thus, it largely outperforms them. The large gap between our proposed algorithm (*PAA-1*) and the others

listed, with regards to system's fairness performance, is a rather logical outcome, since most of these power-allocation algorithms were designed to maximise the system's throughput; whereas ours has been designed to maximise the system's fairness. This reaffirms that, our proposed power-allocation algorithm (*PAA-1*) indeed successfully achieves its design goal.

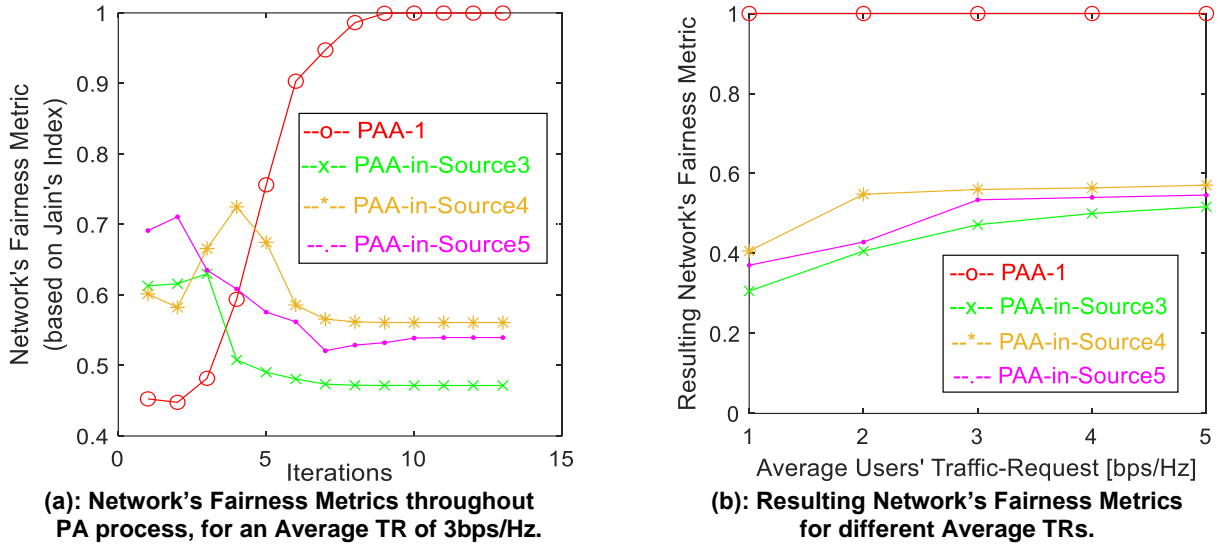


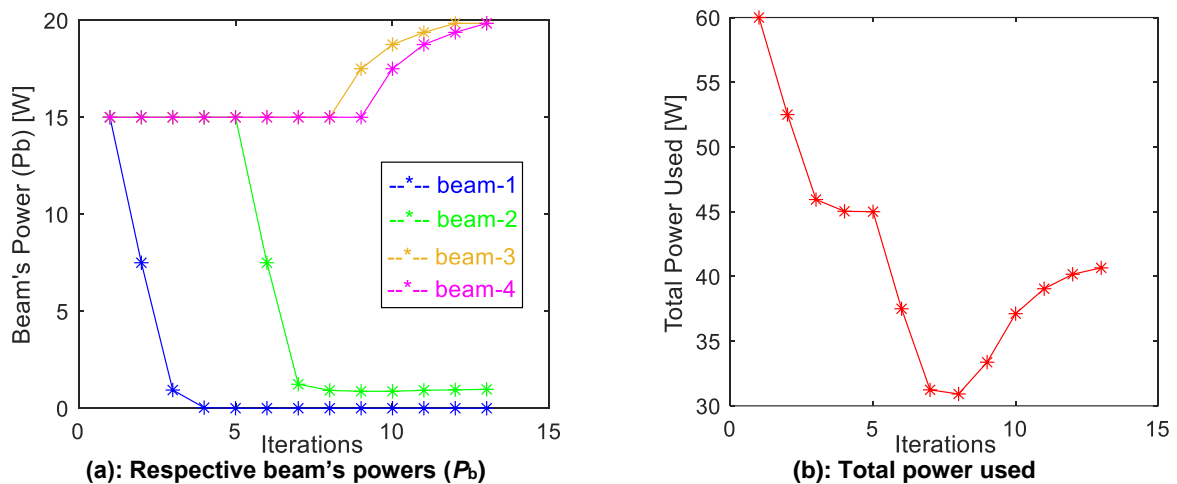
Figure 7.14: Fairness-Metric of various PAAs.

7.2.8. PAA-2's Code running and results discussion

7.2.8.1. Test results

The proposed Maximum-Minimum Fairness Power-Allocation Algorithm (*PAA-2*) was tested in a similar way to the tests done on the *OCTR*-ratios convergence power-allocation Algorithm (*PAA-1*). That is, after obtaining all the input-parameters required by the power-allocation subsystem as listed in the *ATP* (Table 7.2 above), they were fed to the code executing the proposed power-allocation algorithm (*PAA-2*). The code was then run, to test its functional performance. In the case of the max-min fairness concept, the code runs over a number of iterations, until there is no more excess-power to redistribute; then it terminates. Again, according to the *PAS's ATP*, the main output parameters of the power-allocation subsystem are the set of allocated beam's power (P_{b-set}), as well as the set of intra-beam power-sharing coefficient of respective beams (α_{b-set}). Again, from these two sets, other parameters are calculated, including the capacities of respective users, their resulting *OCTR*-ratios; as well as the resulting system's fairness-metric. Since the code is running over multiple iterations before it terminates, we have opted to output the " P_{b-set} " and " α_{b-set} " at each iteration. Subsequently, we are able to calculate respective users' capacities, *OCTR*-ratios, as well as the system fairness-metric, at each iteration. This also allows us to monitor the evolution of the system's fairness metric throughout the power-allocation process; in order to indeed verify that it is being maximised. Figure 7.15, to Figure 7.19 below displays the results obtained from running the

code for *PAA-2*, for the case of 4-satellite's antennas; using the relevant network's parameters defined in Table 7.3 above, the 8-users' traffic-requests listed in Table 7.4 above, the 8-users' channel-vectors displayed in Table 7.6 above, the 4-user-pairs shown in Table 7.8 above, as well as the 4-precoding weight-vectors displayed in Table 7.24 above. Consequently, Figure 7.15 displays the respective beam's power (P_b) over the different run iterations (a); as well as the total power used ($P_{\text{tot-used}}$) at each iteration (b). Then, Figure 7.16 displays intra-beam power sharing coefficient (α_b) of respective beams at each iteration. Note that, the power-sharing coefficients of beam-2 and beam-3 do not appear clearly on the graph because their values are extremely small (in the order of 10^{-12}) compared to values of power-sharing coefficients in beam-1 and beam-4 (which are in the order of 10^{-2}). Also, Figure 7.17 displays the respective beam's capacities over the different run iterations (a); as well as the total achieved throughput at each iteration (b). Furthermore, Figure 7.18 displays the respective beam's *OCTR*-ratios over the different run iterations. Finally, Figure 7.19 displays the system's fairness-metric over the different run iterations. To verify reliability of the proposed code, the code was also executed over 100 times; to check that the results are still the same in each execution.



(a): Respective beam's powers (P_b)
 (b): Total power used
Figure 7.15: Beams' powers per iteration and Total power used on Satellite.

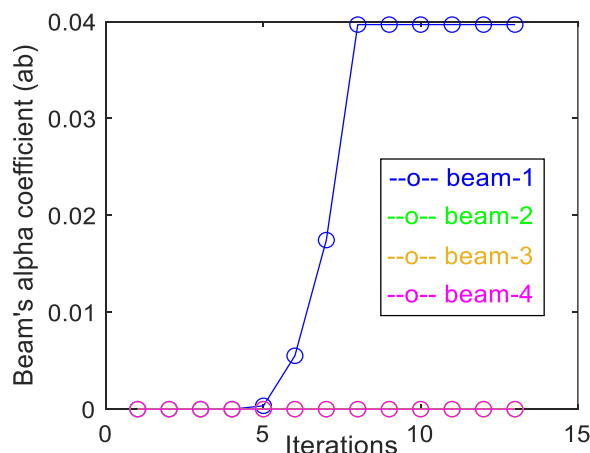
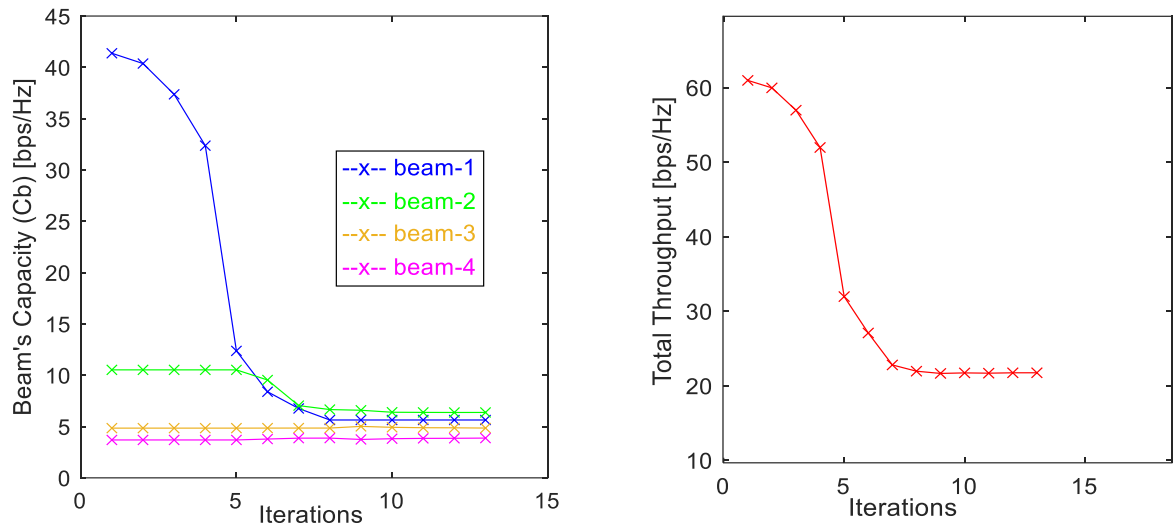


Figure 7.16: Intra-beam power-sharing coefficient (α_b) of respective beams, per iteration.



(a): Respective beam's Capacities (b): Total achievable Capacity
 Figure 7.17: Beams' capacities per iteration and total satellite's throughput.

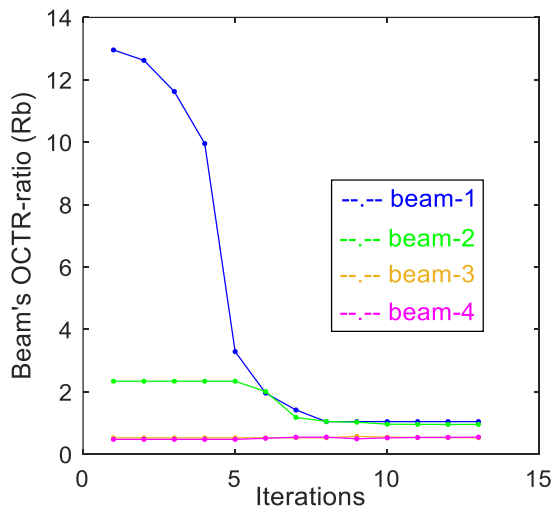


Figure 7.18: OCTR-ratio (R_b) of respective beams at each iteration.

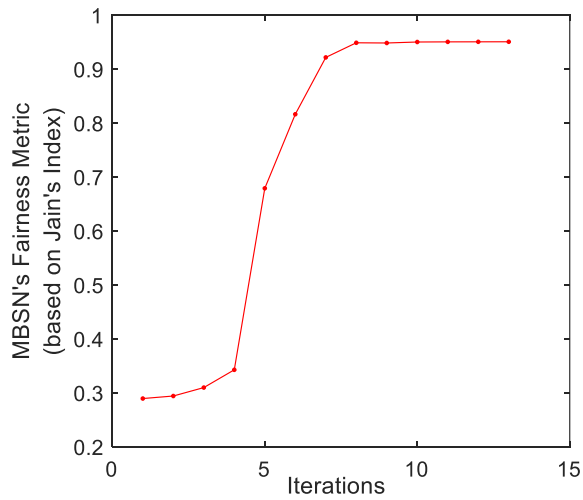


Figure 7.19: Fairness-Metric of the Multi-Beam Satellite's Network per iteration of the PAA-2.

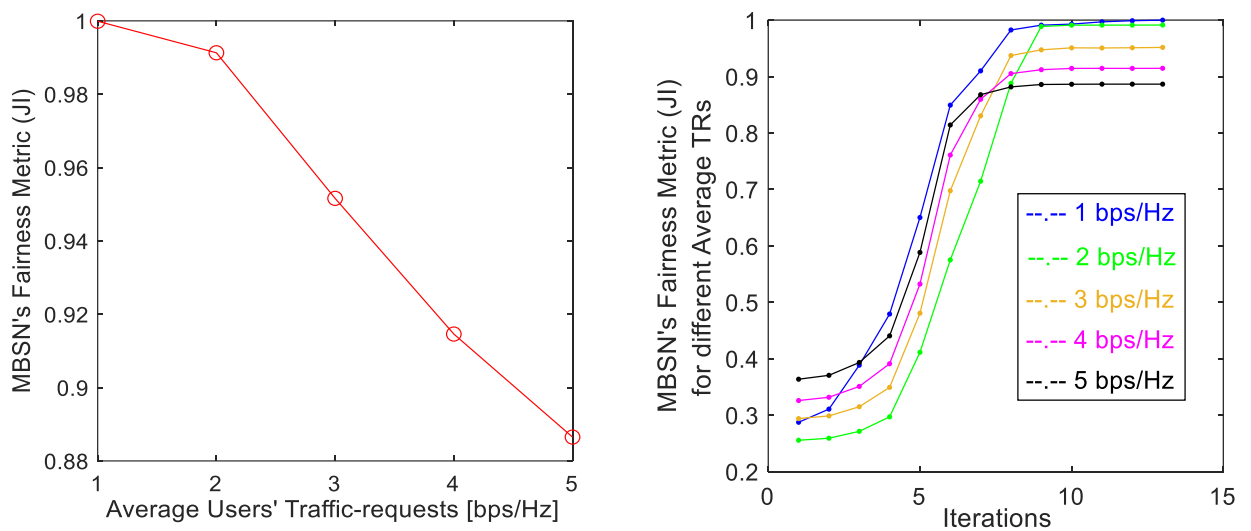
7.2.8.2. Performance validation

As indicated supra, according to Jain's Index, the fairness metric is bounded between 0 and 1; with 0 being the worst and 1 being the best system's fairness metrics. Thus, the graph in Figure 7.19 above shows that, the algorithm indeed maximises the network's fairness; from an initial minimum obtained with equal beam's power allocation, to a maximum value obtained with the final beam's power allocation. *It therefore, satisfies the principal design requirement of the proposed power-allocation algorithm, as indicated in the ATP of the PAS (see Table 7.2 above).* When looking at the graphs in Figure 7.15 (a) and Figure 7.18 above simultaneously, it can be seen that, the power of over-satisfied beams (see beam-1 and beam-2) are respectively reduced until their *OCTR*-ratios are equal to 1; then the excess power is given to unsatisfied beams (see beam-3 and beam-4). It should further be observed from these Figures that, when the unsatisfied beams have reached the maximum possible beam's power (see iteration-13 in Figure 7.15 (a)), the respective powers of beams with *OCTR*-ratio equal 1 are not reduced. This is to preserve the right of these users; which is the main positive characteristic of the Maximum-Minimum Fairness concept. The advantage of this fact is that, the powers of users with good channel conditions are not ridiculously reduced below their deserving shares just to accommodate the *OCTR*-ratios of users with poor channel conditions. Thus, by preserving the right of all users, the system's fairness metric is maximised, while simultaneously, the achievable total system's throughput is increased considerably; which is the other positive characteristic of the max-min fairness concept. This is observable on Figure 7.17 (b) above, where the total achievable throughput is about 22bps/Hz (see iteration-13), as opposed to the 12bps/Hz achievable by the *OCTR*-ratio convergence algorithm (see Figure 7.10 (b) above). The results obtained from running this algorithm show that, while the resulting total system's throughput is preserved to a relatively high value, at the same time, the system's fairness-metric is maximised to about 0.95 as shown in Figure 7.19 above; which is very close to the maximum fairness-metric of 1 achieved by the *OCTR*-ratios convergence algorithm. *Therefore, these two observations certify that indeed, the proposed algorithm (PAA-2) execute well, the Maximum-Minimum Fairness concept; and thus, indeed satisfies the power-allocation design requirements set for this NOMA-based MBSN.*

7.2.8.3. Effect of different average-TRs on the network's Fairness-Metric

Similar to the work done for the proposed *PAA-1*, the functional performance of the proposed Power-Allocation Algorithm-2 (*PAA-2*) was tested for different average values of the 8-users' traffic requests. Here again, to achieve these tests, in each test, we considered the same set of channel-vectors for the 8-users as listed in Table 7.6 above, and we used one of the sets presented in Table 7.26 above for the traffic-requests. Then, we fed the two input-data sets to the code executing the *PAA-2*. In each case, the code provided a final set of beams' powers

which ensure that max-min fairness conditions are satisfied for all users; thus, providing a maximum system's fairness metric. Thus, Figure 7.20 (a) below gives a plot of the final network's fairness-metric obtained from running the proposed *PAA-2*, at different average traffic-requests ranging from 1 to 5 bps/Hz respectively. The graph shows that, as the average traffic-requests increases, the network's fairness metric decreases. This is a logical outcome, because higher traffic-requests of respective users, implies there will be little excess power to redistribute since the initial *OCTR*-ratios of most users will be relatively low. Similarly, Figure 7.20 (b) shows the evolution of the network's fairness-metric over run-iterations of the *PAA-2*, for different average traffic-requests ranging from 1 to 5 bps/Hz. The plots show that, for all the average traffic-requests, the algorithm always maximises the network's fairness metric.



(a): Final Network's Fairness Metric in each run
 (b): Network's Fairness Metrics for different Average TRs
Figure 7.20: Achievable fairness-metric of the PAA-2 for different average traffic-requests.

7.2.8.4. Superiority of the proposed algorithm PAA-2 over existing PAAs

To demonstrate the superiority of our proposed *PAA-2* over some existing *PAAs*, in terms of achievable network's fairness, we followed the exact same process presented earlier in section 7.2.8.4 above for the case of *PAA-1*. Here also, "*PAA-in-source3*" refers to the "*Algorithm-3*" in Zhu et al., (2017:2261); "*PAA-in-source4*" refers to the algorithm in "*Figure-3*" in Liu et al., (2015:4); and "*PAA-in-source5*" refers to the "*Algorithm-1*" in Sun et al., (2019:5). Thus, again, Figure 7.21 (a) below displays the measured system's fairness-metric of each *PAA*, throughout the power-allocation process; for an average users' traffic-requests of 3bps/Hz. Then Figure 7.21 (b) displays the final system's fairness-metric obtained after executing each *PAA* completely; for different average traffic-requests. Graphs in Figure 7.21 (b) shows that, in terms of resulting system's fairness-fairness, over different average traffic-requests, our proposed *PAA-2* always delivers a higher system's fairness metric than the other algorithms; and thus, largely outperforms them. Again, the large gap between our proposed algorithm (*PAA-2*) and the others listed, with regards to system's fairness performance, is a rather logical outcome,

since most of these power-allocation algorithms were designed to maximise the system’s throughput; whereas ours has been designed to maximise the system’s fairness. This reaffirms that, our proposed power-allocation algorithm (*PAA-2*) indeed successfully achieves its design goal.

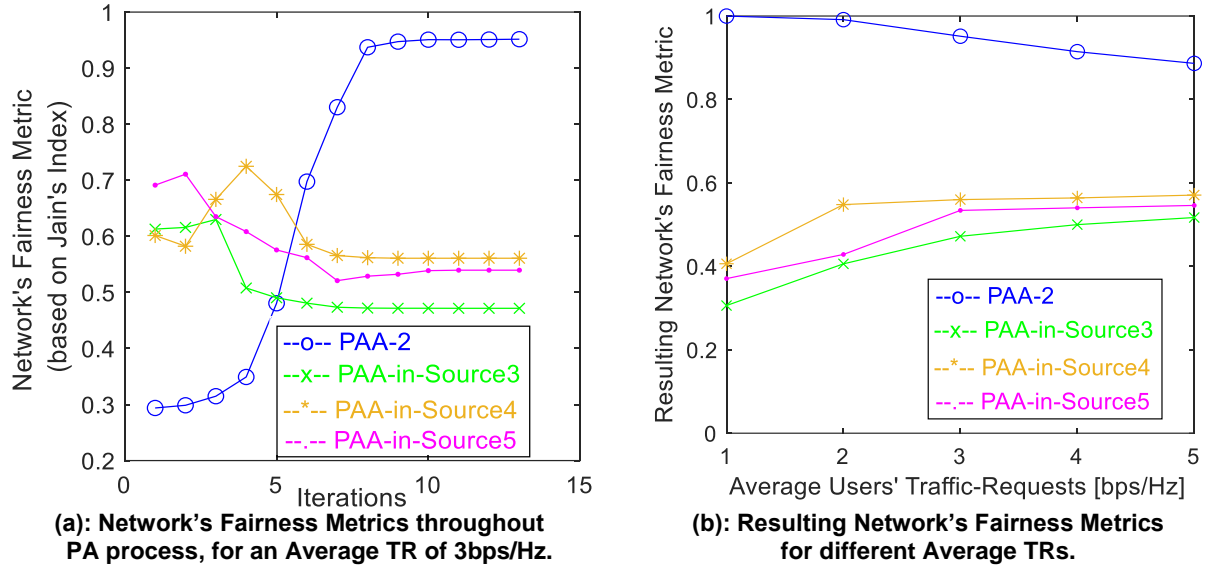


Figure 7.21: Fairness-Metric of various PAAs.

7.3. On-Processor Implementation, Testing and Validation

7.3.1. Implementation

After satisfaction with the performance of the proposed algorithms on the *matlab* platform, we went on to implement the algorithms on the *processor*. In this regards, we used the “*Arm Cortex-R5*” real-time processor, available on the *Zynq Ultra-Scale+ MPSoC* developed by Xilinx. The *Zynq-Ultra-Scale+ MPSoC* has been packaged by Xilinx on a System-On-Module (SoM) called *KRIA-KV260*. This SoM is then used as a daughter-board on a development board known as *KV260-Starter-Kit* (see green board in Figure 7.22 below). below displays our *On-Chip* implementation and testing set-up. In this set-up, the written codes for our proposed algorithms are running on the *Arm Cortex-R5* processor available on the *Zynq Ultra-Scale+ MPSoC*, which is present on the *KRIA-KV260 SoM*, as shown on the figure.



Figure 7.22: Zynq UltraScale+ MPSoC running codes of our proposed algorithms.

We generated bare-metal applications (codes) for our algorithms, which run on the Arm Cortex-R5 processor, which is a real-time processor. For the generation and integration of these codes, we used the *VITIS* platform; which provides the opportunity to develop codes using C/C++ and compile them. Appendix-B: Vitis Codes for the “On-Processor Implementation” of the Algorithms provides some “top-level-functions” generated on Vitis for the implementation of the respective proposed algorithms. Appendix-B1: The “MA-Encoder Function” which calls the UGA, PCA, PAA-1 & PAA-2 shows the written code on Vitis for the MA-Encoder function which calls the functions written for the *UGA*, *PCA* and *PAA-1 and PAA-2*. Appendix-B2: The Top-Level-Function of the “proposed-UGA”, Appendix-B3: The Top-Level-Function of the “PCA”, Appendix-B4: The Top-Level-Function of the “PAA-1” and Appendix-B5: The Top-Level-Function of the “PAA-2” respectively show the codes written on Vitis for the Top-Level-Functions of the *UGA*, *PCA*, *PAA-1* and *PAA-2* respectively. Note that, all other codes for the sub-functions of the respective algorithms have been stored in a drive.

7.3.2. Tests process and input-data generation

In order to run the generated codes for our proposed algorithms on the Arm Cortex-R5 processor, and test their functional performances, the test process was similar to the one outlined earlier for the case of the *matlab implementation*. The *ATP* for each system (i.e. the

UGS and *PAS*) are still the same as listed in Table 7.1 and Table 7.2 above respectively. We considered the same network's parameters' specification outlined in Table 7.3 above. For the generation of the input-data sets (users' traffic-requests and users' channel-vectors) needed by the codes to execute, we proceeded in the same manner as discussed earlier. In essence, given that the network's capacity in this application is $2M$ -users, we considered that $10 \times 2M$ -users are active in the network, and the network service time-slot is T_{NS} . Thus, at each T_{NS} , we generated from our local computer, the traffic-requests and channel-vectors for the $20M$ active-users, as indicated in earlier in 7.2.4.1 and 7.2.4.2 above respectively. Then, we randomly selected $2M$ -users to be served, and grouped their respective traffic-requests and channel-vectors to form the two input-data sets to must be fed to the codes running on the remote *R5*-processor on the *KRIA-KV260 SoM*. The question now was, how to do we get these input-data set from our computer to the Cortex-R5 processor running on the *SoM*? To achieve this, we made use of the "Ethernet" link capability available on the *Zynq Ultra-Scale+ MPSoC*; for which there is an *Ethernet* ports on the *KV260-Start-Kit board*. Thus, from our local computer, at each network's service time-slot (T_{NS}), the set of traffic-requests and channel-vectors for the $2M$ -users selected, are sent to the *R5*-processor via the *Ethernet* link. For simplicity of testing the functionality of the proposed algorithms, other parameters such as the number of antennas on the satellite, the number of users per *NOMA* beam, the total power on the satellite ($P_{tot-sat}$), and maximum antenna power (P_b), were defined as global variables in the main function of each algorithm.

Once the input-data sets, have been received by the processor, the user grouping algorithm will start executing, in order to produce the required M -pairs which will be stored into the *DDR*-memory available on the *SoM*. Once done, the precoding weight-vector calculation will execute, considering the generated pairs, and will provide the M -weight-vectors for the M -antennas; which will also be stored on the *DDR*-memory. Thereafter, having the channel-vectors of all $2M$ -users, the M -pairs, the M -weight-vectors, the power allocation algorithm will commence its execution. At each of its iteration, the allocated power sets (both P_{b-set} and α_{b-set}) as well as the corresponding users capacities, users' *OCTR*-ratios and eventually system's fairness metric, are stored on the *DDR*-memory. When the *PAA* is done executing, all the results stored in the *DDR*-memory during execution of respective codes are sent to the local computer via *Ethernet* link, for visualization. These include, the generated M -pairs from the *UGA*, the generated M -weigh-vectors from the *PCA*, as well as the information obtained from each iteration of the *PAA*, such as the Power-sets, users capacities, beam's *OCTR*-ratios, and network' fairness-metric. The data received on the local computer from the *R5*-processor are then stored in relevant files, and thereafter displayed for visualization in form of graphs or tables, where applicable. Thus, plotting the data received from the *R5*-processor regarding the

power-allocation process allows us to visualize the evolution of the network's fairness-metric throughout the power-allocation process.

To obtain the results below, we considered the specifications of network's parameters listed in Table 7.3 above; that is, 4-satellite's antennas, which means 8-users be served and 80 active-users in the network's coverage. At a given network's service time-slot (T_{NS}), we generated traffic-requests and channel-vectors for 80-users, from which we randomly selected 8-users; and the respective traffic-requests and channel-vectors of these 8-users formulated the two input-data sets that we sent to the *R5*-processor on the board via *Ethernet* link. Table 7.27 below lists the traffic-requests of these 8-users. Note that, the average-*TR* of this set is 4bps/Hz. Table 7.28 below lists the channel-vectors of these 8-users.

Table 7.27: Ground distances and Angle-of-Arrivals of selected 8-users.

Average [bps/Hz]	D _{u1} [bps/Hz]	D _{u2} [bps/Hz]	D _{u3} [bps/Hz]	D _{u4} [bps/Hz]	D _{u5} [bps/Hz]	D _{u6} [bps/Hz]	D _{u7} [bps/Hz]	D _{u8} [bps/Hz]
4	4.503	4.4864	3.3762	1.9070	3.1395	2.6972	1.4845	5.1648

Table 7.28: Channel-vectors of the respective 8-users

h_1	h_2	h_3	h_4
0.0236 + 0.0270i	0.0226 - 0.0378i	0.0123 - 0.0129i	0.0056 + 0.0097i
0.0174 + 0.0314i	0.0121 - 0.0423i	0.0095 - 0.0152i	0.0029 + 0.0108i
-0.0190 + 0.0304i	-0.0374 - 0.0233i	-0.0078 - 0.0161i	-0.0097 + 0.0056i
-0.0358 - 0.0019i	-0.0327+0.0295i	-0.0178 - 0.0019i	-0.0079 - 0.0079i
h_5	h_6	h_7	h_8
0.0325 + 0.0185i	0.0079 + 0.0010i	0.0048 + 0.0327i	-0.0004 + 0.0117i
0.0299 + 0.0225i	0.0079 + 0.0013i	-0.0069 + 0.0323i	-0.0049 + 0.0106i
0.0103 + 0.0360i	0.0076 + 0.0025i	-0.0302 - 0.0134i	-0.0075 - 0.0090i
-0.0134 + 0.0349i	0.0071 + 0.0036i	0.0194 - 0.0267i	0.0113 - 0.0030i

7.3.3. Results and Validation of the UGA's Code

The set of pairs received from the processor after running the code of the *UGA* are listed in Table 7.29 below. Then, Table 7.30 below lists the channel-gain ratio of each pair; and indicates that, the channel-gain ratios (C_{gr}) of the respective pairs are all greater than 1.5, which was the defined minimum. *This therefore, means that, all the generated pairs satisfy the minimum channel-gain ratio requirement; and thus, the algorithm once again satisfies the design requirement (b) on the UGS's ATP (Table 7.1 above).* Furthermore, Table 7.31 below displays the channel-correlation coefficients (C_3) of the respective pairs. It indicates that all the pairs have very high C_3 , with the minimum being 0.7147. *This means that, all the pairs satisfy the requirement for high channel-correlation; and therefore, the algorithms satisfies once again satisfies the design requirement (c) on the UGS's ATP table.* Finally, the grouping fairness-metric obtained using the C_3 of all the pairs is also extremely high, in this case 0.9518, as displayed in Table 7.31 below. This indicates that in generating the resulting pairs, the

algorithm achieved very high fairness with regards to C_3 of the resulting pairs. Thus, it once again satisfies the design requirement (d) on the UGS's ATP table. Consequently, the results obtained from running the proposed users-grouping algorithm on a processor attest that, the algorithm satisfies all the design requirements sets, as listed on the Table 7.1 above of the UGS's ATP. This include that: the algorithm can generate M -pairs (a); that each of the M -pairs satisfies a minimum channel-gain margin for successful implementation of NOMA concept (b); that each pair satisfies a high channel-correlation coefficient in order for all beam's users to mitigate ICI using the generated beam's precoding weight-vector (c); and that there is high fairness amongst all the generated with regards to channel-correlation coefficients of resulting beams (d).

Table 7.29: Resulting pairs from the UGA-Code

(a): Resulting set of pairs		(b): The 4-pairs highlighted on the C_3 -matrix				
Near-user	Far-user	fu\ngu	2	5	1	7
2	3	3	0.7836	0	0	0.2995
5	6	8	0.4910	0.2478	0.1507	0.8998
1	4	4	0.1955	0.4015	0.9106	0.7087
7	8	6	0.2307	0.7147	0	0.1008

Table 7.30: Channel-gain ratio of resulting pairs.

Pair No	[nu-fu]	$ h_{nu} $	$ h_{fu} $	$C_{gr} = h_{nu} / h_{fu} $	C_{gr-min}
1	[2-3]	0.0881	0.0357	2.4643	1.5
2	[5-6]	0.0748	0.0160	4.6699	
3	[1-4]	0.0718	0.0223	3.2161	
4	[7-8]	0.0660	0.0234	2.8224	

Table 7.31: C_3 of resulting pairs and the achieved grouping fairness-metric.

Pair No	[nu-fu]	Channel-correlation coefficient (C_3)	UGA's C_3 fairness_metric
1	[2-3]	0.7836	0.9518
2	[5-6]	0.7147	
3	[1-4]	0.9106	
4	[7-8]	0.8998	

7.3.4. Results and Validation of the Zero-forcing Precoding Code

Table 7.32 below lists the precoding weigh-vectors generated by the code developed to implement the zero-forcing precoding calculation. Here again, the Q-matrix displays on Table 7.33 below which is a product of the H_{nu} and W , as ($Q = H_{nu}^H W$), is an identity matrix; which indicates that the weight-vectors matrix is indeed a zero-forcing weight-vectors matrix.

Table 7.32: precoding weight-vectors of the 4 respective antennas

W_1	W_2	W_3	W_4
1.7210 -29.3553i	-178.72 - 223.52i	-31.25 + 155.62i	407.42 + 23.89i
6.5839 +37.5549i	232.86 + 220.93i	29.49 - 188.68i	-463 + 155i
-12.1055 - 2.8096i	-74.96 - 49.22i	-9.32 + 56.13i	124.49 - 31.19i
2.2118 - 2.9727i	51.08 - 11.09i	-2.29 - 24.25i	-52.47 + 49.77i

Table 7.33: The Q-Matrix obtained

Q_1	Q_2	Q_3	Q_4
1.0000 - 0.0000i	-0.0000 - 0.0000i	-0.0000 + 0.0000i	0.0000 + 0.0000i
0.0000 - 0.0000i	1.0000 - 0.0000i	-0.0000 - 0.0000i	-0.0000 + 0.0000i
-0.0000 + 0.0000i	-0.0000+0.0000i	1.0000 + 0.0000i	-0.0000 - 0.0000i
0.0000 + 0.0000i	0.0000 - 0.0000i	0.0000 - 0.0000i	1.0000 + 0.0000i

7.3.5. Results and Validation of the PAA-1's Code

Figures below display the data obtained from the code executing the *PAA-1* on the processor; at each iteration of the power-allocation process. Figure 7.23 (a) displays the powers (P_b) of the respective beams over different run iterations; and Figure 7.23 (b) shows the total power used at each iteration. Similarly, Figure 7.24 (a) displays the respective beams' capacities over different run iterations; and Figure 7.24 (b) gives the total throughput achieved at each iteration. Also, Figure 7.25 (a) displays the respective user's *OCTR*-ratios over different run iterations. Finally, Figure 7.25 (b) displays the system's fairness metric over different run iterations.

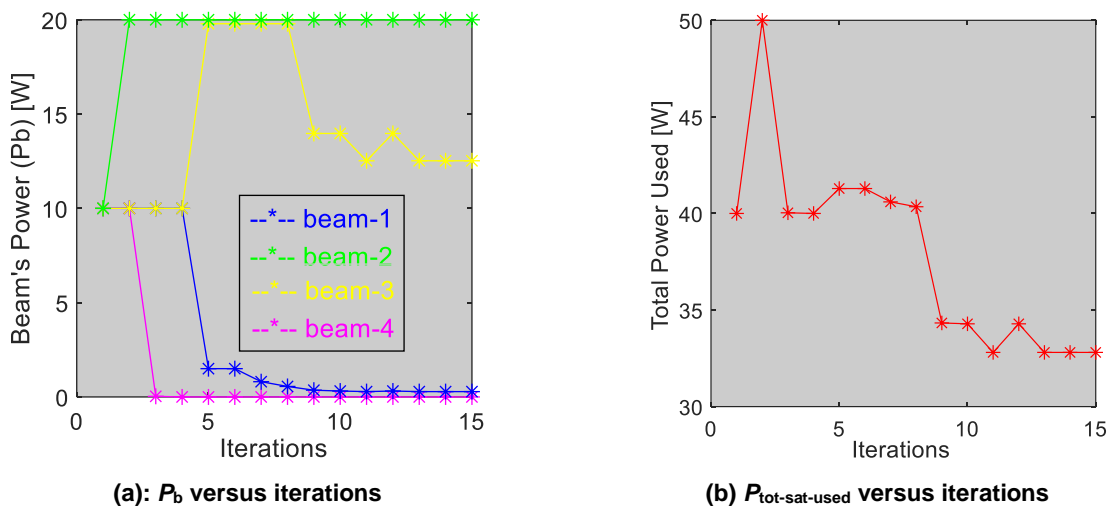


Figure 7.23: Beam's powers and Total power used, per iteration of the PAA-1.

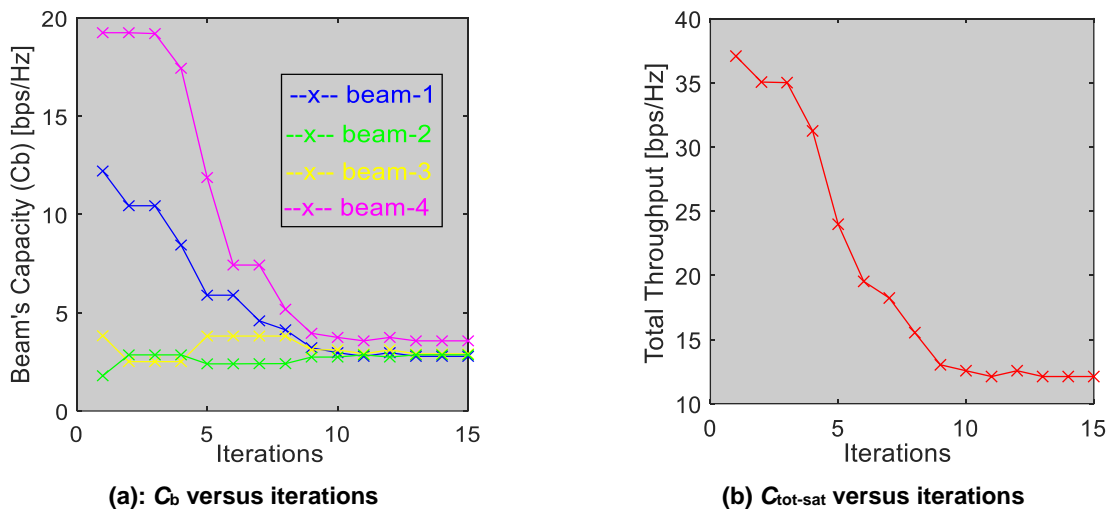


Figure 7.24: Beam's Capacities and Total networks throughput, per iteration of the PAA-1.

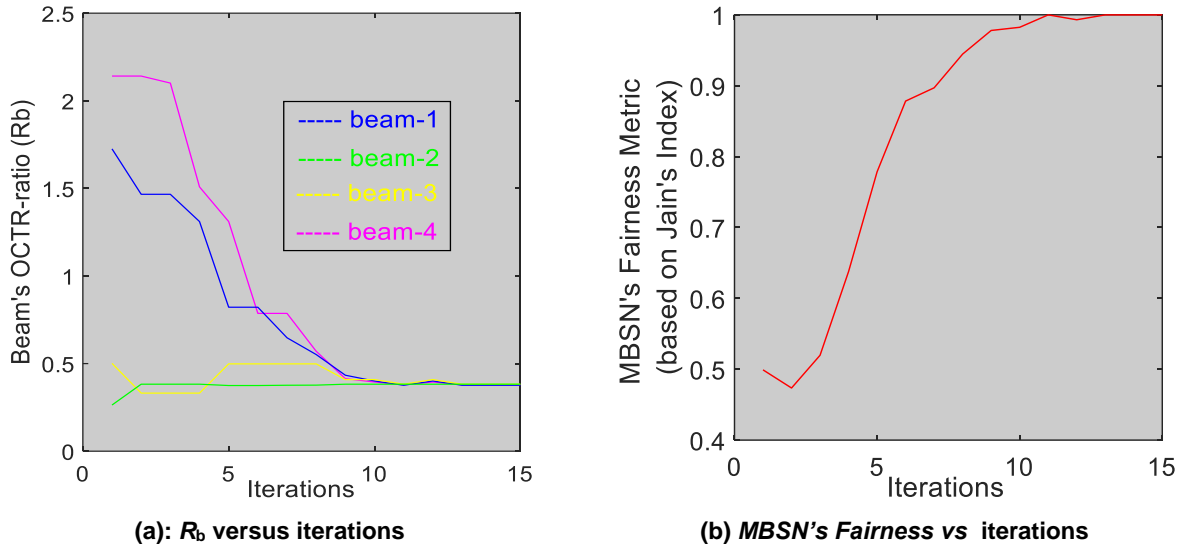
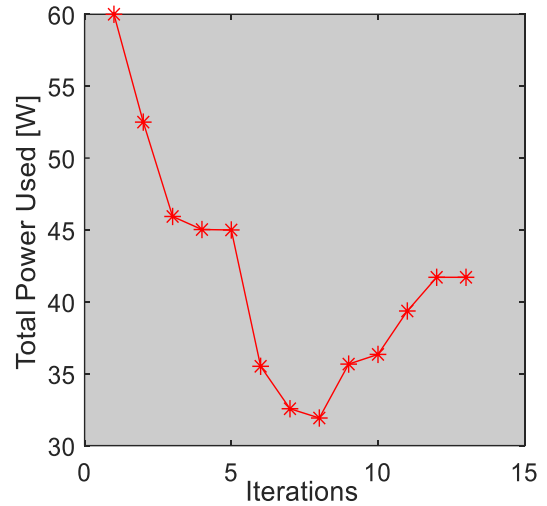
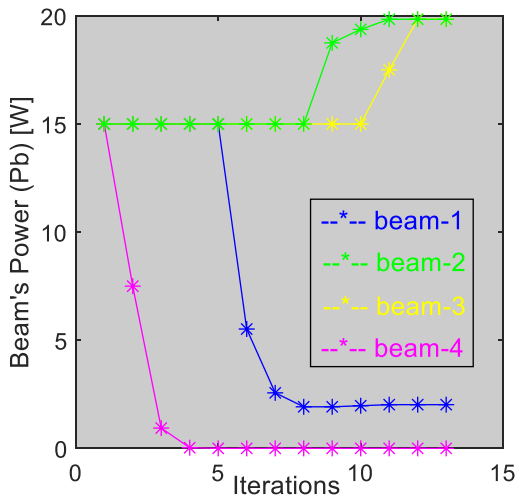


Figure 7.25: Beam's OCTR-ratios and resulting network's Fairness-metric, per iteration of the PAA-1.

Results displayed on Figure 7.25 (a) above show that, the OCTR-ratio of all beams indeed converge after a certain amount of iterations of the power-allocation algorithm. *This then, reinforces that the proposed algorithm indeed implements the OCTR-ratios convergence concept.* Furthermore, results displayed on Figure 7.25 (b) show that, the algorithm indeed maximizes the network's fairness metric throughout the power-allocation process; and produces a final fairness-metric of 1, which is the maximum possible. *This again, reinforces that, the PAA-1 indeed implements that OCTR-ratios convergence concept, as it converges the OCTR-ratios of all network's users; and thus, maximises the system's fairness metric to 1.* However, results from Figure 7.23 (b) and Figure 7.25 (a) indicate that, the algorithm leaves out a lot of the available power, while some users are still not satisfied; thus leading to an extreme limitation in the achievable throughput of the system, as observed in Figure 7.24 (b). This is a well-known drawback of the OCTR-ratio convergence concept, which therefore reinforces that the proposed PAA-1 is indeed a well implemented power-allocation algorithm based on the OCTR-ratio convergence concept.

7.3.6. Results and Validation of the PAA-2's Code

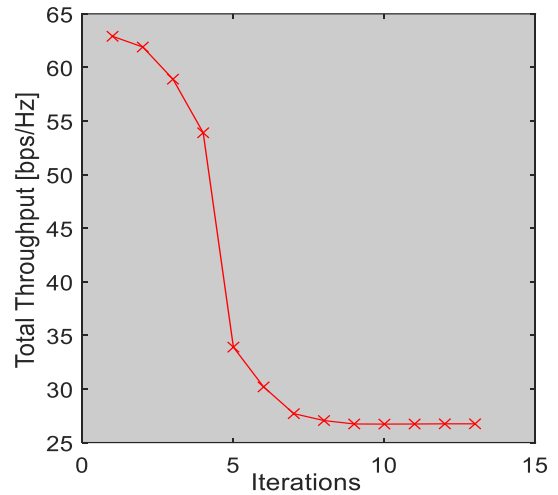
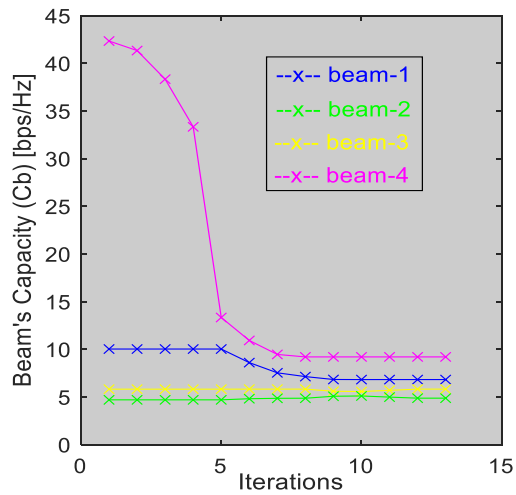
Similar to above discussion for case of the PAA-1, Figures below display the data obtained from the code executing the PAA-2 on the processor; at each iteration of the power-allocation process. Figure 7.26 (a) displays the powers (P_b) of the respective beams over different run iterations; and Figure 7.26 (b) shows the total power used at each iteration. Similarly, Figure 7.27 (a) displays the respective beams' capacities over different run iterations; and Figure 7.27 (b) gives the total throughput achieved at each iteration. Furthermore, Figure 7.28 (a) displays the respective user's OCTR-ratios over different run iterations. Finally, Figure 7.28 (b) displays the system's fairness metric over different run iterations.



(a): P_b versus iterations

(b) $P_{\text{tot-sat-used}}$ versus iterations

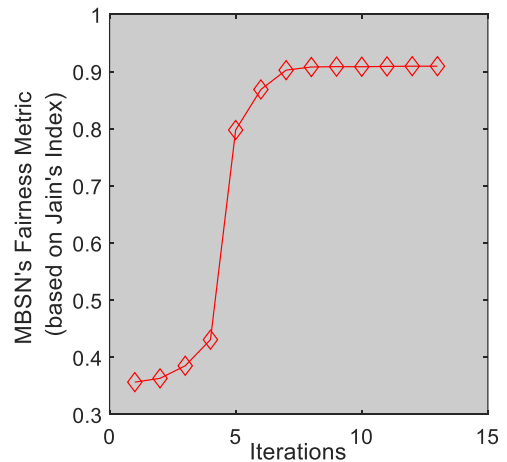
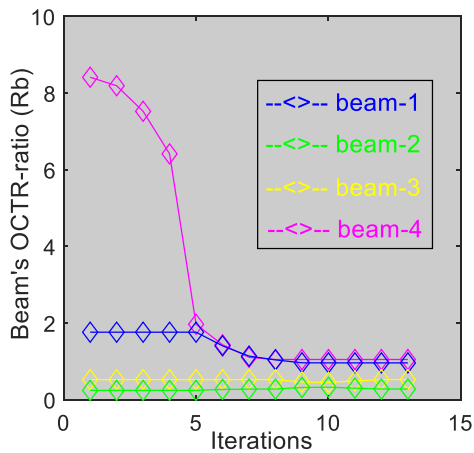
Figure 7.26: Beam's powers and Total power used, per iteration of the PAA-2.



(a): C_b versus iterations

(b) $C_{\text{tot-sat}}$ versus iterations

Figure 7.27: Beam's Capacities and Total networks throughput, per iteration of the PAA-2.



(a): R_b versus iterations

(b) MBSN's Fairness vs iterations

Figure 7.28: Beam's OCTR-ratios and resulting network's Fairness-metric, per iteration of the PAA-2.

Results displayed in Figure 7.28 (b) re-enforce that the proposed PAA-2 indeed maximizes the network's fairness metric throughout the power-allocation process. Also, results displayed in Figure 7.26 (a) and Figure 7.28 (a) show that, the power of respective beams is only reduced until the beam's OCTR-ratio is equal to 1; and no beam's power (P_b) is reduced further when its OCTR-ratio is less than 1. This is the fundamental principle of the max-min fairness concept which is well outlined in these results. Thus, these results re-enforce that, the proposed PAA-2 indeed, implements the max-min fairness concept very well. The good implementation of the max-min fairness concept leads to both, the maximization of the network's fairness metric, as shown in Figure 7.28 (b); as well as the increase in total network's throughput, as shown in Figure 7.27 (b), when compared to the total throughput of the OCTR-ratio convergence concept (see Figure 7.24 (b)). Therefore, in sum, the results obtained from running the proposed PAA-2 on the processor re-enforce that, the proposed algorithm indeed satisfies the main design for the PAS in this NOMA-based MBSN, which is to maximize the network's fairness.

7.4. Chapter summary

This chapter presented the implementation, testing and validation of all the generated algorithms, including, the users' grouping algorithm (UGA), the power-allocation algorithm based on OCTR-ratios convergence concept (PAA-1) and the power-allocation algorithm based on Maximum-Minimum Fairness concept (PAA-2). The algorithms were first implemented on the Matlab environment. The results of the UGA showed that it satisfies all three design requirements, including, ensuring high channel-gain margin and channel-correlation coefficient between paired users; as well as ensuring high fairness amongst resulting pairs in terms of their respective channel-correlation coefficients. These results also showed that, the proposed UGA outperforms other existing UGA in terms of resulting grouping's fairness. The results of the PAA-1 and PAA-2 showed that, the algorithms indeed maximize the system's fairness. They furthermore, demonstrated that, the proposed PA algorithms (PAA-1 and PAA-2) outperforms other existing PA algorithms, in terms of system fairness. After Matlab implementation, the proposed algorithms were also implemented on a programmable hardware; a real-time processor (Arm Cortex-R5), to evaluate their on-chip performance. The results obtained for all three proposed algorithms, correlated well with the initial results obtained from Matlab implementation. These results indicated that, each algorithm respectively, satisfied the design requirements; and outperforms the existing algorithms.

CHAPTER 8: CONCLUSION AND RECOMMENDATIONS

8.1. Conclusion

8.1.1. Summary

In this work, we have proposed a novel users-grouping algorithm and two novel power-allocation algorithms, which maximize the users-fairness of 2users-*NOMA-MBSNs*, intended for 5G mobile networks implementation.

The proposed users-grouping algorithm (*UGA*) was developed based on the combination of the following concepts: the bipartite-matching concept, to generate pairs between the far-users set and the near-users set; the minimum channel-gains margin restriction concept, to satisfy the distinct channel-gains requirement between paired users; as well as the minimum channel-correlation coefficient restriction concept, to satisfy the high channel-correlation requirement between paired users. The combination of all these three concepts formulated the users-grouping problem into a “restricted bipartite-matching problem”. To address this problem while ensuring that the solution (i.e. resulted set of pairs) delivers high fairness amongst the respective pairs in terms of channel-correlation, and thus satisfy the high-fairness requirement, the Hungarian-Method was employed. Subsequently, the “restricted bipartite-matching problem” was then turned into a restricted Hungarian-Matrix of channel-correlation coefficients between all far and near users; which was then solved by means of the Restricted-Hungarian-Method. The resulting *UGA* was then implemented and tested on *Matlab* first. The results indicated that the algorithm satisfies all 3 design requirements defined. They furthermore showed that, the proposed algorithm displays remarkable superiority over other existing users-grouping algorithms, in terms of the fairness performance. The proposed algorithm was also thereafter, implemented on a *real-time processor (Arm Cortex-R5)*, to evaluate its on-chip performance. The results correlated well with the primary results obtained from the *Matlab* implementation, and indicated that the algorithm satisfies all the requirements defined; including, distinct channel-gains and high channel-correlation between paired users, as well as high fairness amongst the resulted pairs in terms of channel-correlation of respective pairs.

The first proposed power-allocation algorithm (*PAA-1*) was developed based on the *OCTR*-ratios convergence concept. The fairness maximization power-allocation requirement was formulated as an optimization problem. The initial problem being non-convex and *NP*-hard was then decomposed into two sub-problems, namely the intra-beam and inter-beam power-allocation problems. These two sub-problems were addressed by means of an intra-beam power-allocation algorithm and an inter-beam power-allocation algorithm respectively; which were respectively developed based on the *OCTR*-ratios convergence concept. The final

algorithm (*PAA-1*) combined the two sub-algorithms, to yield the global solution to the original problem. The developed *PAA-1* was then implemented and tested on the *Matlab* platform first. The results demonstrated that, the algorithm indeed maximises the network's fairness; and thus satisfies the design requirement defined. The results furthermore demonstrated that, the proposed *PAA-1* exhibits large superiority over other existing power-allocation algorithms, in terms of achievable network's fairness. The algorithm (*PAA-1*) was thereafter implemented and tested on a *real-time processor (Arm Cortex-R5)*, to have its on-chip performance. The results obtained re-affirmed that the algorithm maximises the network's fairness; and thus satisfies all the principal design requirement for the power-allocation subsystem.

To address some limits of the first power-allocation (*PAA-1*) related to total power-management, the second proposed power-allocation algorithm (*PAA-2*) was developed based on the Maximum-Minimum Fairness concept. Similarly, the fairness maximization power-allocation requirement was formulated as an optimization problem. The initial problem being non-convex and NP-hard was then decomposed into the intra-beam and inter-beam power-allocation sub-problems. These two sub-problems were then addressed by means of an intra-beam power-allocation algorithm and an inter-beam power-allocation algorithm respectively; which were respectively developed based on the Max-Min Fairness concept. The final algorithm (*PAA-2*) combined the two sub-algorithms, to yield the global solution to the original problem. The developed *PAA-2* was then implemented and tested on the *Matlab* platform first. The results demonstrated that, the algorithm indeed maximises the network's fairness; and thus satisfies the design requirement defined. The results furthermore showed that, the proposed *PAA-2* also demonstrates large superiority over other existing power-allocation algorithms, in terms of achievable network's fairness. Thereafter, the algorithm (*PAA-2*) was also implemented and tested on a *real-time processor (Arm Cortex-R5)*, to evaluate its on-chip performance. The results obtained re-affirmed that the algorithm maximises the network's fairness; and thus satisfies the principal design requirement defined for the power-allocation subsystem. Furthermore, the results from the *PAA-2* demonstrated that, it realises a better total power management than *PAA-1*; and thus, can simultaneously maximize the system's fairness, while also ensuring increased network's total capacity than *PAA-1*.

To the best of authors knowledge, the three algorithms proposed are all original additions to existing literature, for 2users-*NOMA-MBSNs* intended for 5G networks. In fact, the knowledge produced in this research can be used in any *NOMA-MIMO* network that seeks to maximise fair service to all users; including terrestrial, aerial as well as satellites applications.

8.1.2. Responses to research questions

Based on the work realised in this research and the results obtained, the following answers can be provided to the research questions initially asked.

- 1) What approach would be adequate for the design of a *UGA* which satisfies the three pairing requirements of a 2-users-*NOMA-MBSN*?

An adequate approach for developing a user-grouping algorithm that would satisfy all three pairing requirements of a 2-users-*NOMA-MBSN* is: *To combine the concept of Bipartite-Matching of the near-users and far-users' sets, with restrictions on pairs that do not meet the minimum channel-gain margin as well as minimum channel-correlation coefficient; and formulate the problem into a restricted Hungarian-matrix of near-user – far-user's channel-correlation coefficients, which is then solved by means of the Hungarian-Method.*

- 2) Which concept would be adequate for the design of a *PAA* that maximizes fairness of a 2-users-*NOMA-MBSN*?

Both the *OCTR*-ratios convergence and the Max-Min fairness concepts are adequate for designing power-allocation algorithms that maximise fairness of *NOMA-MBSNs*. However, the max-min fairness concept displays superior performance in that, it performs a better power-management than the *OCTR*-ratios convergence; and thus, achieves simultaneously maximization of network's fairness and increase of network's total capacity. Therefore, it is deemed more appropriate for the purpose.

- 3) What approach would be suitable to solve the non-convex and *NP*-hard fairness maximization power-allocation problem, for 2-users-*NOMA-MBSNs*?

To solve this outlined optimization problem, an adequate approach would be to decompose the original problem into two sub-optimization problems; namely, the intra-beam and inter-beam fairness maximization power-allocation problems. Then each problem is solved by means of either the *OCTR*-ratios convergence concept or the Max-Min fairness concept, to produce a sub power-allocation algorithm. Thereafter, combine the two produced power-allocations algorithms into yield a global power-allocation that is a solution to the original problem and thus maximize the fairness of the overall 2-users-*NOMA-MBSN*.

8.2. Recommendations

In the current work, the near-users in each group was used to calculate the precoding weight-vector of the pairs. Thus, near users optimally mitigate ICI from other beams; and thus achieve better link's capacities. Since near users already by default have better conditions and thus are prompt to achieving better capacities, we recommend that to further improve the network's

fairness, the option of using the far-user of each beam for precoding weight-vector calculation instead of the near user, be investigated. This would certainly allow the far-users to optimally mitigate *ICIs* from beams, and thus, achieved improved capacities; which the imply, better system's fairness.

In the current work, only one fairness maximization concept (i.e *OCTR*-ratios convergence or Max-Min fairness) was used at the time, to solve the two sub-problems (intra-beam and inter-beam). Therefore, it is recommended that the option of mixing the two concepts when solving the original problem be investigated. This means that, if *OCTR*-ratio convergence is used to solve the intra-beam sub-problem, then the Max-Min fairness should be used to solve the inter-beam sub-problem; and vice-versa.

In the design of the intra-beam power-allocation based on the max-min fairness concept, our interpretation of "beam's users have same right to available beam's resource" was that "they must receive at their terminal the same power". We therefore recommend that, the option of interpreting the above as "they must receive same capacity" be implemented to investigate whether or not that would lead to better system's fairness.

REFERENCES

- Aldababsa, M., Toka, M., Gökçeli, S., Kurt, G.K. & Kucur, O. 2018. A Tutorial on Nonorthogonal Multiple Access for 5G and Beyond. *Wireless Communications and Mobile Computing*: 1-24, June 28.
- Ali, E., Ismail, M., Nordin, R. & Adulah, N.F. 2017. Beamforming techniques for massive MIMO systems in 5G: overview, classification, and trends for future research. *Frontiers of Information Technology & Electronic Engineering*, 18(6): 753-772.
- An, K., Li, Y., Yan, X. & Liang, T. 2019. On the Performance of Cache-Enable Hybrid Satellite-Terrestrial Relay Networks. *IEEE Wireless Communications Letters*, 8(5): 1506-1509.
- An, K., Yan, X., Liang, T. & Lu, W. 2019. NOMA Based Satellite Communication Networks: Architectures, Techniques and Challenges. *2019 IEEE 19th International Conference on Communication Technology*: 1105-1110.
- Anwar, A., Seet, B., Hasan, M.A. & Li, X.J. 2019. A Survey on Application of Non-Orthogonal Multiple Access to Different Wireless Networks. *Electronics*, 8:1-46, November.
- Attiah, A., Amjad, M.F., Chatterjee, M. & Zou, C. 2018. An evolutionary routing game for energy balance in Wireless Sensor Networks. *Computer Networks*, 138(2018): 31-43.
- Awad, S.D., Sali, A., Al-saegh, A.M., Al-wani, M.M., Abdullah, R.S.A.R. & Singh, M.S.J. 2020. Beamforming and Scheduling Techniques for Multibeam DVB-S2X Over Rainy Fading Satellite Channel. *IEEE Access*, 8:41116- 41127.
- Balyan, V. 2020. Outage Probability of Cognitive Radio Network Utilizing Non Orthogonal Multiple Access. *7th International Conference on Signal Processing and Integrated Networks (SPIN)*, *IEEE Access*, 751-755.
- Balyan, V. 2021. Cooperative relay to relay communication using NOMA for energy efficient wireless communication. *Telecommunication Systems*, 77:271-281.
- Balyan, V. & Gupta, D. 2021. Device-to-Device and mobile user communication with queuing in NOMA-based network. *International Journal on Smart Sensing and Intelligent Systems*, 14(1):1-5.
- Beigi, N.A.K. & Soleymani, M.R. 2018. Interference Management Using Cooperative NOMA in Multi-Beam Satellite Systems. *IEEE Access*:1-6.
- Beigi, N.A.K. & Soleymani, R. 2018. On the Capacity of Asynchronous Cooperative NOMA in Multibeam Satellite Systems. *36th International Communications Satellite Systems Conference (ICSSC-2018)*. Niagara Falls, 15-18 October 2018, IEEE: 1-6.

- Bharathi, S., Nandita, L., Venkateswaran, N. & Subhashini, R. 2017. Performance Analysis of Non Orthogonal Multiple Access Technique with Precoding. *IEEE WiSPNET 2017 conference*: 1878-1882.
- Biyoghe, J. & Balyan, V. 2020. A comprehensive survey of existing researches in NOMA Based Integrated Satellite-Terrestrial Networks for 5G. *5th International Conference on Information and Communication Technology for Competitive Strategies (ICTCS-2020)*, India, 11-12 December, 2020, pp 369-378.
- Biyoghe, J. & Balyan, V. 2021a. A Survey of Existing Studies on NOMA Application to Multi-Beam Satellite Systems for 5G. *5th International Conference on Inventive Systems and Control (ICISC)*, Coimbatore, 7-8 January 2021, pp. 244-255.
- Biyoghe, J. & Balyan, V. 2021b. NOMA Application to Satellite Communication Networks for 5G: A comprehensive Survey of Existing Studies. *Journal of Communications*, 16(6): 217-227, June.
- Botsinis, P., Alanis, D., Xu, C., Babar, Z., Chandra, D., Xin, S.N.G. & Hanzo, L. 2018. Air-to-Ground NOMA Systems for the "Internet-Above-the-Clouds". *IEEE Access*, 6: 47442- 47460.
- Caus, M., Vazquez, M.A. & Neira, A.I.P. 2016. NOMA and Interference Limited Satellite Scenarios. *IEEE Asilomar*:497-501.
- Chistopoulos, D., chatzinotas, S. & Ottersten, B. 2015. Multicast Multigroup Precoding and User Scheduling for Frame-Based Satellite Communications. *IEEE Transactions on Wireless Communications*, 14(9): 4695-4707, September.
- Chowdhury, S. 2019. Matching theory for cognitive radio networks: An overview. *ICT Express (KICS)*, 5:12-15.
- Comisso, M. 2008. Beamforming Techniques for Wireless Communications in Low-Rank Channels: Analytical Models and Synthesis algorithms. Unpublished PhD Thesis, University of Trieste, Italy.
- Dai, L., Wang, B., Ding, Z., Wang, Z., Chen, S. & Hanzo, L. 2018. A Survey of Non-Orthogonal Multiple Access for 5G. *IEEE communications surveys & tutorials*, 20(3): 2294-2322, third quarter.
- Dai, L., Wang, Z. & Yuan, Y. 2015. Non-Orthogonal Multiple Access for 5G: Solutions, Challenges, Opportunities, and Future Research Trends. *IEEE Communications Magazine*: 74-81, September.
- Daniels, R. & Balyan, V. 2020. Resource allocation for NOMA based network using relays: cell centre and cell edge users. *International Journal on Smart Sensing and Intelligent Systems*, 13(1):1-18.
- Daniels, R. & Balyan, V. 2022. Outage probability for a multiuser NOMA-based network using energy harvesting relays. *Nonlinear Engineering*, 11: 672-679.

- Ding, Z., Fan, P. & Poor, H.V. 2016. Impact of User Pairing on 5G Nonorthogonal Multiple-Access Downlink Transmissions. *IEEE Transactions on Vehicular Technology*, 65(8): 6010-6023, August.
- Ejaz, W., Sharma, S.K., Saadat, S., Naeem, M., Anpalagan, A. & Chughtai, N.A. 2020. A comprehensive survey on resource allocation for CRAN in 5G and beyond Networks. *Journal of Network and Computer Applications*, 160:1-24, March.
- Ernest, T.Z.H., Madhukumar, A.S., Sirigina, R.P. & Krishna, A.K. 2020. Addressing spectrum efficiency through hybrid-duplex UAV communications: Challenges and opportunities. *Vehicular Communications*, 24: 1-24.
- Fenech, H., Tomatis, A., Amos, S., Soumholphakdy, V. & Velarde D.S. 2012. Future High Throughput Satellite Systems. *IEEE*: 991-997.
- Goldsmith, A. 2004. *Wireless Communications*. Stanford: Stanford University Press.
- Guidotti, A. & Coralli, A.V. 2018. Geographical Scheduling for Multicast Precoding in Multi-Beam Satellite Systems. *2018 9th Advanced Satellite Multimedia Systems Conference and the 15th Signal Processing for Space Communications Workshop (ASMS/SPSC)*: 1-8.
- Guidotti, A. & Coralli, A.V. 2019. Clustering Strategies for Multicast Precoding in Multi-Beam Satellite Systems. *IEEE Access*:1-33.
- Habid, A. & Moh, S. 2019. Wireless Channel Models for Over-the-Sea Communication: A Comparative Study. *Applied Sciences*, 9(443): 1-32.
- Han, Z., Gu, Y. & Saad, W. 2017. *Matching Theory for Wireless Networks*. Switzerland: Springer.
- Hu, S. & Rusek, F. 2017. A Generalised Zero-Forcing Precoder with Successive Dirty-Paper Coding in MISO. *IEEE Transactions on Wireless Communications*, 16(6): 3632-3645.
- Islam, S.M.R, Avazov, N., Dobre, O.A., & Kwak, K. 2017. Power-Domain Non-Orthogonal Multiple Access (NOMA) in 5G Systems: Potentials and Challenges. *IEEE communications surveys & tutorials*, 19 (2):721-742, second quarter 2017.
- Jamali, M. & Ghiasian, A. 2019. Randomised scheduling algorithm for virtual output queuing switch at the presence of non-uniform traffic. *The Institution of Engineering and Technology (Networks)*, 8(2): 138-142.
- Jiao, J., Sun, Y., Wu, S., Wang, Y. & Zhang, Q. 2019. Network Utility Maximization Resource Allocation for NOMA in Satellite-based Internet of Things. *IEEE Internet of Things Journal*:1-13.
- Joyce, D. 2015. Norm and inner products in C_n and abstract inner product spaces. University Lecture Notes, Linear Algebra, Clark University: 1-2.

- Keshav, S. 1997. *An Engineering Approach to Computer Networking*. New York: Addison-Wesley.
- Khan, U.U., Dilshad, N., Rehmani, M.H. & Umer, T. 2016. Fairness in Cognitive Radio Networks: Models, measurement methods, applications, and future research directions. *Journal of Network and Computer Applications*, 73(2016):12-26.
- Kumar, A., Manjunath, D. & Kuri, J. 2008. *Wireless Networking*. Burlington: Morgan Kaufmann Publishers.
- Kumar, S. & Kumar, K. 2020. Multiple access schemes for Cognitive Radio networks: A survey. *Physical Communication*, 38:1-31.
- Le-Boudec, J.Y. 2021. Rate adaptation, Congestion Control and Fairness: A Tutorial. University Lecture Notes, Ecole Polytechnique Federale de Lausanne: 1-54.
- Li, X., Wang, Q., Peng, H., Zhang, H., Do, D.T., Rabie, K.M., Kharel, P. & Cavalcante, C.C. 2020. A Unified Framework for HS-UAV NOMA Networks: Performance Analysis and Location Optimization. *IEEE Access*, 8: 13329-13340.
- Ligwa, M. & Balyan, V. 2022. A comprehensive Survey of NOMA-Based Cooperative Communication Studies for 5G Implementation. *Expert Clouds and Applications*, Lecture Notes in Networks and Systems, 209.
- Lin, Z., Lin, M., Wang, J.B., Cola, T., & Wang, J. 2019. Joint Beamforming and Power Allocation for Satellite-Terrestrial Integrated Networks With Non-Orthogonal Multiple Access. *IEEE Journal of Selected Topics in Signal Processing*, 13(3):657-670, June.
- Liu, G & Jiang, D. 2016. 5G: Vision and Requirements for Mobile Communication System towards Year 2020. *Chinese Journal of Engineering*: 1-9, March.
- Liu, X., Zhai, X.B., Lu, W. & Wu, C. 2015. QoS-guarantee Resource Allocation for Multibeam Satellite Industrial Internet of Things with NOMA. *IEEE Transaction of Industrial Informatics, Journal of latex class files*, 14(8):1-10, AUGUST.
- Mahmood, K., Moinuddin, M., Saeed, M.O.B. 2015. Rayleigh fading channel estimation using MMSE estimator for MIMO-CDMA system. *IEEE Access*: 1-5.
- Marinescu, D.C. 2018. *Cloud Computing: Theory and Practice*. 2nd ed. Cambridge: Margan Kaufmann Publishers.
- Marsic, I. 2013. *Computer Networks: Performance and Quality of Service*. New Jersey: Rutgers University Press.
- Neira, A.I.P., Caus, M. & Vázquez, M.A. 2019. Non-Orthogonal Transmission Techniques for Multibeam Satellite Systems. *IEEE Communications Magazine: Mobile Communications and Network*:58-63, December.

- Neira, A.I.P., Ibars, C., Serra, J., Coso, A., Vilardebo, J.G., Caus, M. & Liolis, K. P. 2011. MIMO channel modeling and transmission techniques for multi-satellite and hybrid satellite-terrestrial mobile networks. *Physical Communication*, 4(2011): 127-139.
- Obaidat, M., Nicopolitidis, P. & Zarai, F. 2015. *Modelling and Simulation of Computer Networks and Systems: Methodologies and Applications*. Waltham: Morgan Kaufmann Publishers.
- Pachon, A., Navarro, A. & Palomares, U.G. 2015. A flexible mid-term frequency domain scheduler for resource allocation in HetNets based on the SINR requested by users. *Computer Networks*, 79(2015): 247-262.
- Panah, A.Y. & Yogeewaran, K. 2016. Optimization for Zero-Forcing Precoding. *United State Patent Application Publication*. September 29: 1-25.
- Parker, M. 2017. *Digital Signal Processing 101: Everything you need to know to get started*. 2nd ed. Cambridge: Newnes.
- Parsons, J.D. 2000. *The Mobile Radio Propagation Channel*. 2nd ed. Chichester: John Wiley & Sons.
- Patzold, M. 2002. *Mobile Fading Channels*. Chichester: John Wiley & Sons.
- Pinto-Roa, D.P., Brizuela, C.A. & Baran, B. 2015. Multi-objective routing and wavelength converter allocation under uncertain traffic. *Optical Switching and Networking*, 16(2015):1-20.
- Pioro, M. & Medhi, D. 2004. *Routing, Flow, and Design in Communication and Computer Networks*. San Francisco: Morgan Kaufmann Publishers.
- Rahayu, Y., Sari, P.I., Ramadhan, D.I. & Ngah, R. 2019. High gain 5G MIMO antenna for mobile station. *International Journal of Electrical and Computer Engineering*, 9(1): 468-476, February.
- Ramirez, T. & Mosquera, C. 2020. Resource management in the multibeam noma-based satellite downlink. *IEEE Conference of ASSP*: 8812- 8816.
- Rao, S.S. 2009. *Engineering Optimization: Theory and Practice*. 4th ed. New Jersey: John Wiley & Sons.
- Reddy, V. C. & Chakravarthula, R. A. 2017. Intelligent Beam Weight Computation for Massive Beamforming. Unpublished MSc thesis, Blekinge Institute of Technology, Sweden.
- Roy, A., Acharya, T. & Dasbit, S. 2018. Quality of service in delay tolerant networks: A survey. *Computer Networks*, 130(2018): 121-133.
- Rusdiana, S., Oktavia, R. & Charie, E. 2019. Application of Hungarian Method in Optimizing the Scheduling of Employee Assignment and Profit of Home Industry Production. *Journal of Research in Mathematics Trends and Technology*, 1(1):24-33.

- Saito, Y., Benjebbour, A., Kishiyama, Y. & Nakamura, T. 2013. System-Level Performance Evaluation of Downlink Non-orthogonal Multiple Access (NOMA). *2013 IEEE 24th International Symposium on Personal, Indoor and Mobile Radio Communications: Fundamentals and PHY Track*: 611-615.
- Salvatore, J. 2007. Bipartite Graphs and Problem Solving. University of Chicago: 1-8
- Shah, D. & Shin, J. 2012. Randomized Scheduling Algorithm for Queuing Networks. *The Annals of Applied Probability*, 22(1): 128-171.
- Shams, F., Bacci, G. & Luise, M. 2014. A survey on resource allocation techniques in OFDMA(A) networks. *Computer Networks*, 65(2014): 129-150.
- Sun, Y., Jiao, J., Wu, S., Wang, Y. & Zhang, Q. 2019. Joint Power Allocation and Rate Control for NOMA-based Space Information Networks. *IEEE*:1-6.
- Sun, Y., Wang, Y., Jiao, J., Wu, S. & Zhang, Q. 2019. Deep Learning-Based Long-Term Power Allocation Scheme for NOMA Downlink System in S-LoT. *IEEE Access*, 7:86288- 86296.
- Trivedi, V.K., Ramadan, K., Kumar, P., Dessouky, M.I., & Abd El-Samie, F.E. 2019. Enhanced OFDM-NOMA for next generation wireless communication: A study of PAPR reduction and sensitivity to CFO and estimation errors. *International Journal of Electronics and Communications (AEÜ)*, 102: 9-24.
- Tse, D. & Viswanath, P. 2005. *Fundamentals of Wireless Communication*. Cambridge: Cambridge University Press.
- Vazquez, M.A., Caus, M. & Neira, A.P. 2016. Performance Analysis of Joint Precoding and MUD Techniques in Multibeam Satellite Systems. *IEEE Access*: 1-5.
- Vázquez, M.A., Neira, A.I.P., Christopoulos, D., Chatzinotas, S., Ottersten, B., Arapoglou, P.D., Ginesi, A. & Taricco, G. 2016. Precoding in Multibeam Satellite Communications: Present and Future Challenges. *IEEE Wireless Communications*: 88-95, December.
- Vouyioukas, D. 2013. A Survey on Beamforming Techniques for Wireless MIMO Relay Networks. *International Journal of Antennas and Propagation*: 1-21.
- Wagner S., Couillet, R., Slock, D. & Debbah, M. 2010. Large System Analysis of Zero-forcing Precoding in MISO Broadcast Channels with Limited Feedback. *11th IEEE International Workshop on Signal Processing Advances in Wireless Communications, Marrakech, June 2010*: 1-5.
- Wan, D., Wen, M., Ji, F., Yu, H. & Chen, F. 2018. Non-Orthogonal Multiple Access for Cooperative Communications: Challenges, Opportunities, and Trends. *IEEE Wireless Communications*:109-117, April.
- Wang, A., Lei, L., Lagunas, E., Neira, A.I.P., Chatzinotas, S. & Ottersten, B. 2019. On Fairness Optimization for NOMA-Enabled Multi-Beam Satellite Systems. *2019 IEEE 30th Annual*

International Symposium on Personal, Indoor and Mobile Radio Communications (PIMRC): Track 3: Mobile and Wireless Networks: 1-6.

Wang, R., Kang, W., liu, G., Ma, R. & li, B. 2020. Admission Control and Power Allocation for NOMA-Based Satellite Multi-Beam Network. *IEEE Access*, 8: 33631-33643.

Wang, X., Na, Z. & Yan, K. 2019. Energy Efficiency Optimization for NOMA-Based Cognitive Radio with Energy Harvesting, *IEEE Access*, 7:139172-139180.

Wang, Y., Ren, B., Sun, S., Kang, S. & Yue, X. 2016. Analysis of Non-Orthogonal Multiple Access for 5G. *China Communications*, 2:52-66.

Wang, Z., Cao, Y. & Gao, P. 2021. User Selection for MIMO Downlink With Digital and Hybrid Maximum Ration Transmission. *IEEE Transactions on Vehicular Technology*, 70(10): 11101-11105, October.

Wegener, I. 2003. *Complexity Theory: Exploring the Limits of Efficient algorithms*. Dortmund: Springer.

Willner, A.E. 2019. *Optical Fiber Telecommunications VII*. Cambridge: Academic Press.

Yan, X., An, K., Liang, T., Zheng, G., Ding, Z., Chatzinotas, S. & Liu, Y. 2019. The Application of Power-Domain Non-Orthogonal Multiple Access in Satellite Communication Networks. *IEEE Access*, 7: 63531–63539.

Yan, X., An, K., Wang, C.X., Zhu, W.P., Li, Y. & Feng, Z. 2020. Genetic algorithm optimized support vector machine in noma-based satellite networks with imperfect csi. *IEEE Conference of ASSP: 8817- 8821*.

Yan, X., Xiao, H., An, K., Zheng, G. & Tao, W. 2018. Hybrid Satellite Terrestrial Relay Networks With Cooperative Non-Orthogonal Multiple Access. *IEEE COMMUNICATIONS LETTERS*, 22(5):978-981, MAY.

Yan, X., Xiao, H., Wang, C.X., An, K., Chronopoulos, A.T. & Zheng, G. 2018. Performance Analysis of NOMA-Based Land Mobile Satellite Networks. *IEEE Access*, 6:31327- 31339.

Yang, H. & Choi, S. 2013. Implementation of a Zero-Forcing Precoding Algorithm Combined with Adaptive Beamforming Based on WiMAX System. *International Journal of Antennas and Propagation: 1-7*.

Yin, Z., Jia, M., Wang, W., Cheng, N., Lyu, F., Guo, Q. & Shen, X. 2019. Secrecy Rate Analysis of Satellite Communications With Frequency Domain NOMA. *IEEE Transactions on Vehicular Technology*, 68(12):11847–11858, December.

Zeng, Y., Wu, X. & Cao, J. 2013. Research and Implementation of Hungarian Method Based on the Structure Index Reduction for DAE Systems. *Journal of Algorithms & Computational Technology*, 8(2): 219-231.

- Zhang, S., Zhu, D. & Wang, Y. 2020. A survey on space-aerial-terrestrial integrated 5G networks. *Computer Networks*, 174:1-18.
- Zhang, X., Guo, D., An, K., Chen, Z., Zhao, B., Ni, Y. & Zhang, B. 2019. Performance Analysis of NOMA-Based Cooperative Spectrum Sharing in Hybrid Satellite-Terrestrial Networks. *IEEE Access*, 7:172321–172329.
- Zhang, Y., Gao, J. & Liu, Y. 2016. MRT precoding in downlink multi-user MIMO systems. *EURASIP Journal on Wireless Communications and Networking*: 241-247.
- Zhu, X., Jiang, C., Kuang, L., Ge, N., & Lu, J. 2017. Non-Orthogonal Multiple Access Based Integrated Terrestrial-Satellite Networks. *IEEE Journal on Selected Areas in Communications*, 35(10):2253-2267, October.
- Zhu, X., Jiang, C., Kuang, L., Ge, N., Guo, S. & Lu, J. 2019. Cooperative Transmission in Integrated Terrestrial-Satellite Networks. *IEEE Network*: 204-210, June.
- Zhu, X., Jiang, C., Yin, L., Kuang, L., Ge, N. & Lu, J. 2018. Cooperative Multigroup Multicast Transmission in Integrated Terrestrial-Satellite Networks. *IEEE Journal on Selected Areas in Communications*, 36(5): 981-992, May.
- Zhu, Y., Delamotte, T. & Knopp, A., 2019. Geographical NOMA-Beamforming in Multi-Beam Satellite-Based Internet of Things. *IEEE Access*: 1-6.

APPENDICES

Appendix-A: Matlab Codes for the “Matlab Implementation” of the Algorithms

Appendix-A1: The “Main Function” which calls the UGA, PCA, PAA-1 and PAA-2

```
%% ***** %
%   THIS IS THE MAIN FUNCTION FOR THE NETWORK'S MA-ENC BLOCK. THIS %
%   THIS FUNCTION CALLS "PROPOSED_UGA", "PCA", "PAA-1", AND "PAA-2". %
%% ***** %
function MA_Encoder_Function()
    %% INITIALIZE ALL NETWORK'S STATIC PARAMETERS
    sat_altitude = 1000;    %km
    d_max_gnd = 1000;      %km
    AoA_span_max = pi;
    fc = 20*10^9;          %20GHz
    BW = 500*10^6;         %500MHz
    Gtx_dBi = 50;          %sat antenna's gain
    Grx_dBi = 0;           %user's antenna gain
    Ptot_sat = 60;         %60W
    Pb_max = 20;           %20W
    No = -174;             %-174dBm/Hz
    M = 4;                 %Numb of Satellite's antennas
    nw_activ_users = 2*M*10;%Numb of active users in network's coverage
    PAA_option = 1;        %Choose the PAA you wish to run (1=PAA1, 2=PAA2)

    %% AWGN POWER LEVEL CALCULATION
    noise_power_dBm = 10*log10(BW) + No; %Noise_power = BNo
    Noise_power_W = (10^(noise_power_dBm/10))/1000;

    %%USERS TRAFFIC-REQUETS GENERATION
    ave_TR_desired = 3;    %3bps/Hz
    sat_users_TR_set = users_TR_gen(nw_activ_users,ave_TR_desired);

    %%USER'S CHANNEL-VECTOR GENERATION
    sat_users_chx_matrix = users_chx_vect_gen(nw_activ_users,d_max_gnd,
                                                AoA_span_max, fc, Gtx_dBi, Grx_dBi, No);

    %%USERS SCHEDULING PROCESS
    [TRs_set_of_2M_users, chx_vect_set_of_2M_users] =
    sat_users_scheduling(sat_users_TR_set,sat_users_chx_matrix,M,r);

    %%USERS GROUPING PROCESS (PROPOSED_UGA)
    generated_pairs_set = uga_proposed(chx_vect_set_of_2M_users,M);

    %%BEAM'S PRECODING WEIGHT-VECTORS CALCULATION
    W= zero_forcing_PC_gen(generated_pairs_set,chx_vect_set_of_2M_users,M);

    %%POWER-ALLOCATION PROCESS (PAA-1 or PAA-2)
    if(PAA_option == 1)
        [Pb_set_adeq, ab_set_adeq] = PAA_1(TRs_set_of_2M_users,
            chx_vect_set_of_2M_users,generated_pairs_set,W,Ptot_sat,
            Pb_max, Noise_power_W,M); %call PAA-1;
    elseif(PAA_option == 2)
        [Pb_set_adeq, ab_set_adeq] = PAA_2(TR_set_for_2M_users,
            chx_vect_set_of_2M_users,generated_pairs_set,W,Ptot_sat,
            Pb_max, Noise_power_W,M); %call PAA-2;
    end
    Pb_set_final = Pb_set_adeq;
    ab_set_final = ab_set_adeq;
end
```

Appendix-A2: The Top-Level-Function of the “proposed-UGA”

```

%% ***** %
%
% THIS IS THE TOP-LEVEL FUNCTION FOR THE PROPOSED-UGA %
%
%% ***** %
function set_of_generated_pairs = uga_proposed(chx_vect_set_of_2M_users,M)
%% 1. INITIAL PARAMETERS DEFINITION
%%initial parameters
Cgr_min_init = 1.5;
Imax = 5;
Cgr_min_decr_step = (Cgr_min_init-1)/Imax;
numb_users = 2*M;

%%calculate channel-gain of each of the 2M users
for u = 1:numb_users
    user_chx_vect = chx_vect_set_of_2M_users(:,u);
    users_chx_gains(u) = user_chx_gain_cal(user_chx_vect);
end

%% 2. GENERATE A SET OF NEAR-USERS AND A SET OF FAR-USERS
[near_users_set, far_users_set] = near_far_sets_gen(users_chx_gains,M);

%% 3. GENERATE THE HUNGARIAN-MATRIX OF C3 BTWN ALL FUs & NUS
C3_hungarian_matrix = C3_hungarian_matrix_gen(near_users_set,
                                                far_users_set, chx_vect_set_of_2M_users);

%% ITERATIVE PROCESS UNTIL PERFECT-MATCHING IS OBTAINED (I.E. M-PAIRS)
perfect_matching = 0;
Cgr_min_new = Cgr_min_init;
while(perfect_matching == 0)
    %% 4. GENERATE RESTRICTED C3-HUNG-MATX BASED ON "Cgr_min"
    Cgr_min = Cgr_min_new;
    restricted_C3_hungarian_matrix = restricted_C3_hungarian_matrix_gen
        (C3_hungarian_matrix, users_chx_gains,Cgr_min);

    %% 5. EXECUTE RESTRICTED-HUNGARIAN-METHOD TO GENERATE THE PAIRS
    produced_pairs = restricted_hungarian_method
        (restricted_C3_hungarian_matrix);

    %% 6. CHECK PAIRING RESULTS AND EITHER TERMINATE OR LOOP-BACK
    %verify if perfect-matching is obtained
    numb_of_pairs_produced = length(produced_pairs);
    if(numb_of_pairs_produced == M)
        perfect_matching = 1;
    else
        perfect_matching = 0;
    end
    %reduce "Cgr_min" in case of "no perfect-matching"
    if(perfect_matching == 0)
        Cgr_min_new = Cgr_min - Cgr_min_decr_step;
    end
end

%% OUTPUT THE GENERATED SET-OF-PAIRS
set_of_generated_pairs = produced_pairs;
end

```

Appendix-A3: The Top-Level-Function of the "PCA"

```

%% *****
%
%   THIS IS THE TOP-LEVEL FUNCTION FOR THE PCA, WHICH CALCULATE
%   THE ZERO-FORCING PRECODING WEIGHT-VECTOR-MATRIX (W)
%
%% *****
function pc_weight_vectors_matrix = zero_forcing_PC_gen
    (generated_pairs_set, chx_vect_set_of_2M_users, M)
    %% PRODUCE THE CHX-MATRIX FOR THE N-NEAR USERS
    sat_NUs_chx_matrix = sat_NUs_chx_matrix_gen(generated_pairs_set,
        chx_vect_set_of_2M_users, M);
    h = sat_NUs_chx_matrix;

    %% CALCULATE THE HERMITIAN OF THE CHANNEL-MATRIX "hH"
    hH = hermitian_operation(sat_NUs_chx_matrix);

    %% CALCULATE THE PRODUCT "h.hH"
    h_hH = h_prod_hH_calculation(h, hH);

    %% CALCULATE THE INVERSE (h.hH)^-1
    inv_h_hH = inverse_matrix_calculation(h_hH);

    %% CALCULATE THE ZERO-FOCRING WEIGHT-VECTOR MATRIX: "W = hH(hhH)^-1"
    W = zeros(M, M);
    for r = 1:M
        c = 1;
        while(c <= M)
            sum = 0;
            for c1 = 1:M
                sum = sum + hH(r, c1)*inv_h_hH(c1, c);
            end
            W(r, c) = sum;
            c = c+1;
        end
    end

    %% VERIFY THE ZERO-FORCING EFFECT USING "Q-MATRIX"
    Q = zeros(M, M);
    for r = 1:M
        c = 1;
        while(c <= M)
            sum = 0;
            for c1 = 1:M
                sum = sum + h(r, c1)*W(c1, c);
            end
            Q(r, c) = sum;
            c = c+1;
        end
    end

    %%OUTPUT THE RESULTS
    pc_weight_vectors_matrix = W;
end

```

Appendix-A4: The Top-Level-Function of the "PAA-1"

```

%% ***** %
%
% THIS IS THE TOP-LEVEL FUNCTION FOR THE PROPOSED-PAA-1 %
%
%% ***** %
function [Pb_set_adeq, ab_set_adeq] = PAA_1(TRs_set_of_2M_users,
      chx_vect_set_of_2M_users,generated_pairs_set,W,Ptot_sat,
      Pb_max, Noise_power_W,M)

%% PROCESS INITIALIZATION
%define
cee = 0.01;
Pb_init = Pb_max/2;

%generate Pb_set_init
for b = 1:M
    Pb_set_init(b) = Pb_init;
end

%% ITERATIVE PROCESS UNTIL "OCTR-ratios Convergence" IS OBTAINED
octr_ratios_convergence = 0;
Pb_set_new = Pb_set_init;
while(octr_ratios_convergence == 0)

    %% RECEIVE THE NEW BEAMS-POWERS SET (Pb_set_new)
    Pb_set = Pb_set_new;

    %% DO INTRA-BEAM PA PROCESS TO OBTAIN "ab" and "Rb" FOR EACH
BEAM(b) :
    %I.E. CALL INTRA-BEAM PA-ALGORITHM BASED ON "OCTR-ratios-CONV"
    for b = 1:M
        [ab, Rb] = intra_beam_paa_ORC(Pb_set,TRs_set_of_2M_users,
            chx_vect_set_of_2M_users, generated_pairs_set,
            W,Noise_power_W);

        ab_set(b) = ab;
        Rb_set(b) = Rb;
    end

    %% DO INTER-BEAM PA PROCESS TO DET IF CONV-REACH OR NEW-Pb_set:
    %I.E. CALL INTER-BEAM PA-ALGORITHM BASED ON ""OCTR-ratios-CONV"
    [Pb_set_new, conv_reached] = inter_beam_paa_ORC(Pb_set, Rb_set,
        Ptot_sat, Pb_max);

    %% CHECK WHETHER TO TERMINATE OR LOOP BACK
    if(conv_reached == 1)
        octr_ratios_convergence = 1;
    elseif(conv_reached == 0)
        octr_ratios_convergence = 0;
    end
end

%% OUTPUT RESULTS
Pb_set_adeq = Pb_set_new;
ab_set_adeq = ab_set;
end

```

Appendix-A5: The Top-Level-Function of the "PAA-2"

```

%% ***** %
%
% THIS IS THE TOP-LEVEL FUNCTION FOR THE PROPOSED-PAA-2 %
%
%% ***** %
function [Pb_set_adeq, ab_set_adeq] = PAA_2(TRs_set_of_2M_users,
      chx_vect_set_of_2M_users,generated_pairs_set,W,Ptot_sat,
      Pb_max, Noise_power_W,M)

%% 1. PROCESS INITIALIZATION
%define
Pb_d = Ptot_sat/M; %users have same right = all equal.

%generate Pb_set_init
for b = 1:M
    Pb_set_init(b) = Pb_d;
end

%% ITERATIVE PROCESS UNTIL "OCTR-ratios Convergence" IS OBTAINED
all_max_min_fair_conds_reached = 0;
Pb_set_new = Pb_set_init;
while(all_max_min_fair_conds_reached == 0)

    %% RECEIVE THE NEW BEAMS-POWERS SET (Pb_set_new)
    Pb_set_cur = Pb_set_new;

    %% DO INTRA-BEAM PA PROCESS TO OBTAIN "ab" & "Rb" FOR EACH BEAM(b):
    %I.E. CALL INTRA-BEAM PA-ALGORITHM BASED ON "OCTR-ratios-CONV"
    for b = 1:M
        [ab, Rb] = intra_beam_paa_MMF(Pb_set,TRs_set_of_2M_users,
            chx_vect_set_of_2M_users,generated_pairs_set,
            W,Noise_power_W);

        ab_set(b) = ab;
        Rb_set(b) = Rb;
    end

    %% DO INTER-BEAM PA PROCESS TO DET IF CONV-REACH OR NEW-Pb_set:
    %I.E. CALL INTER-BEAM PA-ALGORITHM BASED ON ""OCTR-ratios-CONV"
    [Pb_set_new, mmf_conds_reached] = inter_beam_paa_MMF(Pb_set_cur,
        Rb_set, Ptot_sat, Pb_max);

    %% CHECK WHETHER TO TERMINATE OR LOOP BACK
    if(mmf_conds_reached == 1)
        all_max_min_fair_conds_reached = 1;
    elseif(mmf_conds_reached == 0)
        all_max_min_fair_conds_reached = 0;
    end
end

%% OUTPUT RESULTS
Pb_set_adeq = Pb_set_new;
ab_set_adeq = ab_set;
end

```

Appendix-B: Vitis Codes for the “On-Processor Implementation” of the Algorithms

Appendix-B1: The “MA-Encoder Function” which calls the UGA, PCA, PAA-1 & PAA-2

```
#include <stdio.h>
#include "xparameters.h"
#include "math.h"
#include "uga_proposed.h"
#include "pca_zf.h"
#include "PAA_1.h"
#include "PAA_2.h"

void MA_Encoder(u32_t M, float Noise_power_W, float
    TRS_set_of_2M_users[2*M],float chx_vect_set_of_2M_users[2*M,M],
    u32_t PAA_option, float *Pb_set_final[M],float *ab_set_final[M])
{
    /*DECLARING GLOBAL CONSTANTS AND VARIABLES TO THE MAIN-FUNCTION*/
    constant u32_t Ptot_sat = 60;           //60W
    constant u32_t Pb_max = 20;           //20W

    u32_t generated_pairs_set[2,M];
    float pc_wv_matrix[M,M];
    float Pb_set_adeq[M];
    float ab_set_adeq[M];

    /*CALLING THE UGA-PROPOSED*/
    uga_proposed(M,TRS_set_of_2M_users,chx_vect_set_of_2M_users,
        *generated_pairs_set);

    /*CALLING THE PCA_ZF*/
    pca_zf(M,generated_pairs_set,chx_vect_set_of_2M_users,*pc_wv_matrix);

    /*CALLING THE PAA (PAA1 = 1 or PAA2 = 2)*/
    if (PAA_option == 1)
    {
        PAA_1(M,TRS_set_of_2M_users,chx_vect_set_of_2M_users,
            generated_pairs_set, pc_wv_matrix,Ptot_sat,Pb_max,
            Noise_power_W,*Pb_set_adeq,*ab_set_adeq); //call PAA-1!
    }
    else
    {
        PAA_2(M,TRS_set_of_2M_users,chx_vect_set_of_2M_users,
            generated_pairs_set, pc_wv_matrix,Ptot_sat,Pb_max,
            Noise_power_W,*Pb_set_adeq,*ab_set_adeq); //call PAA-2!
    }

    /*RETURN RESULTS OF THE TOP-LEVEL FUNCTION*/
    Pb_set_final = Pb_set_adeq;
    ab_set_final = ab_set_adeq;
}
```

Appendix-B2: The Top-Level-Function of the “proposed-UGA”

```
#include <stdio.h>
#include "xparameters.h"
#include "math.h"
#include "uga_proposed.h"
#include "user_chx_gain_cal.h"
#include "near_far_sets_gen.h"
#include "C3_hungarian_matrix_gen.h"
#include "restricted_C3_hungarian_matrix_gen.h"
#include "restricted_hungarian_method.h"

void uga_proposed(u32_t M, float TRS_set_of_2M_users[2*M],
float chx_vect_set_of_2M_users[2*M,M], u32_t *generated_pairs_set[2,M])
{

    /*local constant to this uga_proposed*/
    constant float Cgr_min_init = 1.5; //
    constant u32_t Imax = 5; //
    constant float Cgr_min_decr_step = (Cgr_min_init-1)/Imax; //
    constant u32_t numb_users = 2*M; //network's capacity
    /*declaration of local variables to uga_proposed*/
    float user_chx_vect[M];
    float user_chx_gain;
    float user_chx_gains[numb_users];
    u32_t near_users_set[M];
    u32_t far_users_set[M];
    float C3_hungarian_matrix[M,M];
    u32_t perfect_matching;
    float Cgr_min_new;
    float rstx_C3_hungarian_matrix[M,M];
    u32_t produced_pairs[2,M];
    u32_t numb_of_pairs_produced;

    /*1. calculate channel-gain of each respective 2M users*/
    for (u = 1; u<=numb_users; u++)
    {
        for (r = 1; r<=M; r++)
        {
            user_chx_vect[r] = chx_vect_set_of_2M_users[u,r];
        }
        user_chx_gain_cal(user_chx_vect,*user_chx_gain);
        user_chx_gains[u] = user_chx_gain;
    }

    /*2. Generate a set of near-users and far-users*/
    near_far_sets_gen(M,user_chx_gains,*near_users_set,*far_users_set);

    /*3. generate the hungarian-matrix of C3*/
    C3_hungarian_matrix_gen(near_users_set,far_users_set,
        chx_vect_set_of_2M_users,*C3_hungarian_matrix);

    /*Iterative pairing process until perfect-matching*/
    perfect_matching = 0;
    Cgr_min_new = Cgr_min_init;
    while (perfect_matching == 0)
    {
        /*4. generate restricted c3-hung-mat based on "cgr_min"*/
        Cgr_min = Cgr_min_new;
        restricted_C3_hungarian_matrix_gen(C3_hungarian_matrix,
            user_chx_gains,Cgr_min,*rstx_C3_hungarian_matrix);
    }
}
```



```

        /*5. execute the restrix-hungarian-method*/
restricted_hungarian_method(rstx_C3_hungarian_matrix, *produced_pairs);

        /*6. check pairing results */
        //verify//
        numb_of_pairs_produced = sizeof(produced_pairs)/
                                sizeof(produced_pairs[1]);

        if(numb_of_pairs_produced == M)
        {
            perfect_matching = 1;
        }
        else
        {
            perfect_matching = 0;
        }

        //reduce "Cgr_min" in case of "no perfect matching"//
        if(perfect_matching == 0)
        {
            Cgr_min_new = Cgr_min - Cgr_min_decr_step;
        }
    }

    /*Return the resulting pairs*/
    generated_pairs_set = produced_pairs;
}

```

Appendix-B3: The Top-Level-Function of the "PCA"

```
#include <stdio.h>
#include "xparameters.h"
#include "math.h"
#include "pca_zf.h"
#include "sat_NUs_chx_matrix_gen.h"
#include "hermitian_operation.h"
#include "h_prod_hH_calculation.h"
#include "inverse_matrix_calculation.h"

void pca_zf(u32_t M, u32_t generated_pairs_set[2,M],
           float chx_vect_set_of_2M_users[2*M,M], float *pc_wv_matrix[M,M])
{
    /* LOCAL VARIABLES DECLARATION */
    float sat_NUs_chx_matrix[M,M];
    float h[M,M];
    float hH[M,M];
    float h_hH[M,M];
    float inv_h_hH[M,M];
    u32_t c;
    float sum;
    float W[M,M];
    float Q[M,M];

    /*PRODUCE THE CHX-MATRIX OF THE NEAR -USERS*/
    sat_NUs_chx_matrix_gen(M,generated_pairs_set,chx_vect_set_of_2M_users,
                          *sat_NUs_chx_matrix);
    h = sat_NUs_chx_matrix;

    /* CALCULATE THE HERMITIAN OF THE CHANNEL-MATRIX "hH" */
    hermitian_operation(h, *hH);

    /* CALCULATE THE PRODUCT "h.hH" */
    h_prod_hH_calculation(h,hH, *h_hH);

    /* CALCULATE THE INVERSE (h.hH)^-1 */
    inverse_matrix_calculation(h_hH, *inv_h_hH);

    /*CALCUL THE ZERO-FOCRING WEIGHT-VECTOR MATRIX: "W = hH(hhH)^-1" */
    for (r = 1; r<= M; r++)
    {
        c = 1;
        while(c <= M)
        {
            sum = 0;
            for (c1=1; c1<=M; c1++)
            {
                sum = sum + hH(r,c1)*inv_h_hH(c1,c);
            }

            W(r,c) = sum;
            c = c+1;
        }
    }

    /* VERIFY THE ZERO-FORCING EFFECT USING "Q-MATRIX" */
    for (r = 1; r<= M; r++)
    {
        c = 1;
        while(c <= M)
```

```
    {
        sum = 0;
        for (c1=1; c1<=M; c1++)
        {
            sum = sum + h(r,c1)*W(c1,c);
        }

        Q(r,c) = sum;
        c = c+1;
    }

    /* RETURN THE RESULTS */
    pc_wv_matrix = W;
}
```

Appendix-B4: The Top-Level-Function of the "PAA-1"

```
#include <stdio.h>
#include "xparameters.h"
#include "math.h"
#include "PAA_1.h"
#include "intra_beam_paa_ORC.h"
#include "inter_beam_paa_ORC.h"

void PAA_1(u32_t M, float TRS_set_of_2M_users[2*M],
          float chx_vect_set_of_2M_users[2*M,M], u32_t generated_pairs_set[2,M],
          float pc_wv_matrix[M,M], u32_t Ptot_sat,u32_t Pb_max,
          float Noise_power_W, float *Pb_set_adeq[M], float *ab_set_adeq[M])
{
    /* Define initial Parameters */
    constant float cee = 0.01;
    constant float Pb_init = Pb_max/2;
    float Pb_set_init[M];
    u32_t octr_ratios_convergence;
    float Pb_set_new[M];
    float Pb_set[M];
    float ab;
    float Rb;
    float ab_set[M];
    float Rb_set[M];
    u32_t conv_reached;

    /* Generate Pb_set_init */
    for (b=1; b<=M; b++)
    {
        Pb_set_init[b] = Pb_init;
    }

    /* ITERATIVE PROCESS UNTIL "OCTR-ratioa convergence" IS OBTAINED */
    octr_ratios_convergence = 0;
    Pb_set_new = Pb_set_init;

    while(octr_ratios_convergence == 0)
    {
        /* Receive the new Beams-Power Set */
        Pb_set = Pb_set_new;

        /* Do Intra-Beam PA Process */
        for (b=1; b<=M; b++)
        {
            intra_beam_paa_ORC(Pb_set,TRs_set_of_2M_users,
                               chx_vect_set_of_2M_users,generated_pairs_set,
                               pc_wv_matrix,Noise_power_W,*ab,*Rb);

            ab_set[b] = ab;
            Rb_set[b] = Rb;
        }

        /* Do Inter-Beam PA Process */
        inter_beam_paa_ORC(Pb_set,Rb_set,Ptot_sat,Pb_max,
                           *Pb_set_new,*conv_reached);

        /*Check whether to Terminate the PAA_1 function */
    }
}
```

```
        if(conv_reached == 1)
        {
            octr_ratios_convergence = 1;
        }
        elseif(conv_reached == 0)
        {
            octr_ratios_convergence = 0;
        }
    }
    /* Return the Results from the PAA_1 function */
    Pb_set_adeq = Pb_set_new;
    ab_set_adeq = ab_set;
}
```

Appendix-B5: The Top-Level-Function of the "PAA-2"

```
#include <stdio.h>
#include "xparameters.h"
#include "math.h"
#include "PAA_1.h"
#include "intra_beam_paa_MMF.h"
#include "inter_beam_paa_MMF.h"

void PAA_2(u32_t M, float TRS_set_of_2M_users[2*M],
float chx_vect_set_of_2M_users[2*M,M], u32_t generated_pairs_set[2,M],
float pc_wv_matrix[M,M], u32_t Ptot_sat,u32_t Pb_max,
float Noise_power_W, float *Pb_set_adeq[M], float *ab_set_adeq[M])
{
    /* Define initial Parameters */
    constant float Pb_deserv = Ptot_sat/M;
    float Pb_set_init[M];
    u32_t all_max_min_fair_conds_reached;
    float Pb_set_new[M];
    float Pb_set[M];
    float ab;
    float Rb;
    float ab_set[M];
    float Rb_set[M];
    u32_t mmf_conds_reached;

    /* Generate Pb_set_init */
    for (b=1; b<=M; b++)
    {
        Pb_set_init[b] = Pb_init;
    }

    /* ITERATIVE PROCESS UNTIL ALL "MAX-MIN-FAIR CONDITIONS" ARE OBTAINED */
    all_max_min_fair_conds_reached = 0;
    Pb_set_new = Pb_set_init;

    while(all_max_min_fair_conds_reached == 0)
    {
        /* Receive the new Beams-Power Set */
        Pb_set = Pb_set_new;

        /* Do Intra-Beam PA Process */
        for(b=1; b<=M; b++)
        {
            intra_beam_paa_ORC(Pb_set,TRS_set_of_2M_users,
                chx_vect_set_of_2M_users,generated_pairs_set,
                pc_wv_matrix,Noise_power_W,*ab,*Rb);

            ab_set[b] = ab;
            Rb_set[b] = Rb;
        }

        /* Do Inter-Beam PA Process */
        inter_beam_paa_ORC(Pb_set,Rb_set,Ptot_sat,Pb_max,
            *Pb_set_new,*conv_reached);

        /*Check whether to Terminate the PAA_1 function */
        if(mmf_conds_reached == 1)
        {
            all_max_min_fair_conds_reached = 1;
        }
    }
}
```

```
        elseif (mmf_conds_reached == 0)
        {
            all_max_min_fair_conds_reached = 0;
        }
    }
    /* Return the Results from the PAA_1 function */
    Pb_set_adeq = Pb_set_new;
    ab_set_adeq = ab_set;
}
```